Studies on cell wall structure during morphological changes in brown algae

（褐藻の形態形成に伴う細胞壁構造の変化に関する研究）

By

Rina Yonamine

Division of Biosphere Science,

Graduate School of Environmental Science,

Hokkaido University

Contents

Acknowledgement

I would like to express my gratitude to the people mentioned below, the research could not be got along and accomplished without anyone of them.

I want to give sincere thanks to my supervisor, Prof. Chikako Nagasato, Muroran Marine Station, Field Science Center for Northern Biosphere, Hokkaido University. She gave me the opportunity to initiate this interesting research, provide knowledge and experiment guidance. I always received warm encouragements from her. I would like to appreciate to emeritus Prof. Taizo Motomura and associate Prof. Kensuke Ichihara in Muroran Marine Station. They gave me kind discussions and essential advices through thesis research.

I would like to appreciate Prof. Etsuro Yamaha, Nanae Fresh Water Science Center for Northern Biosphere, Hokkaido Univ and Prof. Yoichiro Hoshino, Experiment Farm, Field Science Center for Northern Biosphere, Hokkaido Univ and Prof. Akira Inoue, School of Fisheries Sciences, Hokkaido Univ for their helpful suggestions and critical reading of the thesis.

I would like to express thank Dr. Cécile Hervé, Station Biologique de Roscoff, France, giving me the antibodies against alginate and sulfated fucan and precise advices. Prof. Shiro Tsuyuzaki, Graduate School of Environmental Earth Science, Hokkaido Univ giving me to teach the statistics method. Dr. Chika Kosugi and Dr. Ko Yoshimura, Advanced Technology Research Laboratories, Nippon Steel, for their valuable advices and suggestions.

Special thanks go to Mr. Teruo Tomioka and Mrs. Saeko Kitabayashi, the members of the laboratory, for their all-time supports and a warm cup of coffee. Supporting from the colleagues who belong to the lab Dr. Shen Yuen, Dr. Mizuho Namba, Mrs. Hinako Aoki, Mr. Minori Harada, Mr. Kengo Sawa and Mrs. Theone van der Merwe who belongs to Daekin Univ, Australia for their generous support and warm encouragement.

I wish to offer sincere thanks to my parents, and relatives who live in Okinawa and Prof. Teruko Konishi, Mrs. Ayana Kotani, and other members of the Departments of Agriculture, University of the Ryukyus.

General introduction

Many types of seaweed inhabit the seashore of Japan, and they are an important group of primary producers in coastal food chains. Species of the orders Laminariales and Fucales have notably become dominant in marine forests and they provide habitats for small sea living things. Seaweeds, including *Saccharina japonica* (Kombu) and *Undaria pinnatifida* (Wakame) are popular foodstuffs in Japan that are closely associated with Japanese food culture. The production of seaweed is increasing worldwide due to an increase in multifaceted commercial uses, such as in cosmetics, food additives, and pharmaceuticals. Characteristic polysaccharides such as carrageenan and agar from red algae, and alginate from brown algae, are the three major useful substances from seaweeds.

These substances can be extracted from cell walls in different ways according to their chemical and physical properties. The extracellular matrix (ECM) in plant cells comprises mainly of carbohydrates, proteins, and phenolic compounds, and the components differ depending on the species and groups. Such components form high-order molecular structures that mechanically protect cells from abiotic and biotic effects, and transduce signal information into cells about the extracellular environment.

Research on the cell walls of terrestrial plants, especially angiosperms, has advanced to include cell wall functions, morphology, components, properties of isolated polysaccharides, and searches for enzymes and genes involved in polysaccharide metabolism. The main polysaccharides in the cell walls of terrestrial plants are cellulose, pectin, and hemicellulose. Cellulose is one of the most abundant carbohydrate polymers on earth. Cellulose microfibrils consist of several β-1,4-linked glucans arranged linearly or in parallel, and they have hydrophobic and crystalline characteristics in the cell wall (Tsekos 1999; Jarvis 2003). Pectin mainly exists as a matrix among cellulose fibrils in cell walls and functions in adhesion between neighboring cells (Daher and Braybrook 2015). Pectin has three polysaccharide domains: homogalacturonan (HG), and rhamnogalacturonans I (RG-I) and II (RG-II) (Willats et al. 2001a). Homogalacturonan is a

linear polymer of α-1,4-linked galacturonic acid. Low methyl-esterified HG can cross-link with Ca^{2+} and form a supramolecular gel. Hemicellulose is a non-pectic polysaccharide that can be extracted with alkali. Xyloglucan, xylan, and mannan are hemicelluloses. The cell walls in terrestrial plants comprise primary and secondary cell walls. The primary cell wall is a flexible matrix that forms during cell expansion. The secondary cell wall is generated beneath the primary cell wall layer when cell expansion stops. It also provides structural strength to plants. The primary cell walls in dicotyledons comprise 20%–30% cellulose, 30%–35% pectin, and hemicellulose 25%–30%. In contrast, monocotyledons comprise 20%–30% cellulose, 1%–5% pectin, and 30%–70% hemicellulose (O'Neill and York 2003). Generally, the cellulose content increases in the secondary cell wall compared with that in the primary cell wall, and a heterogeneous phenolic propanoic polymer, lignin, is deposited (Meents et al. 2018). Lignin links between cellulose microfibrils through hemicellulose and ferulic acid restricts cell wall swelling and reduces hydraulic conductivity.

Cellulose is a dominant component in the cell wall of terrestrial plants and it is regarded as a scaffold for ECM formation. Isotropic turgor pressure on the cell drives cell growth, and the orientation of cellulose microfibrils affects anisotropic cell growth. The cell extends perpendicular to the cellulose microfibrils (Cosgrove 2016). Some mechanisms regulate the elasticity of the cell wall by changing the orientation of the cellulose microfibrils. Xyloglucan, a hemicellulose, binds to cellulose *via* hydrogen bonds (Scheller and Ulbskov 2010). Xyloglucan endotransglucosylase/hydrolase (XTH) can cut off xyloglucan, which binds to cellulose microfibrils and reconnects the edge of the polymer to a new xyloglucan acceptor (Rose et al. 2002). The role of XTH might be to loosen and tighten the cellulose microfibrils. Expansin is a glycoprotein located in the extracellular region. Expansin has no catalytic properties, but it can expand cell walls under low pH by loosening and inducing the slippage of cellulose microfibrils (Wu et al. 1996; Cosgrove 2018). In addition to changes in the arrangement of cellulose microfibrils, new cell wall components, such as pectin, are secreted at the tips of pollen tubes and

root hairs (Rounds and Bezanilla 2013).

The cell walls of seaweeds contain < 10% cellulose (Kloareg and Quatrano 1988). Furthermore, seaweeds contain unique sulfated polysaccharides (Kloareg and Quatrano 1988; Popper et al. 2011). For example, sulfated polysaccharides are found in ulvan from *Ulva* species of green algae, agar and carrageenan from red algae, and sulfated fucan from brown algae (Kloareg and Quatrano 1988; Kidgell et al. 2019). Seaweeds would have acquired them to adapt to their habitats. The cell walls of seaweeds function as a simultaneously rigid and flexible armor to protect them from the harsh tidal flow, desiccation, and osmotic pressure of coastal environments.

Brown algae belong to the stramenopiles, whereas green and red algae belong to Archaeplastida. All species of brown algae are multicellular and most of them inhabit marine environments. Some brown algae, such as *Laminaria* species, are the largest marine multicellular photosynthetic organisms. They have evolved the unique cell wall components alginate, cellulose, and sulfated fucan. Alginate is a polysaccharide with 1,4-linked mannuronic acid (M) and guluronic acid (G), and it is the most abundant polysaccharide in brown algal cell walls. The weight ratio of alginate to the other main polysaccharides, cellulose and sulfated fucan, is 3-fold that of *Fucus spiralis, Fucus ceranoides, Fucus vesiculosus, Fucus serratus, Bifurcaria bifurcate* (Fucales), and *Laminaria digitata* (Laminariales) (Mabeau and Kloareg 1987). Alginate might be embedded between cellulose microfibrils, and sulfated fucan is linked with cellulose between cellulose microfibrils (Deniaud-Bouët et al. 2014). How all this affects the physical characteristics of the cell wall remains unknown.

In addition to interactions among polysaccharides, sugar components in alginate and sulfated fucan affect the physical properties of the cell wall of brown algae. M-rich polymers in alginate are soft and elastic, whereas G-rich polymers are firm and brittle (Kloareg and Quatrano 1988). The ratio of M and G differs among species, developmental stage, tissues, and seasons (García-Ríos et al. 2012; Bertagnolli et al. 2014). Young sporophytes of *Costaria costata* and *S.*

japonica of the Laminariales have a high M/G ratio, which gradually decreases during development (Wu et al. 2014; Zhang et al. 2021a). Sulfated fucans comprise L-fucose (L-Fuc) polymers with a sulfate group, and glucuronic acid (GlcA), xylose, mannose (Man), and L-arabinose side chains (Kloareg and Quatrano 1988; Deniaud-Bouët et al. 2017). Sulfated fucan in brown algae differs in terms of bonding style, degree of sulfation, and monosaccharide composition of the side chains depending on the tissues, species, and season (Zvyagintseva et al. 2003; Fletcher et al. 2017).

Phlorotannin, a phloroglucinol polymer, is a polyphenolic component of the brown algal cell wall (Meslet-Cladière et al. 2013). Phenolic compounds are hydrophobic and link to alginate or proteins in the cell wall to protect cells against abiotic and biotic effects and support adherence to the substratum (Vreeland et al. 1998; Schoenwaelder and Wiencke 2000; Schoenwaelder 2002; Salgado et al. 2009; Deniaud-Bouët et al. 2014). Proteins are also considered as important components of brown algal cell walls, but their characterization is still unexplored (Terauchi et al. 2017).

To date, whole genomes of the brown algae *Ectocarpus siliculosus* (Cock et al. 2010), *S. japonica* (Ye et al. 2015), *Cladosiphon okamuranus* (Nishitsuji et al. 2016), *Nemacystus decipiens* (Nishitsuji et al. 2019), *Sargassum fusiforme* (Wang et al. 2020) and *Undaria pinnatifida* (Shan et al. 2020) have been completed. The cellulose, alginate, and sulfated fucan biosynthesis pathways have been predicted in *E. siliculosus*, *S. japonica*, *C. okamuranus*, and *N. decipiens*. However, most genes are still in the prediction stage, and their functions have not been clarified. Michel et al. (2010b) predicted four cellulose synthases (CESA) and a GT2 family glycosyltransferase in *E. siliculosus*. Cellulose synthases are included in terminal complexes (TCs) on the plasma membrane of terrestrial plants, and cellulose microfibrils are assembled through TCs from uridine diphosphate-glucose (UDP-Glc) towards the extracellular region. The movement of TCs is guided by the cortical microtubules located just beneath the plasma membrane; thus, the orientation of cellulose microfibrils is almost parallel to that of microtubules

(Paredez et al. 2006; Duncombe et al. 2021). Linear TCs have been identified (Tamura et al. 1996; Schüßler et al. 2003). However, brown algal cells do not have cortical microtubules (Katsaros and Galatis 1992; Bisgrove and Kropf 2004), therefore, the regulation of the orientation of cellulose microfibrils in brown algae remains debatable. The *Ectocarpus* genome does not contain genes encoding cellulase, and homologs of XTH and expansin are undetectable (Michel et al. 2010b). Although candidate CESAs have been identified in brown algae, the mechanisms that regulate the orientation of cellulose microfibers might differ from those of land plants.

The morphology of brown algal cell walls has been analyzed using electron microscopy. Ultrastructural findings have shown that the cell wall has a fiber structure with a matrix filler (Evans and Holligan 1972; Novotny and Forman 1975; Callow et al. 1978; Karyophyllis et al. 2000; Bisgrove and Kropf 2001; Terauchi et al. 2016). Cellulose comprises electronegatively stained fibrils; thus, the visible fibers of the cell wall in brown algae are thought to be alginate (Terauchi et al. 2016). The appearance of the cell wall varies depending on the cellular types and species, and the layers are distinguishable by stainability and the arrangement of fibrils (Evans and Holligan 1972; Callow et al. 1978). Attempts have been directed towards histochemically defining differences in cell wall components by metachromatic staining. Toluidine blue stains alginate under pH 6.8 while it stained sulfated fucan under pH 0.5 (Novotny and Forman 1975; Callow et al. 1978; Burns et al. 1982a; Mariani et al. 1985). Periodic acid-Schiff (PAS) stained β-1,4-linked glycan, namely cellulose and alginate in brown algae (Novotny and Forman 1975; Callow et al. 1978; Burns et al. 1982a). For example, toluidine blue at pH 0.5, stains only the rhizoid cell wall, whereas PAS stains entire cells in *F. gardneri* zygotes (Novotny and Forman 1975). However, metachromatic staining is insufficient to identify specific sugars. The specificity of polysaccharides in cell walls can be determined *in situ* using anti-alginate and anti-sulfated fucan antibodies under immunofluorescence microscopy (Vreeland et al. 1984; Mizuno et al. 2009; Torode et al. 2015, 2016), and immunoelectron microscopy (Chi et al. 1999; Nagasato et al. 2010; Terauchi et al. 2016). Additionally, cell wall digestive enzymes such as cellulase or

alginate lyase labeled with gold particles can be localized using transmission electron microscopy (TEM) (Nagasato et al. 2010; Terauchi et al. 2016).

The cell walls in land plants and brown algae function to maintain cell morphology and protect cells from abiotic and biotic effects. Conversely, morphological changes in cells might be caused by changes in the cell wall structure. However, few studies have investigated the relationship between morphogenesis and cell wall structure in brown algae using morphological and molecular approaches.

Objective and approach

This study aimed to determine changes in cell wall structure accompanying morphogenesis and thus focused on conspicuous morphological changes in brown algae, namely rhizoid formation in fucoid zygotes of *Silvetia babingtonii* (Chapter 1), and gametogenesis in *S. japonica* (Chapter 2). The fucoid zygotes used in Chapter 1 have served as experimental models to investigate the mechanism of cell polarity for > 100 years. Unfertilized eggs and early zygotes have a uniform distribution of cytoplasm and a perfect spherical shape. However, "polarity," thallus and rhizoid poles, are established before the first mitosis, and the rhizoid elongation and the asymmetrical cell division produce thallus and rhizoid cells. Many ultrastructural studies have identified cell walls in polarized zygotes; however, the mechanism through which rhizoids elongate from the preexisting cell wall has remained obscure. I attempted to clarify this mechanism by rapid freezing and freeze substitution for ultrastructural assessment and transcriptome analysis. The genome of *S. japonica* described in Chapter 2 has been sequenced, and a large volume of transcriptomic data from different culture conditions, developmental stages, and generations (gametophytes and sporophytes) have accumulated. The morphological changes in gametogenesis of *S. japonica* comprise the formation of antheridia in male gametophytes and oogonia in female gametophytes. These organs are formed by protruding from extant walls in filamentous cells. Therefore, I considered that the relationship between cell wall structure and

morphological changes could be clarified by focusing on this developmental stage and would generate new findings about cell wall metabolism in gametophytes.

I assessed the ultrastructure of the cell wall by TEM and immunoelectron microscopy using anti-alginate, then analyzed transcriptomes, and the relationship between morphological changes and modifications of the cell wall architecture in brown algae.

Chapter 1. Change of cell wall structure and gene expression during rhizoid formation of *Silvetia babingtonii* (Fucales, Phaeophyceae) zygotes

Introduction

Many seaweeds grow in the intertidal region where environmental factors, including temperature, wave shock, intensity and quality of light, salinity, and drying, are changeable. The cell wall protects cells from physical shocks and unfavorable factors, such as herbivores. Therefore, seaweeds develop characteristic polysaccharides in the cell wall to enhance stress tolerance (Kloareg and Quatrano 1988; Popper et al. 2011). In brown algae, the main components of the cell wall are alginates, sulfated fucans, and cellulose. The mature sporophyte of laminarialean species contains three times more alginate than cellulose and sulfated fucan, whereas that of fucalean species contains more than twice the alginate compared to cellulose and sulfated fucan (Mabeau and Kloareg 1987; Skriptsova et al. 2012). Alginate consists of 1,4-linked mannuronic acid (M) and guluronic acid (G) residues. M-rich blocks produce flexible gels, while G-rich blocks cause rigidity. Accordingly, the M/G ratio relates to the properties of the cell wall, such as gel strength and stretching. Young sporophytes of *Costaria costata* show a high M/G ratio, and the ratio gradually decreases with thallus growth (Wu et al. 2014). The conversion of M residue into G residue is carried out by different mannuronan C5-epimerases (MC5Es) expressed in different developmental stages and environmental conditions (Nyvall et al. 2003; Tonon et al. 2008). The alginate biosynthesis pathway in brown algae is not fully resolved, especially the first production of a polymer of M residues (mannuronan) (Michel et al. 2010b). It is predicted that, shortly after synthesis, the alginate should consist of M-rich blocks; therefore, the M-rich region might hold the clues to the understanding of alginate synthesis.

There are some ultrastructural observations of the cell walls of the brown algae. The results showed that three or more cell wall layers were identified in the apical cell of *Sphacelaria rigidula* (Karyophyllis et al. 2000), the meristematic epidermal cells of *Dictyota dichotoma*

(Evans and Holligan 1972), zygotes of fucoid algae (Novotny and Forman 1975; Callow et al. 1978; Bisgrove and Kropf 2001), and the lateral cell wall in gametophytes and sporophytes of *Ectocarpus siliculosus* (Terauchi et al. 2016). The cell wall layers were distinguished by the distribution of the cell wall fibers and the matrix. Terauchi et al. (2016) clarified the quantification of the frequency of the electron-opaque fibrils (alginate fibrils) and their junction based on three-dimensional analysis using rapid freezing fixation and electron microscopy and tomography. The results showed that the alginate fibers were distributed more densely and in a more complex arrangement in the inner layer than in the middle layer.

Tip-growing apical cells of *Sphacelaria* showed a characteristic cell wall structure. In *Sphacelaria rigidula*, the apical dome of the tip cell had a two-layered cell wall. A very thin amorphous layer (L1) covered the cell, and the fibrous layer (L2) existed just beneath the L1 layer. Other parts of the tip cell and the thallus cells were covered with four layers of cell walls, with L3 and L4 added to L1 and L2 (Karyophyllis et al. 2000). In *Sphacelaria furcigera*, bud (branch) formation was observed (Burns et al. 1982a, b). The axial cell wall is composed of four layers (CW1–CW4), but the initial bud region is covered by two newly synthesized layers (CWO and CWI). Burns et al. (1982a) suggested that alginates are abundant in CW2, CW4, and CWI, while sulfated fucans were prominent in CW1, CW3, and CWO by metachromatic analysis. Cell wall structure on the rhizoid tip in fucoid zygotes has been observed (Novotny and Forman 1975; Callow et al. 1978; Bisgrove and Kropf 2001). Deposition of the highly sulfated fucan occurs in the tip growth region (Quatrano and Crayton 1973; Quatrano and Steven 1976; Callow et al. 1978; Brawley and Quatrano 1979; Torode et al. 2016). However, the changes occurring in the cell wall structure during rhizoid development remain unclear.

Different appearances in the multilayered cell wall could reflect differences in cell wall components, which would produce different physicochemical properties. To examine the distribution of polysaccharides on the cell wall, immunoelectron microscopy using anti-alginate antibody (Chi et al. 1999; Nagasato et al. 2010; Terauchi et al. 2012; Terauchi et al. 2016), an

anti-fucoidan antibody (Nagasato et al. 2010), and a binding assay using a conjugation of cellulase or alginate lyase-colloidal gold were applied (Nagasato et al. 2010; Terauchi et al. 2016). At the light microscopic level, metachromatic analysis using toluidine blue and periodic acid-Schiff (PAS) was performed to detect alginate and sulfated fucan (Novotny and Forman 1975; Burns et al. 1982a). Recently, monoclonal antibodies that recognize the different structures of alginate and sulfated fucan were produced, and immunofluorescence data on the localization of these epitopes in some brown algal species were collected (Torode et al. 2016; Linardić and Braybrook 2017; Rabillé et al. 2019; Linardić et al. 2020). Antibodies recognizing different epitopes showed spatial and temporal differences in localization. By analyzing the localization of these antibodies through immunoelectron microscopy, it was expected that I could obtain more useful information relating to the multilayered cell wall of the brown algae.

In brown algae, there is little existing information on how the cell wall changes to generate tip-growth from the thallus cell. To address this question, I observed cell wall structure during rhizoid growth in the fucoid alga *S. babingtonii* zygotes, using the rapid freezing and freeze substitution technique for TEM. This method prevents loss of soluble polysaccharides, namely alginate and sulfated fucan. In this study, I focused on localization of the alginate by immunoelectron microscopy using antibodies that recognize different epitopes. Moreover, to examine the synthesis regulation of alginate on rhizoid growth. I carried out transcriptomic analysis using mRNA obtained from zygotes before and after germination.

Materials and methods

Materials

Mature *Silvetia babingtonii* (Harvey) E.A. Serrão, T.O. Cho, S.M. Boo & Brawley was collected from September to November 2006-2010 at Charatsunai, and 2018 at Botofurinai, Muroran, Hokkaido, Japan. The collected mature thalli were brought to the laboratory and wiped with gauze after washing with sterile seawater. The zygote preparation procedure was the same

as in the previous paper (Abe 1970; Nagasato et al. 2010). They were placed in continuous light (30-40 μmol photons m^{-2} s^{-1}) at 18 °C overnight. Then, the thalli were transferred to a cool chamber at 4 °C for 2 h after darkening with aluminum foil. Adding fresh seawater induced the release of eggs and sperm into the medium. The age of the zygotes was counted from 1 h after pouring seawater. Zygotes were cultured in PES medium (Provasoli 1968) containing 40 μg mL^{-1} chloramphenicol at 18 °C in continuous light.

Electron microscopy and Immunoelectron microscopy

Zygotes were cultured on gel support films (ATTO Co., Tokyo, Japan). Before fixation, the films were cut into small triangle shapes less than 1cm. Rapid freezing and freeze substitution procedures were performed according to previous reports (Nagasato and Motomura 2002b; Nagasato et al. 2010). Finally, the samples were embedded in a Spurr low-viscosity resin (Polysciences, Warrington, USA). Ultrathin sections were cut using a diamond knife on an ULTRACUT ultramicrotome (Reichert-Jung, Vienna, Austria). Sections were picked up on a formvar-coated one-slot copper grid, stained with EM stainer (Nisshin EM, Tokyo, Japan), an alternative stain for uranyl acetate based on lanthanide salts, and then lead citrate (Reynolds 1963). Observations were performed using a JEM-1011 electron microscope (JEOL, Tokyo, Japan).

Localization of the alginate was examined using antibodies against various alginate blocks (Torode et al. 2016). Nickel grids with sections were incubated with blocking solution (2.5% skimmed milk, 5% normal goat serum, and 0.05% NaN_3 in PBS; 137 mM NaCl, 2.7 mM KCl, 4.9 mM Na_2HPO_4, 1.5 mM KH_2PO_4, pH 7.4) for 30 min at 37 °C and then transferred to anti-alginate antibodies, BAM6 (M-rich epitopes) and BAM7 (MG epitopes) diluted 1:5 with PBS for 1 h at 37 °C. The grids were then washed with PBS three times and incubated for 1 h at 37 °C with a goat anti-rat IgG (whole molecule) conjugated with 10 nm colloidal gold particles (Sigma, St. Louis, Missouri, USA) diluted 1:20 with blocking solution. After washing with PBS and distilled water, sections on the grids were treated with EM stainer in this case.

Quantification of colloidal gold particles

To quantify the distribution of alginate in the thallus cell wall (TCW) and rhizoid-tip cell wall (RTCW), the distance between each colloidal gold particle and plasma membrane was measured using ImageJ 64 (NIH, Bethesda, MD, USA). Measurements were made within three replicate rectangle regions of cell wall. Each rectangle stretched from the plasma membrane to the outer edge of the cell wall and had 0.75 μm wide sides over the plasma membrane and at the surface of the cell wall (Plate 1). Three different zygotes were measured (n=9). The thickness of the cell wall differed in each sample; thus, the relative length between the plasma membrane and the edge of the cell wall was set as 0-1. The distance of gold particles was assumed to follow a beta distribution because the distance was continuous and ranged from 0 to 1. Because the number of particles differed between the antibodies, the relative density of distance was used to investigate the distributions. The kernel function and bandwidth obtained the function to express the density. Assessment of the function was confirmed by goodness of fit tests (GFT). Beta regression was used to investigate the effects of antibodies (BAM6 and BAM7), and the cell wall regions (TCW and RTCW) used as explanatory variables, on the distance, used as a response variable. Since interactions between these three explanatory variables were unlikely, the analyses were conducted on the respective explanatory variables. All statistical analyses were performed using R software (version 4.0.2) (R Core Team 2020) with the libraries fitdistrplus (Delignette-Muller and Dutang 2015) and betareg (Cribari-Neto and Zeileis 2010).

RNA-seq and differential expression analysis

Total RNA was extracted from zygotes at 3, 10, and 24 h after fertilization using cetyltrimethylammonium bromide (CTAB) buffer (Pearson et al. 2006). The extract was purified with a chloroform-isoamyl alcohol solution (24:1 v/v). After precipitation with 3 M LiCl, contaminating DNA was removed with an RNase-free DNase Set (Qiagen, Hilden, Germany).

Total RNA samples with OD260/280 >1.8, OD260/230>2.0, were used for library construction.

The cDNA library construction, sequencing with Illumina Novaseq6000 (150 bp paired-ends), and generating clean reads by filtering raw reads were performed by Filgen Inc. (Nagoya, Japan). The clean reads were assembled using Trinity software (Haas et al. 2013). The assembled contigs were clustered and filtered out using CD-HIT-EST on CD-HIT suite server (Li and Godzik 2006) with 90% similarity, and the longest open reading frame (ORF) sequences were identified by TransDecoder (v5.5.0) (Haas et al. 2013). Sequences with fewer than 100 amino acids were discarded. The longest ORF sequences were annotated using the annotation pipeline on Maser (Management and Analysis System for Enormous Reads) platform (https://cell-innovation.nig.ac.jp) (Kinjo et al. 2018). Clean reads were aligned onto the longest ORF sequences and quantified using Salmon (Patro et al. 2017). Data normalization and identification of differentially expressed genes (DEGs) without replicates were performed using an iterative *deseq* pipeline in the TCC package (Sun et al. 2013). False discovery rates (FDR) ≤ 0.05 were considered as DEGs. The Z-scores based on the transcripts per million (TPM) were calculated using R software (3.6.2; http://www.R-project.org/), and the heatmap of genes for the biosynthetic pathway of alginates was drawn using the gplots (3.0.1.2) package. The Bioconductor package topGO version 2.38.1 (Alexa et al. 2006) were used for Gene Ontology (GO) enrichment analysis in R software. Over-representative GO terms in up-regulated or down-regulated genes in three comparisons (3 h AF vs 10 h AF, 3 h AF vs 24 h AF and 10 h AF vs 24 h AF) were identified by Fisher's exact test in combination with the 'weight' algorithm, using a minimum p-value cut-off of 0.01.

Real-Time qPCR analysis

To analyze the transcriptional expression of DEG, RT-qPCR was performed. Synthesize of cDNA as template was performed by PrimeScript™ RT reagent Kit with gDNA Eraser (TaKaRa, Shiga, Japan) using total RNA 50 ng in 20 µl reaction mixture according to the

manufacturer's protocol. Specific primers for each contig were designed using Primer-BLAST (Table 1). The reaction mixture contained 5 µL SYBR Premix Ex Taq II (TaKaRa), 0.4 µl specific primers (10 µM), and 1 µl cDNA template in a total of 10 µl. qPCR was performed using Eco Real-Time PCR system (Illumina, San Diego, CA, USA). After 95 °C for 30 s, the cycling parameters were 95 °C for 5 s, and 60 °C for 1 min and were performed for 40 cycles. The melting curve analysis was as follows: 95 °C for 15 s, 55 °C for 15 s, and 95 °C for 15 s. Transcript levels corresponding to the comp32408_c2_seq24.p1 and comp33109_c0_seq1.p1 genes (candidate mannuronan C5-epimerase) were compared with the transcript levels of the actin gene (actin; comp21090_c0_seq1.p1) (Table S1). The RT-qPCR was performed in triplicate using three RNA samples from each zygote at the ages of 3, 10, and 24 h. The differences in mean relative expression level between the developmental hours (3, 10, and 24 h) were examined by Tukey's multiple comparison test.

Identifying mannuronan C5-epimerase from *S. babingtonii* assembled contigs and molecular phylogenetic analysis

A reciprocal blast search against 24,486 proteins of the brown alga *Ectocarpus siliculosus* (http://bioinformatics.psb.ugent.be/orcae/overview/EctsiV2) was also conducted to identify genes for enzymes in the biosynthetic pathway of alginates using BLAST+ version 2.7.1 (ftp://ftp.ncbi.nlm.nih.gov/blast/executables/blast+/LATEST). To construct the MC5E phylogenetic tree, 36 sequences from *E. siliculosus* (https://bioinformatics.psb.ugent.be/orcae/overview/EctsiV2), one sequence from *Saccharina japonica* (Inoue et al. 2016), and seven sequences from assembled *S. babingtonii* contigs were gathered. Three bacterial AlgG sequences from *Azotobacter vinelandii* (uniprotkb: P70805), *Pseudomonas aeruginosa* (uniprotkb: Q51371), *and P. fluorescens* (uniprotkb: P59828) were added to the alignment file as an outgroup. Phylogenetic analysis of amino acid sequences of MC5E was carried out using web service NGphylogeny.fr (https://ngphylogeny.fr/) (Lemoine et

al. 2019). The sequences were aligned using MAFFT with the iterative refinement method and the scoring matrix BLOSUM62 (Katoh et al. 2002). Ambiguously aligned non-informative regions were removed with BMGE (Criscuolo and Gribaldo 2010). Twenty sequences were removed due to insufficient sequence length or having identical sequences to the others from the phylogenetic analysis. The model test for maximum likelihood (ML) method was carried out by SMS (Lefort et al. 2017), and phylogenetic analysis was performed using PhyML (Guindon et al. 2010). The best-fit model was BLOSUM62 + G + I + F based on Akaike information criteria (AIC). Bootstrap values (Felsenstein 1985) were obtained from the analyses of 100 pseudoreplicates with Booster (Lemoine et al. 2018). Domain searches against the InterPro server (https://www.ebi.ac.uk/interpro/) were also carried out.

Results

Immediately after fertilization, the *Silvetia* zygotes showed a spherical shape (Plate 2a). Rhizoid formation was initiated at 12 h after fertilization (AF) (Plate 2b). The first and second cytokinesis occurred at 20 h and 24 h AF, respectively (Plate 2c, d). I observed the ultrastructure and occurrence of alginate in cell walls of the zygotes at 12 h and 24 h AF. Three cell areas were observed in terms of cell wall structures (illustration on the left in Plate 1): (i) the thallus cell wall (TCW), (ii) the rhizoid-flank cell wall (RFCW), and (iii) the rhizoid-tip cell wall (RTCW).

At 12 h AF, the TCW had an electron-opaque structure with parallel-oriented fibrils (Plate 3a). In the RFCW, three layers with different contrasts, dark-light-dark, were visible (Plate 3b). The RTCW was less stained and had irregularly oriented fibrils (Plate 3c). The cell wall structure in the TCW at 24 h AF (Plate 4a) was dependent on the cutting angle of sections relative to the plasma membrane. Obliquely cut sections in which the lipid bilayer of plasma membrane was unclear revealed three distinct layers with different opacities and fiber orientations (Plate 4b). The cell wall was roughly divided into the inner layer (IL) having a rough fibrous net with porous, middle layer (ML) showing the fine fibrous net, and outer layer (OL) with a rough fibrous

net. The width of the layers was calculated. Each layer was almost the same width representing 32, 37, and 31% of the whole cell wall in IL, ML, and OL, respectively. The percentage showed the mean value from the result by triplicated counting on each of three zygotes (Table 2). However, it was difficult to define each layer on a perpendicular section of the cell wall to the plasma membrane, because the difference of orientation among the three layers was hard to be clarified by narrow fiber spacing and high electron-opacity (Plate 4c), as in 12 hour-old zygotes (Plate 3a). In the RFCW, the outer and middle layers were hardly observed (Plate 4d, e). First, the outer layer was not apparent at the thallus pole-facing side of the rhizoid tip (the site indicated by a double arrowhead in Plate 4a) and the middle layer disappeared toward the tip proper. The remaining inner layer became thicker closer to the rhizoid tip (Plate 4f). While well-structured in other regions, the distribution of fibrils was irregular or wavy closer to the tip. The mucilage material covered the outside of the rhizoid. The amorphous mucilaginous layer was not included in the numbering of the cell wall layer in this study.

To locate alginate epitopes in the different cell wall regions, immunoelectron microscopy using anti-alginate antibodies was used at 24 h AF (Plate 5). Localization of M-rich blocks with BAM6 antibody was evident in the inner half of the TCW, RFCW, and RTCW (Plate 5a, b, c). Fewer M-rich blocks were recognized in the RFCW (Plate 5b, Table 3), compared to the other two regions. With BAM7-conjugated gold particles, MG-alginates appeared more uniformly and abundantly distributed in the cell wall than M-rich blocks (Plate 5d, e, f). The mean value of the number of gold particles using BAM7 was shown in Table 3. The mean value of gold particle number with BAM7 was higher as RTCW>RFCW>TCW. However, Tukey's multiple comparison tests showed no significant difference in the number of gold particles with BAM6 and BAM7 among TCW, RFCW, and RTCW.

To make comparisons across different antibodies, the width of the cell wall between the plasma membrane and the edge of the cell wall was divided into ten segments. Distributional patterns of gold particles in the cell wall over the relative distance (0-1) were estimated by the

function fitted at 10 segments (GFT, $P < 0.01$ for all cases) (Plate 6). The density of particles binding to BAM6 peaked at a distance of approximately 0.3 in TCW, and it was flattened through 0.7 while decreasing. And it dropped after 0.7 toward 1.0. The high density segments were at 0.1 to 0.7, which was consistent with the region of the half of the inner layer and whole a middle layer. The high density distribution with BAM7 in TCW was with a range of 0 to 0.7, which was flatter than it with BAM6 in TCW. These results showed that the gold particles binding to BAM7 were distributed closer to the plasma membrane compared with BAM6 in TCW (beta regression, $Z=-6.193$, $P<0.001$). In RTCW, the density of particles binding to BAM6 peaked at a distance of approximately 0.2, and became flatter between 0.5 to 0.9 after a peak. Compared with BAM6 in TCW, the high density segments were shifted closer to plasma membrane (beta regression, $Z=-6.726$, $P<0.001$). In the density distributions of gold particle with BAM7 in RTCW was flat with a range of 0 to 1.0, and a plateau was observed from 0.1 to 0.4. There was no significant difference in the distribution of density of gold particle between BAM7 in RTCW and BAM7 in TCW, or BAM6 in RTCW.

To understand the genes involved in early development of the zygotes, transcriptomic analysis was performed at three different developmental stages (3 h AF: time of increased wall thickness, 10 h AF: time of initiation of rhizoid germination, and 24 h AF: time when the second cytokinesis finished and the rhizoid elongated) under the current culture condition (Plate 7). The timeline might change depending on the cultural condition, so the event of characteristic morphological change in the early development of fucoid zygotes was treated in this study. The short read data are summarized in Table 4. *De novo* assembly produced 97,825 contigs. Filtering with CD-HIT-EST reduced the size of the assembly to 78,268 contigs, and the 27,622 longest ORF contigs were detected by TransDecoder. A total of 11,087 contigs (40%) were annotated by BLASTX with the UniProt database, and 61-63% of reads were mapped to the 25,890 longest ORF contigs. Then, differentially expressed genes (DEGs) were detected for 107 contigs in 3 h AF vs. 10 h AF, 47 contigs in 3 h AF vs. 24 h AF, 125 contigs in 10 h AF vs. 24 h AF of the 25,890

contigs (Plate7; Tables 5-7). GO enrichment analysis indicates that sulfotransferase activity (GO:0008146) and extracellular region (GO:0005576) were significant in the regulated genes at 24 h AF (Table 8).

Mannuronan C-5 epimerase (MC5E) is involved in the conversion of mannuronic acid into its C5-epimer, guluronic acid in alginate biosynthesis. Reciprocal best-hit blast against *E. siliculosus* reference proteins recovered 39.6% (9,699) proteins in the group of longest ORFs in *S. babingtonii*. The BLAST search indicated that seven MC5Es, were conserved in *S. babingtonii*. The expression patterns of the enzymes' genes are summarized in Plate 8. Five MC5Es (comp12459_c0_seq1.p1, comp21318_c0_seq3.p1, comp25876_c0_seq1.p1, comp32408_c2_seq24.p1 and comp32951_c0_seq4.p1) were upregulated as the developmental stage proceeded, and one (comp33109_c0_seq1.p1) was slightly suppressed in 24 h AF (Plate 8).

To clarify the molecular function, domain search and phylogenetic analysis of MC5Es were performed. The catalytic MC5E domain and the signal peptide region were detected in four contigs (comp21318_c0_seq3.p1, comp32408_c2_seq24.p1, comp33109_c0_seq1.p1, comp25876_c0_seq1.p1) (Plate 9). The phylogenetic tree of MC5Es shows five clades supported with high to moderate value (42-100%) and seven MC5Es homologs of *S. babingtonii* were scattered within these five clades (Plate 10). Two MC5E homologs (comp32408_c2_seq24.p1 and comp33109_c0_seq1.p1) were detected as DEGs in the different developmental stages of the zygotes. RT-qPCR was carried out on two contigs (comp32408_c2_seq24.p1 and comp33109_c0_seq1.p1) (Plate 11). The expression level of comp32408_c2_seq24.p1 stayed lower until 10 h AF and increased eight times at 24 h AF. Comp33109_c0_seq1.p1 expression level declined to one-fifth at 10 h AF from 3 h AF.

Discussion

Ultrastructural comparisons of cell walls of the rhizoid and thallus parts of fucoid zygotes have been reported (Novotny and Forman 1975; Vreugdenhil et al. 1976; Callow et al.

1978; Bisgrove and Kropf 2001). Previous studies showed that the cell wall of the thallus region consists of two layers, while the rhizoid cell wall had one or two layers (Novotny and Forman 1975; Vreugdenhil et al. 1976; Callow et al. 1978; Bisgrove and Kropf 2001). I observed three layers in the TCW in *S. babingtonii* zygotes at 24 h AF. Occasionally, it was difficult to define the number of layers in the TCW, even in the same zygote. The cutting angle of the section affected the ultrastructural appearance of the cell wall structure (Terauchi et al. 2016). To avoid this, I prepared consecutive serial sections in each zygote and observed the cell wall structure. Bisgrove and Kropf (2001) mentioned a porous area adjacent to the plasma membrane within the thicker inner layer using chemical fixation. Although they did not count it as another layer, I considered that the porous area corresponds to the inner layer observed in the present study using rapid-freezing and freeze substitution (Plate 4b).

Regarding the rhizoid cell wall, I observed that the two outer and middle layers from the cell wall of the thallus were not apparent along the rhizoid flank (RFCW), and only the inner layer surrounded the rhizoid tip. The inner layer became gradually thicker, and the cell wall fibrils showed an irregular orientation close to the rhizoid tip. This observation is the first to explain how cell wall structure changes during rhizoid elongation in fucoid zygotes at the ultrastructural level. I considered that the cleavage of the two outer layers occurred during rhizoid elongation, not during its initiation. In the RTCW of the zygote at 12 h AF, namely, the stage of initiation of rhizoid elongation, the cell wall layer could not be clearly seen (Plate 3c); however, the three layers were observed in the RFCW (Plate 3b). At the beginning of tip growth, the three layers were present; and the outer two layers might break due to the extension of the cell during further tip outgrowth. On the other hand, the inner layer could be extended by the addition of new cell wall materials and remodeling. Ultrastructural observation in the pollen tube growth of *Lycopersicum peruvianum* and *Lilium longiflorum* showed that a part of the cell wall is broken on the germination (Cresti et al. 1977; Miki-Hirosige and Nakamura 1982). During germination, new cell wall subdivided into pectic outer layer and callosic inner layer is synthesized between

the intine and plasma membrane. The apical dome of pollen tube is always covered with the callosic inner layer. The outer pectic layer breaks in lily pollen germination with the intine. Newly synthesized polysaccharide is important for the tip growth in this case. In the zygotes of *S. babingtonii*, the appearance timing of three layers is not known, however, there is the possibility that a newly synthesized inner cell wall layer before rhizoid formation would be essential for its elongation as in the pollen tube growth of lily.

While, in the growing root hair of *Arabidopsis thaliana,* breaks of cell wall has not been observed. The growing root hair cell wall shows a single layer, and the mature one is surrounded by two layers with different textures and orientation of microfilaments (MFs) (Akkerman et al. 2012). A similar pattern has been observed in *Equisetum hyemale* (Emons and Wolters-Arts 1983). Expansin, a protein that promotes cell wall loosening without degradation of cell wall polymers, is involved in root hair initiation and elongation in many land plants (Cho and Cosgrove 2002; Cosgrove 2015). The apical dome of the pollen tube consists of an outer layer with pectin and a translucent inner layer with callose and cellulose in *A. thaliana* (Dardelle et al. 2010; Chebli et al. 2012) and *Nicotiana tabacum* (Geitmann et al. 1995; Ferguson et al. 1998). In the apical dome of the outer layer, highly esterified pectin deposits are created by exocytosis, while localization of low-esterified pectin increases from the transition area between the apex and axial region in *A. thaliana* (Chebli et al. 2012). De-esterified pectin is produced by pectin methyl esterase from methyl esterified pectin, and the degree and pattern of methyl-esterification of pectin influence the elasticity of the gel (Willats et al. 2001b). In the transition area, remodeling of the cell wall by accumulation of callose and cellulose with de-esterification of pectin occurs, and this affects the aperture of the pollen tube and promotes tip-growth in *A. thaliana* (Chebli et al. 2012).

I had expected that elongation of the rhizoid cell wall would be caused by secretion of new cell wall material and remodeling of existing components in the zygotes of *S. babingtonii*. I focused on the spatial distribution of alginate because it is the main polysaccharide of the brown algal cell wall and affects its mechanical properties. Therefore, immunoelectron microscopy using

antibodies against the different epitopes, BAM6 and BAM7, was conducted against the TCW and the RTCW. There was no significant difference in the distribution of gold particles of BAM7 between the thallus and rhizoid regions. The high density of the gold particle with BAM6 was observed close to the plasma membrane in the RTCW, which differs from the situation in the TCW (Plate 6). Alginate synthesis pathways in brown algae are not fully understood. However, it is considered that alginate is initially synthesized as a polymer of mannuronic acid (mannuronan) by alginate synthase, and a part of the mannuronic acid (M) is converted into guluronic acid (G) reside by mannuronan C5-epimerases (MC5Es) (Michel et al. 2010b). In other words, the M residue-rich area would be considered to be the relatively newly synthesized alginate. However, this study showed that the distribution of gold particles binding to BAM7 was wider than BAM6 at the sites adjacent to the plasma membrane at TCW and RTCW. From this result, it was expected that parts of M in mannuronan would be rapidly converted to G after polymerization. In this study, the outer layer was labeled as neither BAM6 nor BAM7. In *E. siliculosus*, the alginate lyase conjugated with gold particles binds to the entire cell wall but labeling with an anti-alginate antibody is limited to the inner two layers of the three (Terauchi et al. 2016). Therefore, it was considered that the outer layer of *S. babingtonii* zygotes contained alginate with different types of MG blocks, which are recognized by BAM6 and BAM7. I also performed immunoelectron microscopy using the anti-alginates BAM8 to BAM11 antibodies which recognize G-rich alginate block compared to BAM6 and BAM7 (Torode et al. 2016), however they were unable to label the outer layer of the cell wall in *S. babingtonii* zygotes.

Transcriptomic analysis was performed in 3-, 10-, and 24-hour-old zygotes of *S. babingtonii* and focused on gene expression related to alginate modification. The enrichment of term "sulfotransferase activity" (GO:0008146) and "extracellular region" (GO:0005576) indicate some cell wall components with sulfated fucan might be actively modified during rhizoidal growth. By constructing a *de novo* transcriptome assembly, I found homologous genes required for alginate modification (Michel et al. 2010b) (Table 9). Previous genomic or transcriptomic

studies revealed that there were 31 MC5E genes in *Ectocarpus* (Michel et al. 2010b), 105 or 143 MC5E genes in *S. japonica* (Ye et al. 2015; Zhang et al. 2021a), and 38 genes in *Sargassum thunbergii* (Liu et al. 2014). In this study, 19 MC5E genes were identified by BLAST against the UniProt database, and the number was smaller than that of other brown algae (Table 9). Because our RNA-seq data are only from the early developmental stages (3-24 h AF), some MC5E genes in *S. babingtonii* might not be expressed. Seven *S. babingtonii*'s MC5Es included a common MC5E domain, but each MC5E included a variety of domain structures similar to genes in *E. siliculosus* (Fischl et al. 2016). This protein domain diversity in the MC5Es family contributes to the regulation of alginate composition and remodeling in the cell wall. Within the data, two MC5E homologs (comp32408_c2_seq24.p1 and comp33109_c0_seq1.p1) showed significantly different gene expression during development of the zygotes. This is consistent with the different transcriptional patterns of MC5E genes related to developmental stage, thallus region, and different phases of an algal life cycle (Nyvall et al. 2003; Tonon et al. 2008; Fischl et al. 2016; Linardić et al. 2020). Some reports show that the transcripts required for rhizoid formation were synthesized prior to 5 h AF (Quatrano 1968; Kropf et al. 1989). From these findings, comp33109_c0_seq1.p1 may support rhizoid germination, while it is also possible that the gene may be related to the expansion of the cell wall and the formation of the multilayer before rhizoid formation. The expression level of comp32408_c2_seq24.p1 increased in 24 h AF, suggesting that the gene would involve cell wall remodeling for rhizoid elongation.

There are some reports showing cross-linking of polyphenol to alginate in the cell wall in brown algae (Salgado et al. 2009; Deniaud-Bouët et al. 2014). It is considered that phenol involves in the adhesion of the zygotes on the substratum and rigidity of the cell wall. Vanadium-dependent bromoperoxidase is a candidate to catalyze alginate-phenol complex. RNA-seq data in this study showed the 4 in 12 candidate vBPO genes were detected as DEG (Table 7). During early development of *F. vesiculosus* zygotes, vBPO activity increases gradually after fertilization (Lemesheva et al. 2020). These results matched this study data. It is expected that how the

alginate-phenol complex affects the property of the cell wall and involved in the morphogenesis becomes clear.

Chapter 2. Cell wall structure and gene expression during gametogenesis of *Saccharina japonica* (Laminariales, Phaeophyceae)

Introduction

Genera in the order Laminariales are major components of marine forests and have a great capacity to improve the coastal environment by fixing carbon dioxide, absorbing excess nitrogen, phosphate, and metals. Moreover, they provide habitats and spawning places for small crustaceans and fish. *Saccharina* and *Undaria* species are widely consumed as traditional foods, especially in Asian countries, and thus have high commercial value. During 2018, 11 and 2 million tons of *Saccharina japonica* and *Undaria pinnatifida* products, respectively, were generated worldwide (FAO 2020). Brown algae contain useful substances, such as alginate, sulfated fucan in the cell wall. Alginate and sulfated fucans are called marine polysaccharides, and these, along with carrageenan and agar in red algae, and are used in the cosmetics, food additive, and pharmaceutical industries. Species in the Laminariales are used as raw materials for marine polysaccharides.

The sporophyte generation of Laminariales is applied as industrial materials. Sauvageau (1915) discovered the life cycle of *Saccorhiza bulbosa*, a laminarialean plant. Generations typically and heteromorphic alternate between macroscopic sporophytes and microscopic gametophyte (Plate 12). Diploid sporophytes produce asexual reproductive cells called zoospores after meiosis (Toth 1976; Henry and Cole 1982a), whereas haploid gametophytes produce eggs and sperm (Henry and Cole 1982b; Motomura and Sakai 1988, Tatewaki et al. 1989). The properties of the cell wall at different developmental stages were examined in sporophytes. Seasonal ratios of mannuronic acid (M) and guluronic acid (G) in alginate, and developmental stages indicate the characteristics of the cell wall (McKee et al. 1992; Wu et al. 2014; Zhang et al. 2021a), in which M- and G-rich blocks cause flexibility or stiffness. The hard stipe of *Macrocystis pyrifera* contains G-rich alginate, whereas swaying blades consist of M-rich alginate

(McKee et al. 1992). Sulfated fucan in the Laminariales is a fucose polymer that contains sulfate groups (Wang et al. 2010). Sulfated fucans have different components of sulfate groups and constituent sugars depending on the developmental time and season (Zvyagintseva et al. 2003; Fletcher et al. 2017). For example, alginate and sulfated fucan account for 40% and ~ 5% of the dry weight of immature *S. japonica* sporophytes (Skriptsova et al. 2012). After maturation, these values are reduced to 20%, and increased to ~10%, respectively. In contrast to sporophytes, information about the cell wall structure and polysaccharide composition of laminarialean gametophytes has remained obscure.

The gametophytes of the laminarialean species have uniseriate filaments. Appropriate temperatures and light intensity for the growth and maturation of laminarialean gametophytes have been examined (Lüning and Neushul 1978; Lüning 1980; Izquierdo et al. 2002). Lüning and Dring (1972, 1975) found that the maturation of female *Laminaria saccharina* (as *Saccharina latissima*) gametophytes is actively induced under blue light (430–450 nm) independently of photosynthesis and growth, and the gametophytes continue vegetative growth under red light. They also found that gametogenesis in the female *L. saccharina* gametophytes could be induced between 8 °C–16 °C, and that it is not affected by the length of the day. In addition, the concentration of iron chelated as EDTA regulates the maturation of several laminarialean plant gametophytes (Motomura and Sakai 1981, 1984; Suzuki et al. 1994; Lewis et al. 2013). Iron deficiency maintains immature gametophytes, whereas iron supplementation induces gametogenesis.

The genes involved in gametogenesis have been evaluated by transcriptomic analysis in *S. latissima* under white light, instead of red light (Pearson et al. 2019). During gametogenesis in the Laminariales, male gametophytes produce antheridia that form sperm, and female gametophytes form oogonia that produce eggs. The expression of genes involved in ribosome biosynthesis, transcription, translation, nutrient acquisition, and pyruvate biosynthesis, all of which are related to gluconeogenesis, is upregulated in male and female gametophytes as an early

response to gametogenesis in *S. latissima* (Pearson et al. 2019). The expression of genes involved in reactive oxygen signaling *via* NADPH oxidase is increased in female gametophytes, whereas genes involved in mitotic cell proliferation, spermatogenesis, and flagella are upregulated in male gametophytes. The gene expression of galactose-3-O-sulfotransferases is also upregulated. it might be associated with the accumulation of sulfated polysaccharides in the cap structure of antheridia from which the sperm is released (Henry and Cole 1982b; Maier 1982; Motomura and Sakai 1984). The transcriptome of gametogenesis has been analyzed after shifting *S. japonica* from seawater containing $NaNO_3$ and KH_2PO_4 to Provasoli enriched seawater medium (PES) (Zhang et al. 2021b). The genes involved in sperm motility, gamete recognition, pheromone biosynthesis, and signaling were differentially expressed in male and female gametophytes during maturation. Some genes related to the pathway of alginate biosynthesis were stable during gametogenesis in both male and female gametophytes. The expression of sulfated fucan-and cellulose-related genes was higher in mature female, than mature male gametophytes.

The whole genome of *S. japonica* has been published (Ye et al. 2015), and transcriptomic data from different culture conditions, developmental stages, and generations (gametophytes and sporophytes) have accumulated (Shao et al. 2019; Zhang et al. 2020; Zhang et al. 2021b). These data have shown that the expression of various genes associated with cell wall metabolism differs depending on the state of materials. A remarkable morphological change during the generation of gametophytes is the formation of oogonia or antheridia that protrude from the lateral sides of filament cells. To form reproductive organs and release gametes, cell wall modification *via* biosynthesis and degradation might be prerequisite. Therefore, I considered that gametogenesis under different conditions could be compared with previous findings of cell wall polysaccharide metabolism and perhaps new knowledge could be gained in this study.

In this chapter, the cell wall structure and polysaccharide metabolism were examined during gametogenesis induced in *S. japonica* by changing the iron concentration in the medium, to elucidate the relationship between morphological changes in reproductive organs and cell wall

structure using electron microscopy and transcriptomic analyses. In addition, fluctuation of gene expression relating to iron uptake and storage, sex-biased genes were searched. Because these genes might be involved in gametogenesis more or less.

Materials and methods

Culture

The mature sporophyte of *S. japonica* (J.E. Areschoug) C. E. Lane, C. Mayes, Druehl, and G. W. Saunders was collected at Charatsunai, Muroran, Hokkaido, Japan (42°3′N, 140°99′E) in November 2014. The mature thallus was washed with sterilized seawater and cut into small pieces. After wiping with a paper towel to remove small organisms on the surface, small pieces of thallus were placed on the glass dishes. The dishes were kept in the dark in a refrigerator (4 °C). The next day, pre-cooled sterilized seawater was poured into the dishes to induce the release of zoospores. The zoospores were isolated using a Pasteur pipette with a lengthened tip and transferred into an iron deficient ASP_{12} NTA medium to keep the gametophytes immature (Table 10, Provasoli 1963; Motomura and Sakai 1981, 1984). An antibiotic mixture was used to prepare axenic gametophytes (Tatewaki et al. 1989; Kawai et al. 2005). Successful sterilization was confirmed on 0.3% agarose in half-strength Marine Broth (Defco Laboratories, Detroit, MI, USA). Male and female gametophytes were cultured separately and kept immature under Fe deficiency at 10 °C and long-day conditions (14 h light:10 h dark) using cool-white fluorescent light (20–40 μmol photons m^{-2} s^{-1}). Gametogenesis was induced by the exchange of medium containing 2 mg L^{-1} iron as ferrous ammonium sulfate (1:1 molar solution with EDTA, Provasoli 1968) and cultured under the same temperature and light conditions as before.

RNA-seq and differential expression analysis

Total RNA was extracted from male and female gametophytes (fresh weight 30–50 mg) under iron deficiency (M_0 and F_0) and 3 and 6 days after iron repletion (M_3, M_6, F_3,

and F_6) using the RNeasy Plant Mini Kit (Qiagen, Hilden, Germany). Total RNA samples with OD260/280 > 2.0 and OD260/230 > 2.0 were used for cDNA library construction. Library construction, sequencing with Illumina Hiseq 4000 (150 bp paired-ends; Illumina, San Diego, CA, USA), and generation of clean reads by filtering raw reads were performed by Filgen Inc. (Nagoya, Aichi, Japan). The data volume was 4 GB per sample. The fastq files of the raw sequence reads were uploaded to DDBJ Sequence Read Archive (accession number DRA013021). Clean reads were mapped to the coding sequences (CDSs) of *S. japonica* (Ye et al. 2015) by TopHat2 (Kim et al. 2013) with default settings. Mapped reads were counted, and fragments per kilobase of transcript per million fragments mapped (FPKM) values were obtained using HTSeq (Anders et al. 2015) FPKM values were normalized with quantile methods using Agilent GeneSpring (Agilent Technologies, CA, USA). MA plots were drawn using ggpubr version 0.2.5 (https://github.com/kassambara/ggpubr) in R version 3.6.2. Venn diagrams for upregulated or downregulated genes in male or female gametophytes under different conditions were generated using jvenn (Bardou et al. 2014). Differentially expressed genes (DEGs) in M_3, M_6, F_3, and F_6 relative to M_0 or F_0 were determined. The CDSs were re-annotated using Blast2GO (BioBam Bioinformatics S.L., Valencia, Spain). A homology search was performed using the NCBI refseq database (https://www.ncbi.nlm.nih.gov/refseq/). The genes related to polysaccharides synthesis were referred in *Ectocarpus* genome (Michel et al. 2010b). Putative genes encoding glycosyltransferase (GT) and glycoside hydrolase (GH) were searched from CAZy database (http://www.cazy.org/). Domain and motif searches were performed using InterProScan (Jones et al. 2014) (https://www.ebi.ac.uk/interpro/). The results were integrated and gene ontology (GO) term annotations were assigned to the predicted gene models of *S. japonica*. The BioConductor package topGO version 2.38.1 (Alexa et al. 2006) was used for GO enrichment analysis in R software. Over-represented GO terms in upregulated or downregulated genes were identified by Fisher's exact test in combination with the 'weight' algorithm using a minimum p-value cut-off of 0.01. The heatmaps of the genes for biosynthetic pathway in alginates, sulfated

fucan, cellulose and laminaran were drawn using gplots (version 3. 1. 1) package on R (version 3. 6. 2). The expression level was based on the normalized FPKM and the genes which showed low expression (FPKM<1) at all condition were removed from the lists.

Preparation of the samples for electron microscopy and immunoelectron microscopy

Female and male gametophytes under iron deficiency and after 6 days of iron addition were fixed by rapid freezing and freeze substitution to prepare for TEM observation (Nagasato and Motomura 2002b). A gel support film (ATTO, Tokyo, Japan) with settled gametophytes was cut into a triangle of less than 1 cm. All samples were rapidly frozen by immersing in liquid propane (prepared by cooling with liquid nitrogen) and immediately transferred into liquid nitrogen. The samples were then placed in cryotubes containing acetone and 2% osmium tetroxide precooled to –180 °C and stored at –85 °C for 2 days. Subsequently, the temperature of the samples was allowed to rise gradually by placing them at –20 °C for 2 h, 4 °C for 2 h, and room temperature for 30 min. The samples were washed with acetone several times and infiltrated in low-viscosity Spurr's epoxy resin (Polysciences, Warrington, USA) to 10% every 12 h, and in 100% resin for 2 days. Polymerization was performed overnight at 60 °C on aluminum foil dishes. Serial sections were cut with a diamond knife on an ULTRACUT ultramicrotome (Reichert-Jung, Vienna, Austria) and mounted on formvar-coated slot grids. The sections were stained with an EM stainer (Nisshin EM, Tokyo, Japan) and lead citrate (Reynolds 1963). Observations were carried out using a JEM-1011 electron microscope (JEOL, Tokyo, Japan).

Localization of sulfated fucan was investigated using BAM2 antibody against specificity to sulfated fucan (Torode et al. 2015, 2016) using male gametophytes at 6 days after iron supplementation. Sections on the nickel grids were treated with 5% H_2O_2 for 5 min at room temperature to enhance accessibility of antibody to the antigen by etching the resin surface, then transferred to blocking solution (2.5% skimmed milk, 5% normal goat serum, 0.05% NaN_3 in PBS; 137 mM NaCl, 2.7 mM KCl, 4.9 mM Na_2HPO_4, 1.5 mM KH_2PO_4, pH7.4) for 30 min at

37 °C. The grids were incubated with the primary antibodies (BAM2) diluted 1:5 with PBS for 1 hour at 37 °C. After washing with PBS three times, the grids were floated on 10 µl drops of a goat anti-rat IgG (whole molecule) conjugated with 10 nm colloidal gold particles (Sigma, St. Louis, Missouri, USA) diluted 1:20 with blocking solution. The grids were washed with PBS and distilled water, and sections on the grids were dyed with EM stainer as described above.

Results and discussion

Morphological observation during maturation

Morphological changes were observed after male and female gametophytes cultivated in iron-deficient ASP_{12} NTA were transferred into ASP_{12} NTA containing 2 mg L^{-1} Fe. Male and female gametophytes showed uniseriate filaments (Plate 13). Compared to female gametophytes, male gametophytes (Plate 13a–c) presented thinner filaments (Plate 13d–f). Male gametophytes did not show distinct morphological changes at 3 days after transferring into the iron repletion medium (Plate 13a, b). At 6 days, protrusions to form antheridia were observed from the lateral side of the filaments (Plate 13c). In female gametophytes, a lateral protrusion from the filaments was observed at 3 days after iron supplementation (Plate 13d, e). After 6 days, developing oogonia were observed (Plate 13f).

Morphological changes in ultrastructure were examined during maturation in cells rescued from iron deficiency. Organelles in male gametophytes under an iron deficiency (Plate 14a) and at 6 days after iron repletion (Plate 14b) were similarly positioned; the nucleus surrounded by Golgi bodies was located in the center of cells and chloroplasts were located beneath the plasma membrane. The shape of the antheridia was triangular (Plate 14c). The sperm possessed a chromatin-condensed nucleus and two flagella, and a space separated the cell wall from the sperm within the antheridium. The space at the top of the antheridium is called a cap structure, from which the sperm is released (Henry and Cole 1982b; Maier 1982; Motomura and Sakai 1984). The cell wall in the cap structure becomes looser compared with that in other regions

of antheridia. Two flagella elongate in the space between sperm body and cell wall. The cell wall of the vegetative cell was uniformly stained, fibers were regularly orientated under iron depletion (Plate 14d), and iron supplementation did not evoke any changes (Plate 14e). The thickness of the cell wall did not significantly differ after iron replacement. The positions of chloroplasts and nuclei were similar between female and male gametophytes regardless of iron limitation (Plate 15a) and supplementation (Plate 15b). The appearance of cell walls in filaments was similar between before and after iron supplementation (Plate 15c, d). Golgi bodies surrounding nuclei (Plate 15e, f) produced transparent vesicles in the cells after 6 days of iron supplementation (Plate 15f). This feature was also found by Motomura and Sakai (1984) in *Saccharina angustata*. The initial stage of oogenesis was indicated by protrusions from the lateral side of uniseriate filaments showed (Plate 15g).

I used brown algae monoclonal antibody 2 (BAM2) (specific to sulfated fucan) to confirm the location of sulfated polysaccharides within the cap structure by immunoelectron microscopy (Torode et al. 2015). The results showed positive staining not only of the cap structure, but also for the space between the plasma membrane and sperm (Plate 16a, b).

Transcriptome sequencing and the expression profiles

Detailed Illumina sequencing data are summarized in Table 11. In total, 17.1 Gb and 13.7 Gb high-quality paired-end reads were obtained from female and male gametophytes, respectively. Whereas 71.1–71.8% of female reads were mapped to the reference CDSs, only 27–27.6% of male reads were mapped. The difference in the mapping rate between the female and male gametophyte reads would be caused by gene models of the reference genome that were predicted from the transcriptomic data of the female gametophyte and sporophyte (Ye et al. 2015).

MA plots showed differentially expressed genes between M_3 or M_6 and M_0, and F_3 or F_6 and F_0 (Plate 17; Tables 12 and 13). There were 1,185 DEGs (723 upregulated genes and 462 downregulated genes) in M_3 vs. M_0, 2,233 (1286 upregulated genes and 947

downregulated genes) in M_6 vs. M_0, 701 (351 upregulated genes and 350 downregulated genes) in F_3 vs F_0 and 1117 (589 upregulated genes and 528 downregulated genes) in F_6 vs. F_0. Venn diagrams sorted upregulated or downregulated genes into seven categories (consensus DEGs in M_3 and M_6 vs M_0, F_3 and F_6 vs F_0; male consensus DEGs in M_3 and M_6; female consensus DEGs in F_3 and F_6; only in M_3; only in M_6; only in F_3; and only in F_6) (Plate 18). Enriched GO terms in each category are listed in Tables 14 and 15. Consensus DEGs included 26 upregulated genes (Plate 18a; Table 12) and 21 downregulated genes (Plate 18b; Table 13). Male consensus DEGs consisted of 585 upregulated genes and 280 downregulated genes. Female consensus DEGs consisted of 136 upregulated and 126 downregulated genes. GO enrichment analysis (biological process, molecular process, and cellular component) of upregulated genes revealed that “intraciliary transport particle B” and “cilium” were detected in consensus DEGs (Table 14). Among the down-regulated genes, the terms “iron ion transmembrane transport”, “cellular response to iron ion starvation”, and “carbohydrate catabolic process” were predominant in the consensus DEGs category (Table 15).

Polysaccharide metabolism

Genes associated with the biosynthesis and degradation pathways of polysaccharides in the brown alga *E. siliculosus* were predicted immediately after the whole genome was analyzed (Michel et al. 2010a, b). *E. siliculosus* possesses 41 GH and 88 GT genes, from 18 GH and 32 GT families, respectively (Michel et al. 2010b). *S. japonica* encodes 82 GH and 131 GT genes belonging to 17 GH and 31 GT families (Ye et al. 2015). In contrast, the land plant *Arabidopsis thaliana* has 730 GH/GT genes (Henrissat et al. 2001). *E. siliculosus* and *S. japonica* had a few GT and GH genes in the CAZy family compared with the land plant model *A. thaliana*.

The almost genes encoding enzymes involved in alginate biosynthesis, ortholog of *Pseudomonas aeruginosa*, was found in the *Ectocarpus* genome (Michel et al. 2010b). The following processes are predicted for the biosynthesis of alginate. Fructose 6-phosphate (Fru-6-

P) is converted into mannose-6-phosphate (Man-6-P) by mannose-6-phosphate isomerase (MPI). Phosphomannomutase (PMM) catalyzes conversion of Man-6-P into mannose-1-P (Man-1-P). Man-1-P is converted into GDP-mannose (GDP-Man) by GDP-mannose pyrophosphorylase (MPG). GDP-Man is oxidized as GDP-mannuronic acid (GDP-ManA) by GDP-mannose dehydrogenase (GMD). GDP-ManA is polymerized to form mannuronan by mannuroran synthase (MS). Homolog of mannuronan synthase (MS) with Alg8 in alginate-producing bacteria *P. aeruginosa* was not found in brown algae (Michel et al. 2010b). Instead, a homolog gene of GT2 family in the actinomycete, *Frankia* sp. is a candidate as MS in brown algae. *Frankia* sp. has alginate degrading enzymes, alginate lyase and has ortholog of GMD and Mannuronan C-5 epimerases (MC5Es) in *E. siliculosus*. These genes are located close to each other. Glycosyltransferase 2 family (GT2) colocalizes with these genes cluster, that is the reason why it candidates as the MS gene. MC5E catalyzes the conversion of mannuronic acid into its C5-epimer, guluronic acid. A heatmap shows gene expression associated with alginate synthesis before and after iron supplementation in male and female gametophytes (Plate 19). Table 16 shows the candidate genes for alginate biosynthesis of *S. japonica* detected herein and annotated using the NCBI database. Four mannose-6-phosphate isomerase (MPI) genes were detected, and the less SJ01610 was compared with the other three MPI candidate genes. Two phosphomannomutase (PMM) genes (Plate 19) and the SJ02279 gene were annotated as PMM/phosphoglucomutase (PGM). Phosphoglucomutase catalyzes the conversion of Glc-6-P into glucose-1-P (Glc-1-P) in the cellulose biosynthesis pathway. SJ02279 might have PMM and PGM activities in *S. japonica* (Chi et al. 2018; Zhang et al. 2018). One guanosine diphosphate (GDP)-mannose pyrophosphorylase (MPG) gene is expressed, and SJ15067 has MPI activity (Chi et al. 2018). Four genes that were predicted to be GDP-mannose dehydrogenase (GMD) were identified. SJ06834 gene in *S. japonica* is similar to the putative mannuronan synthase (MS) in *E. siliculosus*. Zhang et al. (2021b) indicated that the MPI, PMM, and GMD genes associated with the alginate biosynthesis pathway (Michel et al. 2010b) are upregulated during female gametogenesis. In this

study, genes involved in alginate biosynthesis until the point of the MC5E reaction were stably expressed without fluctuation during both male and female gametogenesis.

The genome of *S. japonica* includes 105 MC5E genes (Ye et al. 2015). Reanalyzed genomic and transcriptomic results have revealed 143 MC5E candidate genes in *S. japonica* (Zhang et al. 2021a). The gene possesses the "right-handed parallel beta-helix repeat-containing protein" domain. Fifty-two genes were identified in the present study. Seven MC5Es (SJ05198, SJ07250, SJ07254, SJ07257, SJ07285, SJ15955, and SJ19999) were downregulated in female consensus DEGs. Different MC5Es are expressed according to the season and development (Nyvall et al. 2003; Fischl et al. 2016; Inoue et al. 2016). The expression of MC5Es differs in *S. babingtonii* zygotes according to the developmental time points of rhizoid elongation (Chapter 1; Yonamine et al. 2021). The formation of oogonia was initiated by cells protruding from the lateral side of the uniseriate filament (Plate 13e, 15g) with partial stretching of the cell wall. The expression of MC5Es can be regulated to modify cell wall strength and form a relatively large oogonium. The MC5E genes are upregulated and downregulated during male and female gametogenesis in *S. japonica* (Zhang et al. 2021b). The genes detected herein differed from the upregulated MC5E genes in previous studies. Gametophyte growth conditions might vary, yielding different cell-wall properties.

Table 16 lists the candidate genes for sulfated fucan biosynthesis detected in *S. japonica* that were annotated using the NCBI database. According to Michel et al. (2010b), two pathways are involved in the production of GDP-fucose (GDP-Fuc) in *E. siliculosus*. One is the *de novo* pathway using GDP-mannose (GDP-Man) synthesized by the same pathway as in alginate (Plate 20). In the *de novo* pathway, GDP-Man is converted into GDP-4-keto-6-deoxymannose by GDP-mannose 4,6-dehydratase (GM46D). GDP-4-keto-6-deoxymannose is catalyzed to GDP-Fuc, which in turn is converted into GDP-4-keto-6-deoxygalactose by GDP-fucose synthase (GFS). Two GM46D and GFS genes were detected in the present study. The other pathway of GDP-Fuc production is the salvage pathway, in which monosaccharide fucose is converted into GDP-Fuc,

which is then converted by fucokinase/GDP-fucose pyrophosphorylase (FKGP) into fucose-1-phosphate (Fuc-1-P). One FKGP gene was also detected. Fucosyltransferase (FT) is required to add GDP-Fuc to fucan. Two FT genes were identified herein. Putative FT genes might belong to the GT10, 23, and 65 families (Michel et al. 2010b). Among the two FT genes detected herein, SJ01987 and SJ11160 respectively belong to the GT23 and GT10 families. Sulfotransferase (ST) is involved in the synthesis of sulfated fucan, but it has not yet been characterized. Here, 67 ST genes annotated as sulfotransferases were selected. I predicted that the synthesis of sulfated fucan would become more active as gametogenesis progressed because immunoelectron microscopy revealed sulfated fucan in the cap structure of the antheridia (Plate 15). However, the expression of genes involved in sulfated fucan synthesis did not significantly change. Although the FT and ST genes were expressed at different levels, this could not explain the formation of cap structures containing sulfated fucan.

A cellulose biosynthesis pathway in *E. siliculosus* has been predicted as follows (Michel et al. 2010b): Glucose-6-phosphate isomerase (GPI) converts fructose 6-phosphate (Fru-6-P) into glucose-6-phosphate (Glc-6-P), which PMG converts into glucose-1-P (Glc-1-P) that is converted into UDP-Glc by UDP-Glc pyrophosphorylase (UGP). Table 16 lists the candidate genes for cellulose biosynthesis of *S. japonica* detected herein and annotated by the NCBI database. Two GPI, four PGM, and two UGP genes were detected (Plate 21). SJ18341 was annotated as PGM; however, this gene is considered to possess UGP activity (Chi et al. 2016). Cellulose synthase (CESA) is involved in the synthesis of cellulose from UDP-Glc. Among 11 CESA genes identified in the present study, SJ01458, SJ01459, and SJ20814 were stable under all experimental conditions. However, the expression of other genes was relatively low.

Other sugar metabolism

Laminaran is a β-1,3-glucan that is stored as a photosynthetic product in brown algae. In the laminaran synthesis pathway, UDP-Glc is predicted to transfer into the β-1,3-glucan

acceptor by β-1,3-glucan synthase (GS). β-1,3-glucan also builds callose in land plants. Callose synthase belongs to the glycosyltransferase 48 family (GT48) (Michel et al. 2010a). Here, seven callose synthase genes were detected. The candidate genes for *S. japonica* laminaran detected herein are listed in Table 16 and were annotated using the NCBI database. Laminaran has branched β-1,3-glucan (Plate 22). A putative β-1,6-transglucosylase (KRE6-like) gene was found that adds UDP-Glc into laminaran as β-1,6-branched glucan. The expression of genes associated with laminaran synthesis did not significantly differ between males and females under all experimental conditions. In contrast, upregulation of putative degrading enzymes of β-1,3-glucanase, SJ10147 with GH81, C-terminal domain, and SJ18897 with GH16_laminarinase_like domain was detected in male consensus DEGs (Table 12, Michel et al. 2010a). Laminaran accumulates in vacuoles in *Scytosiphon lomentaria* (Nagasato and Motomura 2002a). Ultrastructural findings showed that the volume of vacuoles decreased during gametogenesis in males (Plate 14c). Thus, storage products might be consumed to form sperm, diminishing the vacuole size.

Several genes were detected in the DEGs using the CAZy database. SJ21362 belonging to GT1 in male consensus DEGs and β-glucuronosyltransferase GlcAT14A (SJ07398; GT14) were upregulated in female consensus DEGs, whereas SJ09104 belonging to GT2 and β-1,4-N-acetylgalactosaminyltransferase bre-4-like (SJ14181; GT7) were downregulated in male consensus DEGs. However, the mechanism of action of these genes in the polysaccharide metabolic processes of *S. japonica* remain unclear.

Iron uptake and storage

In this study, regulation of maturation by iron deficiency and iron repletion to the gametophytes of *S. japonica* was performed as previously described (Motomura and Sakai 1981, 1984). However, it is an opened question how iron deficiency keeps the laminarialean gametophytes immature, and iron supplementation induces gametogenesis. Additionally, the

mechanism of iron uptake in brown algae is unclear. Iron is a trace essential metal for cellular activity in organisms; however, available iron is limited in the environment because of the formation of insoluble ferric hydroxide complexes in the presence of oxygen that limits the growth of organisms (Gledhill and Buck 2012). Therefore, organisms have evolved strategies to increase iron uptake from the external environment. In land plants, two basic strategies for iron uptake are known (Kobayashi et al. 2019; Zhang et al. 2019). Non-graminaceous monocots and dicots use a reductase-based scheme known as Strategy I (Robinson et al. 1999; Vert et al. 2002). Via this mechanism, ferric ions [Fe(III)] are reduced to ferrous ions [Fe(II)] and transported into the epidermal cells of roots via transporters on the plasma membrane. In graminaceous monocots, phytosiderophores are synthesized and secreted by the plants, which form phytosiderophore-Fe(III) complexes in the rhizosphere and are incorporated into the root cells through transporters (Curie et al. 2001; Murata et al. 2006; Kobayashi et al. 2019). This iron uptake is known as Strategy II. In the ocean, ferric iron bound to organic ligands is present as dissolved Fe, the form that can be taken up by the organisms (Gledhill and Buck 2012).

The response to iron limitation in diatom was examined by transcriptome analysis (Allen et al. 2008; Lommer et al. 2012). The predicted genes related to iron uptake and accumulation are highly expressed in the pennate diatom, *Phaeodactylum tricornutum*, and the centric diatoms *Thalasiosira oceanica*, and *T. pseudonana* cultured in iron-starved medium than in an iron-sufficient medium. It is indicated that there are two major iron uptake mechanisms in diatoms: reduction and non-reduction iron uptake. In iron uptake by reduction, Fe(III) bound to organic ligands is separated from the ligands as ferrous iron by ferrireductase (FRE). Ferrous iron is re-oxidized by ferroxidase (FET), and ferric iron is channeled across the plasma membrane by iron permease (FTR) into the cells (Shaked et al. 2005; Kustka et al. 2007). ISIPs (iron starvation induced proteins) involve in incorporation and accumulation of iron are found in the iron limited medium. ISIP1 is found in *P. tricornutum* and is involved in the incorporation of siderophore-iron complexes by endocytosis (Kazamia et al. 2018; Coale et al. 2019). ISIP2, grouped with

phytotransferrin, binds to ferric ions via carbonate ions to incorporate them by endocytosis (Baker et al. 2003; Morrissey et al. 2015; McQuaid et al. 2018); it has been identified in *P. tricornutum* and *T. pseudonana*. ISIP1 and ISIP2 relate to non-reduction iron uptake. While ISIP3 could involve in iron storage because it possesses domain of unknown function 305 (DUF305) that belongs to the ferritin superfamily (Behnke and LaRoche 2020). Ferritin, a protein that forms large protein cages with a cavity coupling oxidized iron, is used to store iron in the cytosol and chloroplasts (Liu and Theil 2005; Marchetti et al. 2009). The captured iron is reversibly released from the cavity via reduction (Liu and Theil 2005). In *P. tricornutum* and *T. pseudonana*, ISIP3 was upregulated under iron-limited conditions.

Like in diatom, it was expected that expression of the genes involved in iron uptake and accumulation would be fluctuated by iron concentration of medium in *S. japonica*. As expected, plasma membrane iron permeases (SJ01641 in consensus DEGs, SJ01662 in male consensus DEGs) containing the "iron permease FTR1 family" domain and seven transmembrane domains were downregulated after iron repletion. Diatom FTR is suggested to transport Fe(III) into cells, that is the mechanism highly homologous to a ferrous iron uptake transporter in *Escherichia coli* (Große et al. 2006; Kustka et al. 2007). Although candidates for reductase and oxidase before transport via FTR in *S. japonica* were not found in the DEGs, it was thought that SJ01641 and SJ01662 could take up iron reductively. Putative iron permease (SJ07047) is a homolog of low iron-inducible periplasmic protein (FEA1; Ec-05_005150) in *E. siliculosus* (Cock et al. 2010). SJ07047 possesses one transmembrane domain and two ISIP2 domains; therefore, it is predicted that this gene could facilitate the incorporation of ferric ions into the cells by endocytosis, as in diatoms (Morrissey et al. 2015). The results of this study indicate the possibility that *S. japonica* could use reduction and non-reducton iron uptake mechanisms similar to diatoms. Iron starvation-induced protein (SJ13085), a homolog of Ec-05_001700, has one transmembrane domain and a signal peptide. The protein encoded by SJ13085 was predicted to function like ferritin because it contains a DUF305 domain similar to ISIP3 of diatoms (Behnke

and LaRoche 2020; Gao et al. 2021).

Cytochrome *b*5 (SJ00644) with a cytochrome *b*5-like heme/steroid-binding domain was downregulated in an iron-replete medium (Table 13). The cytochrome *b*5 domain possesses heme localized in a hydrophobic pocket via two conserved histidine side chains and functions as an electron donor on the endoplasmic reticulum (ER) and mitochondrial outer membrane (Donaldson and Luster 1991; Schenkman and Jansson 2003). *P. tricornutum* cultured in iron-limited medium showed suppressed expression of cytochrome *b*5 gene compared to iron-replete medium (Allen et al. 2008). In contrast, this study showed that cytochrome *b*5 was downregulated by the addition of iron to the medium. The function and subcellular localization of cytochrome *b*5 in *S. japonica* are unknown, and it is unclear why gene expression was suppressed after iron depletion.

Nitrogen uptake

In this study, after iron repletion, in consensus DEGs, SJ18910, annotated as ammonium transporter 1 member 1-like, was upregulated (Table 12). The gene possesses an ammonium transporter domain and eight transmembrane domains. The enzyme is involved in acquiring ammonium ions from the environment in *A. thaliana* and the pennate diatom *Cylindrotheca fusiformis* (Gazzarrini et al. 1999; Hildebrand 2005). In the iron-deficient medium used in this study, the source of nitrogen is nitrate. Ammonium became the available nitrogen resource in the iron-replete medium because iron was added in the form of ferrous sulfate ammonium. In plants and algae, ammonium is more easily absorbed by the cells than nitrate (Hildebrand 2005), and it was considered that the ammonium transporter gene was upregulated in response to ammonium in this study (Table 12). Ammonium repression of nitrate/nitrite reductase is related to nitrate/nitrite assimilation in plants and algae (Gazzarrini et al. 1999; Song and Ward 2004). In this study, nitrite/nitrate transporter genes that acquire nitrite or nitrate ions from the environment were expressed constantly in male and female gametophytes before and after iron repletion.

SJ11978 with Rieske [2Fe-2S] domain, NirD-type, in consensus DEGs and nitrite reductase large subunit (SJ14266) in male consensus DEGs involved in the reduction of nitrite to ammonium (Allen et al. 2005; Frada et al. 2013) were downregulated (Table 13). Male and female gametophytes of *S. latissima* show upregulation of genes involved in nitrogen metabolism one day after transferring from red to white light (Pearson et al. 2019). In particular, the expression levels of nitrate/nitrite transporter (NRT) strongly increased. Accompanying N-accumulation, the genes for the stock of glutamate in the cytosol with fixation and release of ammonium, chloroplast ferredoxin-dependent glutamate synthase (Fd-GOGAT; GLT1), cytosolic NAD(P)H-dependent glutamate synthase (NADPH-GOGAT; gltD), and glutamate dehydrogenase (GDH) were upregulated. In this study, there was no evidence that amino acid synthesis was induced during gametogenesis.

Flagella formation and cell-to-cell recognition on fertilization

Laminarialean sperms show a short anterior flagellum with mastigonemes and a long posterior flagellum (Henry and Cole 1982b; Maier and Müller 1982, Motomura 1989). In addition, eggs possess vestigial and anchor flagella without mobility and abnormal structures showing an 8 + 2 arrangement of the axoneme in *S. angustata* (Motomura and Sakai 1988; Motomura 1990, 1991; Klochkova et al. 2019), different from the case of brown algal swarmers (O'Kelly and Floyd 1984; O'Kelly 1989). Pearson et al. (2019) identified 91 homologs from the *S. latissima* transcriptome of 93 genes in *Ectocarpus* genome data. Forty-five of these genes were expressed only in male gametophytes. Several genes including intraflagellar transport (IFT) and dynein assembly proteins were upregulated after 8 days of switching to white light (Pearson et al. 2019). Zhang et al. (2021b) showed that 69 genes were upregulated after maturation in males.

In this study, many GO terms-categorized genes related to flagella increased at 3 days after iron addition. In consensus DEGs, upregulation of five genes for the formation and maintenance of flagella was detected (Table 12). These were IFTs (SJ06468, SJ09523, SJ10052),

thought to carry the flagellar component (Rosenbaum and Witman 2002); a flagellar-associated protein (SJ06274) identified in flagellar proteomics of *Chlamydomonas reinhardtii* (Pazour et al. 2005); and sperm flagellar protein 2-like (SJ08387), a linker protein that interacts with dynein protein complex and cargo transport along microtubules in *Mus musculus* (Lehti et al. 2017). In male consensus DEGs, 53 flagellar-related genes were identified as upregulated genes (Table 12). The genes for flagella associated proteins (SJ06251, SJ11626, SJ11627), dynein related genes (SJ01154, SJ02564, SJ02566, SJ02567, SJ02568, SJ02680, SJ06649, SJ06892, SJ06893, SJ06894, SJ12100, SJ12472, SJ12967, SJ12968, SJ12969, SJ12971, SJ13884, SJ15145, SJ16419, SJ17941, SJ20996, SJ20997, SJ20998, SJ20999, SJ21069), IFT (SJ01025, SJ16352, SJ16353), kinesin like protein (SJ01517, SJ06264, SJ08465, SJ12145, SJ13811, SJ16076, SJ16627, SJ18326, SJ18328, SJ18578, SJ19904, SJ19937, SJ20994), and radial spoke protein (SJ05175, SJ11382) were upregulated (Table 12). The two genes, SJ17116, a homolog of tubular mastigoneme-related protein in *E. siliculosus* (Ec-04_001260) and a chrysophycean alga, *Ochromonas danica* (AB264616), and SJ01652, mastigoneme-like protein, were also upregulated. Both genes possess an EGF domain that is familiar with mastigonemes (Blackman et al. 2011). Mastigonemes are characteristic structures that bind to the surface of the anterior flagellum on the stramenopiles and are thought to contribute to the driving force in the movement of swarmers. Mastigoneme protein in *O. danica* (AB264616) is localized in the shaft region and is composed of three parts: a basal portion, a shaft, and a terminal (Bouck 1971, Yamagishi et al. 2009). In male consensus DEGs, connectin/titin putative gene (SJ12980), a high homolog of the connectin/titin isoform N2-B (CBJ30163) which possesses a large molecular mass of 1,822 kDa in *E. siliculosus*, was detected (Cock et al. 2010). Connectin/titin is found only in the isolated anterior flagellum of the brown alga *Colpomenia bullosa* and might be related to the connection between mastigoneme and flagellar axoneme (Fu et al. 2014). Creatine kinase (CK; SJ06630) was listed in the upregulated genes of the male consensus DEGs. Two CKs were found in the genome of *E. siliculosus* (Fu et al. 2014). Analysis of flagellar proteomics in *Colpomenia bullosa* indicated

that one is localized in flagella and the second has been predicted to localize in mitochondria (Fu et al. 2014). It has been shown in sea urchin sperm that creatine phosphate (PCr) is synthesized in mitochondria and supplied to the flagella tail (Tombes and Shapiro 1985; Wallimann et al. 2011). PCr can synthesize ATP that can be used as the power source for flagellar motility. CK generates PCr and ATP reversibly through the creatine shuttle (Kaldis et al. 1997; Wallimann et al. 2011). SJ06630 possesses one transmembrane domain, a signal peptide domain, and homology with Ec-14_00205 predicted in the mitochondria. Putative tubulin polyglutamylase genes with tubulin-tyrosine ligase/tubulin polyglutamylase domain were detected in male consensus DEGs (SJ15555, SJ18654, SJ19490). In *C. reinhardtii*, FAP234 (flagella-associated protein) is suggested to function as tubulin polyglutamylase, promoting glutamination at tubulin in flagella and polyglutamylation involved in flagella elongation, stability, and motility (Kubo and Oda 2019). In *S. japonica*, tubulin polyglutamylase genes would be involved in formation of functional flagella.

The involvement of glycoproteins in cell-to-cell recognition between male and female gametes has been suggested in studies on brown algae, *E. siliculosus,* and *Fucus serratus*. In the isogamous *E. siliculosus*, male gametes pretreated with GlcNAc residues or female gametes preincubated with a lectin, wheat germ agglutinin (specific for GlcNAc residues), were not fused with untreated opposite sex gametes (Schmid 1993; Schmid et al. 1994). In the oogamous *F. serratus*, sperm preincubated with polysaccharides containing mannosyl-residues and fucosyl-residues or eggs pretreated with the lectins, ConA (Concanavalin A; specific for GlcNAc) and FBP (fucose-binding protein; specific for fucose) inhibited fertilization (Bolwell et al. 1979; Catt et al. 1983). However, the involvement of glycoproteins in the cell-to-cell recognition of *S. japonica* is still unknown. Klochkova et al. (2019) indicated that unfertilized eggs were labeled with PNA-FITC (peanut agglutinin; specific for β-D-galactose, D-galactose-β-galactosamine). In this study, concanavalin A-like lectin/glucanase, subgroup (SJ17402, SJ17403), and lectin domain-containing protein (SJ09924) were detected in the male consensus DEGs (Table 12).

SJ09924 belongs to a galactose-binding-like domain superfamily. It is suggested that SJ09924 is involved in the cell-to-cell recognition of sperm and eggs in *S. japonica*.

Summary

Chapter 1 focused on the cell wall structure during rhizoid formation in fucoid *Silvetia babingtonii* zygotes. Changes in the cell wall structure during rhizoid elongation were assessed at the ultrastructural level, and alginates were immunolocalized using specific antibodies against M-rich and MG blocks. The cell wall structure was compared between the thallus and rhizoid cell wall in zygotes aged 12 hours before rhizoid formation, and in those aged 24 hours during rhizoid elongation. The cell walls of 12-hour-old zygotes comprised inner, middle, and outer layers with different fibril distributions. The thallus region of the 24-hour-old zygotes also had a cell wall comprising three layers, but only the inner layer was apparent near the rhizoid tip. This indicated that the outer two layers might break due to the reaching the limit of extension according to further outgrowth. Immunoelectron microscopy using antibodies revealed different alginate epitopes (M-rich and MG block) on the inner half of the cell wall, irrespective of the layer number in the thallus and rhizoid regions. The MG blocks covered a slightly wider area than the M-rich alginate blocks. The conversion of the M, into the G residue is achieved by various mannuronan C5-epimerases (MC5Es). Although details about intracellular mannuronan synthase localization and location where it synthesizes mannuronan remain unknown, alginate might be synthesized as poly-mannuronate form close to the plasma membrane before subsequent maturation, and MG-block generation in the wall. This could explain how cell wall structure changes during rhizoid elongation in fucoid zygotes, and the localization of alginate using specific antibodies at the ultrastructural level. Transcriptomes of 3-, 10-, and 24 hour-old zygotes were analyzed after fertilization to determine fluctuations in gene expression toward rhizoid formation and elongation. A transcriptome assembly was constructed *de novo* to identify homologous genes required for alginate synthesis and modification. One MC5E homolog was suppressed in a 10-hour-old zygote just before rhizoid elongation, and the expression of another was increased in a 24-hour-old zygote. These findings indicates that the downregulated MC5E homolog works for rhizoid germination, but the gene might be related to expansion of the cell wall and formation of a

multilayer before rhizoid formation. The upregulated MC5E might be involved in cell wall modification for rhizoid elongation.

In chapter 2, the focus was on the cell wall structure during gametogenesis in *S. japonica* induced by rescue from iron deficiency. The ultrastructure of the cell wall was examined in male and female gametophytes before and after iron supplementation. Antheridia formed in male gametophytes six days after iron supplementation. These antheridia were triangular, and the cell wall became looser at the tip of the cell. The space at the tip of an antheridium is called a cap structure from which the sperm is released. While cells protruded to form oogonia in female gametophytes, oogenesis was not completed under this experimental condition. Changes in the cell wall structure were not conspicuous in female gametophytes during oogenesis. Male gametophytes were assessed by immunoelectron microscopy to confirm the distribution of sulfated fucan on the cap structure of antheridia. Fluctuations in gene expression were examined in male and female gametophytes under iron deficiency followed by iron replacement at 3 and 6 days. Genes involved in mannuronan synthesis are stably expressed during gametogenesis in male and female gametophytes. The expression of seven mannuronan C5-epimerase genes was suppressed only in female gametophytes. Oogenesis was not completed, but the properties of alginate might become directed towards oogenesis.

The present findings revealed changes in the expression of genes involved in cell wall metabolism associated with morphological changes in the rhizoid elongation of *S. babingtonii* and gametogenesis in *S. japonica*. However, most genes are still in the prediction stage, and their real function has not been clarified. Immunoelectron microscopy using specific epitopes against polysaccharides, as described herein, is a useful tool to determine cell wall composition *in situ*. In the future, more specific antibodies against sugar chains will enable further understanding of the relationship between morphogenesis and cell wall structure. Additionally, CRISPR-Cas9 for genome editing will be a valid tool for revealing the functions of predicted genes for cell wall biosynthesis and modification.

References

Abe M (1970) Method of inducing egg liberation in *Fucus evanescens*. Bot Mag Tokyo 83:254-255

Akkerman M, Franssen-Verheijen MAW, Immerzeel P, Hollander LD, Schel JHN, Emons AMC (2012) Texture of cellulose microfibrils of root hair cell walls of *Arabidopsis thaliana*, *Medicago truncatula*, and *Vicia sativa*. J Microsc 247:60-67

Alexa A, Rahnenführer J, Lengauer T (2006) Improved scoring of functional groups from gene expression data by decorrelating GO graph structure. Bioinformatics 22:1600-1607

Allen AE, LaRoche J, Maheswari U, Lommer M, Schauer N, Lopez PJ, Finazzi G, Fernie AR, Bowler C (2008) Whole-cell response of the pennate diatom *Phaeodactylum tricornutum* to iron starvation. Proc Nat Acad Sci 105:10438-10443

Allen AE, Ward BB, Song B (2005) Characterization of diatom (bacillariophyceae) nitrate reductase genes and their detection in marine phytoplankton communities. J Phycol 41:95-104

Anders S, Pyl PT, Huber W (2015) HTSeq-a Python framework to work with high-throughput sequencing data. Bioinformatics 31:166-169

Baker HM, Anderson BF, Baker EN (2003) Dealing with iron: common structural principles in proteins that transport iron and heme. Proc Nat Acad Sci 100:3579-3583

Bardou P, Mariette J, Escudié F, Djemiel C, Klopp C (2014) jvenn: an interactive Venn diagram viewer. BMC Bioinformatics 15:1-7

Behnke J, LaRoche J (2020) Iron uptake proteins in algae and the role of Iron Starvation-Induced Proteins (ISIPs). Eur J Phycol 55:339-360

Bertagnolli C, Espindola APD, Kleinübing SJ, Tasic L, da Silva MGC (2014) *Sargassum filipendula* alginate from Brazil: Seasonal influence and characteristics. Carbohydr Polym

111:619-623

Bisgrove SR, Kropf DL (2001) Cell wall deposition during morphogenesis in fucoid algae. Planta 212:648-658

Bisgrove SR, Kropf DL (2004) Cytokinesis in brown algae: studies of asymmetric division in fucoid zygotes. Protoplasma 223:163-173

Blackman LM, Arikawa M, Yamada S, Suzaki T, Hardham AR (2011) Identification of a mastigoneme protein from *Phytophthora nicotianae*. Protist 162:100-114

Bolwell GP, Callow JA, Callow ME, Evans LV (1979) Fertilization in brown algae. II. Evidence for lectin-sensitive complementary receptors involved in gamete recognition in *Fucus serratus*. J Cell Sci 36:19-30

Bouck GB (1971) The structure, origin, isolation, and composition of the tubular mastigonemes of the *Ochromonas* flagellum. J Cell Biol 50:362-384

Brawley SH, Quatrano RS (1979) Sulfation of fucoidin in Fucus embryos: IV. Autoradiographic investigations of fucoidin sulfation and secretion during differentiation and the effect of cytochalasin treatment. Dev Biol 73:193-205

Burns AR, Oliveira L, Bisalputra T (1982a) A histochemical study of bud initiation in the brown alga *Sphacelaria furcigera*. New Phytol 92:297-307

Burns AR, Oliveira L, Bisalputra T (1982b) A morphological study of bud initiation in the brown alga *Sphacelaria furcigera*. New Phytol 92:309-325

Callow ME, Coughlan SJ, Evans LV (1978) The role of Golgi bodies in polysaccharide sulphation in *Fucus* zygotes. J Cell Sci 32:337-356

Catt JW, Vithanage HIMV, Callow JA, Callow ME, Evans LV (1983) Fertilization in brown algae: V. Further investigations of lectins as surface probes. Exp Cell Res 147:127-133

Chebli Y, Kaneda M, Zerzour R, Geitmann A (2012) The cell wall of the Arabidopsis pollen

tube—spatial distribution, recycling, and network formation of polysaccharides. Plant Physiol 160:1940-1955

Chi ES, Henry EC, Kawai H, Okuda K (1999) Immunogold‐labeling analysis of alginate distributions in the cell walls of chromophyte algae. Phycol Res 47:53-60

Chi S, Feng YJ, Liu T (2016) Molecular cloning, characterization, and comparison of UDP-glucose pyrophosphorylase from *Gracilaria chouae* and *Saccharina japonica*. J Appl Phycol 28:2051-2059

Chi S, Liu T, Wang X, Wang R, Wang S, Wang G, Shan G, Liu C (2018) Functional genomics analysis reveals the biosynthesis pathways of important cellular components (alginate and fucoidan) of *Saccharina*. Curr Genet 64:259-273

Cho HT, Cosgrove DJ (2002) Regulation of root hair initiation and expansin gene expression in Arabidopsis. Plant Cell 14:3237-3253

Coale TH, Moosburner M, Horák A, Oborník M, Barbeau KA, Allen AE (2019) Reduction-dependent siderophore assimilation in a model pennate diatom. Proc Nat Acad Sci 116:23609-23617

Cock JM, Sterck L, Rouzé P, Scornet D, Allen AE, Amoutzias G, Anthouard V, Artiguenave F, Aury JM, Badger JH, Beszteri B, Billiau K, Bonnet E, Bothwell JH, Bowler C, Boyen C, Brownlee C, Carrano CJ, Charrier B, Cho GY, Coelho SM, Collén J, Corre E, Da Silva C, Delage L, Delaroque N, Dittami SM, Doulbeau S, Elias M, Farnham G, Gachon CMM, Gschloessl B, Heesch S, Jabbari K, Jubin C, Kawai H, Kimura K, Kloareg B, Küpper FC, Lang D, Le Bail A, Leblanc C, Lerouge P, Lohr M, Lopez PJ, Martens C, Maumus F, Michel G, Miranda-Saavedra D, Morales J, Moreau H, Motomura T, Nagasato C, Napoli CA, Nelson DR, Nyvall-Collén P, Peters AF, Pommier C, Potin P, Poulain J, Quesneville H, Read B, Rensing SA, Ritter A, Rousvoal S, Samanta M, Samson G, Schroeder DC, Ségurens

B, Strittmatter M, Tonon T, Tregear JW, Valentin K, von Dassow P, Yamagishi T, Van de Peer Y, Wincker P (2010) The *Ectocarpus* genome and the independent evolution of multicellularity in brown algae. Nature 465:617-621

Cosgrove DJ (2015) Plant expansins: diversity and interactions with plant cell walls. Curr Opin Plant Biol 25:162-172

Cosgrove DJ (2016) Plant cell wall extensibility: connecting plant cell growth with cell wall structure, mechanics, and the action of wall-modifying enzymes. J Exp Bot 67:463-476

Cosgrove DJ (2018) Diffuse growth of plant cell walls. Plant Physiol 176:16-27

Cresti M, Pacini E, Ciampolini F, Sarfatti G (1977) Germination and early tube development in vitro of *Lycopersicum peruvianum* pollen: ultrastructural features. Planta 136:239-247

Cribari-Neto F, Zeileis A (2010) Beta regression in R. J Stat Softw 34:1-24

Criscuolo A, Gribaldo S (2010) BMGE (Block Mapping and Gathering with Entropy): A new software for selection of phylogenetic informative regions from multiple sequence alignments. BMC Evol Biol 10

Curie C, Panaviene Z, Loulergue C, Dellaporta SL, Briat JF, Walker EL (2001) Maize yellow stripe1 encodes a membrane protein directly involved in Fe (III) uptake. Nature 409:346-349

Daher FB, Braybrook SA (2015) How to let go: pectin and plant cell adhesion. Front Plant Sci 6:523

Dardelle F, Lehner A, Ramdani Y, Bardor M, Lerouge P, Driouich A, Mollet JC (2010) Biochemical and immunocytological characterizations of Arabidopsis pollen tube cell wall. Plant Physiol 153:1563-1576

Delignette-Muller ML, Dutang C (2015) fitdistrplus: An R package for fitting distributions. J Stat Softw 64:1-34

Deniaud-Bouët E, Hardouin K, Potin P, Kloareg B, Hervé C (2017) A review about brown algal cell walls and fucose-containing sulfated polysaccharides: Cell wall context, biomedical properties and key research challenges. Carbohydr Polym 175:395-408

Deniaud-Bouët E, Kervarec N, Michel G, Tonon T, Kloareg B, Hervé C (2014) Chemical and enzymatic fractionation of cell walls from Fucales: insights into the structure of the extracellular matrix of brown algae. Ann Bot 114:1203-1216

Donaldson RP, Luster DG (1991) Multiple forms of plant cytochromes P-450. Plant Physiol 96:669-674

Duncombe SG, Chethan SG, Anderson CT (2021) Super-resolution imaging illuminates new dynamic behaviors of cellulose synthase. Plant Cell https://doi.org/10.1093/plcell/koab227

Emons AMC, Wolters-Arts AMC (1983) Cortical microtubules and microfibril deposition in the cell wall of root hairs of *Equisetum hyemale*. Protoplasma 117:68-81

Evans LV, Holligan MS (1972) Correlated light and electron microscope studies on brown algae I. Localization of alginic acid and sulphated polysaccharides in *Dictyota*. New Phytol 71:1161-1172

FAO (2020) The State of World Fisheries and Aquaculture 2020. Sustainability in action. Rome. https://doi.org/10.4060/ca9229en

Felsenstein J (1985) Confidence limits on phylogenies: an approach using the bootstrap. Evolution 39:783-791

Ferguson C, Teeri TT, Siika-aho M, Read SM, Bacic A (1998) Location of cellulose and callose in pollen tubes and grains of *Nicotiana tabacum*. Planta 206:452-460

Fischl R, Bertelsen K, Gaillard F, Coelho S, Michel G, Klinger M, Boyen C, Czjzek M, Hervé C (2016) The cell-wall active mannuronan C5-epimerases in the model brown alga *Ectocarpus*: From gene context to recombinant protein. Glycobiology 26:973-983

Fletcher HR, Biller P, Ross AB, Adams JMM (2017) The seasonal variation of fucoidan within three species of brown macroalgae. Algal Res 22:79-86

Frada MJ, Burrows EH, Wyman KD, Falkowski PG (2013) Quantum requirements for growth and fatty acid biosynthesis in the marine diatom *Phaeodactylum tricornutum* (Bacillariophyceae) in nitrogen replete and limited conditions. J Phycol 49:381-388

Fu G, Nagasato C, Oka S, Cock JM, Motomura T (2014) Proteomics analysis of heterogeneous flagella in brown algae (Stramenopiles). Protist 165:662-675

Gao X, Bowler C, Kazamia E (2021) Iron metabolism strategies in diatoms. J Exp Bot 72:2165-2180

García-Ríos V, Ríosv-Leal E, Robledo D, Freile-Pelegrin Y (2012) Polysaccharides composition from tropical brown seaweeds. Phycol Res 60:305-315

Gazzarrini S, Lejay L, Gojon A, Ninnemann O, Frommer WB, von Wirén N (1999) Three functional transporters for constitutive, diurnally regulated, and starvation-induced uptake of ammonium into Arabidopsis roots. Plant Cell 11:937-947

Geitmann A, Li YQ, Cresti M (1995) Ultrastructural immunolocalization of periodic pectin depositions in the cell wall of *Nicotiana tabacum* pollen tubes. Protoplasma 187:168-171

Gledhill M, Buck KN (2012) The organic complexation of iron in the marine environment: a review. Front Microbiol https://doi.org/10.3389/fmicb.2012.00069

Große C, Scherer J, Koch D, Otto M, Taudte N, Grass G (2006) A new ferrous iron-uptake transporter, EfeU (YcdN), from *Escherichia coli*. Mol Microbiol 62:120-131

Guindon S, Dufayard JF, Lefort V, Anisimova M, Hordijk W, Gascuel O (2010) New algorithms and methods to estimate maximum-likelihood phylogenies: Assessing the performance of PhyML 3.0. Syst Biol 59:307-321

Haas BJ, Papanicolaou A, Yassour M, Grabherr M, Blood PD, Bowden J, Couger MB, Eccles D,

Li B, Lieber M, MacManes MD, Ott M, Orvis J, Pochet N, Strozzi F, Weeks N, Westerman R, William T, Dewey CN, Henschel R, LeDuc RD, Friedman N, Regev A (2013) *De novo* transcript sequence reconstruction from RNA-seq using the Trinity platform for reference generation and analysis. Nat Protoc 8:1494-1512

Henrissat B, Coutinho PM, Davies GJ (2001) A census of carbohydrate-active enzymes in the genome of *Arabidopsis thaliana*. Plant Mol Biol 47:55-72

Henry EC, Cole KM (1982a) Ultrastructure of swarmers in the Laminariales (Phaeophyceae). I. Zoospores. J Phycol 18:550-569

Henry EC, Cole KM (1982b) Ultrastructure of swarmers in the Laminariales (Phaeophyceae). II. Sperm. J Phycol 18:570-579

Hildebrand M (2005) Cloning and functional characterization of ammonium transporters from the marine diatom *Cylindrotheca fusiformis* (Bacillariophyceae). J Phycol 41:105-113

Inoue A, Satoh A, Morishita M, Tokunaga Y, Miyakawa T, Tanokura M, Ojima T (2016) Functional heterologous expression and characterization of mannuronan C5-epimerase from the brown alga *Saccharina japonica*. Algal Res 16:282-291

Izquierdo J, Pérez-Ruzafa IM, Gallardo T (2002) Effect of temperature and photon fluence rate on gametophytes and young sporophytes of *Laminaria ochroleuca* Pylaie. Helgol Mar Res 55:285-292

Jarvis M (2003) Cellulose stacks up. Nature 426:611-612

Jones P, Binns D, Chang HY, Fraser M, Li W, McAnulla C, McWilliam H, Maslen J, Mitchell A, Nuka G, Pesseat S, Quinn AF, Sangrador-Vegas A, Scheremetjew M, Yong SY, Lopez R, Hunter S (2014) InterProScan 5: genome-scale protein function classification. Bioinformatics 30:1236-1240

Kaldis P, Kamp G, Piendl T, Wallimann T (1997) Functions of creatine kinase isoenzymes in

spermatozoa. Adv Dev Biochem 5:275-312

Karyophyllis D, Katsaros C, Galatis B (2000) F-actin involvement in apical cell morphogenesis of *Sphacelaria rigidula* (Phaeophyceae): mutual alignment between cortical actin filaments and cellulose microfibrils. Eur J Phycol 35:195-203

Katoh K, Misawa K, Kuma KI, Miyata T (2002) MAFFT: a novel method for rapid multiple sequence alignment based on fast Fourier transform. Nucleic Acids Res 30:3059-3066

Katsaros C, Galatis B (1992) Immunofluorescence and electron microscopic studies of microtubule organization during the cell cycle of *Dictyota dichotoma* (Phaeophyta, Dictyotales). Protoplasma 169:75-84

Kawai H, Motomura T, Okuda K (2005) Isolation and purification techniques for macroalgae. In: Andersen RA (ed) Algal Culture Techniques. Elsevier Academic Press, London, pp 133-143

Kazamia E, Sutak R, Paz-Yepes J, Dorrell RG, Vieira FRJ, Mach J, Morrissey J, Leon S, Lam F, Pelletier E, Camadro JM, Bowler C, Lesuisse E (2018) Endocytosis-mediated siderophore uptake as a strategy for Fe acquisition in diatoms. Sci Adv 4:eaar4536

Kidgell JT, Magnusson M, de Nys R, Glasson CR (2019) Ulvan: A systematic review of extraction, composition and function. Algal Res 39:101422

Kim D, Pertea G, Trapnell C, Pimentel H, Kelley R, Salzberg SL (2013) TopHat2: accurate alignment of transcriptomes in the presence of insertions, deletions and gene fusions. Genome Biol 14:1-13

Kinjo S, Monma N, Misu S, Kitamura N, Imoto J, Yoshitake K, Gojobori T, Ikeo K (2018) Maser: One-stop platform for NGS big data from analysis to visualization. Database 2018:1-12

Kloareg B, Quatrano RS (1988) Structure of cell walls of marine algae and ecophysiological functions of the matrix polysaccharides. Oceanogr Mar Bio Annu Rev 26:259-315

Klochkova TA, Motomura T, Nagasato C, Klimova AV, Kim GH (2019) The role of egg flagella in the settlement and development of zygotes in two *Saccharina* species. Phycologia 58:145-153

Kobayashi T, Nozoye T, Nishizawa NK (2019) Iron transport and its regulation in plants. Free Radic Biol Med 133:11-20

Kropf DL, Hopkins R, Quatrano RS (1989) Protein synthesis and morphogenesis are not tightly linked during embryogenesis in *Fucus*. Dev Biol 134:452-461

Kubo T, Oda T (2019) *Chlamydomonas* as a tool to study tubulin polyglutamylation. Microscopy 68:80-91

Kustka AB, Allen AE, Morel FM (2007) Sequence analysis and transcriptional regulation of iron acquisition genes in two marine diatoms. J Phycol 43:715-729

Lefort V, Longueville JE, Gascuel O (2017) SMS: Smart Model Selection in PhyML. Mol Biol Evol 34:2422-2424

Lehti MS, Zhang FP, Kotaja N, Sironen A (2017) SPEF2 functions in microtubule-mediated transport in elongating spermatids to ensure proper male germ cell differentiation. Development 144:2683-2693

Lemesheva V, Birkemeyer C, Garbary D, Tarakhovskaya E (2020) Vanadium-dependent haloperoxidase activity and phlorotannin incorporation into the cell wall during early embryogenesis of *Fucus vesiculosus* (Phaeophyceae). Eur J Phycol 55:275-284

Lemoine F, Correia D, Lefort V, Doppelt-Azeroual O, Mareuil F, Cohen-Boulakia S, Gascuel O (2019) NGPhylogeny.fr: new generation phylogenetic services for non-specialists. Nucleic Acids Res 47:W260-265

Lemoine F, Entfellner JBD, Wilkinson E, Correia D, Felipe MD, De Oliveira T, Gascuel O (2018) Renewing Felsenstein's phylogenetic bootstrap in the era of big data. Nature 556:452-456

Lewis RJ, Green MK, Afzal ME (2013) Effects of chelated iron on oogenesis and vegetative growth of kelp gametophytes (Phaeophyceae). Phycol Res 61:46-51

Li W, Godzik A (2006) Cd-hit: A fast program for clustering and comparing large sets of protein or nucleotide sequences. Bioinformatics 22:1658-1659

Linardić M, Braybrook SA (2017) Towards an understanding of spiral patterning in the *Sargassum muticum* shoot apex. Sci Rep 7:13887

Linardić M, Cokus SJ, Pellegrini M, Braybrook SA (2020) Growth of the *Fucus* embryo: insights into wall-mediated cell expansion through mechanics and transcriptomics. bioRxiv https://doi.org/10.1101/2020.01.29.925107

Liu F, Sun X, Wang W, Liang Z, Wang F (2014) De novo transcriptome analysis-gained insights into physiological and metabolic characteristics of *Sargassum thunbergii* (Fucales, Phaeophyceae). J Appl Phycol 26:1519-1526

Liu X, Theil EC (2005) Ferritins: dynamic management of biological iron and oxygen chemistry. Acc Chem Res 38:167-175

Lommer M, Specht M, Roy AS, Kraemer L, Andreson R, Gutowska MA, Wolf J, Bergner SV, Schilhabel MV, Klostermeier UC, Beiko RG, Rosenstiel P, Hippler M, LaRoche J (2012) Genome and low-iron response of an oceanic diatom adapted to chronic iron limitation. Genome Biol 13:1-21

Lüning K (1980) Critical levels of light and temperature regulating the gametogenesis of three *Laminaria* species (Phaeophyceae). J Phycol 16:1-15

Lüning K, Dring MJ (1972) Reproduction induced by blue light in female gametophytes of *Laminaria saccharina*. Planta 104:252-256

Lüning K, Dring MJ (1975) Reproduction, growth and photosynthesis of gametophytes of *Laminaria saccharina* grown in blue and red light. Mar Biol 29:195-200

Lüning K, Neushul M (1978) Light and temperature demands for growth and reproduction of laminarian gametophytes in southern and central California. Mar Biol 45:297-309

Mabeau S, Kloareg B (1987) Isolation and analysis of the cell walls of brown algae: *Fucus spiralis*, *F. ceranoides*, *F. vesiculosus*, *F. serratus*, *Bifurcaria bifurcata* and *Laminaria digitata*. J Exp Bot 38:1573-1580

Maier I (1982) New aspects of pheromone-triggered spermatozoid release in *Laminaria digitata* (Phaeophyta). Protoplasma 113:137-143

Maier I, Müller DG (1982) Antheridium fine structure and spermatozoid release in *Laminaria digitata* (Phaeophyceae). Phycologia 21:1-8

Marchetti A, Parker MS, Moccia LP, Lin EO, Arrieta AL, Ribalet F, Murphy MEP, Maldonado MT, Armbrust EV (2009) Ferritin is used for iron storage in bloom-forming marine pennate diatoms. Nature 457:467-470

Mariani P, Tolomio C, Braghetta P (1985) An ultrastructural approach to the adaptive role of the cell wall in the intertidal alga *Fucus virsoides*. Protoplasma 128:208-217

McKee JWA, Kavalieris L, Brasch DJ, Brown MT, Melton LD (1992) Alginate content and composition of *Macrocystis pyrifera* from New Zealand. J Appl Phycol 4:357-369

McQuaid JB, Kustka AB, Oborník M, Horák A, McCrow JP, Karas BJ, Zheng H, Kindeberg T, Andersson AJ, Barbeau KA, Allen AE (2018) Carbonate-sensitive phytotransferrin controls high-affinity iron uptake in diatoms. Nature 555:534-537

Meents MJ, Watanabe Y, Samuels AL (2018) The cell biology of secondary cell wall biosynthesis. Ann Bot 121:1107-1125

Meslet-Cladière L, Delage L, Leroux CJJ, Goulitquer S, Leblanc C, Creis E, Gall EA, Stiger-Pouvreau V, Czjzek M, Potin P (2013) Structure/function analysis of a type III polyketide synthase in the brown alga *Ectocarpus siliculosus* reveals a biochemical pathway in

phlorotannin monomer biosynthesis. Plant Cell 25:3089-3103

Michel G, Tonon T, Scornet D, Cock JM, Kloareg B (2010a) Central and storage carbon metabolism of the brown alga *Ectocarpus siliculosus*: insights into the origin and evolution of storage carbohydrates in Eukaryotes. New Phytol 188:67-81

Michel G, Tonon T, Scornet D, Cock JM, Kloareg B (2010b) The cell wall polysaccharide metabolism of the brown alga *Ectocarpus siliculosus*. Insights into the evolution of extracellular matrix polysaccharides in Eukaryotes. New Phytol 188:82-97

Miki-Hirosige H, Nakamura S (1982) Process of metabolism during pollen tube wall formation. Microscopy 31:51-62

Mizuno M, Nishitani Y, Tanoue T, Matoba Y, Ojima T, Hashimoto T, Kanazawa K (2009) Quantification and localization of fucoidan in *Laminaria japonica* using a novel antibody. Biosci Biotechnol Biochem 73:335-338

Morrissey J, Sutak R, Paz-Yepes J, Tanaka A, Moustafa A, Veluchamy A, Thomas Y, Botebol H, Bouget FY, McQuaid JB, Tirichine L, Allen AE, Lesuisse E, Bowler C (2015) A novel protein, ubiquitous in marine phytoplankton, concentrates iron at the cell surface and facilitates uptake. Curr Biol 25:364-371

Motomura T (1989) Ultrastructural study of sperm in *Laminaria angustata* (Laminariales, Phaeophyta), especially on the flagellar apparatus. Jpn J Phycol 37:105-116

Motomura T (1990) Ultrastructure of fertilization in *Laminaria angustata* (Phaeophyta, laminariales) with emphasis on the behavior of centrioles, mitochondria and chloroplasts of the sperm. J Phycol 26:80-89

Motomura T, Sakai Y (1981) Effect of chelated iron in culture media on oogenesis in *Laminaria angustata*. Jpn Soc Sci Fish 47:1535-1540

Motomura T, Sakai Y (1984) Ultrastructural studies of gametogenesis in *Laminaria angustata*

(Laminariales, Phaeophyta) regulated by iron concentration in the medium. Phycologia 23:331-343

Motomura T, Sakai Y (1988) The occurrence of flagellated eggs in *Laminaria angustata* (Phaeophyta, Laminariales). J Phycol 24:282-285

Murata Y, Ma JF, Yamaji N, Ueno D, Nomoto K, Iwashita T (2006) A specific transporter for iron (III)-phytosiderophore in barley roots. Plant J 46:563-572

Nagasato C, Inoue A, Mizuno M, Kanazawa K, Ojima T, Okuda K, Motomura T (2010) Membrane fusion process and assembly of cell wall during cytokinesis in the brown alga, *Silvetia babingtonii* (Fucales, Phaeophyceae). Planta 232:287-298

Nagasato C, Motomura T (2002a) New pyrenoid formation in the brown alga, *Scytosiphon lomentaria* (Scytosiphonales, Phaeophyceae). J Phycol 38:800-806

Nagasato C, Motomura T (2002b) Ultrastructural study on mitosis and cytokinesis in *Scytosiphon lomentaria* zygotes (Scytosiphonales, Phaeophyceae) by freeze-substitution. Protoplasma 219:140-149

Nishitsuji K, Arimoto A, Higa Y, Mekaru M, Kawamitsu M, Satoh N, Shoguchi E (2019) Draft genome of the brown alga, *Nemacystus decipiens*, Onna-1 strain: fusion of genes involved in the sulfated fucan biosynthesis pathway. Sci Rep 9:1-11

Nishitsuji K, Arimoto A, Iwai K, Sudo Y, Hisata K, Fujie M, Arakaki N, Kushiro T, Konishi T, Shinzato C, Shoguchi E (2016) A draft genome of the brown alga, *Cladosiphon okamuranus*, S-strain: a platform for future studies of 'mozuku'biology. DNA Res 23:561-570

Novotny AM, Forman M (1975) The composition and development of cell walls of *Fucus* embryos. Planta 122:67-78

Nyvall P, Corre E, Boisset C, Barbeyron T, Rousvoal S, Scornet D, Kloareg B, Boyen C (2003) Characterization of mannuronan C-5-epimerase genes from the brown alga *Laminaria*

digitata. Plant Physiol 133:726-735

O'Kelly CJ (1989) The evolutionary origin of the brown algae: information from studies of motile cell ultrastructure. In JC Green, BSC Leadbeater, WL Diver (Eds) The Chromophyte Algae: Problems and Perspectives, Oxford University Press, Oxford, pp 255-278

O'Kelly CJ, Floyd GL (1984) The absolute configuration of the flagellar apparatus in zoospores from two species of *Laminariales* (Phaeophyceae). Protoplasma 123:18-25

O'Neill MA, York WS (2003) The composition and structure of plant primary cell walls. In Rose JKC (ed) Plant cell wall, Blackwell Publishing, Oxford, pp 1-54

Paredez AR, Somerville CR, Ehrhardt DW (2006) Visualization of cellulose synthase demonstrates functional association with microtubules. Science 312:1491-1495

Patro R, Duggal G, Love MI, Irizarry RA, Kingsford C (2017) Salmon provides fast and bias-aware quantification of transcript expression. Nat Methods 14:417-419

Pazour GJ, Agrin N, Leszyk J, Witman GB (2005) Proteomic analysis of a eukaryotic cilium. J Cell Biol 170:103-113

Pearson G, Lago-Leston A, Valente M, Serrão E (2006) Simple and rapid RNA extraction from freeze-dried tissue of brown algae and seagrasses. Eur J Phycol 41:97-104

Pearson GA, Martins N, Madeira P, Serrão EA, Bartsch I (2019) Sex-dependent and -independent transcriptional changes during haploid phase gametogenesis in the sugar kelp *Saccharina latissima*. PloS one 14:e0219723

Popper ZA, Michel G, Hervé C, Domozych DS, Willats WGT, Tuohy MG, Kloareg B, Stengel DB (2011) Evolution and diversity of plant cell walls: from algae to flowering plants. Annu Rev Plant Biol 62:567-590

Provasoli L (1963) Growing marine seaweeds. In DeVirville D, Feldmann J (eds) Proceedings of the fourth international seaweed symposium, vol 4. Pergamon Press, Oxford, pp 9-17

Provasoli L (1968) Media and prospects for the cultivation of marine algae. In Watanabe A, Hattori A (eds) Cultures and Collections of Algae (Proc Jap Conf Hakone, 1966), Jap Soc Plant Physiol, pp 63-75

Quatrano RS (1968) Rhizoid formation in *Fucus* zygotes: dependence on protein and ribonucleic acid syntheses. Science 162:468-470

Quatrano RS, Crayton MA (1973) Sulfation of fucoidan in *Fucus* embryos: I. Possible role in localization. Dev Biol 30:29-41

Quatrano RS, Stevens PT (1976) Cell wall assembly in *Fucus* zygotes: I. Characterization of the polysaccharide components. Plant Physiol 58:224-231

R Core Team (2020) R: A language and environment for statistical computing. Version 4. 0. 2. R Foundation for Statistical Computing, Vienna, Austria

Rabillé H, Billoud B, Tesson B, Le Panse S, Rolland É, Charrier B (2019) The brown algal mode of tip growth: Keeping stress under control. PLoS Biol 17:e2005258

Reynolds ES (1963) The use of lead citrate at high pH as an electron-opaque stain in electron microscopy. J Cell Biol 17:208-212

Robinson NJ, Procter CM, Connolly EL, Guerinot ML (1999) A ferric-chelate reductase for iron uptake from soils. Nature 397:694-697

Rose JK, Braam J, Fry SC, Nishitani K (2002) The XTH family of enzymes involved in xyloglucan endotransglucosylation and endohydrolysis: current perspectives and a new unifying nomenclature. Plant Cell Physiol 43:1421-1435

Rosenbaum JL, Witman GB (2002) Intraflagellar transport. Nat Rev Mol Cell Biol 3:813-825

Rounds CM, Bezanilla M (2013) Growth mechanisms in tip-growing plant cells. Annu Rev Plant Biol 64:243-265

Salgado LT, Cinelli LP, Viana NB, Tomazetto de Carvalho R, de Souza Mourao PA, Teixeira VL,

Farina M, Filho AGMA (2009) A vanadium bromoperoxidase catalyzes the formation of high-molecular-weight complexes between brown algal phenolic substances and alginates. J Phycol 45:193-202

Sauvageau C (1915) Sur le développement et la biologie d'une Laminaire (*Saccorhiza bulbosa*). Comptes rendus de l'Académie des Sciences [Paris] 160:445-448

Scheller HV, Ulvskov P (2010) Hemicelluloses. Annu Rev Plant Biol 61:263-289

Schenkman JB, Jansson I (2003) The many roles of cytochrome *b*5. Pharmacol Ther 97:139-152

Schmid CE (1993) Cell-cell-recognition during fertilization in *Ectocarpus siliculosus* (Phaeophyceae). Hydrobiologia 260/261:437-443

Schmid CE, Schroer N, Müller DG (1994) Female gamete membrane glycoproteins potentially involved in gamete recognition in *Ectocarpus siliculosus* (Phaeophyceae). Plant Sci 102:61-67

Schoenwaelder ME (2002) The occurrence and cellular significance of physodes in brown algae. Phycologia 41:125-139

Schoenwaelder ME, Wiencke AC (2000) Phenolic compounds in the embryo development of several northern hemisphere fucoids. Plant Biol 2:24-33

Schüßler A, Hirn S, Katsaros C (2003) Cellulose synthesizing terminal complexes and morphogenesis in tip‐growing cells of *Syringoderma phinneyi* (Phaeophyceae). Phycol Res 51:35-44

Shaked Y, Kustka AB, Morel FM (2005) A general kinetic model for iron acquisition by eukaryotic phytoplankton. Limnol Oceanogr 50:872-882

Shan T, Yuan J, Su L, Li J, Leng X, Zhang Y, Gao H, Pang S (2020) First genome of the brown alga *Undaria pinnatifida*: chromosome-level assembly using PacBio and Hi-C technologies. Front genet 11:140

Shao Z, Zhang P, Lu C, Li S, Chen Z, Wang X, Duan D (2019) Transcriptome sequencing of *Saccharina japonica* sporophytes during whole developmental periods reveals regulatory networks underlying alginate and mannitol biosynthesis. BMC Genom 20:1-15

Skriptsova AV, Shevchenko NM, Tarbeeva DV, Zvyagintseva TN (2012) Comparative study of polysaccharides from reproductive and sterile tissues of five brown seaweeds. Mar biotechnol 14:304-311

Song B, Ward BB (2004) Molecular characterization of the assimilatory nitrate reductase gene and its expression in the marine green alga *Dunaliella tertiolecta* (Chlorophyceae). J Phycol 40:721-731

Sun J, Nishiyama T, Shimizu K, Kadota K (2013) TCC: An R package for comparing tag count data with robust normalization strategies. BMC Bioinformatics 14:219

Suzuki Y, Kuma K, Matsunaga K (1994) Effect of iron on oogonium formation, growth rate and pigment synthesis of *Laminaria japonica* (Phaeophyta). Fish Sci 60:373-378

Tamura H, Mine I, Okuda K (1996) Cellulose‐synthesizing terminal complexes and microfibril structure in the brown alga *Sphacelaria rigidula* (Sphacelariales, Phaeophyceae). Phycol Res 44:63-68

Tatewaki M, Wang XY, Wakana I (1989) A simple method of red seaweed axenic culture by spore-washing. Jpn J Phycol 37:150-152

Terauchi M, Nagasato C, Inoue A, Ito T, Motomura T. (2016) Distribution of alginate and cellulose and regulatory role of calcium in the cell wall of the brown alga *Ectocarpus siliculosus*. Planta 244:361-377

Terauchi M, Nagasato C, Kajimura N, Mineyuki Y, Okuda K, Katsaros C, Motomura T (2012) Ultrastructural study of plasmodesmata in the brown alga *Dictyota dichotoma* (Dictyotales, Phaeophyceae). Planta 236:1013-1026

Terauchi M, Yamagishi T, Hanyuda T, Kawai H (2017) Genome-wide computational analysis of the secretome of brown algae (Phaeophyceae). Mar Genom 32:49-59

Tombes RM, Shapiro BM (1985) Metabolite channeling: a phosphorylcreatine shuttle to mediate high energy phosphate transport between sperm mitochondrion and tail. Cell 41:325-334

Tonon T, Rousvoal S, Roeder V, Boyen C (2008) Expression profiling of the Mannuronan C5-Epimerase multigenic family in the brown alga *Laminaria Digitata* (phaeophyceae) under biotic stress conditions. J Phycol 44:1250-1256

Torode TA, Marcus SE, Jam M, Tonon T, Blackburn RS, Hervé C, Knox JP (2015) Monoclonal antibodies directed to fucoidan preparations from brown algae. PLoS One 10:e0118366

Torode TA, Siméon A, Marcus SE, Jam M, Le Moigne MA, Duffieux D, Knox JP, Hervé C (2016) Dynamics of cell wall assembly during early embryogenesis in the brown alga *Fucus*. J Exp Bot 67:6089-6100

Toth R (1976) The release, settlement and germination of zoospores in *Chorda tomentosa* (Phaeophyceae, laminariales). J Phycol 12:222-233

Tsekos I (1999) The sites of cellulose synthesis in algae: diversity and evolution of cellulose‐synthesizing enzyme complexes. J Phycol 35:635-655

Vert G, Grotz N, Dédaldéchamp F, Gaymard F, Guerinot ML, Briat JF, Curie C (2002) IRT1, an Arabidopsis transporter essential for iron uptake from the soil and for plant growth. Plant Cell 14:1223-1233

Vreeland V, Slomich M, Laetsch WM (1984) Monoclonal antibodies as molecular probes for cell wall antigens of the brown alga, *Fucus*. Planta 162:506-517

Vreeland V, Waite JH, Epstein L (1998) Minireview—polyphenols and oxidases in substratum adhesion by marine algae and mussels. J Phycol 34:1-8

Vreugdenhil D, Dijkstra ML, Libbenga KR (1976) The ultrastructure of the cell wall of normal

and apolar embryos of *Fucus vesiculosus*. Protoplasma 88:305-313

Wallimann T, Tokarska-Schlattner M, Schlattner U (2011) The creatine kinase system and pleiotropic effects of creatine. Amino acids 40:1271-1296

Wang J, Zhang Q, Zhang Z, Zhang H, Niu X (2010) Structural studies on a novel fucogalactan sulfate extracted from the brown seaweed *Laminaria japonica*. Int J Biol Macromol 47:126-131

Wang S, Lin L, Shi Y, Qian W, Li N, Yan X, Zou H, Wu M (2020) First draft genome assembly of the seaweed *Sargassum fusiforme*. Front Genet 11:1228

Willats WG, McCartney L, Mackie W, Knox JP (2001a) Pectin: cell biology and prospects for functional analysis. Plant Mol Biol 47:9-27

Willats WG, Orfila C, Limberg G, Buchholt HC, van Alebeek GJW, Voragen AG, Marcus SE, Christensen TMIE, Mikkelsen JD, Murray BS, Knox JP (2001b) Modulation of the degree and pattern of methyl-esterification of pectic homogalacturonan in plant cell walls: implications for pectin methyl esterase action, matrix properties, and cell adhesion. J Biol Chem 276:19404-19413

Wu Y, Sharp RE, Durachko DM, Cosgrove DJ (1996) Growth maintenance of the maize primary root at low water potentials involves increases in cell-wall extension properties, expansin activity, and wall susceptibility to expansins. Plant Physiol 111:765-772

Wu X, Wang G, Fu X (2014) Variations in the chemical composition of *Costaria costata* during harvest. J Appl Phycol 26:2389-2396

Yamagishi T, Motomura T, Nagasato C, Kawai H (2009) Novel proteins comprising the Stramenopile tripartite mastigoneme in *Ochromonas danica* (Chrysophyceae). J Phycol 45:1110-1115

Ye N, Zhang X, Miao M, Fan X, Zheng Y, Xu D, Wang J, Zhou L, Wang D, Gao Y, Wang Y, Shi

W, Ji P, Li D, Guan Z, Shao C, Zhuang Z, Gao Z, Qi J, Zhao F (2015) *Saccharina* genomes provide novel insight into kelp biology. Nat Commu 6:1-11

Yonamine R, Ichihara K, Tsuyuzaki S, Hervé C, Motomura T, Nagasato C (2021) Changes in cell wall structure during rhizoid formation of *Silvetia babingtonii* (Fucales, Phaeophyceae) zygotes. J Phycol 57:1356-1367

Zhang J, Li Y, Luo S, Cao M, Zhang L, Li X (2021b) Differential gene expression patterns during gametophyte development provide insights into sex differentiation in the dioicous kelp *Saccharina japonica*. BMC Plant Biol 21:1-15

Zhang L, Cao Z, Liang G, Li X, Wu H, Yang G (2020) Comparative transcriptome analysis reveals candidate genes related to structural and storage carbohydrate biosynthesis in kelp *Saccharina japonica* (Laminariales, Phaeophyceae). J Phycol 56:1168-1183

Zhang P, Chang L, Zhanru S, Fuli L, Jianting Y, Delin D (2021a) Genome-wide transcriptome profiling and characterization of mannuronan C5-epimerases in *Saccharina japonica*. Algal Res 60:102491

Zhang P, Shao Z, Li L, Liu S, Yao J, Duan D (2018) Molecular characterisation and biochemical properties of phosphomannomutase/phosphoglucomutase (PMM/PGM) in the brown seaweed *Saccharina japonica*. J Appl Phycol 30:2687-2696

Zhang X, Zhang D, Sun W, Wang T (2019) The adaptive mechanism of plants to iron deficiency via iron uptake, transport, and homeostasis. Int J Mol Sci 20:2424

Zvyagintseva TN, Shevchenko NM, Chizhov AO, Krupnova TN, Sundukova EV, Isakov VV (2003) Water-soluble polysaccharides of some far-eastern brown seaweeds. Distribution, structure, and their dependence on the developmental conditions. J Exp Mar Bio Ecol 294:1-13

Table 1. List of RT-qPCR specific primers in *Silvetia babingtonii*

Contig name	Description		Primer sequence	Product size (bp)	Tm (˚C)
comp21090_c0_seq1.p1	actin	Forward	5'-CTCCCCGACGGAAATGTGAT-3'	114	58.4
		Reverse	5'-GAAGGTGCAATCGTGGATGC-3'		58.4
comp32408_c2_seq24.p1	Mannuronan C-5 epimerase	Forward	5'-GGGGTGGAGGGAAGTGATTG-3'	110	60.4
		Reverse	5'-TGCATTCACAAGGATGGCCT-3'		56.3
comp33109_c0_seq1.p1	Mannuronan C-5 epimerase	Forward	5'-AACCACCGATCATAAGCGCA-3'	102	56.3
		Reverse	5'-CGGATTTCACGATGCACACC-3'		58.4

Table 2. The ratio of TCW layers width in 24-hour zygotes in *Silvetia babingtonii*

zygote number	outer layer (%)	middle layer (%)	inner layer (%)
No.1	29.3	37.3	33.3
	32.6	34.7	32.7
	35.9	33.8	30.3
No.2	34.9	31.7	33.3
	35.3	33.8	30.9
	34.8	32.6	32.6
No.3	24.8	41.3	33.9
	26.9	46.4	26.7
	32.6	38.9	28.5
Average	32 ± 1.3	37 ± 1.6	31 ± 0.8

Values show average ±SE of triplicated counting on the three zygotes (n=9).
Tukey's multiple comparison tests show no significant differences between each zygote ($P < 0.01$).

Table 3. The number of gold particles conjugated with BAM6 and BAM7 in three cell wall regions of 24-hour old zygotes (/0.25 μm^2) in *Silvetia babingtonii*

	BAM6	BAM7
TCW	13 ± 4	23 ± 3
RFCW	5 ± 1	34 ± 4
RTCW	11 ± 2	47 ± 12

Values show average ± SE of triplicated counting on the three zygotes.

Table 4. Summary of RNA-seq data in *Silvetia babingtonii*

Sample name	Reads raw data	Reads filtered	> = Q 30	GC (%)	Mapped to longest ORF	BioProject	DRA Submission	BioSample
3h AF	27905740	27145445	95.06	54.66	63.13%	PRJDB10740	DRA011652	SAMD00282835
10h AF	27018797	26311700	94.8	54.71	63.32%	PRJDB10740	DRA011652	SAMD00282836
24h AF	29303100	28807364	95.04	54.46	61.34%	PRJDB10740	DRA011652	SAMD00282837

Table 5. DEGs in 3 h AF vs. 10 h AF in *Silvetia babingtonii*

Contig name	a.value	m.value	p.value	q.value	rank	description	Uniprot ID	Organism
comp29434_c0_seq1.p1	-20.930567	29.4887419	2.24E-11	5.79E-07	1			
comp19835_c0_seq1.p1	8.96585572	5.73341624	2.95E-09	3.82E-05	2			
comp30946_c0_seq1.p2	8.53524858	5.61613952	9.71E-09	8.38E-05	3			
comp12763_c0_seq1.p1	8.70953592	5.44809022	1.73E-08	9.80E-05	4			
comp24437_c0_seq1.p2	0.43698535	16.5285844	1.89E-08	9.80E-05	5			
comp29637_c0_seq2.p1	9.13713605	5.27887814	2.36E-08	0.00010193	6			
comp32255_c0_seq10.p1	10.000636	5.06276241	3.35E-08	0.00012401	7			
comp31851_c1_seq1.p1	8.30736012	5.42324803	3.88E-08	0.00012572	8			
comp32609_c0_seq16.p2	9.59980386	5.04536514	4.83E-08	0.00013903	9			
comp30740_c1_seq24.p1	-20.930567	28.3983891	6.72E-08	0.00017396	10	RNA polymerase sigma factor rpoD3	Q31QG5	*Synechococcus elongatus* (strain PCC 7942)
comp12039_c0_seq1.p1	8.66935901	5.14042282	8.37E-08	0.00019711	11			
comp31426_c1_seq11.p1	10.3919691	4.76603864	1.14E-07	0.00024694	12	DnAJ-like protein slr0093	P50027	*Synechocystis* sp. (strain PCC 6803 / Kazusa)
comp31851_c1_seq2.p1	7.84172355	5.255871	2.08E-07	0.00041477	13			
comp30049_c0_seq1.p1	-20.930567	28.1904431	2.73E-07	0.00050481	14	Mitogen-activated protein kinase kinase 2	Q9S7U9	*Arabidopsis thaliana*
comp29471_c0_seq2.p1	9.05994903	4.779644	2.97E-07	0.00051243	15	Probable E3 ubiquitin-protein ligase HERC1	Q15751	*Homo sapiens*
comp31851_c1_seq4.p1	7.05961882	5.47305219	4.61E-07	0.00074586	16			
comp27441_c0_seq5.p2	9.22841575	4.58849889	6.33E-07	0.00096461	17	Probable urea active transporter 1	O94469	*Schizosaccharomyces pombe* (strain 972 / ATCC 24843)
comp32647_c0_seq22.p1	7.98304027	4.93098519	6.96E-07	0.0010013	18			
comp28285_c0_seq1.p1	6.76278211	5.41605726	1.51E-06	0.00206085	19			
comp32897_c0_seq8.p1	-1.1325332	18.3337062	1.64E-06	0.00212398	20			
comp31948_c0_seq11.p1	5.02012245	7.01401068	2.18E-06	0.00266857	21	Calcium/calmodulin-dependent protein kinase type II subunit gamma	P11730	*Rattus norvegicus*
comp27441_c0_seq8.p1	9.49036547	4.25884701	2.33E-06	0.00266857	22	Probable urea active transporter 1	O94469	*Schizosaccharomyces pombe* (strain 972 / ATCC 24843)
comp30731_c0_seq2.p1	-20.930567	27.8543449	2.37E-06	0.00266857	23			
comp30809_c0_seq1.p1	10.0791373	4.14718641	2.63E-06	0.00283177	24			
comp32125_c0_seq11.p2	6.82734466	5.20533236	3.17E-06	0.00328411	25	NEDD4-like E3 ubiquitin-protein ligase WWP1	Q8BZZ3	*Mus musculus*
comp32537_c0_seq3.p1	11.7401026	3.93774902	3.97E-06	0.00395107	26	Catalase-peroxidase	B4RW28	*Alteromonas macleodii* (strain DSM 17117 / Deep ecotype)
comp25257_c0_seq2.p1	9.72257003	4.07691987	4.60E-06	0.00441185	27			
comp22476_c0_seq1.p1	9.9065544	4.02519426	5.18E-06	0.00479209	28			
comp13072_c0_seq1.p3	6.65403197	5.19855699	5.38E-06	0.00480094	29			
comp31731_c2_seq2.p1	7.33688222	4.7504763	6.17E-06	0.00532781	30	Putative RNA (cytidine(34)-2'-O)-methyltransferase	Q042B4	*Lactobacillus gasseri* (strain ATCC 33323 / DSM 20243)
comp24503_c0_seq3.p1	11.0032373	3.86107918	6.77E-06	0.00565312	31			
comp32527_c0_seq69.p1	8.23908367	4.33697804	7.07E-06	0.00572291	32			
comp19956_c0_seq1.p1	7.23365678	-4.7590348	7.31E-06	0.00573881	33			
comp21979_c1_seq1.p1	9.49374701	3.99210007	8.03E-06	0.00594971	34			
comp32615_c1_seq31.p1	6.49897777	5.18436999	8.04E-06	0.00594971	35			
comp29480_c0_seq3.p1	7.66554891	4.50648685	8.89E-06	0.00639563	36	Short transient receptor potential channel 4	Q9QUQ5	*Mus musculus*
comp31297_c0_seq1.p1	7.55473228	4.50410258	1.12E-05	0.00785173	37			
comp27949_c0_seq1.p1	8.88952567	4.00376435	1.32E-05	0.0090242	38			
comp30780_c0_seq2.p1	-20.930567	27.5540865	1.39E-05	0.00920385	39	Serine/threonine-protein kinase/endoribonuclease IRE1	P32361	*Saccharomyces cerevisiae* (strain ATCC 204508 / S288c)
comp12509_c0_seq1.p1	8.19367957	4.18906395	1.42E-05	0.00921778	40	Alcohol dehydrogenase	P42327	*Geobacillus stearothermophilus*
comp32240_c0_seq4.p1	10.7586465	3.7105402	1.47E-05	0.00927716	41			
comp19957_c0_seq2.p1	8.54265768	4.05694517	1.57E-05	0.0096543	42			
comp12933_c0_seq1.p1	10.8451805	3.68411959	1.61E-05	0.00968632	43	Probable serine/threonine-protein kinase CCRP1	P0C8M8	*Zea mays*
comp29173_c0_seq1.p1	9.13413819	3.9002034	1.65E-05	0.00968652	44			
comp32905_c0_seq22.p1	9.94727995	3.75143637	1.76E-05	0.00998157	45			
comp34050_c0_seq1.p1	9.6870957	3.78175048	1.81E-05	0.00998157	46			
comp32812_c1_seq1.p1	8.34223185	4.07910172	1.85E-05	0.00998157	47	Probable glutamine amidotransferase DUG3	P53871	*Saccharomyces cerevisiae* (strain ATCC 204508 / S288c)
comp31368_c0_seq3.p1	11.3892808	3.61801302	1.87E-05	0.00998157	48			
comp26119_c0_seq1.p1	7.89820952	4.23438524	1.89E-05	0.00998157	49			
comp29838_c1_seq2.p1	5.54327787	5.80141012	2.04E-05	0.01038078	50	D-xylose-proton symporter-like 3, chloroplastic	Q0WWW9	*Arabidopsis thaliana*
comp29139_c1_seq2.p1	-5.1362789	25.4810724	2.04E-05	0.01038078	51			
comp32858_c2_seq18.p1	6.8342241	4.640078	3.31E-05	0.01530986	52			
comp32024_c0_seq4.p1	7.39019174	4.32413227	3.32E-05	0.01530986	53			
comp24321_c0_seq2.p2	9.15214655	3.73714877	3.32E-05	0.01530986	54	Xylosyltransferase sqv-6	Q5QQ52	*Caenorhabditis briggsae*
comp29876_c0_seq1.p1	8.23397561	3.97879515	3.33E-05	0.01530986	55			
comp29543_c0_seq1.p1	9.80376259	3.62474235	3.37E-05	0.01530986	56	UPF0187 protein alr2987	Q8YSU5	*Nostoc* sp. (strain PCC 7120 / UTEX 2576)
comp30494_c2_seq3.p1	8.26644278	3.96574123	3.37E-05	0.01530986	57			
comp32035_c0_seq4.p2	9.31964611	-3.6820317	3.64E-05	0.0162595	58			
comp30844_c0_seq1.p1	6.87837043	4.56853717	3.80E-05	0.01669139	59			
comp26636_c0_seq4.p1	-20.930567	27.345344	4.23E-05	0.01807683	60			
comp13145_c0_seq1.p1	8.67735908	3.7893703	4.26E-05	0.01807683	61	Putative ankyrin repeat protein R873	Q5UP39	*Acanthamoeba polyphaga mimivirus*
comp11702_c0_seq1.p1	7.94653696	4.01828088	4.35E-05	0.01815779	62	ABC transporter G family member 14	Q9C6W5	*Arabidopsis thaliana*
comp20554_c0_seq1.p1	10.5558558	3.47355809	4.57E-05	0.01879232	63	Nephrocystin-3	Q7TNH6	*Mus musculus*
comp30565_c0_seq11.p1	-20.930567	-27.398652	4.73E-05	0.01914779	64	Protein MOS2	Q9C801	*Arabidopsis thaliana*
comp29535_c0_seq4.p1	-20.930567	27.3170485	4.99E-05	0.0196056	65			
comp29976_c0_seq1.p1	9.18474477	3.63421667	5.04E-05	0.0196056	66			
comp26873_c0_seq1.p1	7.27955346	4.27467428	5.18E-05	0.0196056	67			
comp29899_c0_seq3.p1	1.14342956	12.5748825	5.21E-05	0.0196056	68			
comp25714_c0_seq1.p1	8.61962479	3.75674156	5.23E-05	0.0196056	69			
comp29273_c0_seq1.p1	7.33088761	4.21241826	5.99E-05	0.02214294	70	2-epi-5-epi-valiolone synthase	Q9ZAE9	*Actinoplanes* sp. (strain ATCC 31044 / CBS 674.73 / SE50/110)
comp32597_c0_seq13.p1	4.106583	7.07724558	6.16E-05	0.02245206	71	Ubiquitin carboxyl-terminal hydrolase 22	A6H8I0	*Danio rerio*
comp31985_c0_seq1.p1	7.58402381	4.07483447	6.41E-05	0.02266689	72	Uncharacterized protein PB7E8.02	Q9C0V4	*Schizosaccharomyces pombe* (strain 972 / ATCC 24843)
comp32686_c0_seq5.p1	9.88827885	-3.4631534	6.46E-05	0.02266689	73			
comp32858_c2_seq8.p1	6.99600718	4.3727324	6.48E-05	0.02266689	74	Zinc transporter ZIP10	Q6PEH9	*Danio rerio*
comp31436_c0_seq2.p1	9.76177964	-3.4713061	6.65E-05	0.02276527	75			
comp14128_c0_seq1.p1	12.0102387	-3.3050771	6.75E-05	0.02276527	76	La-related protein 7	Q05CL8	*Mus musculus*
comp26937_c0_seq4.p1	4.66124105	-6.4553116	6.77E-05	0.02276527	77	Exportin-7	Q5ZLT0	*Gallus gallus*
comp32374_c8_seq4.p1	4.02651674	-7.1237729	6.90E-05	0.02276767	78	Uncharacterized acyltransferase C1718.04	Q9P7P0	*Schizosaccharomyces pombe* (strain 972 / ATCC 24843)
comp34646_c0_seq1.p1	8.79576087	3.64428831	6.95E-05	0.02276767	79			

comp32920_c1_seq24.p1	9.8959518	3.43415402	7.32E-05	0.02368625	80	Probable cysteine desulfurase	Q9K7A0	*Bacillus halodurans* (strain ATCC BAA-125 / DSM 18197 / FERM 7344 / JCM 9153 / C-125)
comp29976_c0_seq2.p1	7.42527806	4.10201488	7.78E-05	0.02485944	81			
comp25609_c0_seq3.p1	7.20094529	4.19905613	8.20E-05	0.02560483	82	Guanine nucleotide-binding protein G(o) subunit alpha	O15976	*Mizuhopecten yessoensis*
comp33138_c0_seq13.p1	8.55972122	3.66508481	8.23E-05	0.02560483	83	Kinesin-like protein KIF11	B2GU58	*Xenopus tropicalis*
comp30350_c0_seq4.p1	-20.930567	27.2129637	8.32E-05	0.02560483	84			
comp30402_c0_seq2.p1	6.88498988	4.37276042	8.41E-05	0.02560483	85	ATP-dependent DNA helicase PIF1	Q9H611	*Homo sapiens*
comp30731_c0_seq3.p1	9.88995729	3.38109115	9.21E-05	0.02751647	86			
comp24536_c0_seq2.p1	3.88255004	7.36664925	9.25E-05	0.02751647	87	Splicing factor U2AF 65 kDa subunit	P90978	*Caenorhabditis elegans*
comp31844_c0_seq1.p1	-20.930567	27.1923122	9.48E-05	0.02785175	88			
comp32255_c0_seq1.p1	10.9196171	3.27208977	9.75E-05	0.02785175	89			
comp31723_c0_seq9.p1	-20.930567	27.1818969	9.90E-05	0.02785175	90.5	HBS1-like protein	Q2KHZ2	*Bos taurus*
comp31941_c0_seq2.p1	-20.930567	27.1816159	9.90E-05	0.02785175	90.5	Major facilitator superfamily domain-containing protein 6	Q8CBH5	*Mus musculus*
comp26299_c0_seq1.p2*	3.80466629	7.49982562	9.97E-05	0.02785175	92	Poly(beta-D-mannuronate) C5 epimerase	Q88NC9	*Pseudomonas putida* (strain KT2440)
comp25123_c0_seq2.p1	6.82247824	4.36552452	0.00010005	0.02785175	93	Heat shock factor protein	P22813	*Drosophila melanogaster*
comp29163_c0_seq6.p1	3.52460409	-7.9694569	0.00010447	0.02870992	94	Dynein heavy chain 1, axonemal	Q63164	*Rattus norvegicus*
comp30593_c0_seq1.p1	9.32665313	3.43462161	0.00010535	0.02870992	95	Probable outer membrane protein pmp6	Q9Z899	*Chlamydia pneumoniae*
comp11912_c0_seq2.p1	5.98659327	4.94481634	0.00010826	0.02919519	96			
comp24770_c0_seq1.p1	9.38403747	3.41446435	0.00010995	0.02934518	97			
comp33218_c0_seq21.p2	-20.930567	27.1463968	0.0001181	0.03119968	98	Putative serine protease K12H4.7	P34528	*Caenorhabditis elegans*
comp33217_c0_seq37.p1	5.77130733	5.09325771	0.00012293	0.03214729	99			
comp32683_c0_seq3.p1	-20.930567	27.1227012	0.00013496	0.03494077	100			
comp32398_c1_seq13.p1	8.07591437	3.66267268	0.00015333	0.03930498	101			
comp32002_c0_seq2.p2*	10.498789	3.17858492	0.00016635	0.04222316	102	GDP-mannose 6-dehydrogenase	P11759	*Pseudomonas aeruginosa* (strain ATCC 15692 / PAO1 / 1C / PRS 101 / LMG 12228)
comp31142_c0_seq4.p1	5.1675788	5.58179446	0.0001697	0.04265446	103	Peptidyl-Asp metalloendopeptidase	B2FQP3	*Stenotrophomonas maltophilia* (strain K279a)
comp32647_c0_seq2.p2	7.71612848	3.75384082	0.00018163	0.04521636	104			
comp31338_c0_seq10.p1	8.2178986	3.56251235	0.00018428	0.04543759	105			
comp32035_c0_seq2.p1	9.01631449	-3.3534966	0.00018756	0.04581135	106			
comp32887_c0_seq19.p1	9.92588693	3.19001809	0.00020239	0.04896971	107			

* confirmation of expression level by RT-qPCR

Table 6. DEGs in 3 h AF vs. 24 h AF in *Silvetia babingtonii*

Contig name	a.value	m.value	p.value	q.value	rank	description	Uniprot ID	Organism
comp30946_c0_seq1.p2	10.18803	8.600961466	2.92E-09	7.28E-05	1			
comp24437_c0_seq1.p2	1.408872	18.15161611	5.62E-09	7.28E-05	2			
comp32408 c2 seq24.p1*	-20.9176	29.3619053	1.69E-07	0.001455497	3	Poly(beta-D-mannuronate) C5 epimerase	Q88NC9	*Pseudomonas putida* (strain KT2440)
comp31851_c1_seq4.p1	7.979959	6.99299002	8.03E-07	0.003855527	4			
comp32647_c0_seq22.p1	9.016417	6.676996719	9.74E-07	0.003855527	5			
comp32167 c4 seq1.p1	-20.9176	28.94082432	9.77E-07	0.003855527	6	RNA-binding protein Musashi homolog 2	Q96DH6	*Homo sapiens*
comp31608_c0_seq3.p1	7.55588	7.06680202	1.07E-06	0.003855527	7			
comp32096_c0_seq7.p1	6.734351	7.423743109	1.32E-06	0.003855527	8			
comp31851_c1_seq1.p1	9.042802	6.57338988	1.34E-06	0.003855527	9			
comp32647_c0_seq14.p1	8.548829	6.604782698	1.63E-06	0.00400072	10			
comp28285_c0_seq1.p1	7.646199	6.862147978	1.70E-06	0.00400072	11			
comp24510_c0_seq2.p1	6.069545	7.708841048	2.31E-06	0.004980454	12			
comp30049 c0 seq1.p1	-20.9176	28.63170418	3.53E-06	0.007034909	13	Mitogen-activated protein kinase kinase 2	Q9S7U9	*Arabidopsis thaliana*
comp30350_c0_seq4.p1	-20.9176	28.57674473	4.46E-06	0.008164305	14			
comp30892_c1_seq2.p1	7.931916	6.386459168	4.73E-06	0.008164305	15			
comp33139_c0_seq6.p1	5.537691	7.952891519	6.10E-06	0.009729369	16			
comp32096_c0_seq8.p1	5.268865	8.107480382	6.41E-06	0.009729369	17			
comp29434_c0_seq1.p1	-20.9176	28.47178845	6.87E-06	0.009729369	18			
comp30844_c0_seq1.p1	7.876202	6.24345778	7.14E-06	0.009729369	19			
comp29637_c0_seq2.p1	9.558728	5.801320592	8.87E-06	0.011487304	20			
comp31948 c0 seq11.p1	5.533306	7.71963485	9.69E-06	0.011949093	21	Calcium/calmodulin-dependent protein kinase type II subunit gamma	P11730	*Rattus norvegicus*
comp32609 c0 seq16.p2	10.06715	5.659315433	1.12E-05	0.012664883	22	HBS1-like protein	Q2KHZ2	*Bos taurus*
comp19835_c0_seq1.p1	9.14727	5.775502396	1.13E-05	0.012664883	23			
comp33139_c0_seq7.p1	6.135426	6.964730927	1.18E-05	0.012750062	24			
comp32588_c0_seq12.p1	5.849862	7.090472891	1.68E-05	0.017420108	25			
comp32647_c0_seq17.p2	4.529311	8.628372514	1.76E-05	0.017518176	26			
comp31142 c0 seq4.p1	6.01292	6.951734315	1.91E-05	0.018073631	27	Peptidyl-Asp metalloendopeptidase	B2FQP3	*Stenotrophomonas maltophilia* (strain K279a)
comp31844_c0_seq1.p1	-20.9176	28.21435993	1.95E-05	0.018073631	28			
comp33139_c0_seq25.p1	-20.9176	28.12553854	2.81E-05	0.025095404	29			
comp32255_c0_seq10.p1	10.26248	5.26571539	3.18E-05	0.02740893	30			
comp32814_c0_seq23.p1	-20.9176	-28.27220615	4.17E-05	0.033844999	31			
comp36711_c0_seq1.p1	7.740805	5.650482408	4.24E-05	0.033844999	32			
comp32158_c1_seq28.p1	7.140679	-5.871064106	4.31E-05	0.033844999	33			
comp26636_c0_seq4.p1	-20.9176	27.98698195	4.84E-05	0.036854067	34			
comp32954_c2_seq3.p1	7.139718	5.849187788	4.99E-05	0.03691921	35			
comp32125 c0 seq11.p2	7.267426	5.764753075	5.31E-05	0.037566611	36	NEDD4-like E3 ubiquitin-protein ligase WWP1	Q8BZZ3	*Mus musculus*
comp31851_c1_seq2.p1	8.099755	5.451192047	5.37E-05	0.037566611	37			
comp26119_c0_seq1.p1	8.587502	5.292228907	5.68E-05	0.038712552	38			
comp30838_c0_seq2.p1	4.980823	7.531396032	5.94E-05	0.03880784	39			
comp29663 c0 seq7.p1	5.581634	6.944639201	6.00E-05	0.03880784	40	Carboxypeptidase N subunit 2	Q9DBB9	*Mus musculus*
comp32686_c0_seq5.p1	9.225519	-5.109415706	6.55E-05	0.041384858	41			
comp12763_c0_seq1.p1	8.734975	5.178226535	7.05E-05	0.042428858	42			
comp25093_c0_seq1.p1	9.2034	5.090663564	7.06E-05	0.042428858	43			
comp31723_c0_seq9.p1	-20.9176	27.88580389	7.21E-05	0.042428858	44			
comp32780_c1_seq6.p1	4.409353	8.119487104	7.62E-05	0.043573102	45			
comp25257_c0_seq2.p1	10.30884	4.928712766	7.74E-05	0.043573102	46			
comp24681_c0_seq1.p1	10.44553	4.859020302	9.07E-05	0.049985551	47			

* confirmation of expression level by RT-qPCR

Table 7. DEGs in 10 h AF vs. 24 h AF in *Silvetia babingtonii*

Contig name	a.value	m.value	p.value	q.value	rank	description	Uniprot ID	Organism
comp31608_c0_seq3.p1	7.226321857	7.9163	3.83E-26	9.92E-22	1			
comp30892_c1_seq2.p1	7.659291447	7.1221	5.00E-24	6.48E-20	2			
comp32408_c2_seq24.p1*	2.572456685	14.336	5.67E-19	4.89E-15	3	Poly(beta-D-mannuronate) C5 epimerase	Q88NC9	*Pseudomonas putida* (strain KT2440)
comp32096_c0_seq7.p1	7.273275199	6.5363	1.85E-18	1.20E-14	4			
comp32948_c1_seq5.p1	10.16825089	4.74	3.23E-18	1.67E-14	5			
comp33139_c0_seq6.p1	-20.928435	29.443	6.58E-18	2.84E-14	6			
comp32954_c2_seq3.p1	6.858590588	6.6018	1.62E-16	5.99E-13	7			
comp27318_c0_seq1.p1	7.71102096	5.7158	3.69E-16	1.20E-12	8			
comp30557_c0_seq3.p1	6.654272361	6.6793	7.29E-16	2.10E-12	9			
comp32167_c4_seq1.p1	-20.928435	29.153	1.14E-15	2.95E-12	10	RNA-binding protein Musashi homolog 2	Q96DH6	*Homo sapiens*
comp31977_c0_seq7.p1	7.018510284	6.2393	1.61E-15	3.80E-12	11	Peptidyl-Asp metalloendopeptidase	B2FQP3	*Stenotrophomonas maltophilia* (strain K279a)
comp33151_c0_seq1.p1	10.29681246	4.1404	7.53E-15	1.62E-11	12	Vanadium-dependent bromoperoxidase	P81701	*Ascophyllum nodosum*
comp32070_c1_seq1.p1	11.36377414	3.7123	1.31E-13	2.61E-10	13			
comp32096_c0_seq8.p1	6.050502326	6.7346	9.95E-13	1.84E-09	14			
comp32647_c0_seq20.p2	6.574400453	6.1117	1.25E-12	2.16E-09	15			
comp27008_c0_seq1.p1	12.28053642	3.2059	2.54E-11	4.11E-08	16	Dual oxidase 2	Q8HZK2	*Sus scrofa*
comp26937_c0_seq4.p1	5.289985454	7.4108	2.89E-11	4.40E-08	17	Exportin-7	Q5ZLT0	*Gallus gallus*
comp31866_c0_seq20.p1	-20.928435	28.473	3.47E-11	4.99E-08	18			
comp32647_c0_seq14.p1	10.20844931	3.4759	4.43E-11	6.04E-08	19			
comp30946_c0_seq1.p2	13.03900907	3.0894	6.20E-11	8.03E-08	20			
comp33139_c0_seq7.p1	7.198170442	5.0296	1.08E-10	1.33E-07	21			
comp33139_c0_seq25.p1	-20.928435	28.338	2.00E-10	2.35E-07	22			
comp28157_c0_seq3.p1	8.499248706	4.0174	2.35E-10	2.64E-07	23			
comp32737_c2_seq1.p1	6.569624383	5.5419	2.59E-10	2.80E-07	24			
comp33151_c0_seq7.p1	10.4574249	3.2608	2.77E-10	2.86E-07	25	Vanadium-dependent bromoperoxidase	P81701	*Ascophyllum nodosum*
comp29719_c0_seq3.p1	7.856570421	4.4075	2.88E-10	2.87E-07	26	Ankyrin-3	Q12955	*Homo sapiens*
comp31490_c1_seq1.p1	8.231663668	4.0919	5.64E-10	5.41E-07	27	Vanadium-dependent bromoperoxidase	P81701	*Ascophyllum nodosum*
comp32174_c0_seq1.p1	10.66692086	2.9518	5.75E-09	5.31E-06	28			
comp33134_c0_seq9.p1	6.686089724	5.0007	1.01E-08	8.98E-06	29			
comp32814_c0_seq23.p1	-20.928435	-28.12	1.22E-08	1.05E-05	30			
comp32647_c0_seq26.p1	5.397260669	6.3606	1.63E-08	1.36E-05	31			
comp28953_c0_seq2.p1	7.261352941	4.4178	1.83E-08	1.48E-05	32	Flavohemoprotein	Q8ETH0	*Oceanobacillus iheyensis* (strain DSM 14371 / JCM 11309 / KCTC 3954 / HTE831)
comp32647_c0_seq17.p2	6.368687001	5.14	4.07E-08	3.20E-05	33			
comp24510_c0_seq2.p1	8.182665166	3.673	4.29E-08	3.27E-05	34			
comp32647_c0_seq4.p1	9.29479604	3.1333	4.47E-08	3.31E-05	35			
comp24681_c0_seq1.p1	11.67578516	2.5889	6.52E-08	4.69E-05	36			
comp33037_c0_seq5.p1	12.71910868	-2.507	6.97E-08	4.88E-05	37	WSC domain-containing protein 1	Q505J3	*Rattus norvegicus*
comp21513_c0_seq2.p1	10.4030795	2.766	7.40E-08	5.04E-05	38	Probable transketolase	Q9URM2	*Schizosaccharomyces pombe* (strain 972 / ATCC 24843)
comp26164_c0_seq1.p1	6.082122799	5.3239	9.78E-08	6.49E-05	39	HHIP-like protein 1	Q96JK4	*Homo sapiens*
comp12523_c0_seq1.p1	9.756099424	2.8677	1.35E-07	8.76E-05	40			
comp31476_c0_seq6.p1	-20.928435	27.737	1.53E-07	9.65E-05	41	Fanconi anemia group D2 protein	Q9BXW9	*Homo sapiens*
comp33139_c0_seq12.p1	-20.928435	27.689	2.36E-07	0.000145283	42			
comp33287_c0_seq7.p1	10.72238388	2.5822	2.61E-07	0.000157002	43	Retrovirus-related Pol polyprotein from transposon TNT 1-94	P10978	*Nicotiana tabacum*
comp31346_c0_seq7.p1	7.704189935	3.756	2.89E-07	0.000169928	44			
comp33955_c0_seq1.p2	10.6881279	-2.573	3.01E-07	0.000173139	45			
comp17843_c1_seq1.p1	5.678326945	5.5454	4.70E-07	0.000264298	46			
comp12401_c0_seq1.p1	9.57787814	-2.75	6.72E-07	0.000369925	47			
comp32717_c0_seq6.p2	9.829906008	2.6615	7.99E-07	0.000427027	48			
comp33037_c0_seq9.p1	15.73153814	-2.217	8.08E-07	0.000427027	49	WSC domain-containing protein 2	A2BGL3	*Danio rerio*
comp13093_c0_seq1.p1	9.305649034	2.813	8.83E-07	0.000457346	50	Probable transketolase	Q9URM2	*Schizosaccharomyces pombe* (strain 972 / ATCC 24843)
comp32276_c1_seq7.p1	6.592465999	4.4926	9.05E-07	0.000459518	51			
comp30413_c0_seq1.p1	5.869217287	5.2021	1.04E-06	0.000518801	52			
comp25475_c0_seq1.p1	7.523278434	3.6801	1.38E-06	0.000673869	53			
comp30103_c0_seq2.p1	4.51431748	6.8321	1.88E-06	0.000903099	54			
comp30740_c1_seq21.p1	2.561050234	10.112	1.94E-06	0.000915279	55	RNA polymerase sigma factor rpoD4	Q31QR8	*Synechococcus elongatus* (strain PCC 7942)
comp32588_c0_seq12.p1	7.779065762	3.4224	2.73E-06	0.001259943	56			
comp26763_c0_seq1.p1	8.98087907	2.7976	2.88E-06	0.001307962	57	L-aspartate oxidase	Q51363	*Pseudomonas aeruginosa* (strain ATCC 15692 / PAO1 / 1C / PRS 101 / LMG 12228)
comp32306_c0_seq15.p1	-20.928435	27.389	3.07E-06	0.001369192	58			
comp32794_c0_seq2.p1	-20.928435	27.379	3.44E-06	0.001509442	59			
comp32944_c0_seq11.p1	8.89243574	2.7643	4.99E-06	0.002154316	60			
comp30557_c0_seq5.p1	-20.928435	27.327	5.15E-06	0.002185009	61			
comp32302_c1_seq10.p1	7.675601495	3.3805	5.70E-06	0.002381323	62			
comp32456_c0_seq12.p1	12.92949282	2.0662	6.14E-06	0.002523254	63			
comp29766_c0_seq1.p1	9.878686556	2.406	7.10E-06	0.002873776	64			
comp29137_c0_seq1.p1	11.62634144	2.1067	8.85E-06	0.003523699	65	CBL-interacting serine/threonine-protein kinase 26	Q84VQ3	*Arabidopsis thaliana*
comp27786_c0_seq3.p1	7.927053752	3.1617	9.16E-06	0.003547728	66			
comp31977_c0_seq8.p1	5.512621691	5.2275	9.18E-06	0.003547728	67	Peptidyl-Asp metalloendopeptidase	B2FQP3	*Stenotrophomonas maltophilia* (strain K279a)
comp24972_c0_seq1.p1	6.357890904	4.3443	9.38E-06	0.003569845	68			
comp32439_c0_seq5.p1	-20.928435	27.232	1.04E-05	0.003885283	69			
comp32609_c0_seq10.p1	5.003133574	5.8098	1.09E-05	0.004031459	70			
comp36711_c0_seq1.p1	9.423473369	2.4755	1.15E-05	0.004178534	71			
comp32736_c0_seq17.p1	8.720537264	2.7298	1.17E-05	0.004195725	72			
comp32374_c8_seq2.p1	3.089622006	-8.449	1.25E-05	0.00442232	73	Uncharacterized acyltransferase C1718.04	Q9P7P0	*Schizosaccharomyces pombe* (strain 972 / ATCC 24843)

comp33068_c1_seq5.p1	5.494273876	5.1773	1.32E-05	0.00462933	74			
comp31266_c0_seq2.p3	13.30885469	1.9714	1.35E-05	0.004665712	75			
comp34620_c0_seq1.p1	9.149689757	2.5401	1.40E-05	0.004727197	76			
comp32858_c2_seq16.p1	9.307502828	2.4869	1.41E-05	0.004727197	77	S-type anion channel SLAH2	Q9ASQ7	*Arabidopsis thaliana*
comp27266_c0_seq1.p1	6.748934877	3.9005	1.69E-05	0.00560557	78	CBL-interacting serine/threonine-protein kinase 24	Q9LDI3	*Arabidopsis thaliana*
comp20142_c0_seq2.p1	12.4003803	1.9796	1.75E-05	0.005750344	79	6-phosphogluconate dehydrogenase, decarboxylating	P21577	*Synechococcus elongatus* (strain PCC 7942)
comp12356_c0_seq1.p1	8.700524005	2.671	1.94E-05	0.006283862	80			
comp32439_c0_seq22.p1	10.97405337	2.0706	2.32E-05	0.007408884	81			
comp33287_c0_seq9.p1	8.439939738	2.7288	2.95E-05	0.009329296	82			
comp32523_c0_seq13.p3	9.224342121	-2.405	3.23E-05	0.010090463	83			
comp23261_c1_seq1.p1	9.356605822	2.3524	3.59E-05	0.010853128	84			
comp24915_c0_seq2.p1	-20.928435	27.056	3.60E-05	0.010853128	85	DNA-binding protein SMUBP-2	P38935	*Homo sapiens*
comp33109_c0_seq7.p1	11.22900544	-1.989	3.61E-05	0.010853128	86			
comp36129_c0_seq1.p1	3.753056517	7.3096	4.00E-05	0.011901657	87	Niemann-Pick C1 protein	O35604	*Mus musculus*
comp32284_c0_seq33.p1	-2.456021205	-19.19	4.16E-05	0.012233704	88	Centrosomal protein of 76 kDa	A7E2V1	*Danio rerio*
comp28201_c0_seq9.p1	-20.928435	27.011	4.87E-05	0.014004234	89.5	DGAT2 DICDI Diacylglycerol O-acyltransferase 2	Q54GC1	*Dictyostelium discoideum*
comp33139_c0_seq3.p1	-20.928435	27.011	4.87E-05	0.014004234	89.5			
comp27817_c0_seq2.p1	7.784478383	2.9928	5.04E-05	0.014342625	91	Ras-related protein Rab-8B	Q2HJI8	*Bos taurus*
comp31407_c0_seq1.p1	9.86096043	2.1665	5.34E-05	0.014903323	92	Superoxide dismutase [Fe]	O15905	*Babesia bovis*
comp11755_c0_seq1.p1	10.1648534	2.0996	5.41E-05	0.014903323	93	Ankyrin repeat, PH and SEC7 domain containing protein secG	Q54KA7	*Dictyostelium discoideum*
comp20554_c0_seq1.p1	11.48494305	-1.917	5.41E-05	0.014903323	94	Nephrocystin-3	Q7TNH6	*Mus musculus*
comp32374_c8_seq4.p1	3.988360376	6.7454	5.56E-05	0.015164978	95	Uncharacterized acyltransferase C1718.04	Q9P7P0	*Schizosaccharomyces pombe* (strain 972 / ATCC 24843)
comp31627_c1_seq3.p1	7.572009403	3.086	6.28E-05	0.016944222	96	Serine acetyltransferase	Q9ZK14	*Helicobacter pylori* (strain J99)
comp29898_c0_seq1.p1	11.14021571	-1.931	6.46E-05	0.017240233	97	Probable outer membrane protein pmp6	Q9Z899	*Chlamydia pneumoniae*
comp33287_c0_seq1.p1	8.200289554	2.7211	6.85E-05	0.018088545	98	Retrovirus-related Pol polyprotein from transposon TNT 1-94	P10978	*Nicotiana tabacum*
comp30996_c0_seq7.p1	-20.928435	26.95	7.01E-05	0.018319988	99	MOUSE Importin-7	Q9EPL8	*Mus musculus*
comp31004_c0_seq2.p1	5.38390919	4.9566	7.14E-05	0.018490689	100			
comp20707_c0_seq3.p1	9.174847808	2.3165	7.24E-05	0.018568726	101			
comp25093_c0_seq1.p1	10.87072523	1.9464	7.46E-05	0.018945067	102			
comp28107_c0_seq3.p1	11.51468942	1.8724	7.77E-05	0.019540396	103	Pheophorbide a oxygenase, chloroplastic	Q9FYC2	*Arabidopsis thaliana*
comp13049_c0_seq1.p1	8.209655341	2.6919	8.17E-05	0.020251721	104	60S ribosomal protein L6	P34091	*Mesembryanthemum crystallinum*
comp27073_c0_seq1.p1	7.897984974	-2.85	8.21E-05	0.020251721	105			
comp33151_c0_seq10.p1	7.852844926	2.8777	8.37E-05	0.020448913	106	Vanadium-dependent bromoperoxidase	P81701	*Ascophyllum nodosum*
comp32647_c0_seq22.p1	11.52481838	1.8506	9.28E-05	0.022447103	107			
comp31602_c0_seq5.p1	8.950114771	-2.343	0.00010082	0.024168725	108	Abhydrolase domain-containing protein FAM108A	Q5XIJ5	*Rattus norvegicus*
comp20385_c0_seq1.p1	11.01487269	-1.889	0.000103013	0.024467873	109	[Pyruvate dehydrogenase [lipoamide]] kinase, mitochondrial	P91622	*Drosophila melanogaster*
comp32927_c0_seq11.p1	7.839567212	2.8388	0.000108496	0.025536017	110			
comp32516_c0_seq9.p1	7.139010977	3.229	0.000144233	0.033641331	111	Probable outer membrane protein pmp6	Q9Z899	*Chlamydia pneumoniae*
comp33109_c0_seq1.p1*	15.30305253	-1.672	0.000155485	0.035942043	112	Poly(beta-D-mannuronate) C5 epimerase	Q88NC9	*Pseudomonas putida* (strain KT2440)
comp32948_c1_seq4.p1	14.02475974	1.6837	0.000158449	0.036303046	113			
comp32924_c0_seq5.p1	6.882559253	3.3887	0.000164298	0.037286375	114			
comp32733_c0_seq1.p1	12.00972628	1.7465	0.000165621	0.037286375	115			
comp26625_c0_seq1.p1	11.43466099	-1.784	0.000172172	0.038427036	116			
comp32116_c0_seq13.p1	7.284365851	-3.077	0.000181946	0.040261348	117			
comp33061_c0_seq20.p1	6.017964062	4.1184	0.000185998	0.040809266	118	CAP-Gly domain-containing linker protein 2	Q9Z0H8	*Mus musculus*
comp28121_c0_seq1.p1	6.628504838	3.5507	0.000197977	0.043072534	119	Heat shock 70 kDa protein	P41753	*Achlya klebsiana*
comp31208_c0_seq3.p1	8.064001502	2.6151	0.00020534	0.044302016	120	Phosphatidylinositol 4-phosphate 5-kinase 3	O48709	*Arabidopsis thaliana*
comp33777_c0_seq1.p1	10.67147184	1.8443	0.000209415	0.044807857	121	3-oxoacyl-[acyl-carrier-protein] reductase 1	P73574	*Synechocystis* sp. (strain PCC 6803 / Kazusa)
comp32728_c0_seq18.p3	-20.928435	26.768	0.000212027	0.044994876	122	Probable methyltransferase TARBP1	Q13395	*Homo sapiens*
comp26942_c0_seq1.p1	9.517956492	-2.059	0.000222853	0.046907841	123	Serine/threonine-protein kinase Nek1	Q96PY6	*Homo sapiens*
comp32243_c2_seq21.p1	-20.928435	26.751	0.000225639	0.047111194	124			
comp32794_c0_seq7.p1	9.50206588	2.0575	0.000233243	0.048309288	125			

* confirmation of expression level by RT-qPCR

Table 8. GO enrichment analysis of DEGs on each timepoint in *Silvetia babingtonii*

	Category	GO.ID	Term	Annotated	Significant	Expected	p value
Up-regulated on the late timepoint							
10h AF vs 24h AF	MF	GO:0004144	diacylglycerol O-acyltransferase activity	10	1	0.01	0.0059
	CC	GO:0000793	condensed chromosome	5	1	0	0.0046
		GO:0005694	chromosome	104	1	0.1	0.0937
Down-regulated on the late timepoint							
3 h AF vs 10h AF	MF	GO:0005215	transporter activity	286	5	0.98	0.0024
10h AF vs 24h AF	BP	GO:0006508	proteolysis	46	2	0.1	0.0037
		GO:0008219	cell death	4	1	0.01	0.0089
	MF	GO:0008146	sulfotransferase activity	10	2	0.05	0.001
		GO:0004366	glycerol-3-phosphate O-acyltransferase activity	11	2	0.05	0.0012
		GO:0016782	transferase activity, transferring sulfur-containing groups	11	2	0.05	0.0012
	CC	GO:0005576	extracellular region	82	3	0.27	0.0016

p value,0.01 was considered significant.

Table 9. The list of expressed mannuronan C-5 epimerase genes in *in Silvetia babingtonii*

Contig name	description	GO.IDs	GO.Names
comp12369_c0_seq1.p1	Mannuronan C-5-epimerase	GO:0016853,GO:0042121,GO:0042121, GO:0042121,GO:0042121,GO:0042597, GO:0042597	isomerase activity,alginic acid biosynthetic process,alginic acid biosynthetic process,alginic acid biosynthetic process,alginic acid biosynthetic process,periplasmic space,periplasmic space
comp12459_c0_seq1.p1	Mannuronan C-5-epimerase	GO:0016853,GO:0042121,GO:0042121, GO:0042597,GO:0042597	isomerase activity,alginic acid biosynthetic process,alginic acid biosynthetic process,periplasmic space,periplasmic space
comp12906_c0_seq3.p2	Mannuronan C-5-epimerase	GO:0016853,GO:0042121,GO:0042121, GO:0042597,GO:0042597	isomerase activity,alginic acid biosynthetic process,alginic acid biosynthetic process,periplasmic space,periplasmic space
comp20964_c0_seq2.p1	Mannuronan C-5-epimerase	GO:0016853,GO:0042121,GO:0042121, GO:0042121,GO:0042121,GO:0042597, GO:0042597	isomerase activity,alginic acid biosynthetic process,alginic acid biosynthetic process,alginic acid biosynthetic process,alginic acid biosynthetic process,periplasmic space,periplasmic space
comp26299_c0_seq1.p2	Mannuronan C-5-epimerase	GO:0016853,GO:0042121,GO:0042121, GO:0042597,GO:0042597	isomerase activity,alginic acid biosynthetic process,alginic acid biosynthetic process,periplasmic space,periplasmic space
comp26622_c0_seq1.p2	Mannuronan C-5-epimerase	GO:0016853,GO:0042121,GO:0042121, GO:0042597,GO:0042597	isomerase activity,alginic acid biosynthetic process,alginic acid biosynthetic process,periplasmic space,periplasmic space
comp28325_c0_seq4.p1	Mannuronan C-5-epimerase	GO:0016853,GO:0042121,GO:0042121, GO:0042121,GO:0042121,GO:0042597, GO:0042597	isomerase activity,alginic acid biosynthetic process,alginic acid biosynthetic process,alginic acid biosynthetic process,alginic acid biosynthetic process,periplasmic space,periplasmic space
comp31023_c0_seq4.p1	Mannuronan C-5-epimerase	GO:0016853,GO:0042121,GO:0042121, GO:0042597,GO:0042597	isomerase activity,alginic acid biosynthetic process,alginic acid biosynthetic process,periplasmic space,periplasmic space
comp31439_c0_seq3.p1	Mannuronan C-5-epimerase	GO:0016853,GO:0042121,GO:0042121, GO:0042121,GO:0042121,GO:0042597, GO:0042597	isomerase activity,alginic acid biosynthetic process,alginic acid biosynthetic process,alginic acid biosynthetic process,alginic acid biosynthetic process,periplasmic space,periplasmic space
comp32226_c0_seq11.p1	Mannuronan C-5-epimerase	GO:0016853,GO:0042121,GO:0042121, GO:0042597,GO:0042597	isomerase activity,alginic acid biosynthetic process,alginic acid biosynthetic process,periplasmic space,periplasmic space
comp32408_c2_seq17.p1	Mannuronan C-5-epimerase	GO:0016853,GO:0042121,GO:0042121, GO:0042597,GO:0042597	isomerase activity,alginic acid biosynthetic process,alginic acid biosynthetic process,periplasmic space,periplasmic space
comp32408_c2_seq19.p1	Mannuronan C-5-epimerase	GO:0016853,GO:0042121,GO:0042121, GO:0042597,GO:0042597	isomerase activity,alginic acid biosynthetic process,alginic acid biosynthetic process,periplasmic space,periplasmic space
comp32408_c2_seq24.p1	Mannuronan C-5-epimerase	GO:0016853,GO:0042121,GO:0042121, GO:0042597,GO:0042597	isomerase activity,alginic acid biosynthetic process,alginic acid biosynthetic process,periplasmic space,periplasmic space
comp32905_c0_seq30.p1	Mannuronan C-5-epimerase	GO:0016853,GO:0042121,GO:0042121, GO:0042597,GO:0042597	isomerase activity,alginic acid biosynthetic process,alginic acid biosynthetic process,periplasmic space,periplasmic space
comp32905_c0_seq33.p1	Mannuronan C-5-epimerase	GO:0016853,GO:0042121,GO:0042121, GO:0042597,GO:0042597	isomerase activity,alginic acid biosynthetic process,alginic acid biosynthetic process,periplasmic space,periplasmic space
comp32951_c0_seq26.p1	Mannuronan C-5-epimerase	GO:0016853,GO:0042121,GO:0042121, GO:0042597,GO:0042597	isomerase activity,alginic acid biosynthetic process,alginic acid biosynthetic process,periplasmic space,periplasmic space
comp32951_c0_seq4.p1	Mannuronan C-5-epimerase	GO:0016853,GO:0042121,GO:0042121, GO:0042597,GO:0042597	isomerase activity,alginic acid biosynthetic process,alginic acid biosynthetic process,periplasmic space,periplasmic space
comp33109_c0_seq1.p1	Mannuronan C-5-epimerase	GO:0016853,GO:0042121,GO:0042121, GO:0042597,GO:0042597	isomerase activity,alginic acid biosynthetic process,alginic acid biosynthetic process,periplasmic space,periplasmic space
comp41009_c0_seq1.p1	Mannuronan C-5-epimerase	GO:0016853,GO:0042121,GO:0042121, GO:0042597,GO:0042597	isomerase activity,alginic acid biosynthetic process,alginic acid biosynthetic process,periplasmic space,periplasmic space

Table 10. Chemical composition of ASP12 NTA medium

	Fe free	Fe-2 mg/L
NaCl	28 g	28 g
$MgSO_4$ $7H_2O$	7 g	7 g
$MgCl_2$ $6H_2O$	4 g	4 g
KCl	700 mg	700 mg
Tris	1 g	1 g
$NaNO_3$	100 mg	100 mg
Na_2 glycerophosphate	10 mg	10 mg
Vitamine B_{12}	0.2 µg	0.2 µg
Biotine	1 µg	1 µg
Thiamine HCl	100 µg	100 µg
PII metals (Fe-free)	10 ml	10 ml
SII metals	10 ml	10 ml
NTA	100 mg	100 mg
Na_2SiO_3 $9H_2O$	150 mg	150 mg
K_3PO_4	10 mg	10 mg
Ca (as Cl^-)	400 mg	400 mg
$(NH_4)_2Fe(SO_4)_2$ (as EDTA 1:1 molar)		2 mg
Total	1000 ml	1000 ml
	pH 7.8-8.0	pH 7.8-8.0

Table 11. Summary of RNA-seq data in *Saccharina japonica*

Sample name	Raw reads	Clean reads	Raw base (G)	Clean base (G)	Q30 (%)	GC (%)	Mapping rate
M_0	15083640	14866911	4.5	4.5	90.97	55.99	27.60%
M_3	15532141	15360756	4.7	4.6	90.81	56.19	27.00%
M_6	15686802	15444915	4.7	4.6	90.68	56.03	27.10%
F_0	16430399	16094874	4.93	4.83	89.35	59.20	71.50%
F_3	22886077	22553541	6.87	6.77	88.56	58.64	71.10%
F_6	18562161	18260215	5.57	5.48	89.1	58.91	71.80%

Table 12. The upregulated genes list on a: Consensus DEGs, b: Male consensus DEGs, e: Female consensus DEGs in *Saccharina japonica*

Name	Description	GO.IDs	GO.Names	Category*
SJ18910	ammonium transporter 1 member 1-like	F:GO:0008519; C:GO:0016021	F:ammonium transmembrane transporter activity; C:integral component of membrane	a
SJ20107	sperm-associated antigen 6	F:GO:0005515	F:protein binding	a
SJ18650	---NA---			a
SJ21804	ESV-1-226			a
SJ20767	---NA---			a
SJ06468	intraflagellar transport protein 56-like	F:GO:0005515; C:GO:0005929; P:GO:0007224; P:GO:0015031; C:GO:0030992; P:GO:0042073	F:protein binding; C:cilium; P:smoothened signaling pathway; P:protein transport; C:intraciliary transport particle B; P:intraciliary transport	a
SJ03135	---NA---			a
SJ10714	hypothetical protein AURANDRAFT_64780	F:GO:0003676; F:GO:0004721; C:GO:0016020; F:GO:0016491; P:GO:0035335; F:GO:0046872	F:nucleic acid binding; F:phosphoprotein phosphatase activity; C:membrane; F:oxidoreductase activity; P:peptidyl-tyrosine dephosphorylation; F:metal ion binding	a
SJ13712	---NA---			a
SJ13944	DUF11 domain-containing protein			a
SJ00920	zinc carboxypeptidase family protein, putative	F:GO:0003899; F:GO:0004181; F:GO:0005515; F:GO:0005524; C:GO:0005730; P:GO:0006144; P:GO:0006206; P:GO:0006351; F:GO:0008270; P:GO:0009069; C:GO:0016459; F:GO:0016905	F:DNA-directed 5'-3' RNA polymerase activity; F:metallocarboxypeptidase activity; F:protein binding; F:ATP binding; C:nucleolus; P:purine nucleobase metabolic process; P:pyrimidine nucleobase metabolic process; P:transcription, DNA-templated; F:zinc ion binding; P:serine family amino acid metabolic process; C:myosin complex; F:myosin heavy chain kinase activity	a
SJ08387	sperm flagellar protein 2-like	F:GO:0005509	F:calcium ion binding	a
SJ06267	dual specificity phosphatase domain protein	F:GO:0008138	F:protein tyrosine/serine/threonine phosphatase activity	a
SJ09523	intraflagellar transport protein 88 homolog isoform X2	F:GO:0005515; C:GO:0031514	F:protein binding; C:motile cilium	a
SJ13066	WSC-domain-containing protein	F:GO:0016798; P:GO:0055114; P:GO:0098869	F:hydrolase activity, acting on glycosyl bonds; P:oxidation-reduction process; P:cellular oxidant detoxification	a
SJ04346	---NA---	F:GO:0000981; C:GO:0005634; F:GO:0008270	F:RNA polymerase II transcription factor activity, sequence-specific DNA binding; C:nucleus; F:zinc ion binding	a
SJ06647	sporangia induced dynein heavy chain	P:GO:0003341; F:GO:0003777; F:GO:0005524; C:GO:0005858; C:GO:0005874; F:GO:0016887	P:cilium movement; F:microtubule motor activity; F:ATP binding; C:axonemal dynein complex; C:microtubule; F:ATPase activity	a
SJ09089	mucin-1 isoform X1			a
SJ07118	ankyrin repeat domain-containing protein	F:GO:0004672; F:GO:0005515; F:GO:0005524; F:GO:0046872	F:protein kinase activity; F:protein binding; F:ATP binding; F:metal ion binding	a
SJ04968	---NA---	F:GO:0005509	F:calcium ion binding	a
SJ06274	flagellar associated protein	F:GO:0005515	F:protein binding	a
SJ12457	predicted protein	F:GO:0005488; C:GO:0016021	F:binding; C:integral component of membrane	a
SJ03241	dnaJ homolog subfamily C member 27-like	F:GO:0003924; F:GO:0005525; C:GO:0005622; P:GO:0007264	F:GTPase activity; F:GTP binding; C:intracellular; P:small GTPase mediated signal transduction	a
SJ21438	phospholipid-transporting ATPase 3	F:GO:0000287; F:GO:0004012; F:GO:0005524; P:GO:0006812; P:GO:0015917; C:GO:0016021	F:magnesium ion binding; F:phospholipid-translocating ATPase activity; F:ATP binding; P:cation transport; P:aminophospholipid transport; C:integral component of membrane	a
SJ10052	intraflagellar transport protein 80 homolog	F:GO:0005515; C:GO:0005813; C:GO:0030992; C:GO:0031514	F:protein binding; C:centrosome; C:intraciliary transport particle B; C:motile cilium	a
SJ15296	---NA---			a
SJ07633	MBL fold metallo-hydrolase	F:GO:0016787	F:hydrolase activity	b
SJ17661	Protein kinase domain containing protein	F:GO:0004672; F:GO:0005524	F:protein kinase activity; F:ATP binding	b
SJ05479	---NA---			b
SJ18385	hypothetical protein AURANDRAFT_64738	F:GO:0005515	F:protein binding	b
SJ07631	MBL fold metallo-hydrolase	F:GO:0016787	F:hydrolase activity	b
SJ08451	---NA---			b
SJ16359	---NA---			b
SJ06086	serine threonine protein phosphatase	F:GO:0004721	F:phosphoprotein phosphatase activity	b
SJ01501	WD repeat-containing protein 19 isoform X1	F:GO:0005515; C:GO:0005929; C:GO:0030991; P:GO:0035721	F:protein binding; C:cilium; C:intraciliary transport particle A; P:intraciliary retrograde transport	b
SJ16199	Acyl-CoA-binding protein	F:GO:0005515	F:protein binding	b
SJ04268	SAM-dependent methyltransferase	C:GO:0005634; P:GO:0006979; P:GO:0030091; F:GO:0031151; F:GO:0033743; P:GO:0051726	C:nucleus; P:response to oxidative stress; P:protein repair; F:histone methyltransferase activity (H3-K79 specific); F:peptide-methionine (R)-S-oxide reductase activity; P:regulation of cell cycle	b
SJ18597	---NA---			b
SJ11559	---NA---			b
SJ20157	glutathione S-transferase	F:GO:0005515; F:GO:0016740	F:protein binding; F:transferase activity	b
SJ14913	AGC/PKA protein kinase	F:GO:0004691; F:GO:0005524; C:GO:0005952; P:GO:0009069	F:cAMP-dependent protein kinase activity; F:ATP binding; C:cAMP-dependent protein kinase complex; P:serine family amino acid metabolic process	b
SJ15436	predicted protein	F:GO:0005509; F:GO:0005515; C:GO:0016021	F:calcium ion binding; F:protein binding; C:integral component of membrane	b
SJ05309	---NA---			b
SJ09751	TIR domain-containing protein	F:GO:0005515	F:protein binding	b

SJ08874	---NA---			b
SJ15072	---NA---			b
SJ01535	B9 domain-containing protein 1	P:GO:0001701; P:GO:0001944; F:GO:0005515; C:GO:0005737; C:GO:0005813; P:GO:0007224; F:GO:0008158; C:GO:0016020; P:GO:0032880; C:GO:0036038; C:GO:0036064; P:GO:0042733; P:GO:0043010; P:GO:0060271; P:GO:0060563	P:in utero embryonic development; P:vasculature development; F:protein binding; C:cytoplasm; C:centrosome; P:smoothened signaling pathway; F:hedgehog receptor activity; C:membrane; P:regulation of protein localization; C:MKS complex; C:ciliary basal body; P:embryonic digit morphogenesis; P:camera-type eye development; P:cilium assembly; P:neuroepithelial cell differentiation	b
SJ20150	Tkp5 protein	C:GO:0000943; F:GO:0003676; F:GO:0003964; F:GO:0008270; P:GO:0015074; C:GO:0016021	C:retrotransposon nucleocapsid; F:nucleic acid binding; F:RNA-directed DNA polymerase activity; F:zinc ion binding; P:DNA integration; C:integral component of membrane	b
SJ14777	ATPase family AAA domain-containing protein 3-B	F:GO:0005524; C:GO:0005739; P:GO:0007005; C:GO:0016021	F:ATP binding; C:mitochondrion; P:mitochondrion organization; C:integral component of membrane	b
SJ05478	---NA---			b
SJ21916	LARGE xylosyl- and glucuronyltransferase 1-like	F:GO:0016740	F:transferase activity	b
SJ04226	---NA---			b
SJ16283	hypothetical protein GUITHDRAFT_151224			b
SJ13698	transmembrane protein, putative	F:GO:0003676; C:GO:0016021; F:GO:0016740; P:GO:0032259	F:nucleic acid binding; C:integral component of membrane; F:transferase activity; P:methylation	b
SJ13959	TRAF3-interacting protein 1	P:GO:0001738; P:GO:0001933; C:GO:0005813; C:GO:0005930; F:GO:0008017; C:GO:0030992; P:GO:0031076; P:GO:0031333; P:GO:0032688; P:GO:0035050; C:GO:0036064; P:GO:0036342; P:GO:0042073; P:GO:0042733; C:GO:0045298; P:GO:0050687; P:GO:0070507; P:GO:1901621	P:morphogenesis of a polarized epithelium; P:negative regulation of protein phosphorylation; C:centrosome; C:axoneme; F:microtubule binding; C:intraciliary transport particle B; P:embryonic camera-type eye development; P:negative regulation of protein complex assembly; P:negative regulation of interferon-beta production; P:embryonic heart tube development; C:ciliary basal body; P:post-anal tail morphogenesis; P:intraciliary transport; P:embryonic digit morphogenesis; C:tubulin complex; P:negative regulation of defense response to virus; P:regulation of microtubule cytoskeleton organization; P:negative regulation of smoothened signaling pathway involved in dorsal/ventral neural tube patterning	b
SJ00987	---NA---			b
SJ09452	Fibrillins and related proteins containing Ca2-binding EGF-like domains	F:GO:0005515; C:GO:0016021	F:protein binding; C:integral component of membrane	b
SJ12407	---NA---			b
SJ16764	predicted protein			b
SJ01703	ubiquitin carboxyl-terminal hydrolase 2-like isoform X1	P:GO:0016579; F:GO:0036459	P:protein deubiquitination; F:thiol-dependent ubiquitinyl hydrolase activity	b
SJ02768	DUF1565 domain-containing protein			b
SJ16200	Acyl-CoA-binding protein			b
SJ01468	predicted protein	F:GO:0004722; C:GO:0008287; F:GO:0046872	F:protein serine/threonine phosphatase activity; C:protein serine/threonine phosphatase complex; F:metal ion binding	b
SJ12100	dynein regulatory complex protein 1-like	C:GO:0005858; P:GO:0070286	C:axonemal dynein complex; P:axonemal dynein complex assembly	b
SJ11626	flagella associated protein	P:GO:0003341; C:GO:0005930; C:GO:0031514; P:GO:0036159; P:GO:0060285	P:cilium movement; C:axoneme; C:motile cilium; P:inner dynein arm assembly; P:cilium-dependent cell motility	b
SJ21382	uncharacterized protein LOC106162378	C:GO:0016020; C:GO:0016021	C:membrane; C:integral component of membrane	b
SJ00974	predicted protein	C:GO:0016021	C:integral component of membrane	b
SJ20611	---NA---	F:GO:0005515	F:protein binding	b
SJ13226	ankyrin repeat domain-containing protein	F:GO:0005515	F:protein binding	b
SJ06208	---NA---			b
SJ21781	phospholipid-translocating P-type ATPase	C:GO:0000139; F:GO:0000287; F:GO:0004012; F:GO:0005524; C:GO:0005802; C:GO:0005886; P:GO:0006812; P:GO:0006886; P:GO:0006892; P:GO:0015917; C:GO:0016021; P:GO:0032456; P:GO:0048194	C:Golgi membrane; F:magnesium ion binding; F:phospholipid-translocating ATPase activity; F:ATP binding; C:trans-Golgi network; C:plasma membrane; P:cation transport; P:intracellular protein transport; P:post-Golgi vesicle-mediated transport; P:aminophospholipid transport; C:integral component of membrane; P:endocytic recycling; P:Golgi vesicle budding	b
SJ20085	---NA---			b
SJ12977	Projectin/twitchin and related proteins	F:GO:0005515	F:protein binding	b
SJ19396	---NA---			b
SJ04255	tubulin beta chain	F:GO:0003924; F:GO:0005200; F:GO:0005525; C:GO:0005737; C:GO:0005874; P:GO:0007017; C:GO:0016021	F:GTPase activity; F:structural constituent of cytoskeleton; F:GTP binding; C:cytoplasm; C:microtubule; P:microtubule-based process; C:integral component of membrane	b
SJ09526	predicted protein	F:GO:0005488; C:GO:0016020	F:binding; C:membrane	b
SJ01297	---NA---			b
SJ04063	---NA---			b
SJ21789	---NA---			b

SJ00718	serine O-acetyltransferase	C:GO:0005737; P:GO:0006535; F:GO:0009001; P:GO:0042967	C:cytoplasm; P:cysteine biosynthetic process from serine; F:serine O-acetyltransferase activity; P:obsolete acyl-carrier-protein biosynthetic process	b
SJ03349	TKL protein kinase	F:GO:0004674; F:GO:0005524; P:GO:0007165; P:GO:0009069	F:protein serine/threonine kinase activity; F:ATP binding; P:signal transduction; P:serine family amino acid metabolic process	b
SJ08449	---NA---			b
SJ04227	---NA---			b
SJ06476	RxLR-like protein	F:GO:0008270; C:GO:0016021; F:GO:0016787; P:GO:0046856	F:zinc ion binding; C:integral component of membrane; F:hydrolase activity; P:phosphatidylinositol dephosphorylation	b
SJ19546	hypothetical protein AURANDRAFT_64519			b
SJ00194	leucine-rich repeat and guanylate kinase domain-containing protein-like	F:GO:0005515; F:GO:0016301	F:protein binding; F:kinase activity	b
SJ14090	---NA---			b
SJ07431	---NA---			b
SJ20267	type IV inositol polyphosphate 5-phosphatase 11	F:GO:0042578; P:GO:0046856	F:phosphoric ester hydrolase activity; P:phosphatidylinositol dephosphorylation	b
SJ02178	---NA---			b
SJ17100	conserved hypothetical protein	F:GO:0003678; C:GO:0005844; P:GO:0006449; C:GO:0010494; P:GO:0032508; F:GO:0046872	F:DNA helicase activity; C:polysome; P:regulation of translational termination; C:cytoplasmic stress granule; P:DNA duplex unwinding; F:metal ion binding	b
SJ06752	E3 ubiquitin protein ligase	F:GO:0005515; C:GO:0016020	F:protein binding; C:membrane	b
SJ10860	---NA---			b
SJ12476	Immunoglobulin-like fold			b
SJ10046	hypothetical protein PPTG_09172	F:GO:0005509	F:calcium ion binding	b
SJ02681	E3 ubiquitin-protein ligase pellino homolog 1	P:GO:0008063	P:Toll signaling pathway	b
SJ16076	kinesin-like protein KIF11	P:GO:0001525; F:GO:0003777; F:GO:0005524; C:GO:0005874; P:GO:0007018; F:GO:0008017; P:GO:0022008; C:GO:0045298; P:GO:0051726	P:angiogenesis; F:microtubule motor activity; F:ATP binding; C:microtubule; P:microtubule-based movement; F:microtubule binding; P:neurogenesis; C:tubulin complex; P:regulation of cell cycle	b
SJ02568	dynein heavy chain 7, axonemal isoform X1	P:GO:0003341; F:GO:0003777; F:GO:0005509; F:GO:0005524; C:GO:0005874; C:GO:0036156; P:GO:0036159	P:cilium movement; F:microtubule motor activity; F:calcium ion binding; F:ATP binding; C:microtubule; C:inner dynein arm; P:inner dynein arm assembly	b
SJ02566	dynein heavy chain 7, axonemal-like	F:GO:0003777; F:GO:0005509; F:GO:0005524; C:GO:0005874; P:GO:0007018; C:GO:0030286	F:microtubule motor activity; F:calcium ion binding; F:ATP binding; C:microtubule; P:microtubule-based movement; C:dynein complex	b
SJ03191	predicted protein	F:GO:0004420; P:GO:0015936; C:GO:0016020; C:GO:0016021; F:GO:0050662; P:GO:0055114	F:hydroxymethylglutaryl-CoA reductase (NADPH) activity; P:coenzyme A metabolic process; C:membrane; C:integral component of membrane; F:coenzyme binding; P:oxidation-reduction process	b
SJ04963	---NA---			b
SJ02337	transmembrane protein, putative	F:GO:0005509; C:GO:0016021	F:calcium ion binding; C:integral component of membrane	b
SJ02567	dynein heavy chain 7, axonemal-like	P:GO:0003341; F:GO:0003777; F:GO:0005509; F:GO:0005524; C:GO:0005874; F:GO:0016887; C:GO:0036156; P:GO:0036159	P:cilium movement; F:microtubule motor activity; F:calcium ion binding; F:ATP binding; C:microtubule; F:ATPase activity; C:inner dynein arm; P:inner dynein arm assembly	b
SJ02520	EF-hand domain-containing protein 1	F:GO:0005509	F:calcium ion binding	b
SJ08221	copper radical oxidase	C:GO:0005783	C:endoplasmic reticulum	b
SJ12971	dynein heavy chain	F:GO:0003777; F:GO:0005524; C:GO:0005874; P:GO:0007018; F:GO:0016887; C:GO:0030286	F:microtubule motor activity; F:ATP binding; C:microtubule; P:microtubule-based movement; F:ATPase activity; C:dynein complex	b
SJ06892	dynein heavy chain 6, axonemal	F:GO:0003777; F:GO:0005524; C:GO:0005858; C:GO:0005874; P:GO:0007018; F:GO:0016887; P:GO:0060285	F:microtubule motor activity; F:ATP binding; C:axonemal dynein complex; C:microtubule; P:microtubule-based movement; F:ATPase activity; P:cilium-dependent cell motility	b
SJ06174	---NA---			b
SJ17089	Leucine-rich repeat, ribonuclease inhibitor subtype	F:GO:0005515	F:protein binding	b
SJ02359	hypothetical protein SDRG_06794	F:GO:0003824; F:GO:0005509; F:GO:0008270	F:catalytic activity; F:calcium ion binding; F:zinc ion binding	b
SJ16016	Chaperone DnaJ-domain superfamily protein	C:GO:0005634; C:GO:0005737; P:GO:0006457	C:nucleus; C:cytoplasm; P:protein folding	b
SJ04773	---NA---			b
SJ20540	---NA---			b
SJ13931	hypothetical protein H310_14689			b
SJ18578	kinesin-like protein	F:GO:0003777; F:GO:0005524; C:GO:0005871; C:GO:0005874; P:GO:0007018; F:GO:0008017; F:GO:0016887; C:GO:0045298	F:microtubule motor activity; F:ATP binding; C:kinesin complex; C:microtubule; P:microtubule-based movement; F:microtubule binding; F:ATPase activity; C:tubulin complex	b
SJ04064	multiple C2 and transmembrane domain-containing protein 1 isoform X2	F:GO:0005515	F:protein binding	b

SJ16651	protein tyrosine phosphatase domain-containing protein 1-like	F:GO:0004725; C:GO:0005634; C:GO:0005737; P:GO:0006570; P:GO:0007224; F:GO:0008138; P:GO:0060271	F:protein tyrosine phosphatase activity; C:nucleus; C:cytoplasm; P:tyrosine metabolic process; P:smoothened signaling pathway; F:protein tyrosine/serine/threonine phosphatase activity; P:cilium assembly	b
SJ16213	Vacuolar protein 8	F:GO:0005515; C:GO:0005634; C:GO:0005774; P:GO:0007033; P:GO:0022607; P:GO:0034727; P:GO:0051641	F:protein binding; C:nucleus; C:vacuolar membrane; P:vacuole organization; P:cellular component assembly; P:piecemeal microautophagy of the nucleus; P:cellular localization	b
SJ09734	hypothetical protein, variant			b
SJ12968	dynein heavy chain	F:GO:0003777; F:GO:0005524; C:GO:0005874; P:GO:0007018; F:GO:0016887; C:GO:0030286; C:GO:0031514	F:microtubule motor activity; F:ATP binding; C:microtubule; P:microtubule-based movement; F:ATPase activity; C:dynein complex; C:motile cilium	b
SJ18100	hydrocephalus-inducing protein	P:GO:0003341	P:cilium movement	b
SJ15719	---NA---			b
SJ22590	probable xyloglucan galactosyltransferase GT19			b
SJ06291	WD repeat-containing protein 17 isoform X2	F:GO:0005515	F:protein binding	b
SJ02066	---NA---			b
SJ05936	probable E3 ubiquitin-protein ligase HERC3 isoform X2	F:GO:0003824; P:GO:0016567	F:catalytic activity; P:protein ubiquitination	b
SJ07234	---NA---			b
SJ02893	---NA---			b
SJ13814	---NA---			b
SJ03661	hypothetical protein PHYSODRAFT_260187	F:GO:0005509; P:GO:0006952; C:GO:0016021	F:calcium ion binding; P:defense response; C:integral component of membrane	b
SJ10675	hypothetical protein EMIHUDRAFT_109098	F:GO:0003677; F:GO:0003916; F:GO:0005524; C:GO:0005694; P:GO:0006265; P:GO:0006511; P:GO:0016579; F:GO:0036459	F:DNA binding; F:DNA topoisomerase activity; F:ATP binding; C:chromosome; P:DNA topological change; P:ubiquitin-dependent protein catabolic process; P:protein deubiquitination; F:thiol-dependent ubiquitinyl hydrolase activity	b
SJ14390	---NA---			b
SJ09326	hypothetical protein AURANDRAFT_66361, partial	F:GO:0005509; C:GO:0016020	F:calcium ion binding; C:membrane	b
SJ03868	ankyrin repeat domain-containing protein	F:GO:0005515	F:protein binding	b
SJ02950	Acyl-CoA-binding protein			b
SJ18654	tubulin polyglutamylase TTLL13-like isoform X4	F:GO:0005524; P:GO:0006464	F:ATP binding; P:cellular protein modification process	b
SJ00312	---NA---			b
SJ15918	PAP2/haloperoxidase-like protein	F:GO:0004601; P:GO:0006804; P:GO:0006979	F:peroxidase activity; P:obsolete peroxidase reaction; P:response to oxidative stress	b
SJ11410	---NA---			b
SJ06893	dynein heavy chain	F:GO:0003777; F:GO:0005524; C:GO:0005858; C:GO:0005874; P:GO:0007018; F:GO:0016887; P:GO:0060285	F:microtubule motor activity; F:ATP binding; C:axonemal dynein complex; C:microtubule; P:microtubule-based movement; F:ATPase activity; P:cilium-dependent cell motility	b
SJ10769	---NA---			b
SJ12873	tetratricopeptide repeat protein	F:GO:0005515; P:GO:0006396; C:GO:0016021	F:protein binding; P:RNA processing; C:integral component of membrane	b
SJ20461	---NA---	F:GO:0005515	F:protein binding	b
SJ13930	---NA---			b
SJ05175	radial spoke head protein 6 homolog A-like	C:GO:0031514	C:motile cilium	b
SJ19829	osmotic avoidance abnormal protein 3 isoform X1	F:GO:0003777; F:GO:0005524; C:GO:0005769; C:GO:0005871; C:GO:0005874; C:GO:0005886; C:GO:0005912; C:GO:0005929; P:GO:0007288; P:GO:0007411; P:GO:0007605; P:GO:0007608; F:GO:0008017; P:GO:0008089; F:GO:0016887; P:GO:0030177; P:GO:0030951; C:GO:0045298; P:GO:1905515	F:microtubule motor activity; F:ATP binding; C:early endosome; C:kinesin complex; C:microtubule; C:plasma membrane; C:adherens junction; C:cilium; P:sperm axoneme assembly; P:axon guidance; P:sensory perception of sound; P:sensory perception of smell; F:microtubule binding; P:anterograde axonal transport; F:ATPase activity; P:positive regulation of Wnt signaling pathway; P:establishment or maintenance of microtubule cytoskeleton polarity; C:tubulin complex; P:non-motile cilium assembly	b
SJ12979	glycosyl hydrolase	F:GO:0005515	F:protein binding	b
SJ08519	protein phosphatase 1 regulatory subunit 12A isoform X1	F:GO:0005515	F:protein binding	b
SJ21070	ankyrin-2 isoform X6	F:GO:0005515; F:GO:0008138	F:protein binding; F:protein tyrosine/serine/threonine phosphatase activity	b
SJ07078	---NA---			b
SJ12209	---NA---	F:GO:0003676; F:GO:0005515	F:nucleic acid binding; F:protein binding	b
SJ10845	calcium/calmodulin-dependent 3',5'-cyclic nucleotide phosphodiesterase 1C isoform X2	F:GO:0004114; P:GO:0006144; P:GO:0007165	F:3',5'-cyclic-nucleotide phosphodiesterase activity; P:purine nucleobase metabolic process; P:signal transduction	b
SJ22184	---NA---	F:GO:0005515	F:protein binding	b
SJ19591	---NA---			b
SJ21710	---NA---			b
SJ16773	disintegrin and metalloproteinase domain-containing protein 9	P:GO:0006508	P:proteolysis	b
SJ06466	---NA---	F:GO:0005515	F:protein binding	b
SJ05091	hypothetical protein	C:GO:0016020; C:GO:0016021	C:membrane; C:integral component of membrane	b

SJ16593	---NA---	F:GO:0005515	F:protein binding	b
SJ13409	RING-H2 finger protein ATL74	F:GO:0008270; C:GO:0016021; P:GO:0016567; C:GO:0044424	F:zinc ion binding; C:integral component of membrane; P:protein ubiquitination; C:intracellular part	b
SJ02562	---NA---			b
SJ13419	hypothetical protein	F:GO:0005509	F:calcium ion binding	b
SJ16029	26S proteasome non-ATPase regulatory subunit 10	F:GO:0005515; C:GO:0005618	F:protein binding; C:cell wall	b
SJ21482	PPE family protein			b
SJ08902	hypothetical protein	P:GO:0006629; F:GO:0008081	P:lipid metabolic process; F:phosphoric diester hydrolase activity	b
SJ02781	echinoderm microtubule-associated protein-like 2 isoform X1	F:GO:0005515	F:protein binding	b
SJ00204	---NA---			b
SJ02345	---NA---			b
SJ04303	cobalamin biosynthesis protein CobT	F:GO:0005515	F:protein binding	b
SJ15993	hypothetical protein AURANDRAFT_61099			b
SJ07233	FOG: RCC1 domain	F:GO:0004842; F:GO:0005515; C:GO:0005634; C:GO:0005737; F:GO:0016874; F:GO:0046872	F:ubiquitin-protein transferase activity; F:protein binding; C:nucleus; C:cytoplasm; F:ligase activity; F:metal ion binding	b
SJ11411	---NA---			b
SJ05255	hypothetical protein SPRG_10950			b
SJ15899	leucine-rich repeat-containing protein 49	F:GO:0005515; C:GO:0016021	F:protein binding; C:integral component of membrane	b
SJ01842	---NA---			b
SJ05617	cleavage induced predicted protein			b
SJ13811	kinesin-like protein KIF9	F:GO:0003777; F:GO:0005524; C:GO:0005871; C:GO:0005874; P:GO:0007018; F:GO:0008017; F:GO:0016887; C:GO:0045298	F:microtubule motor activity; F:ATP binding; C:kinesin complex; C:microtubule; P:microtubule-based movement; F:microtubule binding; F:ATPase activity; C:tubulin complex	b
SJ16627	kinesin-like protein	F:GO:0003777; F:GO:0005524; C:GO:0005871; C:GO:0005874; P:GO:0007018; F:GO:0008017; C:GO:0016021; F:GO:0016887; P:GO:0030705; C:GO:0030993; P:GO:0034606; P:GO:0034608; C:GO:0045298	F:microtubule motor activity; F:ATP binding; C:kinesin complex; C:microtubule; P:microtubule-based movement; F:microtubule binding; C:integral component of membrane; F:ATPase activity; P:cytoskeleton-dependent intracellular transport; C:axonemal heterotrimeric kinesin-II complex; P:response to hermaphrodite contact; P:vulval location; C:tubulin complex	b
SJ09914	predicted protein	F:GO:0005524; C:GO:0005739; P:GO:0007005; C:GO:0016021	F:ATP binding; C:mitochondrion; P:mitochondrion organization; C:integral component of membrane	b
SJ13704	---NA---			b
SJ16771	---NA---			b
SJ01605	calmodulin-like protein 3	F:GO:0005509; C:GO:0070062	F:calcium ion binding; C:extracellular exosome	b
SJ03373	cyclic nucleotide-binding-like protein	C:GO:0005952; F:GO:0008603; F:GO:0030552	C:cAMP-dependent protein kinase complex; F:cAMP-dependent protein kinase regulator activity; F:cAMP binding	b
SJ21343	---NA---			b
SJ18101	hydrocephalus-inducing protein, putative	P:GO:0003341; C:GO:0016020	P:cilium movement; C:membrane	b
SJ16952	---NA---			b
SJ20996	dynein heavy chain 2, axonemal-like isoform X1	F:GO:0003777; F:GO:0005524; C:GO:0005874; P:GO:0007018; F:GO:0016887; C:GO:0030286; C:GO:0031514	F:microtubule motor activity; F:ATP binding; C:microtubule; P:microtubule-based movement; F:ATPase activity; C:dynein complex; C:motile cilium	b
SJ14602	ankyrin-3 isoform X22	P:GO:0000226; P:GO:0007605; P:GO:0007614; F:GO:0008092; P:GO:0019233; C:GO:0031594; C:GO:0036062; C:GO:0043195; P:GO:0045887; P:GO:0048675; P:GO:0070050; P:GO:1900074	P:microtubule cytoskeleton organization; P:sensory perception of sound; P:short-term memory; F:cytoskeletal protein binding; P:sensory perception of pain; C:neuromuscular junction; C:presynaptic periactive zone; C:terminal bouton; P:positive regulation of synaptic growth at neuromuscular junction; P:axon extension; P:neuron cellular homeostasis; P:negative regulation of neuromuscular synaptic transmission	b
SJ10850	leucine-rich repeat-containing protein 49-like	F:GO:0005515	F:protein binding	b
SJ22248	DUF4962 domain-containing protein	F:GO:0003824	F:catalytic activity	b
SJ20322	---NA---			b
SJ09732	---NA---			b
SJ02759	hypothetical protein SPRG_05045			b
SJ13025	---NA---			b
SJ02954	---NA---			b
SJ07487	rab9 effector protein with kelch motifs-like isoform X2	F:GO:0005515	F:protein binding	b
SJ04052	tenascin-like protein			b
SJ12980	titin, putative	F:GO:0005515	F:protein binding	b
SJ02805	CMGC/MAPK protein kinase	F:GO:0004707; F:GO:0005524; C:GO:0005634; P:GO:0007178; P:GO:0009069	F:MAP kinase activity; F:ATP binding; C:nucleus; P:transmembrane receptor protein serine/threonine kinase signaling pathway; P:serine family amino acid metabolic process	b
SJ03386	dual specificity phosphatase, catalytic domain containing protein	F:GO:0004672; F:GO:0005524; P:GO:0006470; F:GO:0016791	F:protein kinase activity; F:ATP binding; P:protein dephosphorylation; F:phosphatase activity	b
SJ04316	response receiver	P:GO:0000160; F:GO:0005515; C:GO:0005622	P:phosphorelay signal transduction system; F:protein binding; C:intracellular	b

SJ06650	sporangia induced dynein heavy chain	P:GO:0003341; F:GO:0003777; F:GO:0005524; C:GO:0005858; C:GO:0005874; F:GO:0016887	P:cilium movement; F:microtubule motor activity; F:ATP binding; C:axonemal dynein complex; C:microtubule; F:ATPase activity	b
SJ19264	rasGAP-activating-like protein 1	F:GO:0005515	F:protein binding	b
SJ19922	---NA---			b
SJ02680	dynein intermediate chain 2, ciliary-like isoform X3	F:GO:0004674; F:GO:0005515; F:GO:0005524; P:GO:0009069; C:GO:0031514	F:protein serine/threonine kinase activity; F:protein binding; F:ATP binding; P:serine family amino acid metabolic process; C:motile cilium	b
SJ00299	cilia- and flagella-associated protein 54 isoform X7			b
SJ15292	---NA---			b
SJ10147	endo-1,3(4)-beta-glucanase, putative	C:GO:0005622; P:GO:0005982; P:GO:0005985; P:GO:0006076; C:GO:0009986; C:GO:0016021; P:GO:0030036; F:GO:0042973; F:GO:0052861	C:intracellular; P:starch metabolic process; P:sucrose metabolic process; P:(1->3)-beta-D-glucan catabolic process; C:cell surface; C:integral component of membrane; P:actin cytoskeleton organization; F:glucan endo-1,3-beta-D-glucosidase activity; F:glucan endo-1,3-beta-glucanase activity, C-3 substituted reducing group	b
SJ01538	---NA---			b
SJ08537	---NA---			b
SJ16254	glycosyltransferase family 77 protein	C:GO:0016020	C:membrane	b
SJ02825	echinoderm microtubule-associated protein-like 6	F:GO:0005515	F:protein binding	b
SJ22498	low-density lipoprotein receptor-related protein 6-like	C:GO:0016020; C:GO:0016021	C:membrane; C:integral component of membrane	b
SJ11673	---NA---	F:GO:0005515	F:protein binding	b
SJ14525	predicted protein	C:GO:0016021; P:GO:0055114	C:integral component of membrane; P:oxidation-reduction process	b
SJ06894	dynein heavy chain	P:GO:0001539; F:GO:0003777; F:GO:0005524; C:GO:0005858; C:GO:0005874; P:GO:0007018; F:GO:0016887	P:cilium or flagellum-dependent cell motility; F:microtubule motor activity; F:ATP binding; C:axonemal dynein complex; C:microtubule; P:microtubule-based movement; F:ATPase activity	b
SJ12909	---NA---	F:GO:0005515	F:protein binding	b
SJ19899	WD domain, G-beta repeat protein	F:GO:0005515	F:protein binding	b
SJ21332	tetratricopeptide repeat protein 21B	F:GO:0005515; C:GO:0005929; C:GO:0016021; C:GO:0030991; P:GO:0035721; P:GO:0060271; P:GO:0061512	F:protein binding; C:cilium; C:integral component of membrane; C:intraciliary transport particle A; P:intraciliary retrograde transport; P:cilium assembly; P:protein localization to cilium	b
SJ01312	guanylyl cyclase	C:GO:0005622; P:GO:0009190; F:GO:0016849; P:GO:0035556	C:intracellular; P:cyclic nucleotide biosynthetic process; F:phosphorus-oxygen lyase activity; P:intracellular signal transduction	b
SJ10421	---NA---			b
SJ17652	predicted protein	C:GO:0016020	C:membrane	b
SJ18978	transmembrane protein, putative	C:GO:0016021	C:integral component of membrane	b
SJ02669	---NA---			b
SJ04058	---NA---	F:GO:0005515	F:protein binding	b
SJ14623	voltage-dependent calcium channel type A subunit alpha-1 isoform X4	C:GO:0001518; F:GO:0005244; F:GO:0005248; F:GO:0005509; P:GO:0019228; P:GO:0034765; P:GO:0070588; P:GO:0086010	C:voltage-gated sodium channel complex; F:voltage-gated ion channel activity; F:voltage-gated sodium channel activity; F:calcium ion binding; P:neuronal action potential; P:regulation of ion transmembrane transport; P:calcium ion transmembrane transport; P:membrane depolarization during action potential	b
SJ22244	---NA---			b
SJ17404	---NA---			b
SJ21941	NAD(P)/FAD-dependent oxidoreductase	F:GO:0016491	F:oxidoreductase activity	b
SJ06630	creatine kinase	F:GO:0005215; F:GO:0005524; P:GO:0006810; C:GO:0016021; F:GO:0016301	F:transporter activity; F:ATP binding; P:transport; C:integral component of membrane; F:kinase activity	b
SJ16774	---NA---			b
SJ13502	predicted protein			b
SJ07662	---NA---			b
SJ10543	---NA---			b
SJ14979	---NA---			b
SJ18722	zinc finger BED domain-containing protein 1-like	F:GO:0003677; F:GO:0046983	F:DNA binding; F:protein dimerization activity	b
SJ19376	hypothetical protein SPRG_02654	F:GO:0004420; F:GO:0005509; P:GO:0006694	F:hydroxymethylglutaryl-CoA reductase (NADPH) activity; F:calcium ion binding; P:steroid biosynthetic process	b
SJ07068	coiled-coil domain-containing protein 180-like			b
SJ17134	ptype atpase	F:GO:0005509	F:calcium ion binding	b
SJ00384	---NA---			b
SJ01885	sperm-tail PG-rich repeat-containing protein 2-like			b

SJ17590	26S proteasome non-ATPase regulatory subunit 10-like	P:GO:0000022; C:GO:0000235; P:GO:0000742; C:GO:0000777; F:GO:0005524; C:GO:0005634; C:GO:0005871; F:GO:0008017; F:GO:0008569; P:GO:0030951; P:GO:0031122; P:GO:0031534; C:GO:0035371; C:GO:0036449; C:GO:0045298; C:GO:0055028; P:GO:0090561	P:mitotic spindle elongation; C:astral microtubule; P:karyogamy involved in conjugation with cellular fusion; C:condensed chromosome kinetochore; F:ATP binding; C:nucleus; C:kinesin complex; F:microtubule binding; F:ATP-dependent microtubule motor activity, minus-end-directed; P:establishment or maintenance of microtubule cytoskeleton polarity; P:cytoplasmic microtubule organization; P:minus-end directed microtubule sliding; C:microtubule plus-end; C:microtubule minus-end; C:tubulin complex; C:cortical microtubule; P:nuclear migration during mitotic telophase	b
SJ20936	hypothetical protein SPRG_00993			b
SJ05161	---NA---			b
SJ09119	predicted protein	C:GO:0031514	C:motile cilium	b
SJ07606	protein OSCP1 isoform X2			b
SJ00713	---NA---	P:GO:0000160	P:phosphorelay signal transduction system	b
SJ07110	---NA---	F:GO:0005515	F:protein binding	b
SJ14171	---NA---			b
SJ01691	---NA---			b
SJ16439	predicted protein	F:GO:0004674; F:GO:0005509; C:GO:0005634; C:GO:0005737; P:GO:0009069; P:GO:0035556	F:protein serine/threonine kinase activity; F:calcium ion binding; C:nucleus; C:cytoplasm; P:serine family amino acid metabolic process; P:intracellular signal transduction	b
SJ16116	---NA---			b
SJ18866	leucine rich repeat protein	F:GO:0004842; F:GO:0005515	F:ubiquitin-protein transferase activity; F:protein binding	b
SJ19861	---NA---			b
SJ19763	annexin D3	F:GO:0005509; F:GO:0005544	F:calcium ion binding; F:calcium-dependent phospholipid binding	b
SJ08602	---NA---			b
SJ12967	dynein heavy chain	F:GO:0003777; F:GO:0005524; C:GO:0005874; P:GO:0007018; F:GO:0016887; C:GO:0030286	F:microtubule motor activity; F:ATP binding; C:microtubule; P:microtubule-based movement; F:ATPase activity; C:dynein complex	b
SJ18328	kinesin-like protein	F:GO:0003777; F:GO:0005524; C:GO:0005871; C:GO:0005874; P:GO:0007018; F:GO:0008017; F:GO:0016887; C:GO:0045298	F:microtubule motor activity; F:ATP binding; C:kinesin complex; C:microtubule; P:microtubule-based movement; F:microtubule binding; F:ATPase activity; C:tubulin complex	b
SJ18326	kinesin-like protein	F:GO:0000166; F:GO:0003777; F:GO:0005524; P:GO:0007018; F:GO:0008017	F:nucleotide binding; F:microtubule motor activity; F:ATP binding; P:microtubule-based movement; F:microtubule binding	b
SJ19904	kinesin-like protein KIF9	F:GO:0003777; F:GO:0005524; C:GO:0005871; C:GO:0005874; P:GO:0007018; F:GO:0008017; F:GO:0016887; C:GO:0045298	F:microtubule motor activity; F:ATP binding; C:kinesin complex; C:microtubule; P:microtubule-based movement; F:microtubule binding; F:ATPase activity; C:tubulin complex	b
SJ13815	hypothetical protein			b
SJ01471	cilia- and flagella-associated protein 74-like			b
SJ00637	---NA---			b
SJ09568	hypothetical protein AURANDRAFT_70522	C:GO:0016020; C:GO:0016021	C:membrane; C:integral component of membrane	b
SJ21607	---NA---	F:GO:0050825	F:ice binding	b
SJ21890	---NA---			b
SJ02814	cyclic nucleotide-binding protein	F:GO:0005249; C:GO:0008076; P:GO:0042391	F:voltage-gated potassium channel activity; C:voltage-gated potassium channel complex; P:regulation of membrane potential	b
SJ11430	probable LRR receptor-like serine/threonine-protein kinase At3g47570	F:GO:0000166; F:GO:0004672; F:GO:0005515; C:GO:0016020	F:nucleotide binding; F:protein kinase activity; F:protein binding; C:membrane	b
SJ17403	Concanavalin A-like lectin/glucanase, subgroup			b
SJ15976	MGC84469 protein	F:GO:0005509; C:GO:0016021; C:GO:0031514	F:calcium ion binding; C:integral component of membrane; C:motile cilium	b
SJ00298	cilia- and flagella-associated protein 54	P:GO:0007283; P:GO:0060294	P:spermatogenesis; P:cilium movement involved in cell motility	b
SJ01402	---NA---			b
SJ06251	flagellar associated protein	P:GO:0006629; F:GO:0008081; C:GO:0031514	P:lipid metabolic process; F:phosphoric diester hydrolase activity; C:motile cilium	b
SJ01652	mastigoneme-like protein	F:GO:0005488; P:GO:0006468; P:GO:0007154; C:GO:0016021; F:GO:0016301	F:binding; P:protein phosphorylation; P:cell communication; C:integral component of membrane; F:kinase activity	b
SJ06603	predicted protein	C:GO:0005929; P:GO:0006909; F:GO:0035091; F:GO:0051015; P:GO:0061512	C:cilium; P:phagocytosis; F:phosphatidylinositol binding; F:actin filament binding; P:protein localization to cilium	b
SJ21069	dynein heavy chain 9, axonemal	P:GO:0000160; F:GO:0003777; F:GO:0005515; F:GO:0005524; C:GO:0005874; C:GO:0005930; P:GO:0007018; F:GO:0016887; C:GO:0030286	P:phosphorelay signal transduction system; F:microtubule motor activity; F:protein binding; F:ATP binding; C:microtubule; C:axoneme; P:microtubule-based movement; F:ATPase activity; C:dynein complex	b

SJ08465	kinesin-like protein kif6	F:GO:0003777; F:GO:0005524; C:GO:0005871; C:GO:0005874; P:GO:0007018; F:GO:0008017; F:GO:0016887; C:GO:0045298	F:microtubule motor activity; F:ATP binding; C:kinesin complex; C:microtubule; P:microtubule-based movement; F:microtubule binding; F:ATPase activity; C:tubulin complex	b
SJ16595	predicted protein	P:GO:0007154; C:GO:0016020; C:GO:0016021	P:cell communication; C:membrane; C:integral component of membrane	b
SJ17665	predicted protein	F:GO:0070403	F:NAD+ binding	b
SJ12950	predicted protein	C:GO:0005634; C:GO:0005930; F:GO:0008233; P:GO:0035082; P:GO:0060294	C:nucleus; C:axoneme; F:peptidase activity; P:axoneme assembly; P:cilium movement involved in cell motility	b
SJ22341	---NA---			b
SJ01262	---NA---			b
SJ11429	LRR receptor-like serine/threonine-protein kinase RCH1	F:GO:0000166; F:GO:0004672; F:GO:0005515; P:GO:0010082; C:GO:0016020	F:nucleotide binding; F:protein kinase activity; F:protein binding; P:regulation of root meristem growth; C:membrane	b
SJ20998	dynein heavy chain 2, axonemal-like isoform X1	F:GO:0003777; F:GO:0005524; C:GO:0005874; P:GO:0007018; F:GO:0016887; C:GO:0030286	F:microtubule motor activity; F:ATP binding; C:microtubule; P:microtubule-based movement; F:ATPase activity; C:dynein complex	b
SJ13929	---NA---			b
SJ20198	Voltage-gated Ion Channel (VIC) Superfamily	F:GO:0005245; F:GO:0005509; C:GO:0005891; P:GO:0034765; P:GO:0086010	F:voltage-gated calcium channel activity; F:calcium ion binding; C:voltage-gated calcium channel complex; P:regulation of ion transmembrane transport; P:membrane depolarization during action potential	b
SJ18689	---NA---			b
SJ05018	---NA---	F:GO:0005515	F:protein binding	b
SJ20435	AGC protein kinase	F:GO:0004674; F:GO:0005524; C:GO:0005634; C:GO:0005737; P:GO:0009069; P:GO:0035556	F:protein serine/threonine kinase activity; F:ATP binding; C:nucleus; C:cytoplasm; P:serine family amino acid metabolic process; P:intracellular signal transduction	b
SJ13277	---NA---			b
SJ00858	predicted protein	C:GO:0016021	C:integral component of membrane	b
SJ06403	predicted protein	F:GO:0005515; F:GO:0008081; C:GO:0016020; P:GO:0018106; P:GO:0050896	F:protein binding; F:phosphoric diester hydrolase activity; C:membrane; P:peptidyl-histidine phosphorylation; P:response to stimulus	b
SJ18826	---NA---			b
SJ01797	---NA---	F:GO:0005515; P:GO:0045292	F:protein binding; P:mRNA cis splicing, via spliceosome	b
SJ11640	---NA---			b
SJ21666	---NA---			b
SJ20997	dynein heavy chain 2, axonemal isoform X1	F:GO:0003777; F:GO:0005524; C:GO:0005874; P:GO:0007018; F:GO:0016887; C:GO:0030286	F:microtubule motor activity; F:ATP binding; C:microtubule; P:microtubule-based movement; F:ATPase activity; C:dynein complex	b
SJ04977	---NA---			b
SJ18579	---NA---			b
SJ16008	predicted protein	F:GO:0003677	F:DNA binding	b
SJ15287	hypothetical protein AURANDRAFT_72164			b
SJ07674	---NA---			b
SJ20215	---NA---			b
SJ12256	RCC1 repeat-containing protein			b
SJ06316	---NA---			b
SJ20547	---NA---			b
SJ05512	---NA---	F:GO:0005515	F:protein binding	b
SJ00342	choline transporter-like protein 1 isoform X3	C:GO:0016021	C:integral component of membrane	b
SJ06834	protein CASC1 isoform X1	P:GO:0065009	P:regulation of molecular function	b
SJ02070	---NA---			b
SJ04708	EF hand protein	F:GO:0003779; F:GO:0005509; P:GO:0006352; P:GO:0006355; P:GO:0007010; F:GO:0008270; P:GO:0016310	F:actin binding; F:calcium ion binding; P:DNA-templated transcription, initiation; P:regulation of transcription, DNA-templated; P:cytoskeleton organization; F:zinc ion binding; P:phosphorylation	b
SJ02186	echinoderm microtubule-associated protein-like 6 isoform X4	F:GO:0005515	F:protein binding	b
SJ09727	cGMP-specific 3',5'-cyclic phosphodiesterase-like isoform X1	F:GO:0005515; C:GO:0005622; P:GO:0009190; F:GO:0016849; P:GO:0035556	F:protein binding; C:intracellular; P:cyclic nucleotide biosynthetic process; F:phosphorus-oxygen lyase activity; P:intracellular signal transduction	b
SJ15981	hypothetical protein PHYSODRAFT_320561			b
SJ10861	Teneurin-1 and related extracellular matrix proteins, contain EGF-like repeats			b
SJ01311	AGC/PKG protein kinase	F:GO:0004674; F:GO:0005524; P:GO:0009069	F:protein serine/threonine kinase activity; F:ATP binding; P:serine family amino acid metabolic process	b
SJ18897	glycoside hydrolase family 16 protein	P:GO:0005982; P:GO:0005985; C:GO:0016021; F:GO:0030246; F:GO:0042972; F:GO:0042973	P:starch metabolic process; P:sucrose metabolic process; C:integral component of membrane; F:carbohydrate binding; F:licheninase activity; F:glucan endo-1,3-beta-D-glucosidase activity	b
SJ14533	CAP domain-containing protein			b
SJ07684	potential E3 ubiquitin-protein ligase ariadne-2	F:GO:0004842; F:GO:0008270	F:ubiquitin-protein transferase activity; F:zinc ion binding	b
SJ00339	hypothetical protein H257_01102	C:GO:0016021	C:integral component of membrane	b

SJ17383	---NA---			b
SJ09281	predicted protein	P:GO:0000724; C:GO:0005657; C:GO:0033063	P:double-strand break repair via homologous recombination; C:replication fork; C:Rad51B-Rad51C-Rad51D-XRCC2 complex	b
SJ16957	---NA---			b
SJ03338	myophilin	F:GO:0003779; F:GO:0004497; F:GO:0005506; F:GO:0005516; C:GO:0016021; F:GO:0016705; F:GO:0020037; P:GO:0031032	F:actin binding; F:monooxygenase activity; F:iron ion binding; F:calmodulin binding; C:integral component of membrane; F:oxidoreductase activity, acting on paired donors, with incorporation or reduction of molecular oxygen; F:heme binding; P:actomyosin structure organization	b
SJ04066	---NA---			b
SJ21362	glycosyltransferase family 1 protein	F:GO:0016740	F:transferase activity	b
SJ10862	hypothetical protein			b
SJ08586	sporangia induced dynein heavy chain	P:GO:0003341; F:GO:0003777; F:GO:0005524; C:GO:0005858; C:GO:0005874; F:GO:0016887	P:cilium movement; F:microtubule motor activity; F:ATP binding; C:axonemal dynein complex; C:microtubule; F:ATPase activity	b
SJ19936	ankyrin repeat and protein kinase domain-containing protein 1	F:GO:0004672; F:GO:0005515; F:GO:0005524	F:protein kinase activity; F:protein binding; F:ATP binding	b
SJ05834	---NA---			b
SJ16118	---NA---			b
SJ19905	wd40 repeat protein	F:GO:0004381; F:GO:0005515; P:GO:0005975; P:GO:0009069; P:GO:0009247; C:GO:0016459; P:GO:0016573; F:GO:0016746; F:GO:0016905	F:fucosylgalactoside 3-alpha-galactosyltransferase activity; F:protein binding; P:carbohydrate metabolic process; P:serine family amino acid metabolic process; P:glycolipid biosynthetic process; C:myosin complex; P:histone acetylation; F:transferase activity, transferring acyl groups; F:myosin heavy chain kinase activity	b
SJ04084	arylsulfatase B-like	P:GO:0008152; F:GO:0008484	P:metabolic process; F:sulfuric ester hydrolase activity	b
SJ18322	predicted protein	C:GO:0031514	C:motile cilium	b
SJ19555	---NA---			b
SJ16214	Vacuolar protein 8	F:GO:0005515; C:GO:0005634; P:GO:0007033; C:GO:0016021; P:GO:0022607; P:GO:0034727; C:GO:0044422; C:GO:0044444; P:GO:0051641	F:protein binding; C:nucleus; P:vacuole organization; C:integral component of membrane; P:cellular component assembly; P:piecemeal microautophagy of the nucleus; C:organelle part; C:cytoplasmic part; P:cellular localization	b
SJ06266	---NA---			b
SJ09726	dual 3',5'-cyclic-AMP and-GMP phosphodiesterase, putative	F:GO:0005515	F:protein binding	b
SJ10478	---NA---			b
SJ15561	rasGAP-activating-like protein 1 isoform X1	F:GO:0000166; F:GO:0004672; P:GO:0043087; P:GO:0050794	F:nucleotide binding; F:protein kinase activity; P:regulation of GTPase activity; P:regulation of cellular process	b
SJ20197	Voltage-gated Ion Channel (VIC) Superfamily	F:GO:0005245; C:GO:0005891; P:GO:0034765; P:GO:0086010	F:voltage-gated calcium channel activity; C:voltage-gated calcium channel complex; P:regulation of ion transmembrane transport; P:membrane depolarization during action potential	b
SJ05619	---NA---			b
SJ07276	hypothetical protein SPRG_22324	F:GO:0005509	F:calcium ion binding	b
SJ09577	---NA---			b
SJ10995	predicted protein			b
SJ00300	---NA---			b
SJ20216	---NA---			b
SJ21348	---NA---			b
SJ13178	---NA---			b
SJ14394	---NA---			b
SJ18920	tnf receptor associated factor 4	F:GO:0005509; F:GO:0008270	F:calcium ion binding; F:zinc ion binding	b
SJ19295	FYVE, RhoGEF and PH domain-containing protein 6-like	F:GO:0005089; F:GO:0016740; P:GO:0035023; P:GO:0043087; P:GO:0044237; P:GO:0044238; P:GO:0071704	F:Rho guanyl-nucleotide exchange factor activity; F:transferase activity; P:regulation of Rho protein signal transduction; P:regulation of GTPase activity; P:cellular metabolic process; P:primary metabolic process; P:organic substance metabolic process	b
SJ10041	basal body-orientation factor 1	C:GO:0036064	C:ciliary basal body	b
SJ18604	cilia- and flagella-associated protein 57	F:GO:0005515	F:protein binding	b
SJ01057	---NA---			b
SJ18856	---NA---			b
SJ14905	cellulose synthase 3	F:GO:0005506; F:GO:0016702; F:GO:0046872; P:GO:0055114	F:iron ion binding; F:oxidoreductase activity, acting on single donors with incorporation of molecular oxygen, incorporation of two atoms of oxygen; F:metal ion binding; P:oxidation-reduction process	b
SJ17941	dynein regulatory complex subunit 7 isoform X2	C:GO:0005737	C:cytoplasm	b
SJ08043	sodium/potassium/calcium exchanger 3-like isoform X2	F:GO:0005262; F:GO:0005432; F:GO:0005509; C:GO:0005887; P:GO:0006874; F:GO:0008273; F:GO:0030955; F:GO:0031402	F:calcium channel activity; F:calcium:sodium antiporter activity; F:calcium ion binding; C:integral component of plasma membrane; P:cellular calcium ion homeostasis; F:calcium, potassium:sodium antiporter activity; F:potassium ion binding; F:sodium ion binding	b
SJ01539	---NA---	F:GO:0005515	F:protein binding	b
SJ02951	hypothetical protein H310_03509			b

SJ20548	TPPP family protein CG45057-like	F:GO:0005515	F:protein binding	b
SJ06573	PKD domain-containing protein	F:GO:0003824; P:GO:0055114	F:catalytic activity; P:oxidation-reduction process	b
SJ02757	---NA---			b
SJ12969	dynein heavy chain	F:GO:0003777; F:GO:0005524; C:GO:0005874; P:GO:0007018; F:GO:0016887; C:GO:0030286; C:GO:0031514	F:microtubule motor activity; F:ATP binding; C:microtubule; P:microtubule-based movement; F:ATPase activity; C:dynein complex; C:motile cilium	b
SJ15438	---NA---			b
SJ18102	hydrocephalus-inducing protein homolog	P:GO:0003341	P:cilium movement	b
SJ00699	Tudor-like, plant	F:GO:0005509	F:calcium ion binding	b
SJ04771	---NA---			b
SJ06210	---NA---			b
SJ15404	hypothetical protein AURANDRAFT_66629	F:GO:0003676; F:GO:0004725; P:GO:0006570; F:GO:0008138; C:GO:0016021; F:GO:0016491; P:GO:0034613; F:GO:0046872	F:nucleic acid binding; F:protein tyrosine phosphatase activity; P:tyrosine metabolic process; F:protein tyrosine/serine/threonine phosphatase activity; C:integral component of membrane; F:oxidoreductase activity; P:cellular protein localization; F:metal ion binding	b
SJ02564	dynein heavy chain 3, axonemal	F:GO:0003777; F:GO:0005524; C:GO:0005874; P:GO:0007018; C:GO:0030286	F:microtubule motor activity; F:ATP binding; C:microtubule; P:microtubule-based movement; C:dynein complex	b
SJ10766	predicted protein	P:GO:0043170; P:GO:0044248	P:macromolecule metabolic process; P:cellular catabolic process	b
SJ06381	tetratricopeptide repeat protein 29 isoform X1	F:GO:0005515; C:GO:0016021	F:protein binding; C:integral component of membrane	b
SJ20999	dynein heavy chain 2, axonemal	F:GO:0003777; F:GO:0005524; C:GO:0005874; P:GO:0007018; F:GO:0016887; C:GO:0030286; C:GO:0031514	F:microtubule motor activity; F:ATP binding; C:microtubule; P:microtubule-based movement; F:ATPase activity; C:dynein complex; C:motile cilium	b
SJ17529	cytosolic enolase 3	C:GO:0000015; P:GO:0000162; F:GO:0000287; F:GO:0004634; P:GO:0006094; P:GO:0006096; P:GO:0006571; P:GO:0009094	C:phosphopyruvate hydratase complex; P:tryptophan biosynthetic process; F:magnesium ion binding; F:phosphopyruvate hydratase activity; P:gluconeogenesis; P:glycolytic process; P:tyrosine biosynthetic process; P:L-phenylalanine biosynthetic process	b
SJ04103	hypothetical protein H310_07131	F:GO:0003676; F:GO:0005515	F:nucleic acid binding; F:protein binding	b
SJ11382	radial spoke protein 7	F:GO:0005509; C:GO:0031514	F:calcium ion binding; C:motile cilium	b
SJ17116	Teneurin-1 and related extracellular matrix proteins, contain EGF-like repeats			b
SJ04702	sodium/potassium/calcium exchanger 4-like isoform X2	C:GO:0016021; P:GO:0055085	C:integral component of membrane; P:transmembrane transport	b
SJ21342	---NA---			b
SJ04106	---NA---	F:GO:0005515	F:protein binding	b
SJ16026	---NA---			b
SJ19181	---NA---			b
SJ19937	kinesin-like protein KIN-14E	F:GO:0003777; F:GO:0005524; C:GO:0005871; C:GO:0005874; P:GO:0007018; F:GO:0008017; F:GO:0016491; F:GO:0016887; C:GO:0045298	F:microtubule motor activity; F:ATP binding; C:kinesin complex; C:microtubule; P:microtubule-based movement; F:microtubule binding; F:oxidoreductase activity; F:ATPase activity; C:tubulin complex	b
SJ08585	sperm-associated antigen 16 protein-like isoform X2	F:GO:0005515; C:GO:0031514	F:protein binding; C:motile cilium	b
SJ02779	echinoderm microtubule-associated protein-like 6	F:GO:0005509; F:GO:0005515	F:calcium ion binding; F:protein binding	b
SJ08290	dyslexia susceptibility 1 candidate gene 1 protein homolog	F:GO:0005515	F:protein binding	b
SJ21298	---NA---			b
SJ19267	hypothetical protein SPRG_18728, partial	F:GO:0005509; C:GO:0005576; P:GO:0005975; P:GO:0045493; F:GO:0046559	F:calcium ion binding; C:extracellular region; P:carbohydrate metabolic process; P:xylan catabolic process; F:alpha-glucuronidase activity	b
SJ12978	Projectin/twitchin and related proteins	F:GO:0005515	F:protein binding	b
SJ01154	cytoplasmic dynein 2 light intermediate chain 1	F:GO:0003774; C:GO:0005868; C:GO:0005874; C:GO:0005930; P:GO:0007368; C:GO:0030990; P:GO:0035721; P:GO:0035735; C:GO:0036064; C:GO:0045177; F:GO:0045504	F:motor activity; C:cytoplasmic dynein complex; C:microtubule; C:axoneme; P:determination of left/right symmetry; C:intraciliary transport particle; P:intraciliary retrograde transport; P:intraciliary transport involved in cilium assembly; C:ciliary basal body; C:apical part of cell; F:dynein heavy chain binding	b
SJ05117	serine/threonine-protein phosphatase BSL3	F:GO:0005515	F:protein binding	b
SJ07230	E3 ubiquitin-protein ligase HECTD3	F:GO:0004842; F:GO:0008270; F:GO:0016874	F:ubiquitin-protein transferase activity; F:zinc ion binding; F:ligase activity	b
SJ01653	hypothetical protein, variant	F:GO:0005515	F:protein binding	b
SJ08141	ef hand family protein	F:GO:0005515	F:protein binding	b
SJ09368	dynein intermediate chain 3, ciliary-like	C:GO:0000123; F:GO:0004402; F:GO:0004806; F:GO:0005515; P:GO:0016042; C:GO:0031514; P:GO:0042967; P:GO:0046486	C:histone acetyltransferase complex; F:histone acetyltransferase activity; F:triglyceride lipase activity; F:protein binding; P:lipid catabolic process; C:motile cilium; P:obsolete acyl-carrier-protein biosynthetic process; P:glycerolipid metabolic process	b
SJ08044	sodium/potassium/calcium exchanger 1-like isoform X1	C:GO:0016021; P:GO:0055085	C:integral component of membrane; P:transmembrane transport	b

SJ06755	---NA---			b
SJ06317	hypothetical protein PHYSODRAFT_442563, partial			b
SJ15259	carbohydrate-binding protein	F:GO:0030246	F:carbohydrate binding	b
SJ18456	H(+)/Cl(-) exchange transporter 7	F:GO:0005247; C:GO:0016021; P:GO:1903959	F:voltage-gated chloride channel activity; C:integral component of membrane; P:regulation of anion transmembrane transport	b
SJ22217	---NA---			b
SJ17663	---NA---			b
SJ17911	ef hand family protein	F:GO:0005509; F:GO:0005515; C:GO:0016020; C:GO:0044450	F:calcium ion binding; F:protein binding; C:membrane; C:microtubule organizing center part	b
SJ01517	kinesin-like protein	F:GO:0003777; F:GO:0005524; C:GO:0005874; P:GO:0007018; F:GO:0008017; C:GO:0045298	F:microtubule motor activity; F:ATP binding; C:microtubule; P:microtubule-based movement; F:microtubule binding; C:tubulin complex	b
SJ12459	predicted protein	P:GO:0009987	P:cellular process	b
SJ08656	---NA---	F:GO:0005515	F:protein binding	b
SJ21073	cilia- and flagella-associated protein 70	F:GO:0005515	F:protein binding	b
SJ20542	---NA---	F:GO:0050825	F:ice binding	b
SJ12938	ankyrin repeat and SOCS box protein 13	F:GO:0005515	F:protein binding	b
SJ18099	hydrocephalus-inducing protein homolog	P:GO:0003341	P:cilium movement	b
SJ17852	class I SAM-dependent methyltransferase			b
SJ16352	intraflagellar transport protein 140 homolog	F:GO:0005515; C:GO:0005930; C:GO:0016021; C:GO:0030991; C:GO:0031514; P:GO:0035721; C:GO:0036064	F:protein binding; C:axoneme; C:integral component of membrane; C:intraciliary transport particle A; C:motile cilium; P:intraciliary retrograde transport; C:ciliary basal body	b
SJ15555	probable tubulin polyglutamylase TTLL2	P:GO:0006464	P:cellular protein modification process	b
SJ12458	predicted protein	F:GO:0005488; C:GO:0016021	F:binding; C:integral component of membrane	b
SJ21468	calmodulin-like protein 3	F:GO:0005509	F:calcium ion binding	b
SJ12145	kinesin-like protein	F:GO:0003777; F:GO:0005524; C:GO:0005871; C:GO:0005874; P:GO:0007018; F:GO:0008017; F:GO:0016887; P:GO:0030705; C:GO:0045298	F:microtubule motor activity; F:ATP binding; C:kinesin complex; C:microtubule; P:microtubule-based movement; F:microtubule binding; F:ATPase activity; P:cytoskeleton-dependent intracellular transport; C:tubulin complex	b
SJ11846	---NA---			b
SJ08588	sporangia induced dynein heavy chain	P:GO:0003341; F:GO:0003777; F:GO:0005524; C:GO:0005858; C:GO:0005874; F:GO:0016887	P:cilium movement; F:microtubule motor activity; F:ATP binding; C:axonemal dynein complex; C:microtubule; F:ATPase activity	b
SJ13963	zinc finger protein DZIP1L isoform X1			b
SJ14391	Insulin-like growth factor binding protein, N-terminal	C:GO:0005576; P:GO:0006030; F:GO:0008061; C:GO:0016021	C:extracellular region; P:chitin metabolic process; F:chitin binding; C:integral component of membrane	b
SJ02804	CMGC/MAPK protein kinase	F:GO:0004707; F:GO:0005524; C:GO:0005622; P:GO:0007178; P:GO:0009069	F:MAP kinase activity; F:ATP binding; C:intracellular; P:transmembrane receptor protein serine/threonine kinase signaling pathway; P:serine family amino acid metabolic process	b
SJ05582	hypothetical protein AURANDRAFT_71571			b
SJ18855	---NA---			b
SJ20945	TKL protein kinase, variant	F:GO:0004672; F:GO:0005524	F:protein kinase activity; F:ATP binding	b
SJ03748	---NA---			b
SJ15919	---NA---			b
SJ19490	tubulin polyglutamylase, putative	F:GO:0004835; F:GO:0005524; P:GO:0006464; P:GO:0006570; F:GO:0008270	F:tubulin-tyrosine ligase activity; F:ATP binding; P:cellular protein modification process; P:tyrosine metabolic process; F:zinc ion binding	b
SJ11972	leucine-rich repeat domain-containing protein	F:GO:0005515	F:protein binding	b
SJ01403	---NA---			b
SJ07232	---NA---			b
SJ17301	CMGC/RCK protein kinase	F:GO:0004674; F:GO:0005524; P:GO:0009069; C:GO:0031514	F:protein serine/threonine kinase activity; F:ATP binding; P:serine family amino acid metabolic process; C:motile cilium	b
SJ00392	serine/threonine-protein phosphatase 6 regulatory ankyrin repeat subunit B-like isoform X1	F:GO:0004842; F:GO:0005515	F:ubiquitin-protein transferase activity; F:protein binding	b
SJ10736	hypothetical protein H257_12373			b
SJ16081	---NA---			b
SJ16755	centrin-3, putative	F:GO:0005509; C:GO:0005813; C:GO:0031965	F:calcium ion binding; C:centrosome; C:nuclear membrane	b
SJ04935	---NA---			b
SJ16463	Protein phosphatase 1, regulatory subunit, and related proteins	F:GO:0005515; C:GO:0019013	F:protein binding; C:viral nucleocapsid	b
SJ00674	diaminopimelate decarboxylase	P:GO:0006596; F:GO:0008836; P:GO:0009089	P:polyamine biosynthetic process; F:diaminopimelate decarboxylase activity; P:lysine biosynthetic process via diaminopimelate	b
SJ08328	tubulin monoglycylase TTLL3-like isoform X1	F:GO:0004835; F:GO:0005524; C:GO:0005737; C:GO:0005856; C:GO:0005929; P:GO:0006308; P:GO:0006570; F:GO:0008854; C:GO:0009338; P:GO:0018094; P:GO:0035082; F:GO:0070737	F:tubulin-tyrosine ligase activity; F:ATP binding; C:cytoplasm; C:cytoskeleton; C:cilium; P:DNA catabolic process; P:tyrosine metabolic process; F:exodeoxyribonuclease V activity; C:exodeoxyribonuclease V complex; P:protein polyglycylation; P:axoneme assembly; F:protein-glycine ligase activity, elongating	b

SJ14388	uncharacterized protein LOC106159584			b
SJ03779	hypothetical protein			b
SJ05207	protein unc-119 homolog A-like	C:GO:0031514	C:motile cilium	b
SJ04304	---NA---			b
SJ05325	---NA---	F:GO:0005515	F:protein binding	b
SJ12949	---NA---			b
SJ14126	---NA---			b
SJ21598	hypothetical protein AURANDRAFT_62556	F:GO:0005509	F:calcium ion binding	b
SJ08658	WW domain-binding protein 4	F:GO:0005515	F:protein binding	b
SJ01654	26S proteasome non-ATPase regulatory subunit 10	F:GO:0005515	F:protein binding	b
SJ06264	kinesin-like protein KIN-14N	F:GO:0003777; F:GO:0005524; C:GO:0005871; C:GO:0005874; P:GO:0007018; F:GO:0008017; F:GO:0016887; C:GO:0045298	F:microtubule motor activity; F:ATP binding; C:kinesin complex; C:microtubule; P:microtubule-based movement; F:microtubule binding; F:ATPase activity; C:tubulin complex	b
SJ09743	---NA---			b
SJ00260	---NA---			b
SJ07617	---NA---	F:GO:0004672; F:GO:0005524	F:protein kinase activity; F:ATP binding	b
SJ21326	ankyrin repeat domain-containing protein 50 isoformX1	F:GO:0005509; F:GO:0005515	F:calcium ion binding; F:protein binding	b
SJ13883	putative dynein heavy chain	F:GO:0003777; F:GO:0005524; C:GO:0005858; C:GO:0005874; P:GO:0007018; C:GO:0016021; F:GO:0016887; P:GO:0060285	F:microtubule motor activity; F:ATP binding; C:axonemal dynein complex; C:microtubule; P:microtubule-based movement; C:integral component of membrane; F:ATPase activity; P:cilium-dependent cell motility	b
SJ16594	DUF4347 domain-containing protein	P:GO:0007154; C:GO:0016021	P:cell communication; C:integral component of membrane	b
SJ10481	capsule biosynthesis phosphatase	P:GO:0008152; P:GO:0009058; F:GO:0016740; F:GO:0016779; F:GO:0070569	P:metabolic process; P:biosynthetic process; F:transferase activity; F:nucleotidyltransferase activity; F:uridylyltransferase activity	b
SJ15459	---NA---			b
SJ00794	---NA---			b
SJ00431	NADAR family protein	F:GO:0016787	F:hydrolase activity	b
SJ00700	---NA---	F:GO:0005509	F:calcium ion binding	b
SJ09527	IPT domain	F:GO:0005509; P:GO:0007156; C:GO:0016021	F:calcium ion binding; P:homophilic cell adhesion via plasma membrane adhesion molecules; C:integral component of membrane	b
SJ11987	---NA---	F:GO:0005515	F:protein binding	b
SJ20364	tetratricopeptide repeat protein	F:GO:0005515; F:GO:0016757	F:protein binding; F:transferase activity, transferring glycosyl groups	b
SJ00022	tetratricopeptide repeat protein			b
SJ12472	dynein heavy chain	F:GO:0003777; F:GO:0005524; C:GO:0005874; P:GO:0007018; F:GO:0016887; C:GO:0030286	F:microtubule motor activity; F:ATP binding; C:microtubule; P:microtubule-based movement; F:ATPase activity; C:dynein complex	b
SJ16030	tetratricopeptide repeat protein	P:GO:0006493; F:GO:0008168; F:GO:0016757	P:protein O-linked glycosylation; F:methyltransferase activity; F:transferase activity, transferring glycosyl groups	b
SJ14174	protein PTHB1-like	C:GO:0016020; C:GO:0034464	C:membrane; C:BBSome	b
SJ00434	---NA---			b
SJ17402	Concanavalin A-like lectin/glucanase, subgroup			b
SJ07524	multiple epidermal growth factor-like domains protein 6	C:GO:0005576; P:GO:0006030; F:GO:0008061; C:GO:0016021	C:extracellular region; P:chitin metabolic process; F:chitin binding; C:integral component of membrane	b
SJ20994	kinesin-like protein KIF16B	F:GO:0003777; F:GO:0003950; F:GO:0004672; F:GO:0005524; C:GO:0005874; F:GO:0008017; C:GO:0045298; P:GO:0072383	F:microtubule motor activity; F:NAD+ ADP-ribosyltransferase activity; F:protein kinase activity; F:ATP binding; C:microtubule; F:microtubule binding; C:tubulin complex; P:plus-end-directed vesicle transport along microtubule	b
SJ01614	serine/threonine-protein kinase ULK4-like	F:GO:0016787	F:hydrolase activity	b
SJ03848	DNA cytosine methyltransferase			b
SJ09924	lectin domain-containing protein	F:GO:0030246	F:carbohydrate binding	b
SJ15071	---NA---			b
SJ17937	---NA---	F:GO:0005515	F:protein binding	b
SJ05869	---NA---			b
SJ11638	EF hand protein	F:GO:0005509; F:GO:0005515	F:calcium ion binding; F:protein binding	b
SJ19589	predicted protein	C:GO:0016020	C:membrane	b
SJ11420	---NA---			b
SJ18289	---NA---			b
SJ16419	dynein heavy chain 3, axonemal-like	F:GO:0000166; P:GO:0001539; P:GO:0003341; F:GO:0003777; F:GO:0005524; C:GO:0005858; P:GO:0007018; F:GO:0016887; C:GO:0030286	F:nucleotide binding; P:cilium or flagellum-dependent cell motility; P:cilium movement; F:microtubule motor activity; F:ATP binding; C:axonemal dynein complex; P:microtubule-based movement; F:ATPase activity; C:dynein complex	b
SJ19336	ADP-ribosylation factor-like protein 13B isoform X1	P:GO:0001947; F:GO:0005525; C:GO:0005930; P:GO:0007224; P:GO:0007264; P:GO:0009953; P:GO:0021532; P:GO:0021830; P:GO:0021943; C:GO:0031514; C:GO:0060170; P:GO:0070986	P:heart looping; F:GTP binding; C:axoneme; P:smoothened signaling pathway; P:small GTPase mediated signal transduction; P:dorsal/ventral pattern formation; P:neural tube patterning; P:interneuron migration from the subpallium to the cortex; P:formation of radial glial scaffolds; C:motile cilium; C:ciliary membrane; P:left/right axis specification	b
SJ11436	---NA---			b

SJ17117	sel1 repeat family protein	F:GO:0005515	F:protein binding	b
SJ05790	protein FAM179B			b
SJ13061	WSC domain containing protein	F:GO:0004601; P:GO:0006804; P:GO:0006979; F:GO:0008237; F:GO:0020037	F:peroxidase activity; P:obsolete peroxidase reaction; P:response to oxidative stress; F:metallopeptidase activity; F:heme binding	b
SJ02311	expressed protein, partial	F:GO:0005515; C:GO:0016021	F:protein binding; C:integral component of membrane	b
SJ10933	PREDICTED: uncharacterized protein LOC105951547			b
SJ06319	zinc finger CCCH domain-containing protein 13 isoform X1	F:GO:0046872	F:metal ion binding	b
SJ17343	ankyrin repeat-containing protein	F:GO:0004674; F:GO:0005515; F:GO:0005524; P:GO:0009069; C:GO:0016021	F:protein serine/threonine kinase activity; F:protein binding; F:ATP binding; P:serine family amino acid metabolic process; C:integral component of membrane	b
SJ21917	capping protein, Arp2/3 and myosin-I linker protein 3-like			b
SJ21962	---NA---			b
SJ16082	CMGC/MAPK protein kinase	F:GO:0004707; F:GO:0005524; C:GO:0005622; P:GO:0007178; P:GO:0009069	F:MAP kinase activity; F:ATP binding; C:intracellular; P:transmembrane receptor protein serine/threonine kinase signaling pathway; P:serine family amino acid metabolic process	b
SJ05456	katanin p60 ATPase-containing subunit A-like 1	C:GO:0000922; F:GO:0005524; C:GO:0005634; C:GO:0005737; C:GO:0005813; C:GO:0005874; P:GO:0007049; F:GO:0008017; F:GO:0008568; P:GO:0031122; C:GO:0045298; P:GO:0051301	C:spindle pole; F:ATP binding; C:nucleus; C:cytoplasm; C:centrosome; C:microtubule; P:cell cycle; F:microtubule binding; F:microtubule-severing ATPase activity; P:cytoplasmic microtubule organization; C:tubulin complex; P:cell division	b
SJ00433	ORF B	F:GO:0003676; F:GO:0004190; F:GO:0008270; P:GO:0015074	F:nucleic acid binding; F:aspartic-type endopeptidase activity; F:zinc ion binding; P:DNA integration	b
SJ22235	---NA---			b
SJ19125	WSC domain-containing protein 2			b
SJ08791	---NA---			b
SJ09528	IPT domain	F:GO:0005261; F:GO:0005509; C:GO:0005576; C:GO:0005886; P:GO:0006030; P:GO:0006816; P:GO:0007156; F:GO:0008061; C:GO:0016021; P:GO:0086010	F:cation channel activity; F:calcium ion binding; C:extracellular region; C:plasma membrane; P:chitin metabolic process; P:calcium ion transport; P:homophilic cell adhesion via plasma membrane adhesion molecules; F:chitin binding; C:integral component of membrane; P:membrane depolarization during action potential	b
SJ03623	subtilisin-like serine peptidase	F:GO:0000166; F:GO:0004252; C:GO:0016021; P:GO:0016311; F:GO:0042626; F:GO:0043167	F:nucleotide binding; F:serine-type endopeptidase activity; C:integral component of membrane; P:dephosphorylation; F:ATPase activity, coupled to transmembrane movement of substances; F:ion binding	b
SJ14772	hypothetical protein H310_07304	F:GO:0005515; C:GO:0005622; F:GO:0008270	F:protein binding; C:intracellular; F:zinc ion binding	b
SJ03938	---NA---			b
SJ13884	dynein heavy chain 6, axonemal isoform X1	F:GO:0003777; F:GO:0005524; C:GO:0005858; C:GO:0005874; P:GO:0007018; F:GO:0016887; P:GO:0060285	F:microtubule motor activity; F:ATP binding; C:axonemal dynein complex; C:microtubule; P:microtubule-based movement; F:ATPase activity; P:cilium-dependent cell motility	b
SJ12557	glutathione S-transferase, putative	F:GO:0005515; F:GO:0016740	F:protein binding; F:transferase activity	b
SJ16353	intraflagellar transport protein 140 homolog isoform X2	C:GO:0001750; F:GO:0005515; C:GO:0005813; C:GO:0005930; P:GO:0007368; P:GO:0007507; P:GO:0008589; C:GO:0016021; P:GO:0021532; C:GO:0030991; C:GO:0031514; C:GO:0032391; P:GO:0035108; P:GO:0035721; P:GO:0035845; C:GO:0036064; P:GO:0048705; P:GO:0060041; P:GO:0061512; P:GO:0072001; P:GO:1902017	C:photoreceptor outer segment; F:protein binding; C:centrosome; C:axoneme; P:determination of left/right symmetry; P:heart development; P:regulation of smoothened signaling pathway; C:integral component of membrane; P:neural tube patterning; C:intraciliary transport particle A; C:motile cilium; C:photoreceptor connecting cilium; P:limb morphogenesis; P:intraciliary retrograde transport; P:photoreceptor cell outer segment organization; C:ciliary basal body; P:skeletal system morphogenesis; P:retina development in camera-type eye; P:protein localization to cilium; P:renal system development; P:regulation of cilium assembly	b
SJ19920	serine/threonine-protein kinase ULK4-like	F:GO:0005488; P:GO:0055114; P:GO:0098869	F:binding; P:oxidation-reduction process; P:cellular oxidant detoxification	b
SJ20757	predicted protein			b
SJ09451	predicted protein	C:GO:0016021	C:integral component of membrane	b
SJ01285	Tudor-like, plant	F:GO:0003824; F:GO:0005509; F:GO:0008270	F:catalytic activity; F:calcium ion binding; F:zinc ion binding	b
SJ20981	LRR-containing protein	F:GO:0005525; C:GO:0005622; P:GO:0007264	F:GTP binding; C:intracellular; P:small GTPase mediated signal transduction	b
SJ10484	protein MAATS1			b
SJ01727	morn domain repeat protein	F:GO:0005515; P:GO:0006554; F:GO:0018024; F:GO:0046872	F:protein binding; P:lysine catabolic process; F:histone-lysine N-methyltransferase activity; F:metal ion binding	b

SJ21779	phospholipid-transporting ATPase, putative	F:GO:0000287; F:GO:0004012; F:GO:0005524; C:GO:0005886; P:GO:0006812; P:GO:0015917; C:GO:0016021	F:magnesium ion binding; F:phospholipid-translocating ATPase activity; F:ATP binding; C:plasma membrane; P:cation transport; P:aminophospholipid transport; C:integral component of membrane	b
SJ18679	3 5-cyclic nucleotide	F:GO:0004114; P:GO:0006144; P:GO:0007165; C:GO:0016021; F:GO:0046872	F:3',5'-cyclic-nucleotide phosphodiesterase activity; P:purine nucleobase metabolic process; P:signal transduction; C:integral component of membrane; F:metal ion binding	b
SJ05894	---NA---			b
SJ15605	potassium sodium hyperpolarization-activated cyclic nucleotide-gated	F:GO:0005249; C:GO:0008076; P:GO:0042391	F:voltage-gated potassium channel activity; C:voltage-gated potassium channel complex; P:regulation of membrane potential	b
SJ08159	UMP-CMP kinase	F:GO:0004127; F:GO:0005524; C:GO:0005634; C:GO:0005737; P:GO:0006207; P:GO:0006221; F:GO:0009041; P:GO:0046939	F:cytidylate kinase activity; F:ATP binding; C:nucleus; C:cytoplasm; P:'de novo' pyrimidine nucleobase biosynthetic process; P:pyrimidine nucleotide biosynthetic process; F:uridylate kinase activity; P:nucleotide phosphorylation	b
SJ15008	coiled-coil domain-containing protein 78 isoform X1	F:GO:0005524; C:GO:0005871; C:GO:0005874; P:GO:0007018; F:GO:0008017; F:GO:0008574; C:GO:0045298	F:ATP binding; C:kinesin complex; C:microtubule; P:microtubule-based movement; F:microtubule binding; F:ATP-dependent microtubule motor activity, plus-end-directed; C:tubulin complex	b
SJ00618	---NA---			b
SJ07651	IQ and AAA domain-containing protein 1-like	F:GO:0005524	F:ATP binding	b
SJ21971	hypothetical protein PPTG_13300	P:GO:0006801	P:superoxide metabolic process	b
SJ03621	---NA---			b
SJ19921	T9SS C-terminal target domain-containing protein	F:GO:0008237; C:GO:0016020	F:metallopeptidase activity; C:membrane	b
SJ05218	signal peptide peptidase-like 3	F:GO:0004252; C:GO:0005765; P:GO:0006465; C:GO:0030660; P:GO:0033619; F:GO:0042500; C:GO:0071458; C:GO:0071556	F:serine-type endopeptidase activity; C:lysosomal membrane; P:signal peptide processing; C:Golgi-associated vesicle membrane; P:membrane protein proteolysis; F:aspartic endopeptidase activity, intramembrane cleaving; C:integral component of cytoplasmic side of endoplasmic reticulum membrane; C:integral component of lumenal side of endoplasmic reticulum membrane	b
SJ03210	tenascin-like protein			b
SJ00444	hypothetical protein AURANDRAFT_72288	F:GO:0005515	F:protein binding	b
SJ02513	---NA---	F:GO:0005515	F:protein binding	b
SJ02159	hypothetical protein, variant			b
SJ04961	transmembrane and TPR repeat-containing protein CG4050	F:GO:0005515; C:GO:0016021	F:protein binding; C:integral component of membrane	b
SJ02833	FAD-dependent oxidoreductase	F:GO:0016491	F:oxidoreductase activity	b
SJ21180	actin, clone 403-like	F:GO:0005524	F:ATP binding	b
SJ00151	tandem-95 repeat protein	F:GO:0005509; P:GO:0007156; C:GO:0016020	F:calcium ion binding; P:homophilic cell adhesion via plasma membrane adhesion molecules; C:membrane	b
SJ04604	---NA---			b
SJ01025	intraflagellar transport protein 122 homolog	P:GO:0001843; F:GO:0005515; C:GO:0005737; C:GO:0005886; P:GO:0007227; P:GO:0010172; P:GO:0021914; C:GO:0030991; C:GO:0032391; P:GO:0035115; P:GO:0035720; P:GO:0035721; P:GO:0035735; C:GO:0036064; P:GO:0042733; P:GO:0048593; P:GO:0050680; P:GO:0060830; P:GO:0060831; P:GO:0060971; P:GO:0061512; P:GO:0072594; C:GO:0097546	P:neural tube closure; F:protein binding; C:cytoplasm; C:plasma membrane; P:signal transduction downstream of smoothened; P:embryonic body morphogenesis; P:negative regulation of smoothened signaling pathway involved in ventral spinal cord patterning; C:intraciliary transport particle A; C:photoreceptor connecting cilium; P:embryonic forelimb morphogenesis; P:intraciliary anterograde transport; P:intraciliary retrograde transport; P:intraciliary transport involved in cilium assembly; C:ciliary basal body; P:embryonic digit morphogenesis; P:camera-type eye morphogenesis; P:negative regulation of epithelial cell proliferation; P:ciliary receptor clustering involved in smoothened signaling pathway; P:smoothened signaling pathway involved in dorsal/ventral neural tube patterning; P:embryonic heart tube left/right pattern formation; P:protein localization to cilium; P:establishment of protein localization to organelle; C:ciliary base	b
SJ00723	glycosyl transferase			b
SJ06181	glucose 1-dehydrogenase	F:GO:0004316; C:GO:0005835; P:GO:0006633; P:GO:0042967	F:3-oxoacyl-[acyl-carrier-protein] reductase (NADPH) activity; C:fatty acid synthase complex; P:fatty acid biosynthetic process; P:obsolete acyl-carrier-protein biosynthetic process	b
SJ15397	---NA---	C:GO:0000124; F:GO:0003712; C:GO:0005667; P:GO:0006355	C:SAGA complex; F:transcription coregulator activity; C:transcription factor complex; P:regulation of transcription, DNA-templated	b
SJ09163	meckelin isoform x1	P:GO:0010826; C:GO:0016021; C:GO:0036038; C:GO:0043227; C:GO:0044446; P:GO:0060271	P:negative regulation of centrosome duplication; C:integral component of membrane; C:MKS complex; C:membrane-bounded organelle; C:intracellular organelle part; P:cilium assembly	b
SJ18825	CHAT domain-containing protein			b
SJ07111	---NA---			b
SJ17439	---NA---	C:GO:0030992; P:GO:0042073	C:intraciliary transport particle B; P:intraciliary transport	b

SJ19346	---NA---			b
SJ15082	---NA---			b
SJ15603	---NA---			b
SJ04479	hypothetical protein			b
SJ21969	T9SS C-terminal target domain-containing protein	F:GO:0008237; C:GO:0016021	F:metallopeptidase activity; C:integral component of membrane	b
SJ18435	---NA---			b
SJ17366	predicted protein	F:GO:0005506; F:GO:0016705; F:GO:0031418	F:iron ion binding; F:oxidoreductase activity, acting on paired donors, with incorporation or reduction of molecular oxygen; F:L-ascorbic acid binding	b
SJ00213	glycosyltransferase	F:GO:0016740; F:GO:0016757	F:transferase activity; F:transferase activity, transferring glycosyl groups	b
SJ18436	---NA---			b
SJ06970	---NA---			b
SJ03597	cilia- and flagella-associated protein 69	F:GO:0005262; C:GO:0016020; C:GO:0031514	F:calcium channel activity; C:membrane; C:motile cilium	b
SJ14603	parkin coregulated gene protein			b
SJ19092	---NA---			b
SJ21848	thaumatin domain-containing protein			b
SJ03599	---NA---			b
SJ06649	dynein heavy chain 1, axonemal	P:GO:0003341; F:GO:0003777; F:GO:0005524; C:GO:0005858; C:GO:0005874; F:GO:0016887	P:cilium movement; F:microtubule motor activity; F:ATP binding; C:axonemal dynein complex; C:microtubule; F:ATPase activity	b
SJ01578	predicted protein	P:GO:0006355; C:GO:0016021	P:regulation of transcription, DNA-templated; C:integral component of membrane	b
SJ09738	---NA---	F:GO:0005515	F:protein binding	b
SJ18098	hydrocephalus-inducing protein-like	P:GO:0003341	P:cilium movement	b
SJ21084	predicted protein	F:GO:0003924; F:GO:0005509; F:GO:0005525	F:GTPase activity; F:calcium ion binding; F:GTP binding	b
SJ02188	microtubule-associated protein, putative	F:GO:0005509; F:GO:0005515	F:calcium ion binding; F:protein binding	b
SJ17405	WD repeat-containing protein 66	F:GO:0005515	F:protein binding	b
SJ11627	flagella associated protein	P:GO:0003341; C:GO:0005930; C:GO:0031514; P:GO:0036159; P:GO:0060285	P:cilium movement; C:axoneme; C:motile cilium; P:inner dynein arm assembly; P:cilium-dependent cell motility	b
SJ21347	---NA---			b
SJ07676	Kelch repeat-containing proteins	F:GO:0005515	F:protein binding	b
SJ02185	microtubule-associated protein, putative	F:GO:0005509; F:GO:0005515	F:calcium ion binding; F:protein binding	b
SJ09752	---NA---			b
SJ12448	predicted protein	F:GO:0005488; P:GO:0009987; C:GO:0016020	F:binding; P:cellular process; C:membrane	b
SJ10480	capsule biosynthesis phosphatase	P:GO:0009058; F:GO:0016779	P:biosynthetic process; F:nucleotidyltransferase activity	b
SJ12260	CMGC/MAPK/ERK7 protein kinase	F:GO:0004707; F:GO:0005524; C:GO:0005622; P:GO:0007178; P:GO:0009069	F:MAP kinase activity; F:ATP binding; C:intracellular; P:transmembrane receptor protein serine/threonine kinase signaling pathway; P:serine family amino acid metabolic process	b
SJ04254	monodehydroascorbate reductase, seedling isozyme-like	C:GO:0016020; F:GO:0016491; F:GO:0050660	C:membrane; F:oxidoreductase activity; F:flavin adenine dinucleotide binding	b
SJ03055	guanylyl cyclase	C:GO:0005622; P:GO:0009190; F:GO:0016849; P:GO:0035556	C:intracellular; P:cyclic nucleotide biosynthetic process; F:phosphorus-oxygen lyase activity; P:intracellular signal transduction	b
SJ20752	---NA---	F:GO:0004535; C:GO:0030014; P:GO:0051252	F:poly(A)-specific ribonuclease activity; C:CCR4-NOT complex; P:regulation of RNA metabolic process	b
SJ01223	tenascin-like protein			b
SJ15188	F-box/LRR-repeat protein 13	F:GO:0005515	F:protein binding	b
SJ07010	---NA---			b
SJ17912	---NA---	F:GO:0005515	F:protein binding	b
SJ15441	IQ motif, EF-hand binding site			b
SJ12951	---NA---			b
SJ05021	calpain-type cysteine protease DEK1	F:GO:0004198; F:GO:0005509; C:GO:0005622	F:calcium-dependent cysteine-type endopeptidase activity; F:calcium ion binding; C:intracellular	b
SJ08610	Uncharacterized conserved protein	C:GO:0016021; F:GO:0046983	C:integral component of membrane; F:protein dimerization activity	b
SJ13298	p25-alpha family protein, putative	F:GO:0005509	F:calcium ion binding	b
SJ17260	---NA---			b
SJ18907	FG-GAP repeat protein	F:GO:0005509; P:GO:0007155; P:GO:0007229; C:GO:0008305	F:calcium ion binding; P:cell adhesion; P:integrin-mediated signaling pathway; C:integrin complex	b
SJ16021	STE/STE7 protein kinase	F:GO:0004674; F:GO:0005524; C:GO:0005737; P:GO:0009069; P:GO:0023014	F:protein serine/threonine kinase activity; F:ATP binding; C:cytoplasm; P:serine family amino acid metabolic process; P:signal transduction by protein phosphorylation	b
SJ07067	hypothetical protein AURANDRAFT_72773			b
SJ15145	dynein heavy chain 10, axonemal-like	F:GO:0003777; F:GO:0005524; C:GO:0005874; P:GO:0007018; F:GO:0016887; C:GO:0030286	F:microtubule motor activity; F:ATP binding; C:microtubule; P:microtubule-based movement; F:ATPase activity; C:dynein complex	b

SJ07231	FOG: RCC1 domain	F:GO:0004842; F:GO:0005515; C:GO:0005634; C:GO:0005737; F:GO:0016874; F:GO:0046872	F:ubiquitin-protein transferase activity; F:protein binding; C:nucleus; C:cytoplasm; F:ligase activity; F:metal ion binding	b
SJ08985	sperm-associated antigen 1	F:GO:0005515	F:protein binding	b
SJ13031	---NA---			b
SJ12456	Proteins containing Ca2-binding EGF-like domains	C:GO:0016021	C:integral component of membrane	b
SJ15301	protein NLRC3	F:GO:0005515; F:GO:0005524; C:GO:0005737; P:GO:0032088; P:GO:0032715; P:GO:0032720; P:GO:0042110; P:GO:0043124	F:protein binding; F:ATP binding; C:cytoplasm; P:negative regulation of NF-kappaB transcription factor activity; P:negative regulation of interleukin-6 production; P:negative regulation of tumor necrosis factor production; P:T cell activation; P:negative regulation of I-kappaB kinase/NF-kappaB signaling	b
SJ13934	IQ and ubiquitin-like domain-containing protein isoform X1	F:GO:0005515	F:protein binding	b
SJ14290	---NA---			b
SJ00044	peptidyl-prolyl cis-trans isomerase FKBP1A	F:GO:0003755; F:GO:0005515; P:GO:0006457	F:peptidyl-prolyl cis-trans isomerase activity; F:protein binding; P:protein folding	b
SJ15898	---NA---	F:GO:0005515	F:protein binding	b
SJ06877	26S proteasome non-ATPase regulatory subunit 10-like	F:GO:0005515; F:GO:0016787	F:protein binding; F:hydrolase activity	b
SJ11381	---NA---			b
SJ06261	ADP-ribosylation factor-like protein 3	C:GO:0000139; P:GO:0000910; P:GO:0001822; F:GO:0003924; F:GO:0005525; C:GO:0005634; C:GO:0005813; C:GO:0005876; C:GO:0005881; P:GO:0006892; P:GO:0007224; P:GO:0007264; F:GO:0008017; P:GO:0015031; F:GO:0019003; C:GO:0030496; C:GO:0032391; P:GO:0042073; P:GO:0042461; C:GO:0045298; F:GO:0046872; P:GO:0060271; C:GO:0070062	C:Golgi membrane; P:cytokinesis; P:kidney development; F:GTPase activity; F:GTP binding; C:nucleus; C:centrosome; C:spindle microtubule; C:cytoplasmic microtubule; P:post-Golgi vesicle-mediated transport; P:smoothened signaling pathway; P:small GTPase mediated signal transduction; F:microtubule binding; P:protein transport; F:GDP binding; C:midbody; C:photoreceptor connecting cilium; P:intraciliary transport; P:photoreceptor cell development; C:tubulin complex; F:metal ion binding; P:cilium assembly; C:extracellular exosome	b
SJ14937	---NA---			b
SJ20235	DEAD/DEAH box helicase	F:GO:0000166; F:GO:0016787	F:nucleotide binding; F:hydrolase activity	b
SJ21184	---NA---	F:GO:0005515	F:protein binding	b
SJ19587	solute carrier family 35 member E3	F:GO:0005338; P:GO:0015780; C:GO:0016021; P:GO:1901679	F:nucleotide-sugar transmembrane transporter activity; P:nucleotide-sugar transmembrane transport; C:integral component of membrane; P:nucleotide transmembrane transport	b
SJ09525	retention module-containing protein	F:GO:0005509; P:GO:0007156; C:GO:0016020; F:GO:0017154	F:calcium ion binding; P:homophilic cell adhesion via plasma membrane adhesion molecules; C:membrane; F:semaphorin receptor activity	b
SJ21854	aspartyl protease family A01A, putative	F:GO:0004190	F:aspartic-type endopeptidase activity	b
SJ12770	hypothetical protein AURANDRAFT_64248	C:GO:0016020	C:membrane	b
SJ07026	---NA---			c
SJ15859	importin subunit alpha-2-like	F:GO:0005515; C:GO:0005643; C:GO:0005654; C:GO:0005829; P:GO:0006607; P:GO:0006952; F:GO:0008139; F:GO:0008565	F:protein binding; C:nuclear pore; C:nucleoplasm; C:cytosol; P:NLS-bearing protein import into nucleus; P:defense response; F:nuclear localization sequence binding; F:protein transporter activity	c
SJ04357	ankyrin-3-like isoform X24	F:GO:0005515	F:protein binding	c
SJ05468	---NA---			c
SJ16366	---NA---			c
SJ19172	probable protein phosphatase 2C 59	F:GO:0004722; C:GO:0005739; C:GO:0008287; F:GO:0046872	F:protein serine/threonine phosphatase activity; C:mitochondrion; C:protein serine/threonine phosphatase complex; F:metal ion binding	c
SJ16765	hypothetical protein AURANDRAFT_67962			c
SJ15730	---NA---			c
SJ02222	Oxoglutarate/iron-dependent dioxygenase			c
SJ11154	DNA cytosine methyltransferase	F:GO:0008168	F:methyltransferase activity	c
SJ03934	---NA---	F:GO:0046872	F:metal ion binding	c
SJ02998	clumping factor A-like			c
SJ04632	protein LIGHT-DEPENDENT SHORT HYPOCOTYLS 9-like	F:GO:0003677; P:GO:0006310; P:GO:0015074	F:DNA binding; P:DNA recombination; P:DNA integration	c
SJ11400	---NA---			c
SJ16158	---NA---			c
SJ08438	NADAR family protein			c
SJ16376	superoxide dismutase	F:GO:0005515	F:protein binding	c
SJ20863	chitin binding	F:GO:0004553; C:GO:0005576; P:GO:0005975; F:GO:0030248	F:hydrolase activity, hydrolyzing O-glycosyl compounds; C:extracellular region; P:carbohydrate metabolic process; F:cellulose binding	e

SJ08296	exostosin-1c-like	F:GO:0005515; C:GO:0005783; C:GO:0005794; P:GO:0006044; P:GO:0006486; P:GO:0007411; P:GO:0008101; P:GO:0008354; P:GO:0008589; P:GO:0015014; C:GO:0016021; P:GO:0016055; P:GO:0030206; P:GO:0030210; P:GO:0048312; P:GO:0048488; F:GO:0050508; F:GO:0050509; P:GO:0050808	F:protein binding; C:endoplasmic reticulum; C:Golgi apparatus; P:N-acetylglucosamine metabolic process; P:protein glycosylation; P:axon guidance; P:decapentaplegic signaling pathway; P:germ cell migration; P:regulation of smoothened signaling pathway; P:heparan sulfate proteoglycan biosynthetic process, polysaccharide chain biosynthetic process; C:integral component of membrane; P:Wnt signaling pathway; P:chondroitin sulfate biosynthetic process; P:heparin biosynthetic process; P:intracellular distribution of mitochondria; P:synaptic vesicle endocytosis; F:glucuronosyl-N-acetylglucosaminyl-proteoglycan 4-alpha-N-acetylglucosaminyltransferase activity; F:N-acetylglucosaminyl-proteoglycan 4-beta-glucuronosyltransferase activity; P:synapse organization	e
SJ09459	---NA---			e
SJ16228	predicted protein	F:GO:0004568; P:GO:0006032; C:GO:0016020; C:GO:0016021; P:GO:0016998	F:chitinase activity; P:chitin catabolic process; C:membrane; C:integral component of membrane; P:cell wall macromolecule catabolic process	e
SJ17787	calcineurin-like phosphoesterase	F:GO:0003993; P:GO:0006771; P:GO:0019497; F:GO:0046872	F:acid phosphatase activity; P:riboflavin metabolic process; P:hexachlorocyclohexane metabolic process; F:metal ion binding	e
SJ15808	---NA---			e
SJ08942	putative germin-like protein 2-1	C:GO:0005576; C:GO:0016021; F:GO:0030145; F:GO:0045735	C:extracellular region; C:integral component of membrane; F:manganese ion binding; F:nutrient reservoir activity	e
SJ05924	predicted protein	F:GO:0005549; C:GO:0016021	F:odorant binding; C:integral component of membrane	e
SJ07758	serine/threonine-protein kinase ULK4-like	F:GO:0016787	F:hydrolase activity	e
SJ07143	Retrovirus-related Gag-Pol polyprotein	C:GO:0000943; F:GO:0003676; F:GO:0008270; P:GO:0015074	C:retrotransposon nucleocapsid; F:nucleic acid binding; F:zinc ion binding; P:DNA integration	e
SJ17542	predicted protein	C:GO:0005887; F:GO:0008271	C:integral component of plasma membrane; F:secondary active sulfate transmembrane transporter activity	e
SJ04511	autotransporter outer membrane beta-barrel domain-containing protein			e
SJ09414	putative calmodulin-binding protein	P:GO:0006468	P:protein phosphorylation	e
SJ19623	predicted protein	F:GO:0005247; F:GO:0005525; C:GO:0016021; P:GO:1903959	F:voltage-gated chloride channel activity; F:GTP binding; C:integral component of membrane; P:regulation of anion transmembrane transport	e
SJ16331	---NA---			e
SJ07352	---NA---			e
SJ10837	DUF11 domain-containing protein	P:GO:0007165; C:GO:0016021	P:signal transduction; C:integral component of membrane	e
SJ04746	acyltransferase-like protein At1g54570, chloroplastic isoform X3	F:GO:0004144; C:GO:0010287; C:GO:0016021; P:GO:0033306; P:GO:0042967; P:GO:0046486	F:diacylglycerol O-acyltransferase activity; C:plastoglobule; C:integral component of membrane; P:phytol metabolic process; P:obsolete acyl-carrier-protein biosynthetic process; P:glycerolipid metabolic process	e
SJ08260	hypothetical protein SARC_02286			e
SJ18355	alkaline phosphatase	F:GO:0005515; P:GO:0007154; C:GO:0016021	F:protein binding; P:cell communication; C:integral component of membrane	e
SJ19782	uracil-DNA glycosylase	F:GO:0004844; C:GO:0005737; P:GO:0006284	F:uracil DNA N-glycosylase activity; C:cytoplasm; P:base-excision repair	e
SJ08253	hypothetical protein SARC_02286			e
SJ05541	ankyrin-2-like isoform X8	F:GO:0005515	F:protein binding	e
SJ12632	RmlC-like cupin	C:GO:0005576; C:GO:0016021; F:GO:0030145; F:GO:0045735	C:extracellular region; C:integral component of membrane; F:manganese ion binding; F:nutrient reservoir activity	e
SJ01831	DNA-directed RNA polymerase II subunit 1-like	F:GO:0003676; P:GO:0015074; C:GO:0016021	F:nucleic acid binding; P:DNA integration; C:integral component of membrane	e
SJ20963	predicted protein	F:GO:0005525	F:GTP binding	e
SJ08435	uncharacterized protein LOC110923835			e
SJ06576	hypothetical protein PHYSODRAFT_501905, partial	F:GO:0003677; P:GO:0006310; P:GO:0015074	F:DNA binding; P:DNA recombination; P:DNA integration	e
SJ07398	beta-glucuronosyltransferase GlcAT14A	F:GO:0008375; C:GO:0016021	F:acetylglucosaminyltransferase activity; C:integral component of membrane	e
SJ00820	predicted protein	C:GO:0005634; C:GO:0005768; C:GO:0005794; C:GO:0005829; P:GO:0015031; P:GO:0032511	C:nucleus; C:endosome; C:Golgi apparatus; C:cytosol; P:protein transport; P:late endosome to vacuole transport via multivesicular body sorting pathway	e
SJ20834	hypothetical protein AURANDRAFT_72082	F:GO:0003824; C:GO:0016021	F:catalytic activity; C:integral component of membrane	e
SJ21540	---NA---	F:GO:0005515	F:protein binding	e
SJ18939	arrestin domain-containing protein 2 isoform X2			e
SJ16886	hypothetical protein PHYSODRAFT_342415	F:GO:0003677; F:GO:0004672; F:GO:0005524; P:GO:0006310; P:GO:0006468; P:GO:0015074	F:DNA binding; F:protein kinase activity; F:ATP binding; P:DNA recombination; P:protein phosphorylation; P:DNA integration	e
SJ01269	LPXTG cell wall anchor domain-containing protein	C:GO:0016020	C:membrane	e
SJ21322	17-beta-hydroxysteroid dehydrogenase type 6	C:GO:0016021; F:GO:0016491	C:integral component of membrane; F:oxidoreductase activity	e
SJ14215	PREDICTED: uncharacterized protein LOC105330442	F:GO:0003676; P:GO:0015074	F:nucleic acid binding; P:DNA integration	e
SJ06937	cell surface receptor IPT/TIG domain-containing protein	P:GO:0007165; C:GO:0016021; F:GO:0016740	P:signal transduction; C:integral component of membrane; F:transferase activity	e

SJ02313	---NA---			e
SJ04157	RmlC-like cupin	C:GO:0005576; C:GO:0016021; F:GO:0030145; F:GO:0045735	C:extracellular region; C:integral component of membrane; F:manganese ion binding; F:nutrient reservoir activity	e
SJ17627	---NA---			e
SJ11357	RmlC-like cupin	C:GO:0005576; C:GO:0016021; F:GO:0030145; F:GO:0045735	C:extracellular region; C:integral component of membrane; F:manganese ion binding; F:nutrient reservoir activity	e
SJ18339	tetratricopeptide repeat protein	F:GO:0003777; F:GO:0005515; C:GO:0005871; C:GO:0005874; P:GO:0007017; C:GO:0016021	F:microtubule motor activity; F:protein binding; C:kinesin complex; C:microtubule; P:microtubule-based process; C:integral component of membrane	e
SJ18286	serine/threonine protein kinase	F:GO:0004672; F:GO:0005524	F:protein kinase activity; F:ATP binding	e
SJ05548	T9SS C-terminal target domain-containing protein			e
SJ02438	DUF1565 domain-containing protein			e
SJ17573	---NA---	F:GO:0003676; F:GO:0008270	F:nucleic acid binding; F:zinc ion binding	e
SJ07081	autotransporter domain-containing protein	C:GO:0005739; F:GO:0008233; C:GO:0009279; C:GO:0016021	C:mitochondrion; F:peptidase activity; C:cell outer membrane; C:integral component of membrane	e
SJ03202	---NA---			e
SJ00904	---NA---			e
SJ15837	---NA---			e
SJ15331	copia protein	F:GO:0003676; F:GO:0008270; P:GO:0015074	F:nucleic acid binding; F:zinc ion binding; P:DNA integration	e
SJ18473	---NA---			e
SJ08259	hypothetical protein SARC_02286			e
SJ16009	---NA---			e
SJ03217	peroxidase	F:GO:0004601; P:GO:0006804; P:GO:0006979; C:GO:0016020; F:GO:0020037	F:peroxidase activity; P:obsolete peroxidase reaction; P:response to oxidative stress; C:membrane; F:heme binding	e
SJ11665	---NA---			e
SJ02282	---NA---			e
SJ01268	hypothetical protein AURANDRAFT_72082	F:GO:0005215; P:GO:0006810; C:GO:0016021; F:GO:0016787; F:GO:0046872	F:transporter activity; P:transport; C:integral component of membrane; F:hydrolase activity; F:metal ion binding	e
SJ06538	platelet glycoprotein V	F:GO:0005515; C:GO:0016021	F:protein binding; C:integral component of membrane	e
SJ09567	---NA---			e
SJ07602	---NA---			e
SJ06887	---NA---			e
SJ01168	histone H1-like	C:GO:0000786; F:GO:0003677; C:GO:0005634; P:GO:0006334	C:nucleosome; F:DNA binding; C:nucleus; P:nucleosome assembly	e
SJ07953	---NA---			e
SJ09846	---NA---			e
SJ22470	---NA---			e
SJ20759	---NA---			e
SJ16628	kinesin-like protein KIF19	F:GO:0003777; F:GO:0005524; C:GO:0005871; C:GO:0005874; P:GO:0007018; F:GO:0008017; F:GO:0016887; C:GO:0045298	F:microtubule motor activity; F:ATP binding; C:kinesin complex; C:microtubule; P:microtubule-based movement; F:microtubule binding; F:ATPase activity; C:tubulin complex	e
SJ04691	enzymatic polyprotein, putative	F:GO:0003676; F:GO:0004190; P:GO:0006278; F:GO:0016779; P:GO:0090305	F:nucleic acid binding; F:aspartic-type endopeptidase activity; P:RNA-dependent DNA biosynthetic process; F:nucleotidyltransferase activity; P:nucleic acid phosphodiester bond hydrolysis	e
SJ13440	WSC-domain-containing protein	P:GO:0055114; P:GO:0098869	P:oxidation-reduction process; P:cellular oxidant detoxification	e
SJ03898	RmlC-like cupin	C:GO:0005576; C:GO:0016021; F:GO:0030145; F:GO:0045735	C:extracellular region; C:integral component of membrane; F:manganese ion binding; F:nutrient reservoir activity	e
SJ08244	---NA---			e
SJ20291	D-beta-hydroxybutyrate dehydrogenase, mitochondrial-like	C:GO:0016021; F:GO:0016491	C:integral component of membrane; F:oxidoreductase activity	e
SJ09268	jerky protein homolog-like	F:GO:0003676	F:nucleic acid binding	e
SJ05935	TBC1 domain family member 31 isoform X1			e
SJ19752	hypothetical protein SDRG_12541	F:GO:0005509	F:calcium ion binding	e
SJ01559	metalloprotease family	F:GO:0003677; F:GO:0008237; F:GO:0046872	F:DNA binding; F:metallopeptidase activity; F:metal ion binding	e
SJ16159	dynein beta chain, ciliary-like	P:GO:0000160; F:GO:0003777; F:GO:0005515; C:GO:0005874; P:GO:0007018	P:phosphorelay signal transduction system; F:microtubule motor activity; F:protein binding; C:microtubule; P:microtubule-based movement	e
SJ18197	hypothetical protein PHYSODRAFT_254578	F:GO:0004672; F:GO:0005524	F:protein kinase activity; F:ATP binding	e
SJ02605	Inositol polyphosphate 5-phosphatase and related proteins	C:GO:0016021	C:integral component of membrane	e
SJ20402	---NA---			e
SJ12611	keratin-associated protein 4-4-like			e
SJ14014	autotransporter domain-containing protein	C:GO:0019867; C:GO:0030312	C:outer membrane; C:external encapsulating structure	e
SJ02216	---NA---			e
SJ01636	copper oxidase	F:GO:0004322; F:GO:0005507; C:GO:0005623; P:GO:0006825; P:GO:0006879; P:GO:0015994	F:ferroxidase activity; F:copper ion binding; C:cell; P:copper ion transport; P:cellular iron ion homeostasis; P:chlorophyll metabolic process	e

SJ19478	WSC-domain-containing protein	F:GO:0016787	F:hydrolase activity	e
SJ07905	---NA---			e
SJ04407	---NA---	F:GO:0005515	F:protein binding	e
SJ11612	---NA---			e
SJ08079	---NA---			e
SJ18518	---NA---			e
SJ09412	Carbohydrate-binding WSC	F:GO:0004601; P:GO:0006804; P:GO:0006979; F:GO:0020037	F:peroxidase activity; P:obsolete peroxidase reaction; P:response to oxidative stress; F:heme binding	e
SJ08708	---NA---			e
SJ09070	---NA---			e
SJ11654	BUB protein kinase	C:GO:0000942; F:GO:0004674; F:GO:0005524; C:GO:0005654; C:GO:0005737; P:GO:0007063; P:GO:0007094; P:GO:0009069; P:GO:0009790; C:GO:0016020; P:GO:0051301; P:GO:2001244	C:condensed nuclear chromosome outer kinetochore; F:protein serine/threonine kinase activity; F:ATP binding; C:nucleoplasm; C:cytoplasm; P:regulation of sister chromatid cohesion; P:mitotic spindle assembly checkpoint; P:serine family amino acid metabolic process; P:embryo development; C:membrane; P:cell division; P:positive regulation of intrinsic apoptotic signaling pathway	e
SJ19612	peptidase S8	F:GO:0004252; P:GO:0016311	F:serine-type endopeptidase activity; P:dephosphorylation	e
SJ05585	EsV-1-163			e
SJ10526	carboxypeptidase N subunit 2-like	F:GO:0005515; C:GO:0016021	F:protein binding; C:integral component of membrane	e
SJ01364	aurora kinase B-like	C:GO:0000780; F:GO:0004712; F:GO:0005524; C:GO:0005876; P:GO:0007052; P:GO:0009069; P:GO:0031577; C:GO:0031616; C:GO:0032133; P:GO:0032467; F:GO:0035174; P:GO:0043988; C:GO:0051233	C:condensed nuclear chromosome, centromeric region; F:protein serine/threonine/tyrosine kinase activity; F:ATP binding; C:spindle microtubule; P:mitotic spindle organization; P:serine family amino acid metabolic process; P:spindle checkpoint; C:spindle pole centrosome; C:chromosome passenger complex; P:positive regulation of cytokinesis; F:histone serine kinase activity; P:histone H3-S28 phosphorylation; C:spindle midzone	e
SJ08258	keratin-associated protein 4-4-like			e
SJ14113	---NA---			e
SJ21038	---NA---			e
SJ02854	---NA---			e
SJ04542	---NA---			e
SJ12285	---NA---	F:GO:0003676; F:GO:0008270	F:nucleic acid binding; F:zinc ion binding	e
SJ01632	uncharacterized protein LOC113380490	P:GO:0000723; F:GO:0003678; C:GO:0005657; P:GO:0006281	P:telomere maintenance; F:DNA helicase activity; C:replication fork; P:DNA repair	e
SJ14280	mcKusick-Kaufman/Bardet-Biedl syndromes putative chaperonin isoform X2	P:GO:0006457; F:GO:0051082; P:GO:0060271	P:protein folding; F:unfolded protein binding; P:cilium assembly	e
SJ00601	---NA---			e
SJ08460	---NA---			e
SJ13896	hypothetical protein SPRG_02099			e
SJ12918	nicotinamide/nicotinic acid mononucleotide adenylyltransferase 2	F:GO:0000309; P:GO:0001522; F:GO:0003723; F:GO:0004515; F:GO:0005524; C:GO:0005794; P:GO:0006769; F:GO:0009982; P:GO:0019357; P:GO:0034628	F:nicotinamide-nucleotide adenylyltransferase activity; P:pseudouridine synthesis; F:RNA binding; F:nicotinate-nucleotide adenylyltransferase activity; F:ATP binding; C:Golgi apparatus; P:nicotinamide metabolic process; F:pseudouridine synthase activity; P:nicotinate nucleotide biosynthetic process; P:'de novo' NAD biosynthetic process from aspartate	e
SJ11264	---NA---	F:GO:0004932; P:GO:0007606; C:GO:0016020; P:GO:0019236	F:mating-type factor pheromone receptor activity; P:sensory perception of chemical stimulus; C:membrane; P:response to pheromone	e
SJ01618	---NA---			e
SJ12641	---NA---			e
SJ16966	---NA---			e
SJ17340	---NA---			e
SJ18204	protein ZINC INDUCED FACILITATOR-LIKE 1 isoform X1	C:GO:0016020	C:membrane	e
SJ18717	---NA---	F:GO:0005262; F:GO:0005515; C:GO:0016020	F:calcium channel activity; F:protein binding; C:membrane	e
SJ20815	glycosyltransferase	P:GO:0005982; P:GO:0005985; P:GO:0006011; C:GO:0016020; F:GO:0016760; P:GO:0030244	P:starch metabolic process; P:sucrose metabolic process; P:UDP-glucose metabolic process; C:membrane; F:cellulose synthase (UDP-forming) activity; P:cellulose biosynthetic process	e
SJ21775	---NA---	F:GO:0003676; F:GO:0008270	F:nucleic acid binding; F:zinc ion binding	e
SJ22575	AIG1-type guanine nucleotide-binding (G) domain-containing protein	F:GO:0005525	F:GTP binding	e
SJ14872	tetratricopeptide repeat protein	F:GO:0003777; F:GO:0005515; C:GO:0005871; C:GO:0005874; P:GO:0006629; P:GO:0007017; P:GO:0007165; F:GO:0043531	F:microtubule motor activity; F:protein binding; C:kinesin complex; C:microtubule; P:lipid metabolic process; P:microtubule-based process; P:signal transduction; F:ADP binding	e
SJ15147	---NA---			e
SJ00383	---NA---			e
SJ08684	---NA---			e
SJ00240	---NA---			e

SJ22172	FNIP repeat-containing protein	F:GO:0004672; F:GO:0005524	F:protein kinase activity; F:ATP binding	e
SJ20796	---NA---			e
SJ05641	ankyrin repeat domain-containing protein	F:GO:0005515	F:protein binding	e
SJ05027	---NA---			e
SJ09789	putative anion transporter 5	C:GO:0016021; P:GO:0055085	C:integral component of membrane; P:transmembrane transport	e
SJ10246	---NA---			e
SJ19204	---NA---			e
SJ05056	predicted protein	F:GO:0005525	F:GTP binding	e
SJ16377	peptidase S8	F:GO:0004252; C:GO:0016020	F:serine-type endopeptidase activity; C:membrane	e

*Alphabet indicate a: Consensus DEGs, b: Male consensus DEGs, e: Female consensus DEGs.

Table 13. The downregulated genes list on a: Consensus DEGs, b: Male consensus DEGs, e: Female consensus DEGs in *Saccharina japonica*

Name	Description	GO.IDs	GO.Names	Category*
SJ16164	---NA---			a
SJ21503	---NA---			a
SJ21636	altered inheritance of mitochondria protein 32-like	C:GO:0005634; C:GO:0016021	C:nucleus; C:integral component of membrane	a
SJ08640	mercuric reductase	F:GO:0004148; C:GO:0005622; P:GO:0006094; P:GO:0006096; P:GO:0006099; P:GO:0006118; P:GO:0006544; P:GO:0006563; P:GO:0006566; F:GO:0009055; C:GO:0016021; F:GO:0016152; P:GO:0035556; P:GO:0045454; F:GO:0050660	F:dihydrolipoyl dehydrogenase activity; C:intracellular; P:gluconeogenesis; P:glycolytic process; P:tricarboxylic acid cycle; P:obsolete electron transport; P:glycine metabolic process; P:L-serine metabolic process; P:threonine metabolic process; F:electron transfer activity; C:integral component of membrane; F:mercury (II) reductase activity; P:intracellular signal transduction; P:cell redox homeostasis; F:flavin adenine dinucleotide binding	a
SJ07047	putative iron permease	F:GO:0003824; F:GO:0005381; C:GO:0016020; C:GO:0016021; P:GO:0018193; C:GO:0033573; P:GO:0034755	F:catalytic activity; F:iron ion transmembrane transporter activity; C:membrane; C:integral component of membrane; P:peptidyl-amino acid modification; C:high-affinity iron permease complex; P:iron ion transmembrane transport	a
SJ13085	iron starvation induced protein	P:GO:0007186	P:G-protein coupled receptor signaling pathway	a
SJ04682	peptidase	F:GO:0004222; P:GO:0007155; C:GO:0016020	F:metalloendopeptidase activity; P:cell adhesion; C:membrane	a
SJ00644	Cytochrome b5	F:GO:0016491; F:GO:0020037; F:GO:0046872	F:oxidoreductase activity; F:heme binding; F:metal ion binding	a
SJ01641	Plasma membrane iron permease	F:GO:0005381; C:GO:0005783; C:GO:0005794; P:GO:0010106; F:GO:0016740; C:GO:0033573	F:iron ion transmembrane transporter activity; C:endoplasmic reticulum; C:Golgi apparatus; P:cellular response to iron ion starvation; F:transferase activity; C:high-affinity iron permease complex	a
SJ01623	---NA---			a
SJ04506	predicted protein	C:GO:0016020	C:membrane	a
SJ04413	predicted protein			a
SJ07046	predicted protein	P:GO:0000272; F:GO:0003824; F:GO:0005509; C:GO:0016021; P:GO:0018193; P:GO:0034755	P:polysaccharide catabolic process; F:catalytic activity; F:calcium ion binding; C:integral component of membrane; P:peptidyl-amino acid modification; P:iron ion transmembrane transport	a
SJ18964	metalloproteinase inhibitor 2-like	F:GO:0008191	F:metalloendopeptidase inhibitor activity	a
SJ20299	---NA---			a
SJ00781	predicted protein	F:GO:0000166; F:GO:0003723; F:GO:0004842; F:GO:0008270; C:GO:0030014	F:nucleotide binding; F:RNA binding; F:ubiquitin-protein transferase activity; F:zinc ion binding; C:CCR4-NOT complex	a
SJ17393	---NA---	F:GO:0005515; P:GO:0006396	F:protein binding; P:RNA processing	a
SJ11978	predicted protein	F:GO:0008942; P:GO:0042128; F:GO:0046872; F:GO:0051537	F:nitrite reductase [NAD(P)H] activity; P:nitrate assimilation; F:metal ion binding; F:2 iron, 2 sulfur cluster binding	a
SJ12702	---NA---			a
SJ03251	protein fucoxanthin chlorophyll a/c protein	P:GO:0009416; C:GO:0009535; P:GO:0009768; C:GO:0016021; F:GO:0016168; P:GO:0018298; F:GO:0031409	P:response to light stimulus; C:chloroplast thylakoid membrane; P:photosynthesis, light harvesting in photosystem I; C:integral component of membrane; F:chlorophyll binding; P:protein-chromophore linkage; F:pigment binding	a
SJ19160	E3 ubiquitin-protein ligase NEDD4 isoform X4	F:GO:0005515	F:protein binding	a
SJ17831	predicted protein	F:GO:0005509; C:GO:0016021	F:calcium ion binding; C:integral component of membrane	b
SJ17829	predicted protein	F:GO:0005509; C:GO:0016021	F:calcium ion binding; C:integral component of membrane	b
SJ04511	autotransporter outer membrane beta-barrel domain-containing protein			b
SJ20834	hypothetical protein AURANDRAFT_72082	F:GO:0003824; C:GO:0016021	F:catalytic activity; C:integral component of membrane	b
SJ04157	RmlC-like cupin	C:GO:0005576; C:GO:0016021; F:GO:0030145; F:GO:0045735	C:extracellular region; C:integral component of membrane; F:manganese ion binding; F:nutrient reservoir activity	b
SJ18582	---NA---			b
SJ06850	subtilisin-like serine peptidase	F:GO:0004252	F:serine-type endopeptidase activity	b
SJ19207	---NA---			b
SJ10968	tetratricopeptide repeat protein	F:GO:0003777; F:GO:0005515; C:GO:0005871; C:GO:0005874; P:GO:0006629; P:GO:0007017; F:GO:0043531	F:microtubule motor activity; F:protein binding; C:kinesin complex; C:microtubule; P:lipid metabolic process; P:microtubule-based process; F:ADP binding	b
SJ20835	DUF11 domain-containing protein	C:GO:0016020	C:membrane	b
SJ08325	hypothetical protein AURANDRAFT_72082	C:GO:0016021	C:integral component of membrane	b
SJ13781	---NA---			b
SJ02605	Inositol polyphosphate 5-phosphatase and related proteins	C:GO:0016021	C:integral component of membrane	b
SJ07657	---NA---			b
SJ12611	keratin-associated protein 4-4-like			b
SJ06275	---NA---			b
SJ17610	---NA---			b
SJ18256	---NA---			b
SJ08786	---NA---			b
SJ02162	---NA---			b
SJ09977	zinc finger BED domain-containing protein 1-like	F:GO:0046983	F:protein dimerization activity	b
SJ01342	ankyrin repeat protein	F:GO:0005515	F:protein binding	b
SJ07853	---NA---			b
SJ09341	---NA---			b
SJ05056	predicted protein	F:GO:0005525	F:GTP binding	b
SJ04680	uncharacterized protein LOC110923835			b
SJ16377	peptidase S8	F:GO:0004252; C:GO:0016020	F:serine-type endopeptidase activity; C:membrane	b
SJ18202	---NA---			b
SJ20920	---NA---			b
SJ09164	---NA---			b
SJ15541	predicted protein			b
SJ21532	---NA---			b

SJ04156	RmlC-like cupin	C:GO:0005576; C:GO:0016021; F:GO:0030145; F:GO:0045735	C:extracellular region; C:integral component of membrane; F:manganese ion binding; F:nutrient reservoir activity	b
SJ02508	predicted protein	F:GO:0046872	F:metal ion binding	b
SJ07947	predicted protein	C:GO:0016021	C:integral component of membrane	b
SJ13310	---NA---			b
SJ10804	---NA---			b
SJ02154	protein ALP1-like			b
SJ21271	arylsulfatase I-like	F:GO:0004252; F:GO:0008484; C:GO:0016021; F:GO:0016740	F:serine-type endopeptidase activity; F:sulfuric ester hydrolase activity; C:integral component of membrane; F:transferase activity	b
SJ01477	TVP38/TMEM64 family protein	C:GO:0016021	C:integral component of membrane	b
SJ02826	hypothetical protein H257_16157	C:GO:0016021	C:integral component of membrane	b
SJ04997	hypothetical protein SARC_12666, partial			b
SJ07357	---NA---			b
SJ20590	WSC domain-containing protein 1			b
SJ20964	predicted protein			b
SJ20185	---NA---			b
SJ11786	calcium/calmodulin-dependent protein kinase type 1B	F:GO:0004674; F:GO:0005524; P:GO:0009069	F:protein serine/threonine kinase activity; F:ATP binding; P:serine family amino acid metabolic process	b
SJ09762	fimbrial protein			b
SJ03282	predicted protein			b
SJ12645	RmlC-like cupin	C:GO:0005576; C:GO:0016021; F:GO:0030145; F:GO:0045735	C:extracellular region; C:integral component of membrane; F:manganese ion binding; F:nutrient reservoir activity	b
SJ01551	hypothetical protein	F:GO:0003676; F:GO:0008168	F:nucleic acid binding; F:methyltransferase activity	b
SJ08334	---NA---			b
SJ03998	predicted protein			b
SJ01480	---NA---			b
SJ20148	---NA---			b
SJ07056	peroxidase	F:GO:0004601; P:GO:0006804; P:GO:0006979; C:GO:0016020; F:GO:0020037	F:peroxidase activity; P:obsolete peroxidase reaction; P:response to oxidative stress; C:membrane; F:heme binding	b
SJ04371	arylsulfatase B	F:GO:0008484	F:sulfuric ester hydrolase activity	b
SJ12423	---NA---	F:GO:0008270	F:zinc ion binding	b
SJ15058	---NA---			b
SJ21021	---NA---			b
SJ01336	---NA---			b
SJ14015	---NA---			b
SJ19294	hypothetical protein AURANDRAFT_61043	F:GO:0003677; C:GO:0005622; C:GO:0016021; F:GO:0016491; F:GO:0046872	F:DNA binding; C:intracellular; C:integral component of membrane; F:oxidoreductase activity; F:metal ion binding	b
SJ14232	predicted protein			b
SJ08925	---NA---			b
SJ04193	phosphoribosylglycinamide formyltransferase	P:GO:0015969; F:GO:0016740	P:guanosine tetraphosphate metabolic process; F:transferase activity	b
SJ12701	---NA---			b
SJ02288	cyanate hydratase	F:GO:0003677; F:GO:0008824; P:GO:0009439; F:GO:0016787	F:DNA binding; F:cyanate hydratase activity; P:cyanate metabolic process; F:hydrolase activity	b
SJ19448	Hsp20/alpha crystallin family protein			b
SJ06926	---NA---			b
SJ11849	---NA---	F:GO:0008191	F:metalloendopeptidase inhibitor activity	b
SJ06744	---NA---			b
SJ03294	thioredoxin family	C:GO:0005623; P:GO:0006662; F:GO:0015035; P:GO:0045454; P:GO:0055114	C:cell; P:glycerol ether metabolic process; F:protein disulfide oxidoreductase activity; P:cell redox homeostasis; P:oxidation-reduction process	b
SJ07140	predicted protein	P:GO:0043170; P:GO:0044248	P:macromolecule metabolic process; P:cellular catabolic process	b
SJ11335	---NA---			b
SJ18295	serine/threonine protein kinase	F:GO:0004672; F:GO:0005524	F:protein kinase activity; F:ATP binding	b
SJ10614	tyrosinase family protein	F:GO:0016491	F:oxidoreductase activity	b
SJ22564	---NA---			b
SJ08041	putative nuclease HARBI1			b
SJ10305	serine-enriched protein isoform X2	P:GO:0051260	P:protein homooligomerization	b
SJ04679	peptidase	F:GO:0004222; P:GO:0007155; C:GO:0016020	F:metalloendopeptidase activity; P:cell adhesion; C:membrane	b
SJ17318	---NA---			b
SJ20852	---NA---			b
SJ08860	synaptic vesicle 2-related protein	C:GO:0016021; F:GO:0022857	C:integral component of membrane; F:transmembrane transporter activity	b
SJ08583	cell surface receptor IPT/TIG domain-containing protein	F:GO:0003824; P:GO:0007165; C:GO:0016020	F:catalytic activity; P:signal transduction; C:membrane	b
SJ13370	hypothetical protein PHYSODRAFT_254279			b
SJ08558	---NA---			b
SJ18257	---NA---			b
SJ07396	H(+)/Cl(-) exchange transporter 7	F:GO:0005247; C:GO:0016021; P:GO:1903959	F:voltage-gated chloride channel activity; C:integral component of membrane; P:regulation of anion transmembrane transport	b
SJ01153	hypothetical protein AURANDRAFT_65957	F:GO:0005488; P:GO:0006470; F:GO:0016491; F:GO:0016791	F:binding; P:protein dephosphorylation; F:oxidoreductase activity; F:phosphatase activity	b
SJ13505	---NA---			b
SJ06612	---NA---			b
SJ18137	---NA---			b
SJ02278	---NA---			b
SJ19300	protein N-lysine methyltransferase METTL21A			b
SJ04754	zinc finger BED domain-containing protein RICESLEEPER 2-like			b
SJ12725	---NA---			b
SJ13229	hypothetical protein PHYSODRAFT_501905, partial	F:GO:0003677; P:GO:0006310; P:GO:0015074	F:DNA binding; P:DNA recombination; P:DNA integration	b
SJ12792	---NA---			b

SJ13750	---NA---			b
SJ13374	---NA---			b
SJ06413	arylsulfatase J-like	P:GO:0006508; F:GO:0008484; C:GO:0016021; F:GO:0016740	P:proteolysis; F:sulfuric ester hydrolase activity; C:integral component of membrane; F:transferase activity	b
SJ01534	---NA---			b
SJ04177	predicted protein	F:GO:0005247; F:GO:0005525; C:GO:0016021; P:GO:1903959	F:voltage-gated chloride channel activity; F:GTP binding; C:integral component of membrane; P:regulation of anion transmembrane transport	b
SJ12417	---NA---			b
SJ09129	pyruvate dehydrogenase (acetyl-transferring) kinase, mitochondrial-like isoform X2	F:GO:0004672	F:protein kinase activity	b
SJ06938	---NA---			b
SJ06869	MFS transporter	P:GO:0008152; C:GO:0016021; F:GO:0016798; P:GO:0055085	P:metabolic process; C:integral component of membrane; F:hydrolase activity, acting on glycosyl bonds; P:transmembrane transport	b
SJ13793	---NA---			b
SJ05329	2OG-Fe(II) oxygenase	P:GO:0018193; P:GO:0055114	P:peptidyl-amino acid modification; P:oxidation-reduction process	b
SJ05022	---NA---			b
SJ09252	DNA-directed RNA polymerase II subunit RPB1-like			b
SJ09542	predicted protein	F:GO:0005525	F:GTP binding	b
SJ07948	predicted protein	F:GO:0005525; F:GO:0015075; C:GO:0016021	F:GTP binding; F:ion transmembrane transporter activity; C:integral component of membrane	b
SJ14561	serine/threonine-protein phosphatase 6 regulatory ankyrin repeat subunit B-like	F:GO:0005515	F:protein binding	b
SJ08080	---NA---			b
SJ19520	---NA---			b
SJ04555	---NA---			b
SJ18296	---NA---	F:GO:0004672; F:GO:0005524	F:protein kinase activity; F:ATP binding	b
SJ02733	---NA---			b
SJ00190	---NA---			b
SJ00432	---NA---			b
SJ03122	---NA---			b
SJ05042	uncharacterized protein LOC110913593	F:GO:0003676; F:GO:0008270	F:nucleic acid binding; F:zinc ion binding	b
SJ07155	---NA---			b
SJ07916	predicted protein	P:GO:0043170; P:GO:0044248	P:macromolecule metabolic process; P:cellular catabolic process	b
SJ08027	---NA---			b
SJ09291	WSC domain-containing protein 1-like			b
SJ18944	---NA---			b
SJ19608	mitogen-activated protein kinase kinase 2	F:GO:0004708; F:GO:0005515; F:GO:0005524; C:GO:0005737; C:GO:0005886; P:GO:0009631; P:GO:0009651; P:GO:0009814; P:GO:0010051; P:GO:0060918	F:MAP kinase kinase activity; F:protein binding; F:ATP binding; C:cytoplasm; C:plasma membrane; P:cold acclimation; P:response to salt stress; P:defense response, incompatible interaction; P:xylem and phloem pattern formation; P:auxin transport	b
SJ19609	peptidase S8	F:GO:0004252	F:serine-type endopeptidase activity	b
SJ20797	---NA---			b
SJ02101	---NA---	F:GO:0003676; F:GO:0008270	F:nucleic acid binding; F:zinc ion binding	b
SJ20594	hypothetical protein crov511			b
SJ08422	phosphatase PAP2 family protein	F:GO:0004601; P:GO:0006804; P:GO:0006979	F:peroxidase activity; P:obsolete peroxidase reaction; P:response to oxidative stress	b
SJ09457	predicted protein			b
SJ13176	malignant fibrous histiocytoma-amplified sequence 1 homolog	P:GO:0007165; F:GO:0008234	P:signal transduction; F:cysteine-type peptidase activity	b
SJ00474	zinc finger BED domain-containing protein 1-like	F:GO:0003676	F:nucleic acid binding	b
SJ07950	---NA---			b
SJ17945	tetratricopeptide repeat protein	F:GO:0005515; C:GO:0016020	F:protein binding; C:membrane	b
SJ17003	---NA---			b
SJ06935	copia protein	C:GO:0000943; F:GO:0003676; F:GO:0008270; P:GO:0015074	C:retrotransposon nucleocapsid; F:nucleic acid binding; F:zinc ion binding; P:DNA integration	b
SJ21135	---NA---			b
SJ08754	protein ZINC INDUCED FACILITATOR-LIKE 1-like	C:GO:0016021; P:GO:0055085	C:integral component of membrane; P:transmembrane transport	b
SJ20451	---NA---			b
SJ06686	---NA---	F:GO:0003700; C:GO:0005667; P:GO:0006355	F:DNA-binding transcription factor activity; C:transcription factor complex; P:regulation of transcription, DNA-templated	b
SJ09104	glycosyltransferase family 2 protein	P:GO:0000272; P:GO:0005982; P:GO:0005985; P:GO:0006011; F:GO:0008810; C:GO:0016021; F:GO:0016760; P:GO:0030244	P:polysaccharide catabolic process; P:starch metabolic process; P:sucrose metabolic process; P:UDP-glucose metabolic process; F:cellulase activity; C:integral component of membrane; F:cellulose synthase (UDP-forming) activity; P:cellulose biosynthetic process	b
SJ15053	probable peptide/nitrate transporter At3g43790 isoform X3	F:GO:0005215; C:GO:0016021; P:GO:0055085	F:transporter activity; C:integral component of membrane; P:transmembrane transport	b
SJ20789	---NA---			b
SJ14610	uncharacterized protein LOC111331083			b
SJ11111	apoptotic protease-activating factor 1	C:GO:0008303; P:GO:0008635; F:GO:0008656; C:GO:0043293; F:GO:0043531	C:caspase complex; P:activation of cysteine-type endopeptidase activity involved in apoptotic process by cytochrome c; F:cysteine-type endopeptidase activator activity involved in apoptotic process; C:apoptosome; F:ADP binding	b
SJ14791	---NA---			b
SJ20882	ExeM/NucH family extracellular endonuclease	F:GO:0004536; P:GO:0006308	F:deoxyribonuclease activity; P:DNA catabolic process	b
SJ10183	---NA---			b
SJ10667	predicted protein	F:GO:0003824; P:GO:0006281; P:GO:0006284	F:catalytic activity; P:DNA repair; P:base-excision repair	b
SJ19258	---NA---			b
SJ02155	---NA---			b
SJ18115	---NA---			b
SJ03682	---NA---			b
SJ11201	---NA---			b

SJ12614	low-density lipoprotein receptor-related protein 1-like			b
SJ13288	jmjC domain-containing protein 8	F:GO:0004347; C:GO:0005737; P:GO:0006094; P:GO:0006096; P:GO:0006457; C:GO:0016020; C:GO:0016021; P:GO:0016311; F:GO:0016791	F:glucose-6-phosphate isomerase activity; C:cytoplasm; P:gluconeogenesis; P:glycolytic process; P:protein folding; C:membrane; C:integral component of membrane; P:dephosphorylation; F:phosphatase activity	b
SJ18958	---NA---			b
SJ21783	lipase family protein	P:GO:0006629	P:lipid metabolic process	b
SJ03892	RmlC-like cupin	C:GO:0005576; C:GO:0016021; F:GO:0030145; F:GO:0045735	C:extracellular region; C:integral component of membrane; F:manganese ion binding; F:nutrient reservoir activity	b
SJ07084	uncharacterized mitochondrial protein AtMg00810-like	F:GO:0003676; F:GO:0008270; P:GO:0015074	F:nucleic acid binding; F:zinc ion binding; P:DNA integration	b
SJ09458	---NA---			b
SJ01479	TVP38/TMEM64 family protein	C:GO:0016021	C:integral component of membrane	b
SJ15712	tetratricopeptide repeat protein	F:GO:0003777; F:GO:0005515; C:GO:0005871; C:GO:0005874; P:GO:0007017; P:GO:0015969; C:GO:0016021; F:GO:0043531	F:microtubule motor activity; F:protein binding; C:kinesin complex; C:microtubule; P:microtubule-based process; P:guanosine tetraphosphate metabolic process; C:integral component of membrane; F:ADP binding	b
SJ05190	autotransporter domain-containing protein	C:GO:0016020	C:membrane	b
SJ06527	predicted protein	C:GO:0016021	C:integral component of membrane	b
SJ07351	---NA---			b
SJ08486	uncharacterized protein LOC110923835			b
SJ09245	DUF2306 domain-containing protein	C:GO:0016020	C:membrane	b
SJ22439	alginate lyase	F:GO:0016829	F:lyase activity	b
SJ13658	keratin-associated protein 4-7-like			b
SJ08364	---NA---			b
SJ07083	---NA---			b
SJ04649	---NA---			b
SJ14559	serine/threonine-protein phosphatase 6 regulatory ankyrin repeat subunit B-like	F:GO:0003676; F:GO:0005515; C:GO:0016020	F:nucleic acid binding; F:protein binding; C:membrane	b
SJ00465	MULTISPECIES: hypothetical protein			b
SJ09063	serine/threonine-protein kinase EDR1-like	F:GO:0004674; F:GO:0005524; C:GO:0005622; P:GO:0009069; P:GO:0009190; C:GO:0016021; F:GO:0016849; P:GO:0035556	F:protein serine/threonine kinase activity; F:ATP binding; C:intracellular; P:serine family amino acid metabolic process; P:cyclic nucleotide biosynthetic process; C:integral component of membrane; F:phosphorus-oxygen lyase activity; P:intracellular signal transduction	b
SJ01117	carbohydrate-binding protein	F:GO:0004553; P:GO:0005975; F:GO:0030246	F:hydrolase activity, hydrolyzing O-glycosyl compounds; P:carbohydrate metabolic process; F:carbohydrate binding	b
SJ14192	exostosin-1c-like	C:GO:0005783; P:GO:0006024; P:GO:0006486; P:GO:0015012; F:GO:0015020; C:GO:0016021	C:endoplasmic reticulum; P:glycosaminoglycan biosynthetic process; P:protein glycosylation; P:heparan sulfate proteoglycan biosynthetic process; F:glucuronosyltransferase activity; C:integral component of membrane	b
SJ15834	---NA---			b
SJ05263	peptidase S8	F:GO:0004252; C:GO:0016020	F:serine-type endopeptidase activity; C:membrane	b
SJ10256	predicted protein	C:GO:0005794; P:GO:0006486; F:GO:0008378; C:GO:0016020	C:Golgi apparatus; P:protein glycosylation; F:galactosyltransferase activity; C:membrane	b
SJ03270	putative leucine-rich repeat-containing protein DDB_G0281931	C:GO:0005739; P:GO:0007165; F:GO:0008233; C:GO:0016021; F:GO:0046872	C:mitochondrion; P:signal transduction; F:peptidase activity; C:integral component of membrane; F:metal ion binding	b
SJ19761	---NA---			b
SJ11985	---NA---			b
SJ19245	keratin-associated protein 4-7-like			b
SJ22387	---NA---			b
SJ12606	keratin-associated protein 4-7-like			b
SJ11395	---NA---			b
SJ07388	---NA---			b
SJ14181	beta-1,4-N-acetylgalactosaminyltransferase bre-4-like	F:GO:0005515; P:GO:0005975; F:GO:0016757	F:protein binding; P:carbohydrate metabolic process; F:transferase activity, transferring glycosyl groups	b
SJ07610	---NA---			b
SJ19359	---NA---			b
SJ12318	---NA---			b
SJ11246	hypothetical protein GUITHDRAFT_50618, partial			b
SJ06522	---NA---			b
SJ17156	---NA---	F:GO:0003677	F:DNA binding	b
SJ21708	---NA---			b
SJ09652	retrovirus-related Pol polyprotein from transposon TNT 1-94	C:GO:0000943; F:GO:0003676; P:GO:0015074	C:retrotransposon nucleocapsid; F:nucleic acid binding; P:DNA integration	b
SJ01176	protein NLP2-like	F:GO:0003677; C:GO:0005634; P:GO:0006355	F:DNA binding; C:nucleus; P:regulation of transcription, DNA-templated	b
SJ04192	tetratricopeptide repeat protein	F:GO:0003777; F:GO:0005515; C:GO:0005871; C:GO:0005874; P:GO:0007017; C:GO:0016021	F:microtubule motor activity; F:protein binding; C:kinesin complex; C:microtubule; P:microtubule-based process; C:integral component of membrane	b
SJ07314	DUF268 domain-containing protein			b
SJ17540	PKD domain-containing protein	C:GO:0016020; C:GO:0016021	C:membrane; C:integral component of membrane	b
SJ00373	notch (DSL) domain-containing protein, putative	P:GO:0043170; P:GO:0044248	P:macromolecule metabolic process; P:cellular catabolic process	b
SJ16126	---NA---			b
SJ11137	predicted protein	C:GO:0005739; C:GO:0005779	C:mitochondrion; C:integral component of peroxisomal membrane	b
SJ19979	---NA---			b
SJ13287	---NA---			b
SJ22540	---NA---			b
SJ19321	---NA---			b
SJ06156	predicted protein	F:GO:0005525	F:GTP binding	b
SJ15786	peroxidase	F:GO:0004601; P:GO:0006804; P:GO:0006979; F:GO:0020037	F:peroxidase activity; P:obsolete peroxidase reaction; P:response to oxidative stress; F:heme binding	b

SJ05300	---NA---			b
SJ04417	predicted protein			b
SJ04662	---NA---			b
SJ01486	ankyrin repeat protein	F:GO:0005515	F:protein binding	b
SJ17617	---NA---			b
SJ03924	ATP-dependent DNA helicase PIF1-like isoform X1	P:GO:0000723; F:GO:0003678; C:GO:0005657; P:GO:0006281	P:telomere maintenance; F:DNA helicase activity; C:replication fork; P:DNA repair	b
SJ09948	serine/threonine-protein phosphatase 6 regulatory ankyrin repeat subunit B-like	F:GO:0005515	F:protein binding	b
SJ18440	---NA---	F:GO:0003676; F:GO:0008270	F:nucleic acid binding; F:zinc ion binding	b
SJ20060	ubiquitin carboxyl-terminal hydrolase 2-like	F:GO:0004843; P:GO:0006511; P:GO:0016579; F:GO:0046872	F:thiol-dependent ubiquitin-specific protease activity; P:ubiquitin-dependent protein catabolic process; P:protein deubiquitination; F:metal ion binding	b
SJ08721	ubiquitin carboxyl-terminal hydrolase 20-like	P:GO:0016579; F:GO:0036459	P:protein deubiquitination; F:thiol-dependent ubiquitinyl hydrolase activity	b
SJ01975	---NA---			b
SJ17120	---NA---			b
SJ02122	SAM-dependent methyltransferase	F:GO:0016429; P:GO:0030488	F:tRNA (adenine-N1-)-methyltransferase activity; P:tRNA methylation	b
SJ07156	WSC-domain-containing protein	F:GO:0016787; P:GO:0055114; P:GO:0098869	F:hydrolase activity; P:oxidation-reduction process; P:cellular oxidant detoxification	b
SJ10293	BTB/POZ domain-containing protein KCTD2	P:GO:0051260	P:protein homooligomerization	b
SJ08689	---NA---			b
SJ17275	---NA---			b
SJ06175	MFS transporter	C:GO:0016021; P:GO:0055085	C:integral component of membrane; P:transmembrane transport	b
SJ05581	hypothetical protein AMSG_02933	F:GO:0004842; F:GO:0046872	F:ubiquitin-protein transferase activity; F:metal ion binding	b
SJ19467	---NA---			b
SJ19009	glutamine-fructose-6-phosphate transaminase	F:GO:0004360; P:GO:0006002; P:GO:0006047; P:GO:0016051; F:GO:0030246; P:GO:1901137	F:glutamine-fructose-6-phosphate transaminase (isomerizing) activity; P:fructose 6-phosphate metabolic process; P:UDP-N-acetylglucosamine metabolic process; P:carbohydrate biosynthetic process; F:carbohydrate binding; P:carbohydrate derivative biosynthetic process	b
SJ01255	monogalactosyldiacylglycerol synthase, chloroplastic	P:GO:0009247; P:GO:0046486; F:GO:0046509	P:glycolipid biosynthetic process; P:glycerolipid metabolic process; F:1,2-diacylglycerol 3-beta-galactosyltransferase activity	b
SJ16994	---NA---			b
SJ15804	---NA---			b
SJ18282	---NA---	F:GO:0005509	F:calcium ion binding	b
SJ06006	DUF1415 domain-containing protein	C:GO:0005634	C:nucleus	b
SJ03519	---NA---			b
SJ14649	---NA---			b
SJ22388	---NA---			b
SJ08756	---NA---			b
SJ06090	---NA---			b
SJ09477	hypothetical protein			b
SJ09898	---NA---			b
SJ05783	---NA---			b
SJ16473	ankyrin repeat domain-containing protein 50-like	F:GO:0005515	F:protein binding	b
SJ00093	leucine-rich repeat serine/threonine-protein kinase 1-like isoform X4	F:GO:0005525; C:GO:0005622; P:GO:0007264	F:GTP binding; C:intracellular; P:small GTPase mediated signal transduction	b
SJ13457	succinate/fumarate mitochondrial transporter	F:GO:0003735; F:GO:0005469; C:GO:0005840; P:GO:0006412; C:GO:0016021; P:GO:0042254	F:structural constituent of ribosome; F:succinate:fumarate antiporter activity; C:ribosome; P:translation; C:integral component of membrane; P:ribosome biogenesis	b
SJ22516	---NA---	F:GO:0003723	F:RNA binding	b
SJ12887	nitrite reductase small subunit NirD	F:GO:0008942; F:GO:0020037; P:GO:0042128; F:GO:0046872; F:GO:0050660; F:GO:0050661; F:GO:0051537; F:GO:0051539	F:nitrite reductase [NAD(P)H] activity; F:heme binding; P:nitrate assimilation; F:metal ion binding; F:flavin adenine dinucleotide binding; F:NADP binding; F:2 iron, 2 sulfur cluster binding; F:4 iron, 4 sulfur cluster binding	b
SJ03732	predicted protein	P:GO:0006486; F:GO:0008417; C:GO:0016021; C:GO:0032580; F:GO:0035091	P:protein glycosylation; F:fucosyltransferase activity; C:integral component of membrane; C:Golgi cisterna membrane; F:phosphatidylinositol binding	b
SJ13204	cytochrome b561 and DOMON domain-containing protein At5g35735	C:GO:0005886	C:plasma membrane	b
SJ21530	predicted protein	F:GO:0003676; F:GO:0004523; P:GO:0051252	F:nucleic acid binding; F:RNA-DNA hybrid ribonuclease activity; P:regulation of RNA metabolic process	b
SJ16284	---NA---			b
SJ01662	Plasma membrane iron permease	F:GO:0005381; C:GO:0005783; C:GO:0005794; P:GO:0010106; F:GO:0016740; C:GO:0033573	F:iron ion transmembrane transporter activity; C:endoplasmic reticulum; C:Golgi apparatus; P:cellular response to iron ion starvation; F:transferase activity; C:high-affinity iron permease complex	b
SJ02441	DUF11 domain-containing protein	C:GO:0016020	C:membrane	b
SJ12636	RmlC-like cupin	C:GO:0005576; C:GO:0016021; F:GO:0030145; F:GO:0045735	C:extracellular region; C:integral component of membrane; F:manganese ion binding; F:nutrient reservoir activity	b
SJ03422	---NA---			b
SJ22277	---NA---			b
SJ16285	serine/threonine-protein kinase STY8-like	F:GO:0004672; F:GO:0005524	F:protein kinase activity; F:ATP binding	b
SJ01002	---NA---			b
SJ14266	nitrite reductase large subunit	F:GO:0008942; F:GO:0020037; P:GO:0042128; F:GO:0046872; F:GO:0050660; F:GO:0050661; F:GO:0051537; F:GO:0051539	F:nitrite reductase [NAD(P)H] activity; F:heme binding; P:nitrate assimilation; F:metal ion binding; F:flavin adenine dinucleotide binding; F:NADP binding; F:2 iron, 2 sulfur cluster binding; F:4 iron, 4 sulfur cluster binding	b
SJ00133	---NA---			b
SJ17135	---NA---			b
SJ07470	---NA---			b
SJ13749	---NA---			b
SJ18343	---NA---			b
SJ19246	low-density lipoprotein receptor-related protein 1-like	F:GO:0005509	F:calcium ion binding	b

SJ15840	coproporphyrinogen III oxidase	F:GO:0004109; P:GO:0006779; F:GO:0008484; P:GO:0015994	F:coproporphyrinogen oxidase activity; P:porphyrin-containing compound biosynthetic process; F:sulfuric ester hydrolase activity; P:chlorophyll metabolic process	b
SJ03140	hypothetical protein H257_02413	F:GO:0005509	F:calcium ion binding	b
SJ06523	endo alpha-1,4 polygalactosaminidase	F:GO:0003824	F:catalytic activity	b
SJ14656	---NA---			b
SJ19892	---NA---			b
SJ10393	2-isopropylmalate synthase	F:GO:0016307	F:phosphatidylinositol phosphate kinase activity	b
SJ01776	hypothetical protein			e
SJ04070	---NA---			e
SJ13628	histone H3	C:GO:0000786; F:GO:0003677; C:GO:0005634; F:GO:0046982	C:nucleosome; F:DNA binding; C:nucleus; F:protein heterodimerization activity	e
SJ07010	---NA---			e
SJ17912	---NA---	F:GO:0005515	F:protein binding	e
SJ06327	UDP-N-acetylglucosamine-peptide N-acetylglucosaminyltransferase 110 kDa subunit, putative	F:GO:0016757	F:transferase activity, transferring glycosyl groups	e
SJ05021	calpain-type cysteine protease DEK1	F:GO:0004198; F:GO:0005509; C:GO:0005622	F:calcium-dependent cysteine-type endopeptidase activity; F:calcium ion binding; C:intracellular	e
SJ07387	hypothetical protein H310_02556	F:GO:0005515	F:protein binding	e
SJ02184	---NA---			e
SJ08610	Uncharacterized conserved protein	C:GO:0016021; F:GO:0046983	C:integral component of membrane; F:protein dimerization activity	e
SJ21388	---NA---			e
SJ09686	---NA---			e
SJ11325	predicted protein	C:GO:0016021	C:integral component of membrane	e
SJ01744	---NA---			e
SJ01838	---NA---			e
SJ03962	---NA---			e
SJ04789	PhoD-like phosphatase	F:GO:0046872	F:metal ion binding	e
SJ06580	NADAR family protein	F:GO:0016787	F:hydrolase activity	e
SJ07600	exonuclease 1	P:GO:0006281; P:GO:0006308; F:GO:0035312	P:DNA repair; P:DNA catabolic process; F:5'-3' exodeoxyribonuclease activity	e
SJ07878	exonuclease 1	F:GO:0004518; P:GO:0006281	F:nuclease activity; P:DNA repair	e
SJ14070	keratin-associated protein 4-7-like			e
SJ16648	---NA---			e
SJ21919	hypothetical protein crov527	P:GO:0006468	P:protein phosphorylation	e
SJ18268	---NA---			e
SJ21148	---NA---			e
SJ04537	---NA---			e
SJ04830	---NA---			e
SJ22484	---NA---			e
SJ16643	---NA---			e
SJ12920	---NA---			e
SJ13298	p25-alpha family protein, putative	F:GO:0005509	F:calcium ion binding	e
SJ18907	FG-GAP repeat protein	F:GO:0005509; P:GO:0007155; P:GO:0007229; C:GO:0008305	F:calcium ion binding; P:cell adhesion; P:integrin-mediated signaling pathway; C:integrin complex	e
SJ16021	STE/STE7 protein kinase	F:GO:0004674; F:GO:0005524; C:GO:0005737; P:GO:0009069; P:GO:0023014	F:protein serine/threonine kinase activity; F:ATP binding; C:cytoplasm; P:serine family amino acid metabolic process; P:signal transduction by protein phosphorylation	e
SJ07067	hypothetical protein AURANDRAFT_72773			e
SJ21656	---NA---			e
SJ07231	FOG: RCC1 domain	F:GO:0004842; F:GO:0005515; C:GO:0005634; C:GO:0005737; F:GO:0016874; F:GO:0046872	F:ubiquitin-protein transferase activity; F:protein binding; C:nucleus; C:cytoplasm; F:ligase activity; F:metal ion binding	e
SJ08985	sperm-associated antigen 1	F:GO:0005515	F:protein binding	e
SJ21205	hypothetical protein CAOG_07946			e
SJ20741	Tetratricopeptide repeat-containing domain	F:GO:0005515	F:protein binding	e
SJ15168	predicted protein	F:GO:0003676; F:GO:0003964; F:GO:0008270; P:GO:0015074; C:GO:0016021	F:nucleic acid binding; F:RNA-directed DNA polymerase activity; F:zinc ion binding; P:DNA integration; C:integral component of membrane	e
SJ01075	peroxidase	F:GO:0004601; P:GO:0006804; P:GO:0006979; F:GO:0020037	F:peroxidase activity; P:obsolete peroxidase reaction; P:response to oxidative stress; F:heme binding	e
SJ02863	abnormal spindle-like microcephaly-associated protein homolog	F:GO:0005515	F:protein binding	e
SJ03293	serine/threonine protein kinase	F:GO:0004672; F:GO:0005524	F:protein kinase activity; F:ATP binding	e
SJ03706	uncharacterized mitochondrial protein AtMg00810-like	F:GO:0003676; F:GO:0008270; P:GO:0015074	F:nucleic acid binding; F:zinc ion binding; P:DNA integration	e
SJ05276	17-beta-hydroxysteroid dehydrogenase type 6	F:GO:0016491	F:oxidoreductase activity	e
SJ05653	---NA---			e
SJ07589	---NA---			e
SJ10127	ankyrin repeat and protein kinase domain-containing protein 1-like	F:GO:0005515; C:GO:0016021; F:GO:0043531	F:protein binding; C:integral component of membrane; F:ADP binding	e
SJ10547	autotransporter outer membrane beta-barrel domain-containing protein	C:GO:0016020	C:membrane	e
SJ13542	---NA---			e
SJ15590	DNRLRE domain-containing protein			e
SJ17055	---NA---			e
SJ18631	---NA---			e
SJ19842	---NA---			e
SJ21457	hypothetical protein PHYSODRAFT_254578			e
SJ21947	hypothetical protein AURANDRAFT_63931	F:GO:0003676; F:GO:0004721; C:GO:0016020; F:GO:0016491; P:GO:0035335; F:GO:0046872	F:nucleic acid binding; F:phosphoprotein phosphatase activity; C:membrane; F:oxidoreductase activity; P:peptidyl-tyrosine dephosphorylation; F:metal ion binding	e
SJ01939	---NA---			e

SJ11851	---NA---	F:GO:0003676; F:GO:0008270	F:nucleic acid binding; F:zinc ion binding	e
SJ03335	saccharopine dehydrogenase	F:GO:0004754; P:GO:0006554; P:GO:0009085	F:saccharopine dehydrogenase (NAD+, L-lysine-forming) activity; P:lysine catabolic process; P:lysine biosynthetic process	e
SJ14782	DUF4281 domain-containing protein	C:GO:0016021	C:integral component of membrane	e
SJ13934	IQ and ubiquitin-like domain-containing protein isoform X1	F:GO:0005515	F:protein binding	e
SJ15898	---NA---	F:GO:0005515	F:protein binding	e
SJ11381	---NA---			e
SJ09466	cytoplasmic dynein 2 heavy chain 1-like	F:GO:0000166; F:GO:0003777; C:GO:0005874; P:GO:0007018	F:nucleotide binding; F:microtubule motor activity; C:microtubule; P:microtubule-based movement	e
SJ06583	transposon Ty3-I Gag-Pol polyprotein			e
SJ02043	predicted protein	F:GO:0005247; F:GO:0005525; C:GO:0016021; P:GO:1903959	F:voltage-gated chloride channel activity; F:GTP binding; C:integral component of membrane; P:regulation of anion transmembrane transport	e
SJ02973	---NA---			e
SJ07285	mannuronate C5-epimerase			e
SJ10009	---NA---			e
SJ10520	putative wsc domain-containing protein	C:GO:0016020	C:membrane	e
SJ17794	---NA---			e
SJ10156	---NA---			e
SJ03729	---NA---			e
SJ17731	keratin-associated protein 4-4-like			e
SJ14937	---NA---			e
SJ05597	---NA---			e
SJ03158	ankyrin repeat protein	F:GO:0005515	F:protein binding	e
SJ01922	---NA---			e
SJ18521	---NA---			e
SJ00953	MYB DNA binding protein/ transcription factor-like protein	F:GO:0003677; C:GO:0005672; P:GO:0006355; P:GO:0006367	F:DNA binding; C:transcription factor TFIIA complex; P:regulation of transcription, DNA-templated; P:transcription initiation from RNA polymerase II promoter	e
SJ01332	tetratricopeptide repeat protein	F:GO:0003777; F:GO:0005515; C:GO:0005871; C:GO:0005874; P:GO:0007017	F:microtubule motor activity; F:protein binding; C:kinesin complex; C:microtubule; P:microtubule-based process	e
SJ01333	tetratricopeptide repeat protein	F:GO:0003777; F:GO:0005515; C:GO:0005871; C:GO:0005874; P:GO:0007017	F:microtubule motor activity; F:protein binding; C:kinesin complex; C:microtubule; P:microtubule-based process	e
SJ04167	---NA---			e
SJ04356	serine/threonine-protein phosphatase 6 regulatory ankyrin repeat subunit B-like	F:GO:0005515	F:protein binding	e
SJ09798	---NA---			e
SJ20179	unnamed protein product	F:GO:0003676; C:GO:0005634; P:GO:0015074	F:nucleic acid binding; C:nucleus; P:DNA integration	e
SJ20315	predicted protein	F:GO:0004697; F:GO:0005524; P:GO:0007165; P:GO:0009069	F:protein kinase C activity; F:ATP binding; P:signal transduction; P:serine family amino acid metabolic process	e
SJ20441	---NA---			e
SJ07001	---NA---			e
SJ04237	---NA---			e
SJ09525	retention module-containing protein	F:GO:0005509; P:GO:0007156; C:GO:0016020; F:GO:0017154	F:calcium ion binding; P:homophilic cell adhesion via plasma membrane adhesion molecules; C:membrane; F:semaphorin receptor activity	e
SJ06579	---NA---			e
SJ14313	---NA---			e
SJ15955	mannuronate C5-epimerase			e
SJ20436	---NA---			e
SJ08482	---NA---			e
SJ21854	aspartyl protease family A01A, putative	F:GO:0004190	F:aspartic-type endopeptidase activity	e
SJ14653	predicted protein			e
SJ04381	---NA---			e
SJ04709	---NA---			e
SJ16266	CAMK protein kinase	F:GO:0004683; F:GO:0005516; F:GO:0005524; C:GO:0005634; C:GO:0005737; P:GO:0009069; F:GO:0009931; P:GO:0018105; P:GO:0035556; P:GO:0046777	F:calmodulin-dependent protein kinase activity; F:calmodulin binding; F:ATP binding; C:nucleus; C:cytoplasm; P:serine family amino acid metabolic process; F:calcium-dependent protein serine/threonine kinase activity; P:peptidyl-serine phosphorylation; P:intracellular signal transduction; P:protein autophosphorylation	e
SJ18310	---NA---			e
SJ19999	mannuronate C5-epimerase			e
SJ05031	autotransporter outer membrane beta-barrel domain-containing protein	C:GO:0019867	C:outer membrane	e
SJ07139	---NA---			e
SJ03991	---NA---			e
SJ20440	---NA---			e
SJ21794	---NA---			e
SJ14197	---NA---			e
SJ08316	predicted protein	C:GO:0016020; C:GO:0016021	C:membrane; C:integral component of membrane	e
SJ19286	---NA---			e
SJ11155	---NA---			e
SJ07250	mannuronate C5-epimerase			e
SJ13248	---NA---			e
SJ20888	lipase family protein	F:GO:0004806; P:GO:0016042; P:GO:0046486	F:triglyceride lipase activity; P:lipid catabolic process; P:glycerolipid metabolic process	e
SJ11323	predicted protein	F:GO:0005515; C:GO:0016021	F:protein binding; C:integral component of membrane	e
SJ20895	lipase family protein	F:GO:0004806; P:GO:0016042; P:GO:0046486	F:triglyceride lipase activity; P:lipid catabolic process; P:glycerolipid metabolic process	e
SJ05198	mannuronate C5-epimerase			e
SJ08635	WSC domain-containing protein 1-like	F:GO:0008146	F:sulfotransferase activity	e
SJ04681	---NA---			e

SJ12639	putative germin-like protein 2-1	C:GO:0005576; F:GO:0030145; F:GO:0045735	C:extracellular region; F:manganese ion binding; F:nutrient reservoir activity	e
SJ07254	mannuronate C5-epimerase			e
SJ15574	DNRLRE domain-containing protein	F:GO:0004553; P:GO:0005975; P:GO:0008152; F:GO:0008810; F:GO:0016787; F:GO:0016798	F:hydrolase activity, hydrolyzing O-glycosyl compounds; P:carbohydrate metabolic process; P:metabolic process; F:cellulase activity; F:hydrolase activity; F:hydrolase activity, acting on glycosyl bonds	e
SJ07257	mannuronate C5-epimerase			e
SJ15576	DNRLRE domain-containing protein	F:GO:0004553; P:GO:0005975; P:GO:0008152; F:GO:0008810; F:GO:0016787; F:GO:0016798	F:hydrolase activity, hydrolyzing O-glycosyl compounds; P:carbohydrate metabolic process; P:metabolic process; F:cellulase activity; F:hydrolase activity; F:hydrolase activity, acting on glycosyl bonds	e
SJ02021	---NA---			e

*Alphabet a: Consensus DEGs, b: Male consensus DEGs, e: Female consensus DEGs.

Table 14. GO enrichment analysis on upregulated gene on a: Consensus DEGs, b: Male consensus DEGs, e: Female consensus DEGs in *Saccharina japonica*

	Category	GO.ID	Term
Consensus DEGs[a]	CC	GO:0030992	intraciliary transport particle B
		GO:0005929	cilium
Male consensus DEGs[b]	BP	GO:0007018	microtubule-based movement
		GO:0044782	cilium organization
		GO:0001539	cilium or flagellum-dependent cell motility
		GO:0036159	inner dynein arm assembly
		GO:0007224	smoothened signaling pathway
		GO:0086010	membrane depolarization during action potential
		GO:0042733	embryonic digit morphogenesis
		GO:0061512	protein localization to cilium
		GO:0007156	homophilic cell adhesion via plasma membrane adhesion molecules
		GO:0043010	camera-type eye development
		GO:0035050	embryonic heart tube development
		GO:0060972	left/right pattern formation
		GO:0007178	transmembrane receptor protein serine/threonine kinase signaling pathway
		GO:0021532	neural tube patterning
		GO:0030951	establishment or maintenance of microtubule cytoskeleton polarity
		GO:0042461	photoreceptor cell development
		GO:0007605	sensory perception of sound
		GO:0051961	negative regulation of nervous system development
		GO:0072001	renal system development
	MF	GO:0003777	microtubule motor activity
		GO:0005509	calcium ion binding
		GO:0005515	protein binding
		GO:0008017	microtubule binding
		GO:0016887	ATPase activity
		GO:0005524	ATP binding
		GO:0004707	MAP kinase activity
		GO:0022843	voltage-gated cation channel activity
		GO:0004835	tubulin-tyrosine ligase activity
	CC	GO:0030286	dynein complex
		GO:0005874	microtubule
		GO:0005930	axoneme
		GO:0005929	cilium
		GO:0045298	tubulin complex
		GO:0030990	intraciliary transport particle
		GO:0036064	ciliary basal body
		GO:0035869	ciliary transition zone
		GO:0005871	kinesin complex
		GO:0005813	centrosome
Female consensus DEGs[c]	BP	GO:0043988	histone H3-S28 phosphorylation
		GO:0008354	germ cell migration
		GO:2001244	positive regulation of intrinsic apoptotic signaling pathway
		GO:0034628	'de novo' NAD biosynthetic process from aspartate
		GO:0015014	heparan sulfate proteoglycan biosynthetic process, polysaccharide chain biosynthetic process
		GO:0008101	decapentaplegic signaling pathway
		GO:0030210	heparin biosynthetic process
	MF	GO:0045735	nutrient reservoir activity
		GO:0030145	manganese ion binding
		GO:0050509	N-acetylglucosaminyl-proteoglycan 4-beta-glucuronosyltransferase activity
		GO:0004515	nicotinate-nucleotide adenylyltransferase activity
		GO:0000309	nicotinamide-nucleotide adenylyltransferase activity
		GO:0004932	mating-type factor pheromone receptor activity
		GO:0008375	acetylglucosaminyltransferase activity
	CC	GO:0005576	extracellular region
		GO:0000942	condensed nuclear chromosome outer kinetochore

p -value,0.01 was considered significant.

BP; Biologycal Process, MF; Molecular Function, CC; Cellular Component

Table 15. GO enrichment analysis on downregulated genes on a: Consensus DEGs, b: Male consensus DEGs, e: Female consensus DEGs in *Saccharina japonica*

	Category	GO.ID	Term
Consensus DEGs[a]	BP	GO:0034755	iron ion transmembrane transport
		GO:0010106	cellular response to iron ion starvation
		GO:0016052	carbohydrate catabolic process
	MF	GO:0005381	iron ion transmembrane transporter activity
		GO:0016152	mercury (II) reductase activity
		GO:0004148	dihydrolipoyl dehydrogenase activity
		GO:0008942	nitrite reductase [NAD(P)H] activity
	CC	GO:0033573	high-affinity iron permease complex
Male consensus DEGs[b]	BP	GO:0015969	guanosine tetraphosphate metabolic process
		GO:0042128	nitrate assimilation
		GO:0009439	cyanate metabolic process
		GO:0008635	activation of cysteine-type endopeptidase activity involved in apoptotic process by cytochrome c
	MF	GO:0045735	nutrient reservoir activity
		GO:0030145	manganese ion binding
		GO:0008942	nitrite reductase [NAD(P)H] activity
		GO:0008484	sulfuric ester hydrolase activity
		GO:0004252	serine-type endopeptidase activity
		GO:0005469	succinate:fumarate antiporter activity
		GO:0008656	cysteine-type endopeptidase activator activity involved in apoptotic process
		GO:0008824	cyanate hydratase activity
	CC	GO:0016020	membrane
		GO:0031224	intrinsic component of membrane
		GO:0043293	apoptosome
		GO:0008303	caspase complex
Female consensus DEGs[c]	MF	GO:0004806	triglyceride lipase activity
		GO:0008810	cellulase activity
		GO:0017154	semaphorin receptor activity
	CC	GO:0005672	transcription factor TFIIA complex

p -value,0.01 was considered significant.

BP; Biologycal Process, MF; Molecular Function, CC; Cellular Component

Table 16. The list of genes related to cell wall synthesis in *Saccharina japonica*

Abbreviation	Name	Description	GO.IDs	GO.Names
MPI	SJ01610	mannose-6-phosphate isomerase	F:GO:0004476; C:GO:0005737; P:GO:0006000; P:GO:0006013; F:GO:0008270; P:GO:0009298	F:mannose-6-phosphate isomerase activity; C:cytoplasm; P:fructose metabolic process; P:mannose metabolic process; F:zinc ion binding; P:GDP-mannose biosynthetic process
MPI	SJ15067	mannose-6-phosphate isomerase 1-like	F:GO:0004476; P:GO:0006000; P:GO:0006013; F:GO:0008270; P:GO:0009298	F:mannose-6-phosphate isomerase activity; P:fructose metabolic process; P:mannose metabolic process; F:zinc ion binding; P:GDP-mannose biosynthetic process
MPI	SJ15069	mannose-6-phosphate isomerase-like	F:GO:0004476; P:GO:0006000; P:GO:0006013; F:GO:0008270; P:GO:0009298	F:mannose-6-phosphate isomerase activity; P:fructose metabolic process; P:mannose metabolic process; F:zinc ion binding; P:GDP-mannose biosynthetic process
MPI	SJ22044	mannose-6-phosphate isomerase	F:GO:0004476; P:GO:0006000; P:GO:0006013; F:GO:0008270; P:GO:0009298	F:mannose-6-phosphate isomerase activity; P:fructose metabolic process; P:mannose metabolic process; F:zinc ion binding; P:GDP-mannose biosynthetic process
PMM	SJ02279	phosphomannomutase/phosphoglucomutase	P:GO:0005975; F:GO:0016868	P:carbohydrate metabolic process; F:intramolecular transferase activity, phosphotransferases
PMM	SJ14545	phosphomannomutase	F:GO:0004615; C:GO:0005737; P:GO:0006000; P:GO:0006013; P:GO:0009298	F:phosphomannomutase activity; C:cytoplasm; P:fructose metabolic process; P:mannose metabolic process; P:GDP-mannose biosynthetic process
MPG	SJ15067	mannose-6-phosphate isomerase 1-like	F:GO:0004476; P:GO:0006000; P:GO:0006013; F:GO:0008270; P:GO:0009298	F:mannose-6-phosphate isomerase activity; P:fructose metabolic process; P:mannose metabolic process; F:zinc ion binding; P:GDP-mannose biosynthetic process
GMD	SJ03911	UDP-glucose/GDP-mannose dehydrogenase family protein	P:GO:0000271; F:GO:0016616; F:GO:0016628; F:GO:0051287	P:polysaccharide biosynthetic process; F:oxidoreductase activity, acting on the CH-OH group of donors, NAD or NADP as acceptor; F:oxidoreductase activity, acting on the CH-CH group of donors, NAD or NADP as acceptor; F:NAD binding
GMD	SJ11024	UDP-glucose/GDP-mannose dehydrogenase family protein	F:GO:0016616; F:GO:0051287	F:oxidoreductase activity, acting on the CH-OH group of donors, NAD or NADP as acceptor; F:NAD binding
GMD	SJ11025	UDP-glucose/GDP-mannose dehydrogenase family protein	F:GO:0016616; F:GO:0051287	F:oxidoreductase activity, acting on the CH-OH group of donors, NAD or NADP as acceptor; F:NAD binding
GMD	SJ11033	UDP-glucose/GDP-mannose dehydrogenase family protein	F:GO:0016616; F:GO:0051287	F:oxidoreductase activity, acting on the CH-OH group of donors, NAD or NADP as acceptor; F:NAD binding
MS	SJ06835	glycosyltransferase family 2 protein	C:GO:0016021; F:GO:0016740	C:integral component of membrane; F:transferase activity
MC5E	SJ01921	right-handed parallel beta-helix repeat-containing protein	C:GO:0016021	C:integral component of membrane
MC5E	SJ02850	right-handed parallel beta-helix repeat-containing protein		
MC5E	SJ03359	right-handed parallel beta-helix repeat-containing protein		
MC5E	SJ04550	right-handed parallel beta-helix repeat-containing protein		
MC5E	SJ05198	right-handed parallel beta-helix repeat-containing protein		
MC5E	SJ07100	right-handed parallel beta-helix repeat-containing protein		
MC5E	SJ07246	right-handed parallel beta-helix repeat-containing protein		
MC5E	SJ07249	right-handed parallel beta-helix repeat-containing protein		
MC5E	SJ07250	right-handed parallel beta-helix repeat-containing protein		
MC5E	SJ07252	right-handed parallel beta-helix repeat-containing protein		
MC5E	SJ07254	right-handed parallel beta-helix repeat-containing protein		
MC5E	SJ07256	right-handed parallel beta-helix repeat-containing protein		
MC5E	SJ07257	right-handed parallel beta-helix repeat-containing protein		
MC5E	SJ07277	right-handed parallel beta-helix repeat-containing protein		
MC5E	SJ07285	right-handed parallel beta-helix repeat-containing protein		
MC5E	SJ07310	right-handed parallel beta-helix repeat-containing protein		
MC5E	SJ08627	right-handed parallel beta-helix repeat-containing protein	F:GO:0016787	F:hydrolase activity
MC5E	SJ09197	right-handed parallel beta-helix repeat-containing protein		
MC5E	SJ10909	right-handed parallel beta-helix repeat-containing protein		
MC5E	SJ10921	right-handed parallel beta-helix repeat-containing protein		
MC5E	SJ10981	right-handed parallel beta-helix repeat-containing protein		
MC5E	SJ12394	right-handed parallel beta-helix repeat-containing protein		
MC5E	SJ12582	right-handed parallel beta-helix repeat-containing protein		
MC5E	SJ12583	right-handed parallel beta-helix repeat-containing protein		
MC5E	SJ12584	right-handed parallel beta-helix repeat-containing protein		
MC5E	SJ12586	right-handed parallel beta-helix repeat-containing protein		
MC5E	SJ12591	right-handed parallel beta-helix repeat-containing protein		
MC5E	SJ12592	right-handed parallel beta-helix repeat-containing protein		
MC5E	SJ12593	right-handed parallel beta-helix repeat-containing protein		
MC5E	SJ15142	right-handed parallel beta-helix repeat-containing protein		
MC5E	SJ15955	right-handed parallel beta-helix repeat-containing protein		
MC5E	SJ16086	right-handed parallel beta-helix repeat-containing protein		
MC5E	SJ16087	right-handed parallel beta-helix repeat-containing protein		
MC5E	SJ16092	right-handed parallel beta-helix repeat-containing protein		
MC5E	SJ18882	right-handed parallel beta-helix repeat-containing protein		
MC5E	SJ19998	right-handed parallel beta-helix repeat-containing protein		
MC5E	SJ19999	right-handed parallel beta-helix repeat-containing protein		
MC5E	SJ20001	right-handed parallel beta-helix repeat-containing protein		
MC5E	SJ21203	right-handed parallel beta-helix repeat-containing protein		
MC5E	SJ21223	right-handed parallel beta-helix repeat-containing protein		
MC5E	SJ21803	right-handed parallel beta-helix repeat-containing protein		
MC5E	SJ22025	right-handed parallel beta-helix repeat-containing protein		
MC5E	SJ22026	right-handed parallel beta-helix repeat-containing protein		
MC5E	SJ22027	right-handed parallel beta-helix repeat-containing protein		
MC5E	SJ22028	right-handed parallel beta-helix repeat-containing protein		
MC5E	SJ22029	right-handed parallel beta-helix repeat-containing protein		
MC5E	SJ22030	right-handed parallel beta-helix repeat-containing protein		
MC5E	SJ22031	right-handed parallel beta-helix repeat-containing protein		
MC5E	SJ22032	right-handed parallel beta-helix repeat-containing protein		
MC5E	SJ22069	right-handed parallel beta-helix repeat-containing protein		
MC5E	SJ22247	right-handed parallel beta-helix repeat-containing protein		
MC5E	SJ22418	right-handed parallel beta-helix repeat-containing protein	C:GO:0016020; C:GO:0016021	C:membrane; C:integral component of membrane
FKGP	SJ13948	L-fucose kinase isoform X1	F:GO:0005524; C:GO:0005737; F:GO:0016301; F:GO:0016773	F:ATP binding; C:cytoplasm; F:kinase activity; F:phosphotransferase activity, alcohol group as acceptor

GM46D	SJ04008	gdp-mannose 4,6-dehydratase	P:GO:0006000; P:GO:0006012; F:GO:0008446; P:GO:0009298; F:GO:0070401	P:fructose metabolic process; P:galactose metabolic process; F:GDP-mannose 4,6-dehydratase activity; P:GDP-mannose biosynthetic process; F:NADP+ binding
GM46D	SJ21655	GDP-mannose 4,6-dehydratase	P:GO:0006000; P:GO:0006012; F:GO:0008446; P:GO:0009298; F:GO:0070401	P:fructose metabolic process; P:galactose metabolic process; F:GDP-mannose 4,6-dehydratase activity; P:GDP-mannose biosynthetic process; F:NADP+ binding
GFS	SJ05880	GDP-L-fucose synthase	P:GO:0006000; P:GO:0006013; P:GO:0019673; P:GO:0019835; P:GO:0042351; F:GO:0050577; F:GO:0050662; C:GO:0070062	P:fructose metabolic process; P:mannose metabolic process; P:GDP-mannose metabolic process; P:cytolysis; P:'de novo' GDP-L-fucose biosynthetic process; F:GDP-L-fucose synthase activity; F:coenzyme binding; C:extracellular exosome
FT	SJ01987	alpha-(1,6)-fucosyltransferase (GT23)	F:GO:0016740	F:transferase activity
FT	SJ11160	putative alpha 1,3-fucosyltransferase (GT10)	P:GO:0006486; F:GO:0008417; C:GO:0016021; C:GO:0032580	P:protein glycosylation; F:fucosyltransferase activity; C:integral component of membrane; C:Golgi cisterna membrane
ST	SJ00041	carbohydrate sulfotransferase 11-like	F:GO:0008146; C:GO:0016021; P:GO:0016051	F:sulfotransferase activity; C:integral component of membrane; P:carbohydrate biosynthetic process
ST	SJ00043	predicted protein	F:GO:0008146; C:GO:0016021; P:GO:0016051	F:sulfotransferase activity; C:integral component of membrane; P:carbohydrate biosynthetic process
ST	SJ00192	amine sulfotransferase-like	F:GO:0008146	F:sulfotransferase activity
ST	SJ00322	cell surface receptor IPT/TIG domain-containing protein	P:GO:0007165; F:GO:0008146; C:GO:0016021; F:GO:0046872	P:signal transduction; F:sulfotransferase activity; C:integral component of membrane; F:metal ion binding
ST	SJ00892	PREDICTED: uncharacterized protein LOC102810117	F:GO:0008146; C:GO:0016021	F:sulfotransferase activity; C:integral component of membrane
ST	SJ00902	NAD-dependent epimerase/dehydratase family protein	F:GO:0008146; F:GO:0008270; P:GO:0009117; P:GO:0009247; C:GO:0009507; F:GO:0046507; F:GO:0050662	F:sulfotransferase activity; F:zinc ion binding; P:nucleotide metabolic process; P:glycolipid biosynthetic process; C:chloroplast; F:UDPsulfoquinovose synthase activity; F:coenzyme binding
ST	SJ00944	heparan sulfate glucosamine 3-O-sulfotransferase 3B1-like	F:GO:0008146	F:sulfotransferase activity
ST	SJ01900	amine sulfotransferase-like	P:GO:0006805; F:GO:0008146; P:GO:0042403; P:GO:0051923	P:xenobiotic metabolic process; F:sulfotransferase activity; P:thyroid hormone metabolic process; P:sulfation
ST	SJ03065	hypothetical protein	F:GO:0008146; C:GO:0016021	F:sulfotransferase activity; C:integral component of membrane
ST	SJ03843	PREDICTED: uncharacterized protein LOC752507	F:GO:0008146; C:GO:0016021	F:sulfotransferase activity; C:integral component of membrane
ST	SJ04014	aryl sulfotransferase	F:GO:0008146	F:sulfotransferase activity
ST	SJ04970	tetratricopeptide repeat protein	F:GO:0008146	F:sulfotransferase activity
ST	SJ05080	---NA---	F:GO:0008146	F:sulfotransferase activity
ST	SJ05081	---NA---	F:GO:0008146	F:sulfotransferase activity
ST	SJ05573	sulfotransferase domain-containing protein	F:GO:0008146	F:sulfotransferase activity
ST	SJ05659	hypothetical protein AURANDRAFT_66449	F:GO:0008146; C:GO:0016021	F:sulfotransferase activity; C:integral component of membrane
ST	SJ05785	galactose-3-O-sulfotransferase 3	F:GO:0001733; C:GO:0005794; P:GO:0006687; P:GO:0009247; C:GO:0016021; F:GO:0016263; P:GO:0016267; C:GO:0019013	F:galactosylceramide sulfotransferase activity; C:Golgi apparatus; P:glycosphingolipid metabolic process; P:glycolipid biosynthetic process; C:integral component of membrane; F:glycoprotein-N-acetylgalactosamine 3-beta-galactosyltransferase activity; P:O-glycan processing, core 1; C:viral nucleocapsid
ST	SJ06276	sulfotransferase 1A3	F:GO:0004062; F:GO:0005515; C:GO:0005829; P:GO:0006584; P:GO:0006805; P:GO:0008202; P:GO:0009812; F:GO:0036498; P:GO:0050427; P:GO:0051923	F:aryl sulfotransferase activity; F:protein binding; C:cytosol; P:catecholamine metabolic process; P:xenobiotic metabolic process; P:steroid metabolic process; P:flavonoid metabolic process; P:IRE1-mediated unfolded protein response; P:3'-phosphoadenosine 5'-phosphosulfate metabolic process; P:sulfation
ST	SJ07550	sulfotransferase 1 family member D1-like	P:GO:0006805; F:GO:0008146; P:GO:0042403; P:GO:0051923	P:xenobiotic metabolic process; F:sulfotransferase activity; P:thyroid hormone metabolic process; P:sulfation
ST	SJ08012	sulfotransferase	F:GO:0008146	F:sulfotransferase activity
ST	SJ08083	predicted protein	F:GO:0008146; C:GO:0016021; P:GO:0018193	F:sulfotransferase activity; C:integral component of membrane; P:peptidyl-amino acid modification
ST	SJ08635	WSC domain-containing protein 1-like	F:GO:0008146	F:sulfotransferase activity
ST	SJ09246	PREDICTED: uncharacterized protein LOC752507	F:GO:0008146; C:GO:0016021	F:sulfotransferase activity; C:integral component of membrane
ST	SJ09270	galactose-3-O-sulfotransferase 3	F:GO:0001733; C:GO:0005794; P:GO:0006687; P:GO:0009247; C:GO:0016021; F:GO:0016263; P:GO:0016267; C:GO:0019013	F:galactosylceramide sulfotransferase activity; C:Golgi apparatus; P:glycosphingolipid metabolic process; P:glycolipid biosynthetic process; C:integral component of membrane; F:glycoprotein-N-acetylgalactosamine 3-beta-galactosyltransferase activity; P:O-glycan processing, core 1; C:viral nucleocapsid
ST	SJ10783	predicted protein	F:GO:0008146; C:GO:0016021; P:GO:0016051	F:sulfotransferase activity; C:integral component of membrane; P:carbohydrate biosynthetic process
ST	SJ11262	carbohydrate sulfotransferase 14	F:GO:0008146; C:GO:0016021; P:GO:0016051	F:sulfotransferase activity; C:integral component of membrane; P:carbohydrate biosynthetic process
ST	SJ11351	hypothetical protein AURANDRAFT_62666	F:GO:0001733; F:GO:0003676; C:GO:0005794; P:GO:0006511; F:GO:0008168; P:GO:0009247; C:GO:0016020; C:GO:0016021; P:GO:0016579; P:GO:0032259; F:GO:0036459	F:galactosylceramide sulfotransferase activity; F:nucleic acid binding; C:Golgi apparatus; P:ubiquitin-dependent protein catabolic process; F:methyltransferase activity; P:glycolipid biosynthetic process; C:membrane; C:integral component of membrane; P:protein deubiquitination; P:methylation; F:thiol-dependent ubiquitinyl hydrolase activity
ST	SJ11352	galactosylceramide sulfotransferase-like	F:GO:0001733; F:GO:0003676; C:GO:0005794; P:GO:0006511; P:GO:0006687; F:GO:0008168; P:GO:0009247; C:GO:0016021; P:GO:0016579; F:GO:0036459	F:galactosylceramide sulfotransferase activity; F:nucleic acid binding; C:Golgi apparatus; P:ubiquitin-dependent protein catabolic process; P:glycosphingolipid metabolic process; F:methyltransferase activity; P:glycolipid biosynthetic process; C:integral component of membrane; P:protein deubiquitination; F:thiol-dependent ubiquitinyl hydrolase activity
ST	SJ12399	putative leucine-rich repeat-containing protein DDB_G0281931	C:GO:0005739; P:GO:0007165; F:GO:0008146; F:GO:0008233; C:GO:0016021; F:GO:0046872	C:mitochondrion; P:signal transduction; F:sulfotransferase activity; F:peptidase activity; C:integral component of membrane; F:metal ion binding
ST	SJ12919	PREDICTED: uncharacterized protein LOC100892323	F:GO:0008146; C:GO:0016021	F:sulfotransferase activity; C:integral component of membrane
ST	SJ13253	putative leucine-rich repeat-containing protein DDB_G0281931	P:GO:0007186; F:GO:0008146; C:GO:0016021	P:G-protein coupled receptor signaling pathway; F:sulfotransferase activity; C:integral component of membrane
ST	SJ13268	putative leucine-rich repeat-containing protein DDB_G0281931	C:GO:0005739; P:GO:0007165; F:GO:0008146; F:GO:0008233; C:GO:0016021; F:GO:0046872	C:mitochondrion; P:signal transduction; F:sulfotransferase activity; F:peptidase activity; C:integral component of membrane; F:metal ion binding
ST	SJ13393	galactose-3-O-sulfotransferase 3-like	F:GO:0001733; C:GO:0005794; P:GO:0006687; P:GO:0009247; C:GO:0016021; F:GO:0016263; P:GO:0016267; C:GO:0019013	F:galactosylceramide sulfotransferase activity; C:Golgi apparatus; P:glycosphingolipid metabolic process; P:glycolipid biosynthetic process; C:integral component of membrane; F:glycoprotein-N-acetylgalactosamine 3-beta-galactosyltransferase activity; P:O-glycan processing, core 1; C:viral nucleocapsid

ST	SJ13394	galactosylceramide sulfotransferase-like	F:GO:0001733; C:GO:0005794; P:GO:0006687; P:GO:0009247; C:GO:0016021; F:GO:0016263; P:GO:0016267; C:GO:0019013	F:galactosylceramide sulfotransferase activity; C:Golgi apparatus; P:glycosphingolipid metabolic process; P:glycolipid biosynthetic process; C:integral component of membrane; F:glycoprotein-N-acetylgalactosamine 3-beta-galactosyltransferase activity; P:O-glycan processing, core 1; C:viral nucleocapsid
ST	SJ13400	galactose-3-O-sulfotransferase 3-like	F:GO:0001733; C:GO:0005794; P:GO:0006687; P:GO:0009247; C:GO:0016021; F:GO:0016263; P:GO:0016267; C:GO:0019013	F:galactosylceramide sulfotransferase activity; C:Golgi apparatus; P:glycosphingolipid metabolic process; P:glycolipid biosynthetic process; C:integral component of membrane; F:glycoprotein-N-acetylgalactosamine 3-beta-galactosyltransferase activity; P:O-glycan processing, core 1; C:viral nucleocapsid
ST	SJ13949	sulfotransferase	F:GO:0008146; C:GO:0016021	F:sulfotransferase activity; C:integral component of membrane
ST	SJ13950	sulfotransferase	F:GO:0008146; C:GO:0016021	F:sulfotransferase activity; C:integral component of membrane
ST	SJ14141	galactose-3-O-sulfotransferase 3	F:GO:0001733; C:GO:0005794; P:GO:0006687; P:GO:0009247; C:GO:0016021; F:GO:0016263; P:GO:0016267; C:GO:0019013	F:galactosylceramide sulfotransferase activity; C:Golgi apparatus; P:glycosphingolipid metabolic process; P:glycolipid biosynthetic process; C:integral component of membrane; F:glycoprotein-N-acetylgalactosamine 3-beta-galactosyltransferase activity; P:O-glycan processing, core 1; C:viral nucleocapsid
ST	SJ14732	carbohydrate sulfotransferase 4	C:GO:0000139; F:GO:0001517; C:GO:0005802; P:GO:0005975; P:GO:0006044; P:GO:0006477; P:GO:0006790; F:GO:0008146; C:GO:0016021; F:GO:0016740	C:Golgi membrane; F:N-acetylglucosamine 6-O-sulfotransferase activity; C:trans-Golgi network; P:carbohydrate metabolic process; P:N-acetylglucosamine metabolic process; P:protein sulfation; P:sulfur compound metabolic process; F:sulfotransferase activity; C:integral component of membrane; F:transferase activity
ST	SJ16079	adenylate kinase	F:GO:0008146; C:GO:0016021	F:sulfotransferase activity; C:integral component of membrane
ST	SJ16123	probable arabinosyltransferase ARAD1	P:GO:0006486; F:GO:0008146; C:GO:0016021; F:GO:0016757	P:protein glycosylation; F:sulfotransferase activity; C:integral component of membrane; F:transferase activity, transferring glycosyl groups
ST	SJ16293	---NA---	F:GO:0008146	F:sulfotransferase activity
ST	SJ16315	predicted protein	F:GO:0004888; F:GO:0005215; C:GO:0005739; P:GO:0006810; P:GO:0006963; P:GO:0007186; P:GO:0007352; P:GO:0008063; F:GO:0008146; F:GO:0008233; P:GO:0009620; C:GO:0016021; F:GO:0046872; P:GO:0050830	F:transmembrane signaling receptor activity; F:transporter activity; C:mitochondrion; P:transport; P:positive regulation of antibacterial peptide biosynthetic process; P:G-protein coupled receptor signaling pathway; P:zygotic specification of dorsal/ventral axis; P:Toll signaling pathway; F:sulfotransferase activity; F:peptidase activity; P:response to fungus; C:integral component of membrane; F:metal ion binding; P:defense response to Gram-positive bacterium
ST	SJ16318	predicted protein	F:GO:0004888; F:GO:0005215; C:GO:0005739; P:GO:0006810; P:GO:0006963; P:GO:0007186; P:GO:0007352; P:GO:0008063; F:GO:0008146; F:GO:0008233; P:GO:0009620; C:GO:0016021; F:GO:0046872; P:GO:0050830	F:transmembrane signaling receptor activity; F:transporter activity; C:mitochondrion; P:transport; P:positive regulation of antibacterial peptide biosynthetic process; P:G-protein coupled receptor signaling pathway; P:zygotic specification of dorsal/ventral axis; P:Toll signaling pathway; F:sulfotransferase activity; F:peptidase activity; P:response to fungus; C:integral component of membrane; F:metal ion binding; P:defense response to Gram-positive bacterium
ST	SJ17072	adenylate kinase	F:GO:0008146; C:GO:0016021	F:sulfotransferase activity; C:integral component of membrane
ST	SJ17294	carbohydrate sulfotransferase 4-like	C:GO:0000139; P:GO:0005975; F:GO:0008146; C:GO:0016020; C:GO:0016021; F:GO:0016740	C:Golgi membrane; P:carbohydrate metabolic process; F:sulfotransferase activity; C:membrane; C:integral component of membrane; F:transferase activity
ST	SJ17636	predicted protein	F:GO:0008146; C:GO:0016021; P:GO:0016051	F:sulfotransferase activity; C:integral component of membrane; P:carbohydrate biosynthetic process
ST	SJ17721	sulfotransferase family protein	F:GO:0008146	F:sulfotransferase activity
ST	SJ17864	carbohydrate sulfotransferase 1-like isoform X2	F:GO:0008146	F:sulfotransferase activity
ST	SJ18080	WSCD family member CG9164-like	F:GO:0008146	F:sulfotransferase activity
ST	SJ18184	galactose-3-O-sulfotransferase 3	F:GO:0001733; C:GO:0005794; P:GO:0006687; P:GO:0009247; C:GO:0016021; P:GO:0032501	F:galactosylceramide sulfotransferase activity; C:Golgi apparatus; P:glycosphingolipid metabolic process; P:glycolipid biosynthetic process; C:integral component of membrane; P:multicellular organismal process
ST	SJ18421	hypothetical protein NGA_0310502	F:GO:0008146; C:GO:0016021	F:sulfotransferase activity; C:integral component of membrane
ST	SJ18674	---NA---	F:GO:0008146; C:GO:0016021	F:sulfotransferase activity; C:integral component of membrane
ST	SJ19194	sulfotransferase 1C2A-like	P:GO:0006805; F:GO:0008146; P:GO:0042403; P:GO:0051923	P:xenobiotic metabolic process; F:sulfotransferase activity; P:thyroid hormone metabolic process; P:sulfation
ST	SJ20074	galactose-3-O-sulfotransferase 3-like	F:GO:0001733; C:GO:0005794; P:GO:0006687; P:GO:0009247; C:GO:0016021	F:galactosylceramide sulfotransferase activity; C:Golgi apparatus; P:glycosphingolipid metabolic process; P:glycolipid biosynthetic process; C:integral component of membrane
ST	SJ20091	carbohydrate sulfotransferase 11	F:GO:0008146; C:GO:0016021; P:GO:0016051	F:sulfotransferase activity; C:integral component of membrane; P:carbohydrate biosynthetic process
ST	SJ20108	heparan sulfate glucosamine 3-O-sulfotransferase 6-like	P:GO:0003341; F:GO:0019111; P:GO:0046718; P:GO:0060271	P:cilium movement; F:phenanthrol sulfotransferase activity; P:viral entry into host cell; P:cilium assembly
ST	SJ21107	tetratricopeptide repeat protein	F:GO:0008146	F:sulfotransferase activity
ST	SJ21189	---NA---	F:GO:0008146; C:GO:0016021	F:sulfotransferase activity; C:integral component of membrane
ST	SJ21222	predicted protein	F:GO:0008146; C:GO:0016021	F:sulfotransferase activity; C:integral component of membrane
ST	SJ21244	ubiquitin domain containing protein	F:GO:0001733; F:GO:0003676; C:GO:0005794; P:GO:0006511; P:GO:0006687; F:GO:0008168; P:GO:0009247; C:GO:0016021; P:GO:0016579; F:GO:0036459	F:galactosylceramide sulfotransferase activity; F:nucleic acid binding; C:Golgi apparatus; P:ubiquitin-dependent protein catabolic process; P:glycosphingolipid metabolic process; F:methyltransferase activity; P:glycolipid biosynthetic process; C:integral component of membrane; P:protein deubiquitination; F:thiol-dependent ubiquitinyl hydrolase activity
ST	SJ21424	heparan sulfate glucosamine 3-O-sulfotransferase 5	F:GO:0008146	F:sulfotransferase activity
ST	SJ21441	galactosylceramide sulfotransferase-like	F:GO:0001733; C:GO:0005794; P:GO:0006687; P:GO:0009247; C:GO:0016021; F:GO:0016263; P:GO:0016267; C:GO:0019013	F:galactosylceramide sulfotransferase activity; C:Golgi apparatus; P:glycosphingolipid metabolic process; P:glycolipid biosynthetic process; C:integral component of membrane; F:glycoprotein-N-acetylgalactosamine 3-beta-galactosyltransferase activity; P:O-glycan processing, core 1; C:viral nucleocapsid
ST	SJ22167	PREDICTED: uncharacterized protein LOC752507	F:GO:0008146; C:GO:0016021	F:sulfotransferase activity; C:integral component of membrane
ST	SJ22623	probable arabinosyltransferase ARAD1	P:GO:0006486; F:GO:0008146; C:GO:0016021; F:GO:0016757	P:protein glycosylation; F:sulfotransferase activity; C:integral component of membrane; F:transferase activity, transferring glycosyl groups

GPI	SJ00085	glucose-6-phosphate isomerase, cytosolic	F:GO:0004347; C:GO:0005829; P:GO:0005982; P:GO:0005985; P:GO:0006094; P:GO:0006096; P:GO:0006098; P:GO:0009817	F:glucose-6-phosphate isomerase activity; C:cytosol; P:starch metabolic process; P:sucrose metabolic process; P:gluconeogenesis; P:glycolytic process; P:pentose-phosphate shunt; P:defense response to fungus, incompatible interaction
GPI	SJ08179	glucose-6-phosphate isomerase, cytosolic	F:GO:0004347; C:GO:0005829; P:GO:0005982; P:GO:0005985; P:GO:0006094; P:GO:0006096; P:GO:0006098; P:GO:0009817	F:glucose-6-phosphate isomerase activity; C:cytosol; P:starch metabolic process; P:sucrose metabolic process; P:gluconeogenesis; P:glycolytic process; P:pentose-phosphate shunt; P:defense response to fungus, incompatible interaction
PGM	SJ02279	phosphomannomutase/phosphoglucomutase	P:GO:0005975; F:GO:0016868	P:carbohydrate metabolic process; F:intramolecular transferase activity, phosphotransferases
PGM	SJ05004	phosphoglucomutase-2 isoform X1	F:GO:0000287; C:GO:0005829; P:GO:0005975; F:GO:0016868	F:magnesium ion binding; C:cytosol; P:carbohydrate metabolic process; F:intramolecular transferase activity, phosphotransferases
PGM	SJ12510	phosphoglucomutase, cytoplasmic	F:GO:0000287; F:GO:0004017; F:GO:0004614; F:GO:0005524; C:GO:0005634; C:GO:0005829; C:GO:0005886; P:GO:0005978; P:GO:0005985; P:GO:0005992; P:GO:0006094; P:GO:0006096; P:GO:0006098; P:GO:0006144; P:GO:0006874; C:GO:0009570; P:GO:0009590; C:GO:0010319; P:GO:0019252; P:GO:0019255; P:GO:0019388; P:GO:0019872; P:GO:0046686; P:GO:0048229; F:GO:0070569	F:magnesium ion binding; F:adenylate kinase activity; F:phosphoglucomutase activity; F:ATP binding; C:nucleus; C:cytosol; C:plasma membrane; P:glycogen biosynthetic process; P:sucrose metabolic process; P:trehalose biosynthetic process; P:gluconeogenesis; P:glycolytic process; P:pentose-phosphate shunt; P:purine nucleobase metabolic process; P:cellular calcium ion homeostasis; C:chloroplast stroma; P:detection of gravity; C:stromule; P:starch biosynthetic process; P:glucose 1-phosphate metabolic process; P:galactose catabolic process; P:streptomycin biosynthetic process; P:response to cadmium ion; P:gametophyte development; F:uridylyltransferase activity
PGM	SJ18341	phosphoglucomutase, cytoplasmic	F:GO:0000287; F:GO:0003983; F:GO:0004614; C:GO:0005829; P:GO:0005978; P:GO:0005982; P:GO:0005985; P:GO:0006011; P:GO:0006094; P:GO:0006096; P:GO:0006098; P:GO:0019388; P:GO:0019872	F:magnesium ion binding; F:UTP:glucose-1-phosphate uridylyltransferase activity; F:phosphoglucomutase activity; C:cytosol; P:glycogen biosynthetic process; P:starch metabolic process; P:sucrose metabolic process; P:UDP-glucose metabolic process; P:gluconeogenesis; P:glycolytic process; P:pentose-phosphate shunt; P:galactose catabolic process; P:streptomycin biosynthetic process
UGP	SJ10502	utp-glucose-1-phosphate uridylyltransferase	F:GO:0003983; P:GO:0005982; P:GO:0005985; P:GO:0006011; P:GO:0006012; P:GO:0009117	F:UTP:glucose-1-phosphate uridylyltransferase activity; P:starch metabolic process; P:sucrose metabolic process; P:UDP-glucose metabolic process; P:galactose metabolic process; P:nucleotide metabolic process
UGP	SJ18341	phosphoglucomutase, cytoplasmic	F:GO:0000287; F:GO:0003983; F:GO:0004614; C:GO:0005829; P:GO:0005978; P:GO:0005982; P:GO:0005985; P:GO:0006011; P:GO:0006094; P:GO:0006096; P:GO:0006098; P:GO:0019388; P:GO:0019872	F:magnesium ion binding; F:UTP:glucose-1-phosphate uridylyltransferase activity; F:phosphoglucomutase activity; C:cytosol; P:glycogen biosynthetic process; P:starch metabolic process; P:sucrose metabolic process; P:UDP-glucose metabolic process; P:gluconeogenesis; P:glycolytic process; P:pentose-phosphate shunt; P:galactose catabolic process; P:streptomycin biosynthetic process
CESA	SJ01458	glycosyltransferase	C:GO:0016020; F:GO:0016757	C:membrane; F:transferase activity, transferring glycosyl groups
CESA	SJ01459	glycosyltransferase	P:GO:0005982; P:GO:0005985; P:GO:0006011; C:GO:0016020; F:GO:0016760; P:GO:0030244	P:starch metabolic process; P:sucrose metabolic process; P:UDP-glucose metabolic process; C:membrane; F:cellulose synthase (UDP-forming) activity; P:cellulose biosynthetic process
CESA	SJ05122	glycosyltransferase family 2 protein	P:GO:0000272; P:GO:0005982; P:GO:0005985; P:GO:0006011; F:GO:0008810; C:GO:0016021; F:GO:0016760; P:GO:0030244	P:polysaccharide catabolic process; P:starch metabolic process; P:sucrose metabolic process; P:UDP-glucose metabolic process; F:cellulase activity; C:integral component of membrane; F:cellulose synthase (UDP-forming) activity; P:cellulose biosynthetic process
CESA	SJ08880	cellulose synthase 3		
CESA	SJ09104	glycosyltransferase family 2 protein	P:GO:0000272; P:GO:0005982; P:GO:0005985; P:GO:0006011; F:GO:0008810; C:GO:0016021; F:GO:0016760; P:GO:0030244	P:polysaccharide catabolic process; P:starch metabolic process; P:sucrose metabolic process; P:UDP-glucose metabolic process; F:cellulase activity; C:integral component of membrane; F:cellulose synthase (UDP-forming) activity; P:cellulose biosynthetic process
CESA	SJ17603	glycosyltransferase family 2 protein	P:GO:0000272; P:GO:0005982; P:GO:0005985; F:GO:0008810; C:GO:0016021; F:GO:0016740	P:polysaccharide catabolic process; P:starch metabolic process; P:sucrose metabolic process; F:cellulase activity; C:integral component of membrane; F:transferase activity
CESA	SJ17604	glycosyltransferase family 2 protein	P:GO:0000272; P:GO:0005982; P:GO:0005985; P:GO:0006011; F:GO:0008810; C:GO:0016021; F:GO:0016760; P:GO:0030244	P:polysaccharide catabolic process; P:starch metabolic process; P:sucrose metabolic process; P:UDP-glucose metabolic process; F:cellulase activity; C:integral component of membrane; F:cellulose synthase (UDP-forming) activity; P:cellulose biosynthetic process
CESA	SJ19851	glycosyltransferase		
CESA	SJ19854	---NA---		
CESA	SJ20814	glycosyltransferase	P:GO:0005982; P:GO:0005985; P:GO:0006011; C:GO:0016020; F:GO:0016760; P:GO:0030244	P:starch metabolic process; P:sucrose metabolic process; P:UDP-glucose metabolic process; C:membrane; F:cellulose synthase (UDP-forming) activity; P:cellulose biosynthetic process
CESA	SJ20815	glycosyltransferase	P:GO:0005982; P:GO:0005985; P:GO:0006011; C:GO:0016020; F:GO:0016760; P:GO:0030244	P:starch metabolic process; P:sucrose metabolic process; P:UDP-glucose metabolic process; C:membrane; F:cellulose synthase (UDP-forming) activity; P:cellulose biosynthetic process
GS	SJ05912	callose synthase 9		
GS	SJ05913	callose synthase 2-like	C:GO:0000148; F:GO:0003843; P:GO:0005982; P:GO:0005985; P:GO:0006075	C:1,3-beta-D-glucan synthase complex; F:1,3-beta-D-glucan synthase activity; P:starch metabolic process; P:sucrose metabolic process; P:(1->3)-beta-D-glucan biosynthetic process
GS	SJ07490	callose synthase 12-like	P:GO:0000003; C:GO:0000148; F:GO:0003843; C:GO:0005794; P:GO:0005982; P:GO:0005985; P:GO:0006075; C:GO:0009506; P:GO:0009555; P:GO:0009870; P:GO:0009965; P:GO:0010150; C:GO:0016021; P:GO:0042742; P:GO:0050832; P:GO:0052544	P:reproduction; C:1,3-beta-D-glucan synthase complex; F:1,3-beta-D-glucan synthase activity; C:Golgi apparatus; P:starch metabolic process; P:sucrose metabolic process; P:(1->3)-beta-D-glucan biosynthetic process; C:plasmodesma; P:pollen development; P:defense response signaling pathway, resistance gene-dependent; P:leaf morphogenesis; P:leaf senescence; C:integral component of membrane; P:defense response to bacterium; P:defense response to fungus; P:defense response by callose deposition in cell wall
GS	SJ14965	callose synthase 5	C:GO:0000148; F:GO:0003843; F:GO:0004553; P:GO:0005982; P:GO:0005985; P:GO:0006075; C:GO:0016021	C:1,3-beta-D-glucan synthase complex; F:1,3-beta-D-glucan synthase activity; F:hydrolase activity, hydrolyzing O-glycosyl compounds; P:starch metabolic process; P:sucrose metabolic process; P:(1->3)-beta-D-glucan biosynthetic process; C:integral component of membrane

GS	SJ14966	callose synthase 12	C:GO:0000148; F:GO:0003843; F:GO:0004553; P:GO:0005982; P:GO:0005985; P:GO:0006075; C:GO:0016021	C:1,3-beta-D-glucan synthase complex; F:1,3-beta-D-glucan synthase activity; F:hydrolase activity, hydrolyzing O-glycosyl compounds; P:starch metabolic process; P:sucrose metabolic process; P:(1->3)-beta-D-glucan biosynthetic process; C:integral component of membrane
GS	SJ14967	callose synthase 9	C:GO:0000148; F:GO:0003843; F:GO:0004553; P:GO:0005982; P:GO:0005985; P:GO:0006075; C:GO:0016021	C:1,3-beta-D-glucan synthase complex; F:1,3-beta-D-glucan synthase activity; F:hydrolase activity, hydrolyzing O-glycosyl compounds; P:starch metabolic process; P:sucrose metabolic process; P:(1->3)-beta-D-glucan biosynthetic process; C:integral component of membrane
GS	SJ14968	callose synthase 5	C:GO:0000148; F:GO:0003843; F:GO:0004553; P:GO:0005982; P:GO:0005985; P:GO:0006075; C:GO:0016021	C:1,3-beta-D-glucan synthase complex; F:1,3-beta-D-glucan synthase activity; F:hydrolase activity, hydrolyzing O-glycosyl compounds; P:starch metabolic process; P:sucrose metabolic process; P:(1->3)-beta-D-glucan biosynthetic process; C:integral component of membrane
GS	SJ17989	callose synthase 3-like	C:GO:0000148; F:GO:0003843; P:GO:0005982; P:GO:0005985; P:GO:0006075	C:1,3-beta-D-glucan synthase complex; F:1,3-beta-D-glucan synthase activity; P:starch metabolic process; P:sucrose metabolic process; P:(1->3)-beta-D-glucan biosynthetic process
KRE6-like	SJ06967	predicted protein	C:GO:0000148; F:GO:0003843; F:GO:0004519; F:GO:0004553; P:GO:0005982; P:GO:0005985; P:GO:0006075; C:GO:0016021	C:1,3-beta-D-glucan synthase complex; F:1,3-beta-D-glucan synthase activity; F:endonuclease activity; F:hydrolase activity, hydrolyzing O-glycosyl compounds; P:starch metabolic process; P:sucrose metabolic process; P:(1->3)-beta-D-glucan biosynthetic process; C:integral component of membrane

Legends of Plates

Plate 1. A diagram showing the measurement area of gold particles bound to antibodies on the cell wall of the *Silvetia babingtonii* zygotes. Measurements are made within three replicate rectangle regions of the thallus cell wall (TCW: diagonal dot line area), the rhizoid-flank cell wall (RFCW: striped area), and the rhizoid-tip cell wall (RTCW: plane area). Each rectangle stretches from the plasma membrane (PM) to the outer edge of the cell wall (CW edge) and has 0.75 μm wide sides over the plasma membrane and at the surface of the cell wall. Three different zygotes are measured (n=9).

Plate 2. *Silvetia babingtonii* zygote development. (a) 30 min AF, (b) 12 h AF, (c) 20 h AF, (d) 24 h AF. Arrows and arrowheads indicate the first and second cytokinetic planes, respectively. Scale bars = 50 μm (a-d).

Plate 3. Ultrastructure of (a) TCW, (b) RFCW, and (c) RTCW in *Silvetia babingtonii* zygotes at 12 h AF. Arrows show the outer edge of cell wall. Arrowheads show plasma membrane. IL; the inner layer, ML; the middle layer, OL; the outer layer. Scale bars = 500 nm.

Plate 4. *Silvetia babingtonii* zygotes at 24 h AF. (a) View of the rhizoid. A double arrowhead indicates the point from which the two outer layers start to be reduced. (b) Oblique section of TCW. The cell wall consists of three layers. (c) Perpendicular section of TCW. (d) RFCW. The outer layer is disappearing. (e) RFCW. The middle layer fades away. (f) RTCW has only one layer, which is made of rough fibrils. Thick mucilage covers the rhizoid. Arrows indicate the outer edge of cell wall. Arrowheads show plasma membrane. IL; the inner layer, ML; the middle layer, OL; the outer layer. Scale bars = 10 μm (a), 500 nm (b-f).

Plate 5. Immunogold localization of alginate within cell wall in the *Silvetia babingtonii* zygotes at 24 h AF. (a), (b), (c) show BAM6 localization. (d), (e), (f) indicate BAM7 localization. (a) (d) TCW, (b) (e) RFCW, (c) (f) RTCW. Arrows show the outer edge of cell wall. Insets show the magnified images of dashed line rectangles. Arrowheads show plasma membrane. Scale bars = 500 nm (a-f), 100 nm (insets).

Plate 6. The distribution of the relative density of relative distance of gold particles binding to BAM6 and BAM7 in TCW and RTCW at 24 h-old *Silvetia babingtonii* zygotes. The relative distance between plasma membrane and the cell-wall edge ranges from 0 to 1. The sum of density is adjusted to 10. Grey lines show the function obtained by kernel function and bandwidth.

Plate 7. MA plots (log expression ratio vs. mean average expression) comparing gene expression during germination of *Silvetia babingtonii* zygotes. Differential expression genes were shown as magenta points (TCC, FDR < 0.05). (a) 3 h AF vs. 10 h AF, (b) 3 h AF vs. 24 h AF, (c) 10 h AF vs. 24 h AF.

Plate 8. The gene expression level of mannuronan C5-epimerase (MC5E) shown as TPM and Z-score during development of *Silvetia babingtonii* zygotes. Asterisks indicate differential expression genes.

Plate 9. Putative protein structure of mannuronan C5-epimerases in *Silvetia babingtonii*. Each shape on the schematic protein sequences indicates the catalytic MC5E domain (purple box), a transmembrane domain (cyan oval), a signal peptide region (orange box), and the WSC domains (green box).

Plate 10. Phylogenetic analysis of mannuronan C5-epimerases in *Silvetia babingtonii*. Numbers

indicate the bootstrap values in the maximum likelihood analysis. Asterisks indicate differential expression genes.

Plate 11. Quantitative analysis of putative mannuronan C5-epimerase genes transcript level in 3, 10, and 24 hour-old zygotes of *Silvetia babingtonii*. (a) comp32408_c2_seq24.p1, (b) comp33109_c0_seq1.p1. The relative gene expression was set at one at 3 h AF. The error bars indicate SDs of three separate experiments. Tukey's multiple comparison tests were conducted to investigate significant differences between the treatment hours. Asterisks (*) indicate significant differences at $P < 0.01$.

Plate 12. Life cycle of *Saccharina japonica*. AF; anterior flagellum; Ch; chroloplast, N; nucleus, PF; posterior flagellum.

Plate 13. Male and female gametophytes of *Saccharina japonica* cultured in iron-deficient and iron-repletion medium. (a) Male gametophytes in iron deficient ASP_{12} NTA. (b) Male gametophytes at 3 days after iron repletion. (c) Male gametophytes at 6 days after iron repletion. Arrows show that protrusions to form antheridia from later of the filament. (d) Female gametophytes in iron deficient ASP_{12} NTA. (e) Female gametophytes at 3 days after iron repletion. Asterisks show that protrusions to form oogonia from lateral of the filament. (f) Female gametophytes at 6 days after iron repletion. Arrows indicate premature oogonia. Cap structure can be seen at the tip. Scale bars = 20 μm.

Plate 14. Ultrastructure of male gametophytes of *Saccharina japonica* cultured in iron-deficient and iron-repletion medium. (a) A filament cell of male gametophyte in iron deficient ASP_{12} NTA. (b) The filament cell of male gametophyte at 6 days after iron repletion. (c) Antheridium on the filament at 6 days after iron repletion. An asterisk shows the cap structure. Double arrowheads

indicate flagella. (d) Cell wall from lateral of filament cultured in iron deficient medium. (e) Cell wall from lateral of filament cultured at 6 days after iron repletion. Arrows show the edge of cell wall. Arrowheads indicate the plasma membrane. Ch; chloroplast, CW; cell wall, M; mitochondria, N; nucleus, V; vacuole. Scale bars = 1 μm (a, b, c), 200 nm (d, e).

Plate 15. Ultrastructure of female gametophytes of *Saccharina japonica* cultured in iron-deficient and iron-repletion medium. (a) The filament cell of female gametophyte in iron deficient ASP_{12}NTA. (b) The filament cell of female gametophyte at 6 days after iron repletion. (c) Cell wall from lateral of filament cultured in iron deficient medium. (d) Cell wall from lateral of filament cultured at 6 days after iron repletion. (e) Golgi bodies in the cell of female gametophyte in iron deficient ASP_{12} NTA. (f) Golgi bodies in the cell of female gametophyte at 6 days after iron repletion. (g) Initial stage of oogenesis. Ch; chloroplast, CW; cell wall, M; mitochondria, N; nucleus, V; vacuole. Scale bars = 2 μm (a, b, g), 200 nm (c, d), 500 nm (e, f).

Plate 16. Immunogold localization of sulfated fucan using BAM2 in antheridium of male gametophytes of *Saccharina japonica*. (a) Cap structure of antheridium, (b) Base of antheridium. Scale bars = 500 nm.

Plate 17. MA-plot (log expression ratio vs. mean average expression) comparing gene expression during 0 vs 3 days or 0 vs 6 days in male and female gametophytes in *Saccharina japonica* respectively. Differential expression genes were shown as red in upregulated and downregulated in blue. Top 10 of DEGs which were upregulation or downregulation were indicated with name plates. (a) SJ01641; Plasma membrane iron permease, SJ02684; dynein heavy chain 7, axonemal isoform X1, SJ03191; predicted protein, SJ03251; protein fucoxanthin chlorophyll a/c protein, SJ07633; MBL fold metallo-hydrolase, SJ10046; hypothetical protein PPTG_09172, SJ11978; predicted protein, SJ12702; N/A, SJ17393; N/A, SJ22590; probable xyloglucan

galactosyltransferase GT19. (b) SJ02566; dynein heavy chain 7, axonemal-like, SJ02568; dynein heavy chain 7, axonemal isoform X1, SJ02681; E3 ubiquitin-protein ligase pellino homolog 1, SJ02684; kinesin-like protein KIF13B isoform X1, SJ03251; protein fucoxanthin chlorophyll a/c protein, SJ10046; hypothetical protein PPTG_09172, SJ11978; predicted protein, SJ12702; N/A, SJ16076; kinesin-like protein KIF11, SJ17393; N/A. (c) SJ03251; protein fucoxanthin chlorophyll a/c protein, SJ03335; saccharopine dehydrogenase, SJ08942; putative germin-like protein 2-1, SJ11978; predicted protein, SJ12702; N/A, SJ15808; N/A, SJ16643; N/A, SJ17393; N/A, SJ18834; chitin binding, SJ21503; N/A. (d) SJ02020; N/A, SJ02023; glycosyl hydrolase family protein, SJ03251; protein fucoxanthin chlorophyll a/c protein, SJ09196; N/A, SJ11978; predicted protein, SJ12702; N/A, SJ12780; predicted protein, SJ13353; predicted protein, SJ13353; predicted protein, SJ17393; N/A.

Plate 18. Venn diagrams of DEGs on (a) upregulation or (b) downregulation by gene expression fluctuation during 0 vs 3 days or 0 vs 6 days in male (M_3, M_6) and female (F_3, F_6) gametophyte in *Saccharina japonica* respectively. The 7 categories are shown in bold letters. [a] Consensus DEGs; Gene expression fluctuation of M_3, M_6 and F_3, F_6 is observed compared to M_0 and F_0. [b] Male consensus DEGs; Gene expression fluctuation of M_3 and M_6 is observed compared to M_0 only. [c] 3 days in male; Gene expression fluctuation of M_3 is observed compared to M_0 only. [d] 6 days in male; Gene expression fluctuation of M_6 is observed compared to M_0 only. [e] Female consensus DEGs; Gene expression fluctuation of F_3 and F_6 is observed compared to F_0 only. [f] 3 days in female; Gene expression fluctuation of F_3 is observed compared to F_0 only. [g] 6 days in female; Gene expression fluctuation of F_6 is observed compared to F_0 only.

Plate 19. Schematic representation of alginate biosynthesis pathway with expression of putative enzymatic genes (FPKM > 1) at 0, 3, and 6 days after iron replacement in male and female

gametophytes in *Saccharina japonica* (M_0, M_3, M_6, F_0, F_3, F_6). Heatmap was generated based on normalized FPKM values for each gene. GDP, guanosine diphosphate; GMD, GDP-mannose dehydrogenase; MC5E, mannuronan C-5 epimerase; MPG, GDP-mannose pyrophosphorylase; MPI, mannose-6-phosphate isomerase; MS, Mannuronan synthase; PMM, phosphomannomutase. Upregulated and downregulated (male or female) consensus DEGs are shown in red and blue, respectively.

Plate 20. Schematic representation of sulfated fucan biosynthesis pathway with expression of putative enzymatic genes (FPKM > 1) at 0, 3, and 6 days after iron replacement in male and female gametophytes in *Saccharina japonica* (M_0, M_3, M_6, F_0, F_3, F_6). Heatmap was generated based on normalized FPKM values for each gene. FKGP; fucokinase/GDP-Fuc pyrophosphorylase, FT; fucosyltransferase, GDP; guanosine diphosphate, GFS; GDP-fucose synthase, GM46D; GDP-mannose 4,6-dehydratase, ST; sulfotransferase.

Plate 21. Schematic representation of cellulose biosynthesis pathway with expression of putative enzymatic genes in *Saccharina japonica* (FPKM > 1) at 0, 3, and 6 days after iron replacement in male and female gametophytes (M_0, M_3, M_6, F_0, F_3, F_6). Heatmap was generated based on normalized FPKM values for each gene. CESA; Cellulose synthase, GDP; guanosine diphosphate, GPI; glucose-6-phosphate isomerase, GS; β-1,3-glucan synthase (family GT48), PGM; phosphoglucomutase, UDP; uridine diphosphate, UGP; UDP-glucose pyrophosphorylase.

Plate 22. Schematic representation of laminaran biosynthesis pathway with expression of putative enzymatic genes in *Saccharina japonica* (FPKM > 1) at 0, 3, and 6 days after iron replacement in male and female gametophytes (M_0, M_3, M_6, F_0, F_3, F_6). Heatmap was generated based on normalized FPKM values for each gene. KRE6-like; putative 1,6-β-transglucosylase (family GH16), UDP; uridine diphosphate.

Plate 1

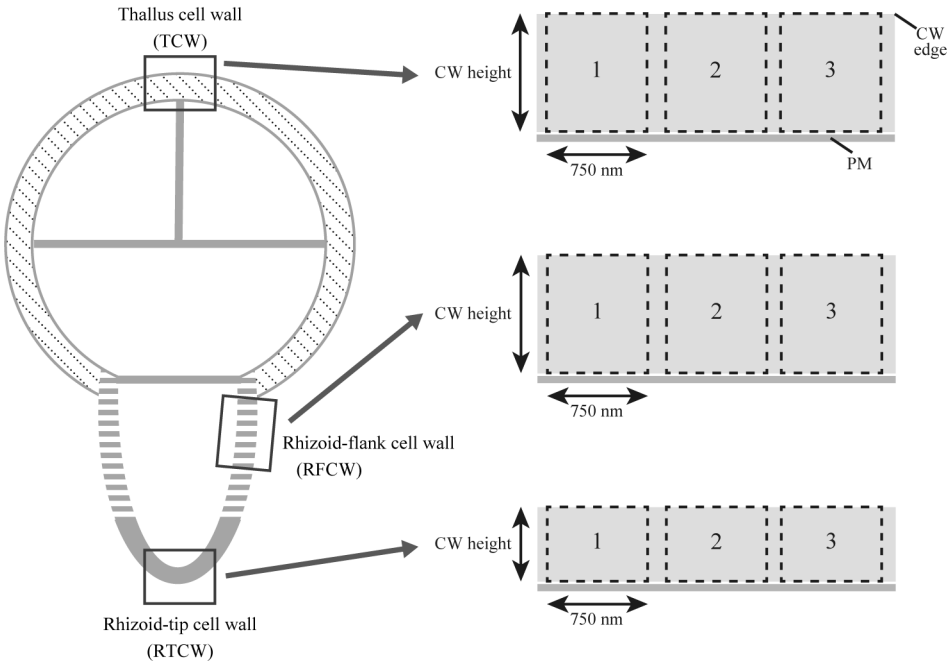
Thallus cell wall
(TCW)
Rhizoid-flank cell wall
(RFCW)
Rhizoid-tip cell wall
(RTCW)
CW height
1
2
3
CW edge
750 nm
PM
CW height
1
2
3
750 nm
CW height
1
2
3
750 nm

Plate 2

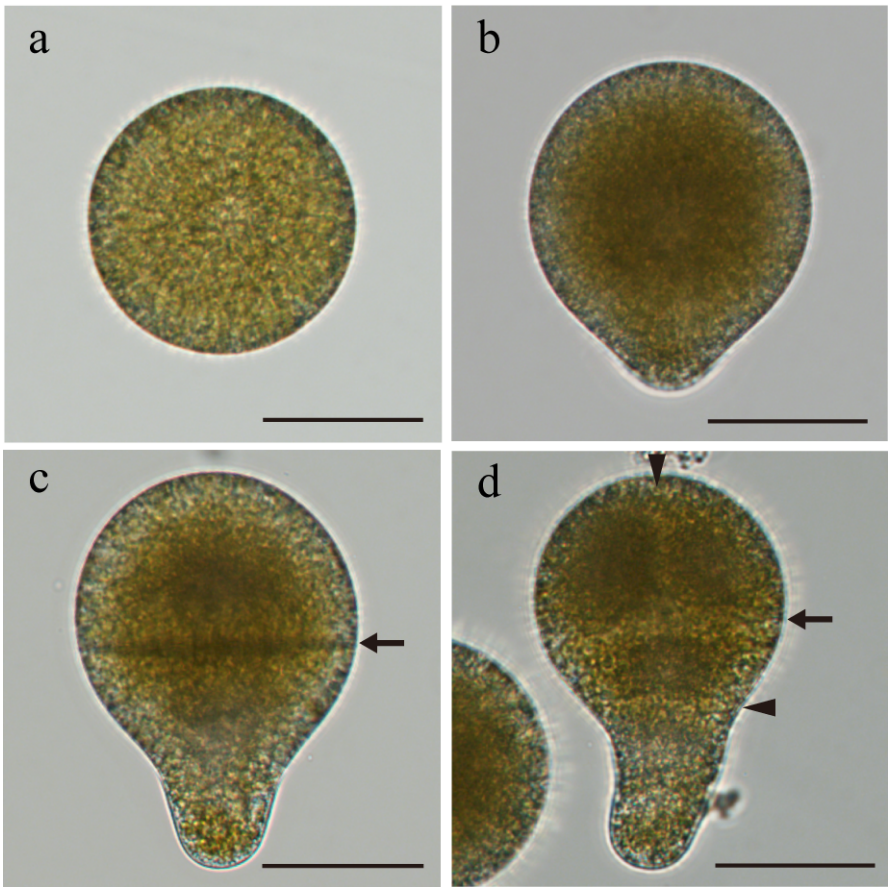

Plate 3

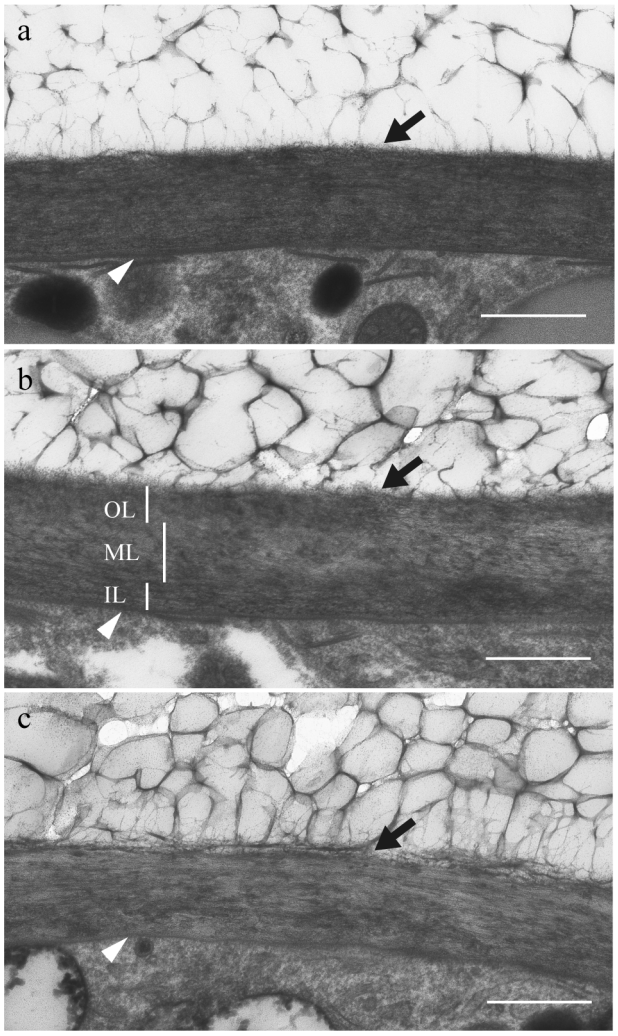

Plate 4

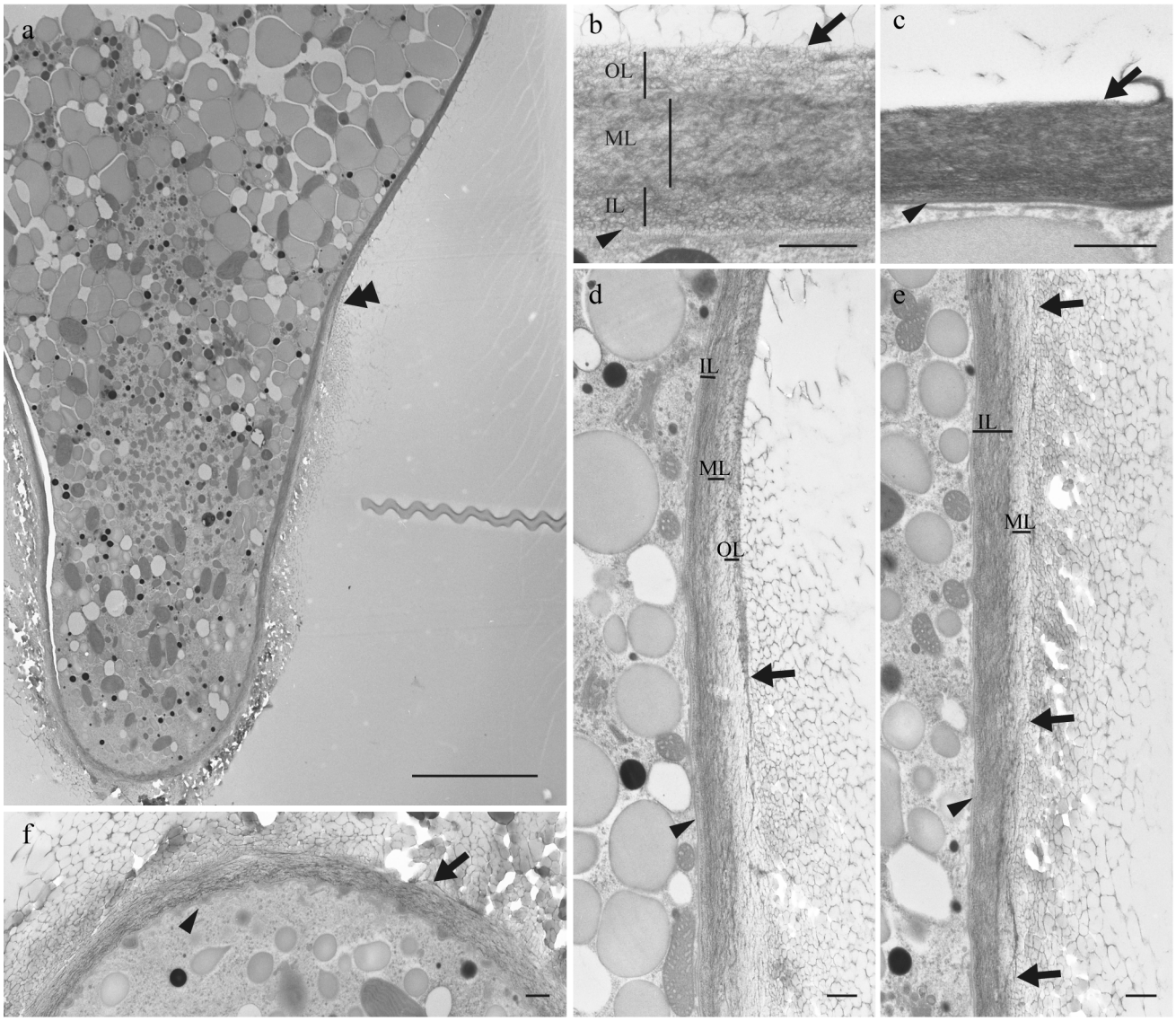

Plate 5

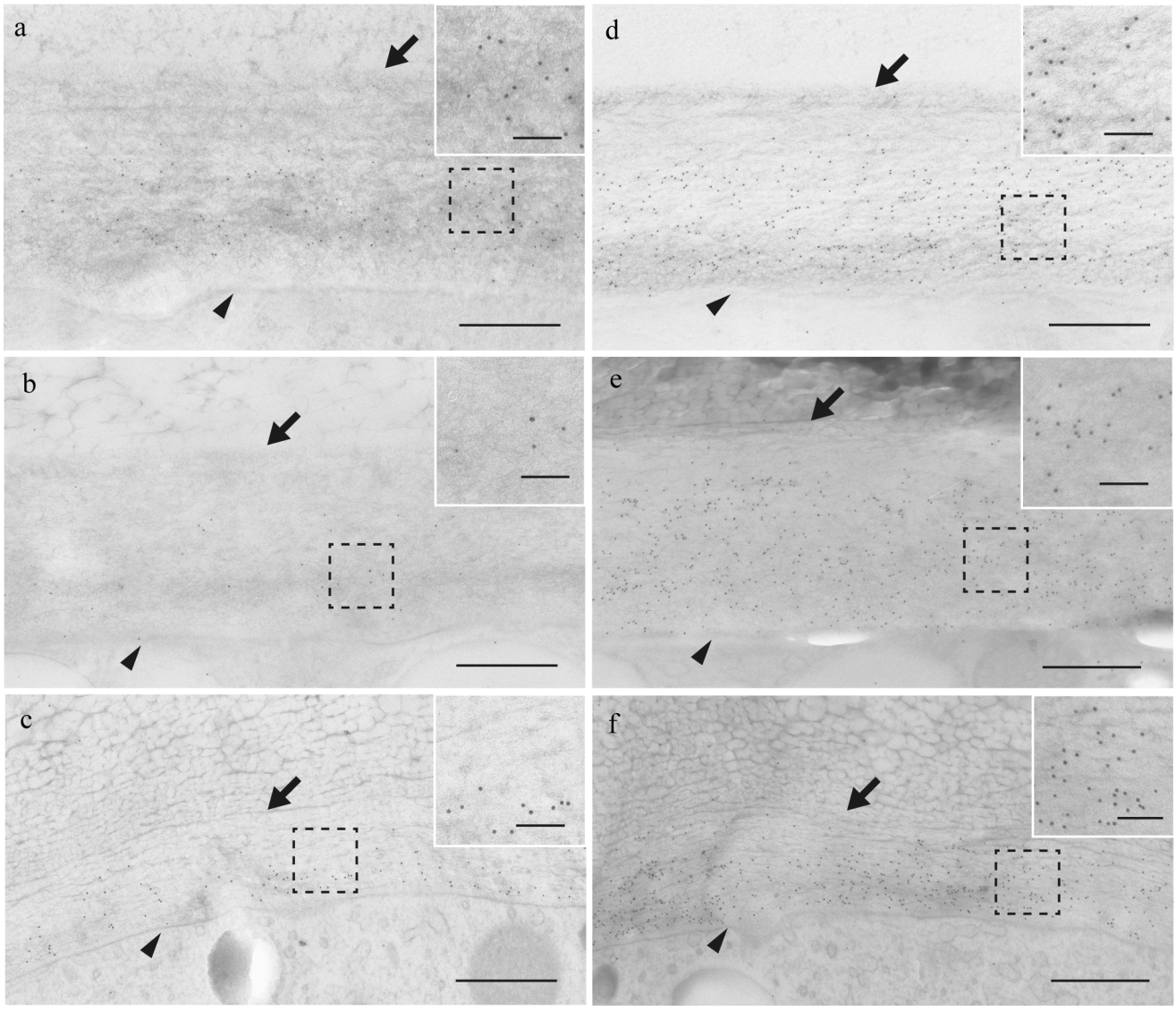

Plate 6

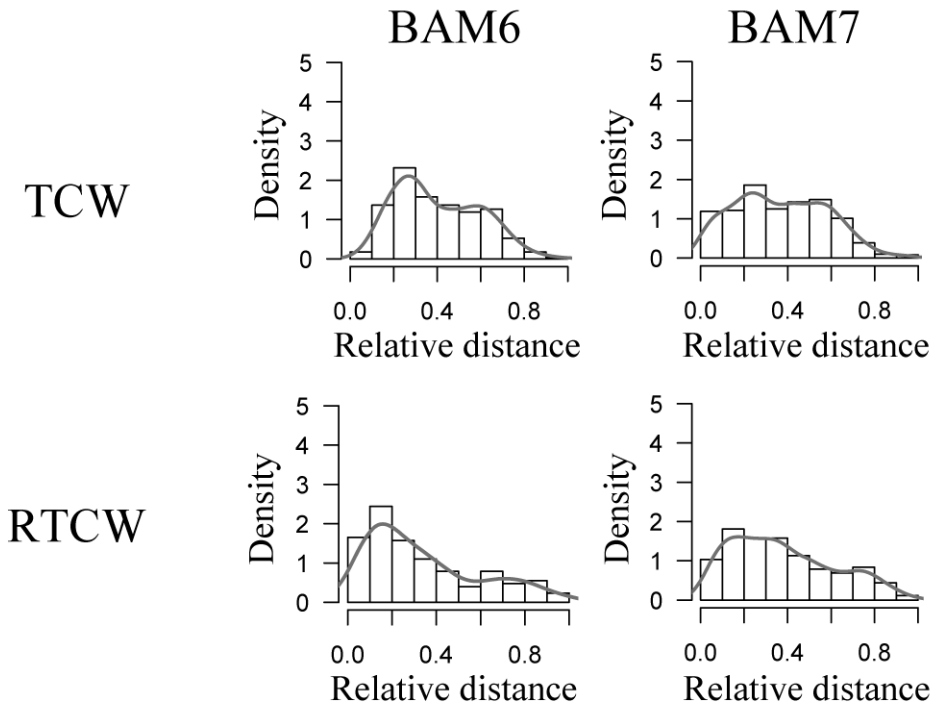
BAM6
BAM7
TCW
RTCW
Density
Relative distance
0.0
0.4
0.8
0
1
2
3
4
5

Plate 7

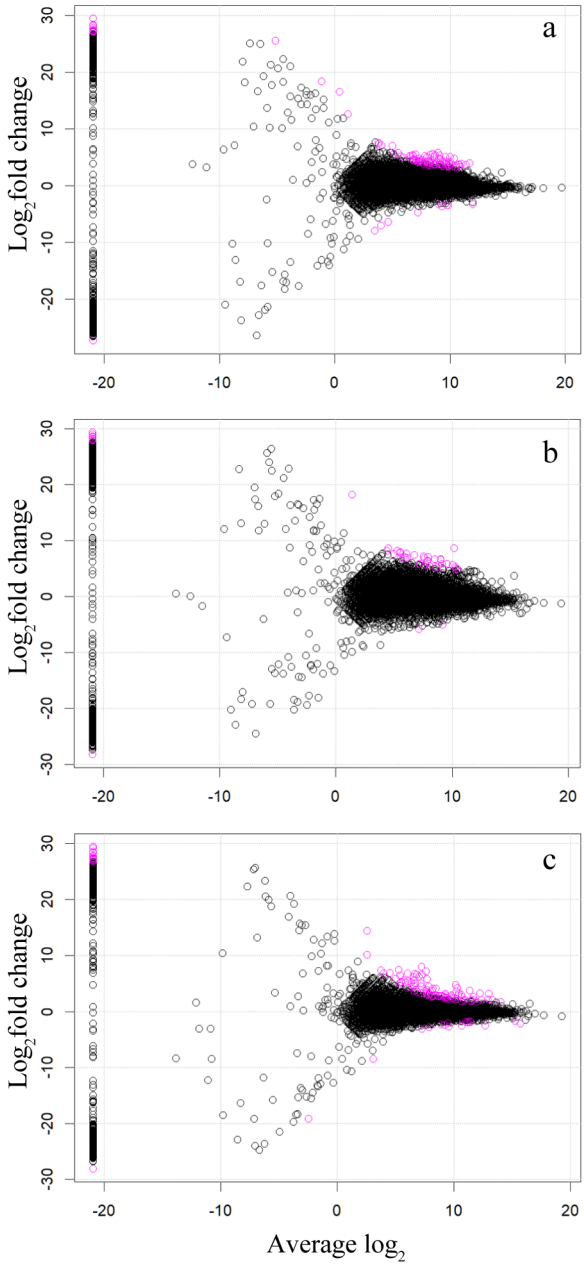
a
b
c
Log2 fold change
Average log2
30
20
10
0
-10
-20
-30
-20
-10
0
10
20

Plate 8

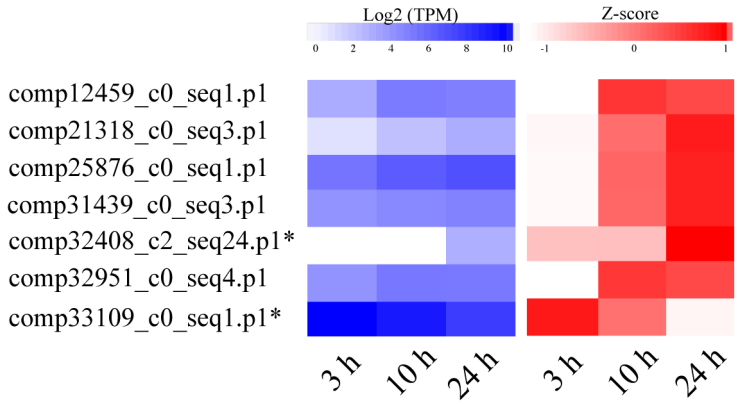
Log2 (TPM)
0
2
4
6
8
10
Z-score
-1
0
1
comp12459_c0_seq1.p1
comp21318_c0_seq3.p1
comp25876_c0_seq1.p1
comp31439_c0_seq3.p1
comp32408_c2_seq24.p1*
comp32951_c0_seq4.p1
comp33109_c0_seq1.p1*
3 h
10 h
24 h
3 h
10 h
24 h

Plate 9

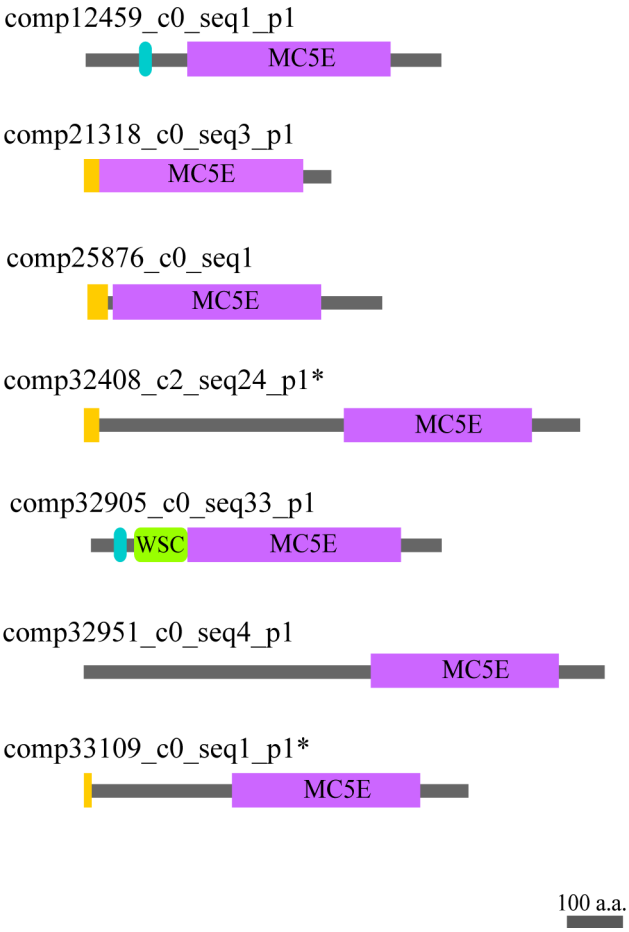
comp12459_c0_seq1_p1
MC5E
comp21318_c0_seq3_p1
MC5E
comp25876_c0_seq1
MC5E
comp32408_c2_seq24_p1*
MC5E
comp32905_c0_seq33_p1
WSC
MC5E
comp32951_c0_seq4_p1
MC5E
comp33109_c0_seq1_p1*
MC5E
100 a.a.

Plate 10

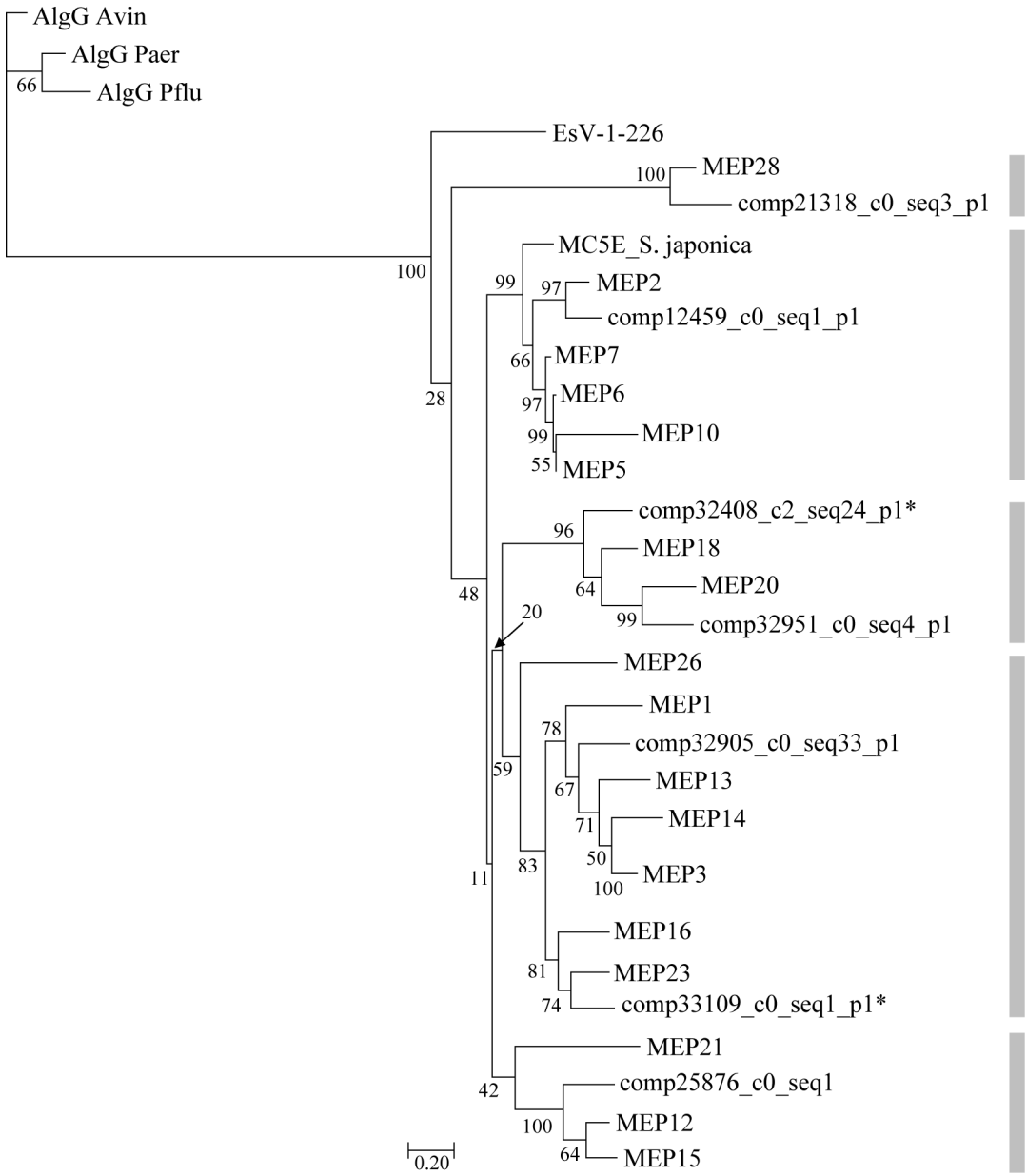
AlgG Avin
AlgG Paer
AlgG Pflu
66
EsV-1-226
100
MEP28
comp21318_c0_seq3_p1
100
MC5E_S. japonica
99
97
MEP2
comp12459_c0_seq1_p1
66
MEP7
28
97
MEP6
99
MEP10
55
MEP5
comp32408_c2_seq24_p1*
96
MEP18
64
MEP20
48
99
comp32951_c0_seq4_p1
20
MEP26
MEP1
78
comp32905_c0_seq33_p1
59
67
MEP13
71
MEP14
50
83
MEP3
11
100
MEP16
81
MEP23
74
comp33109_c0_seq1_p1*
MEP21
42
comp25876_c0_seq1
100
MEP12
64
MEP15
0.20

Plate 11

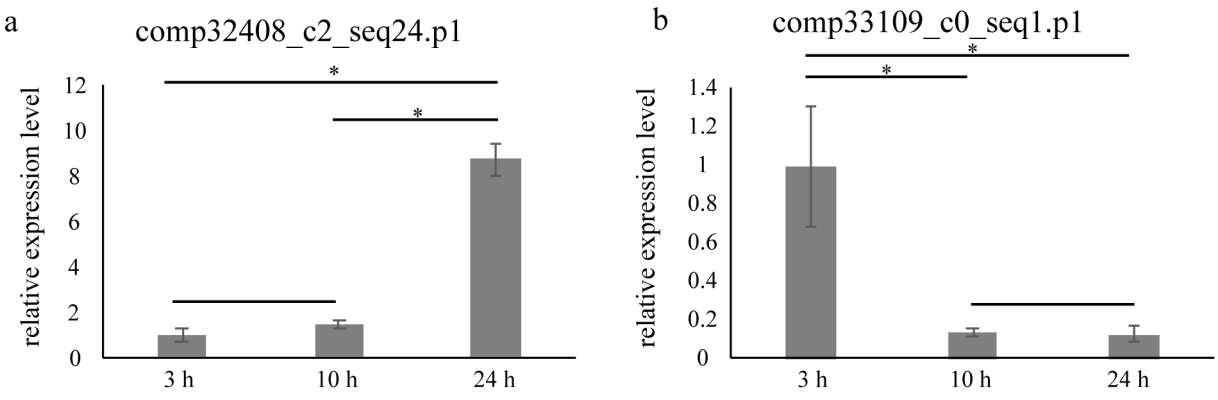
a
comp32408_c2_seq24.p1
relative expression level
12
10
8
6
4
2
0
*
*
3 h
10 h
24 h
b
comp33109_c0_seq1.p1
relative expression level
1.4
1.2
1
0.8
0.6
0.4
0.2
0
*
*
3 h
10 h
24 h

Plate 12

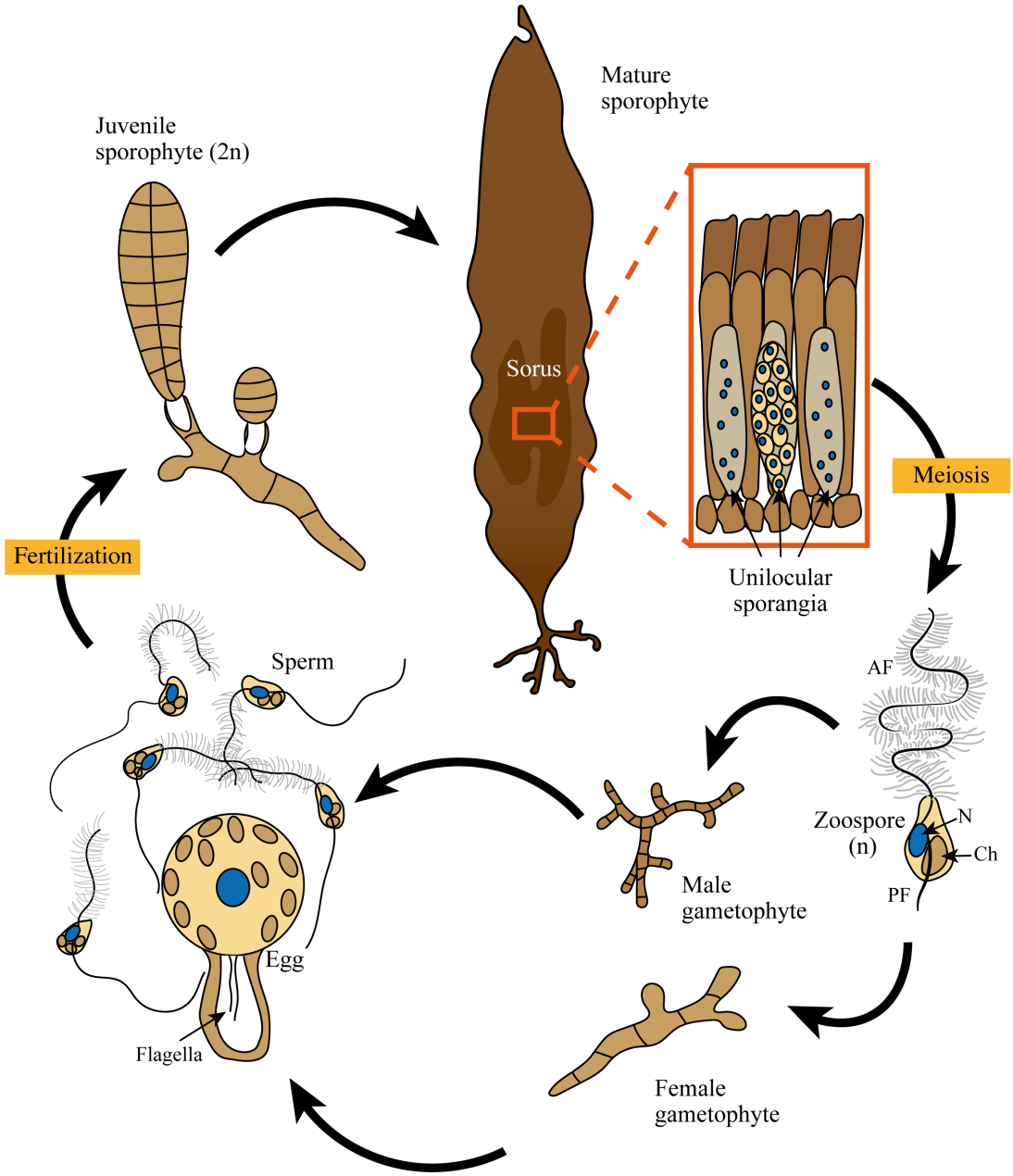
Mature
sporophyte
Juvenile
sporophyte (2n)
Sorus
Meiosis
Unilocular
sporangia
Fertilization
AF
Sperm
Zoospore
(n)
N
Ch
PF
Male
gametophyte
Egg
Flagella
Female
gametophyte

Plate 13

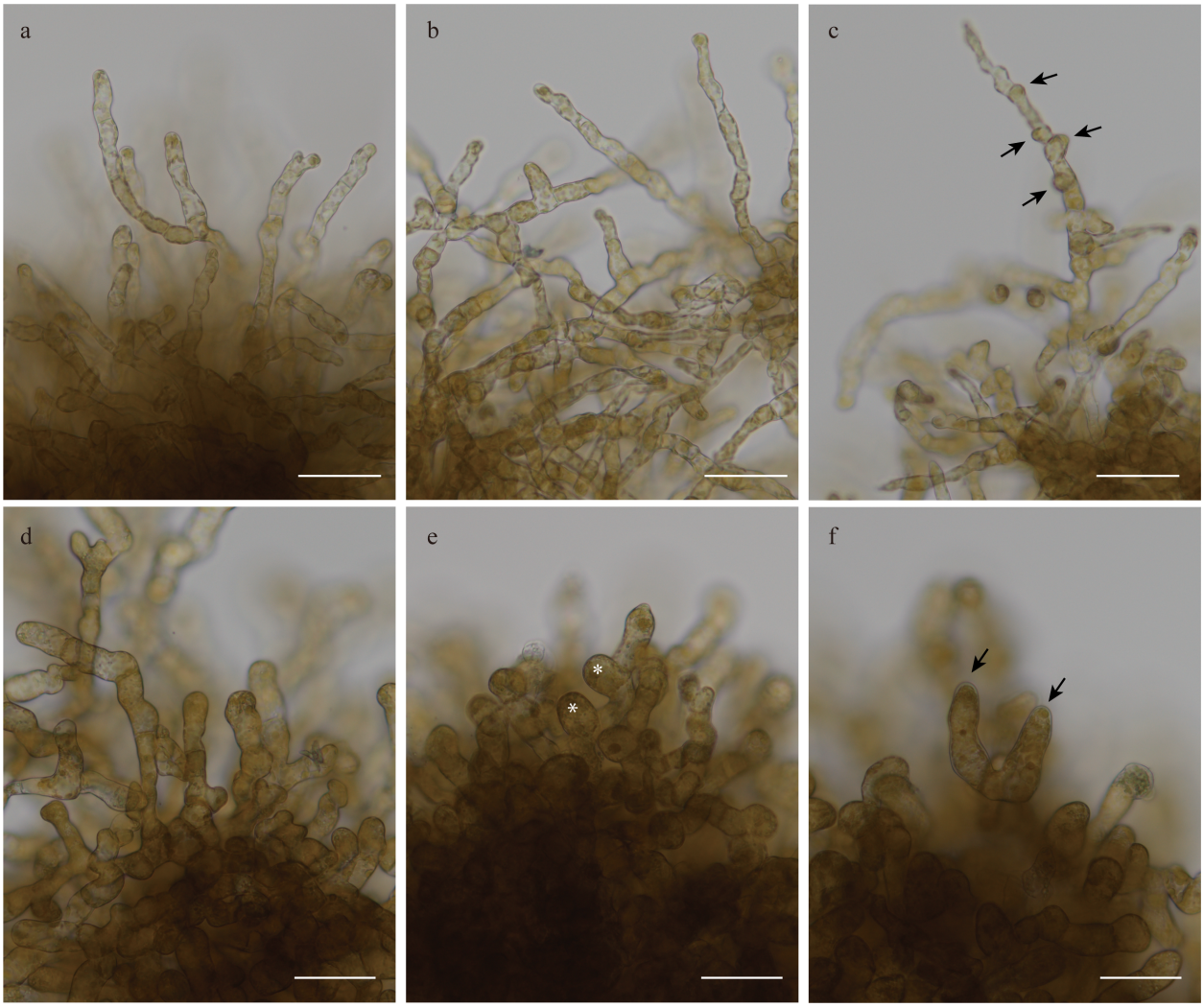

Plate 14

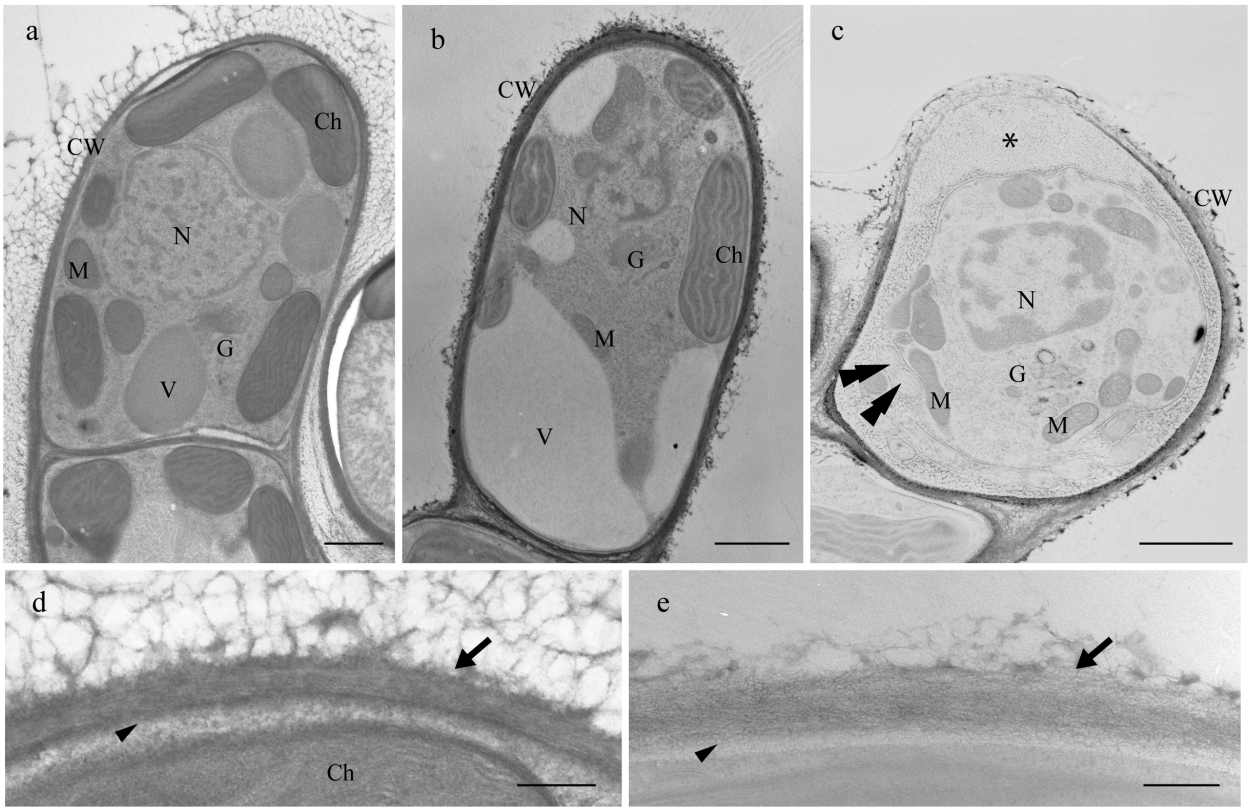

Plate 15

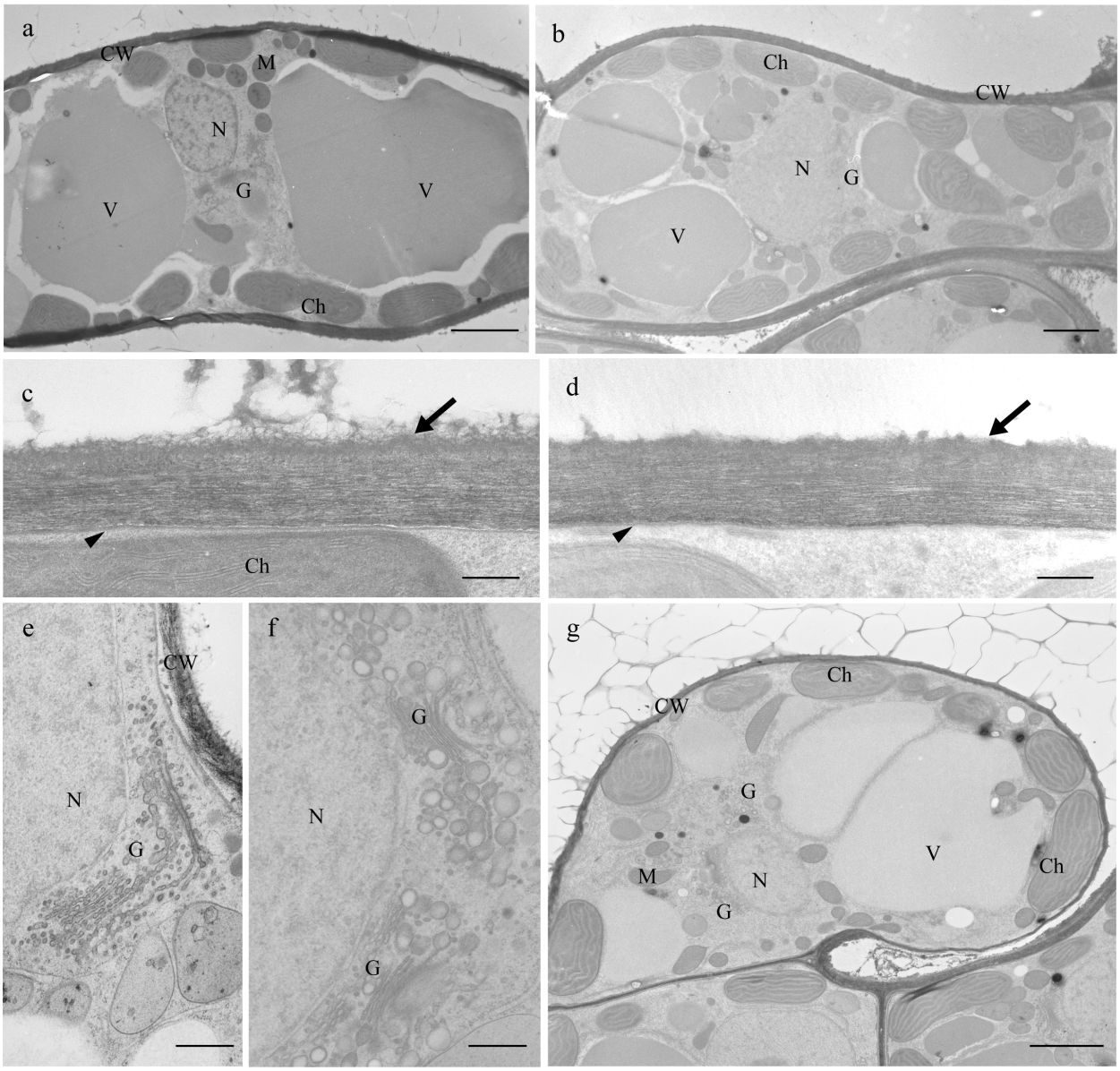

Plate 16

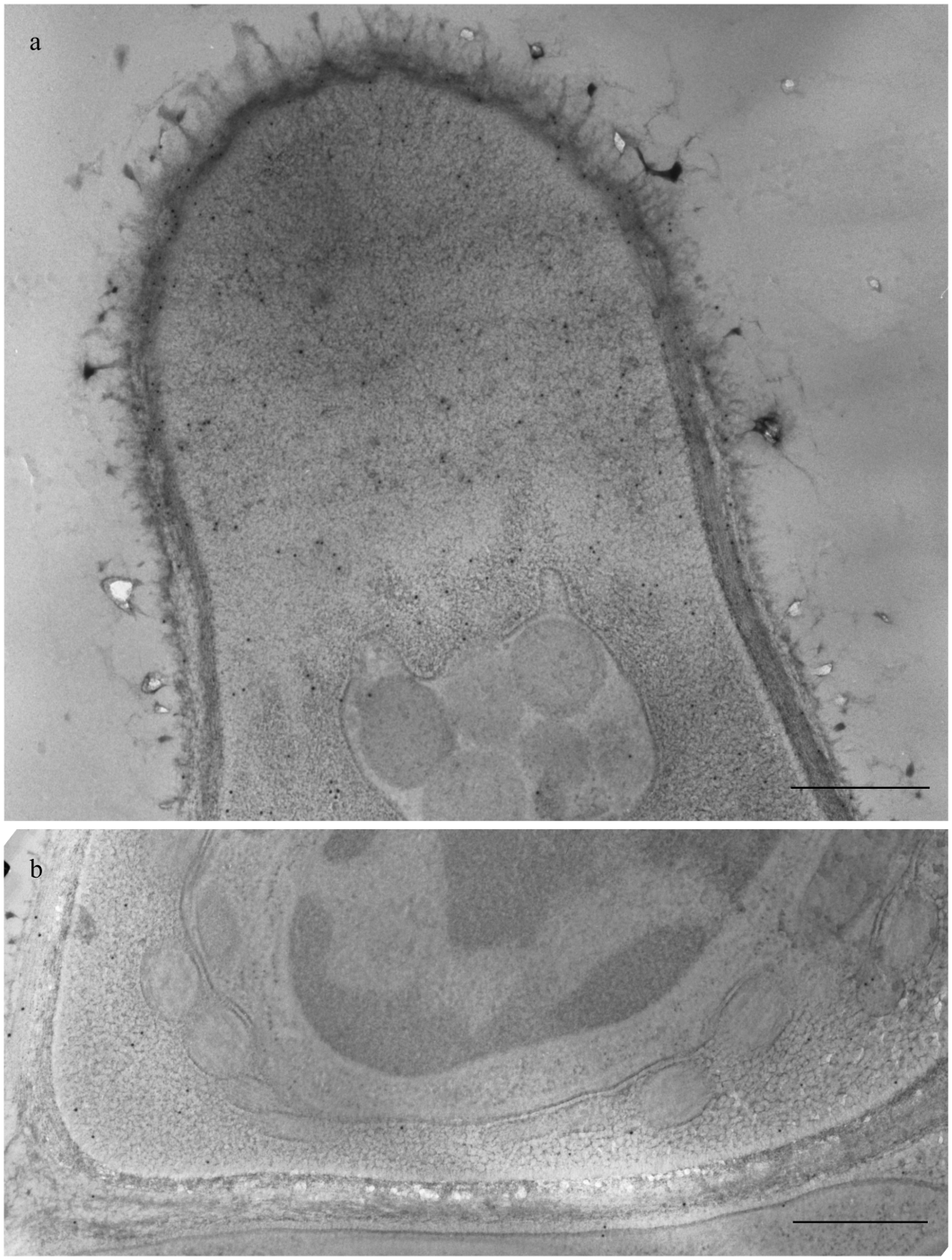

Plate 17

Male

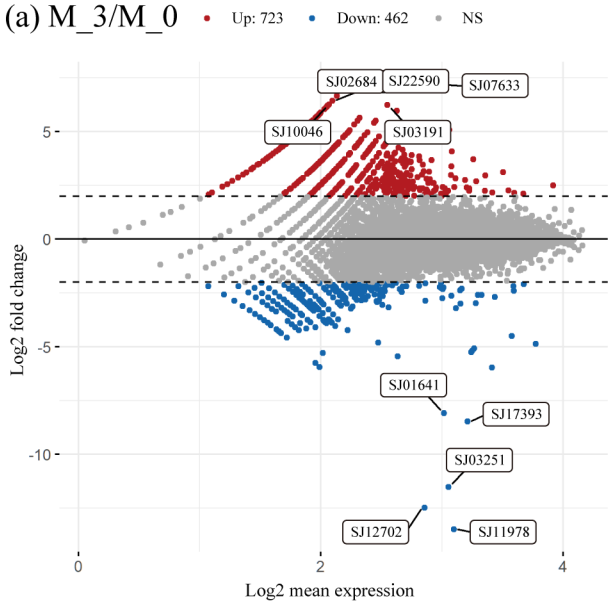

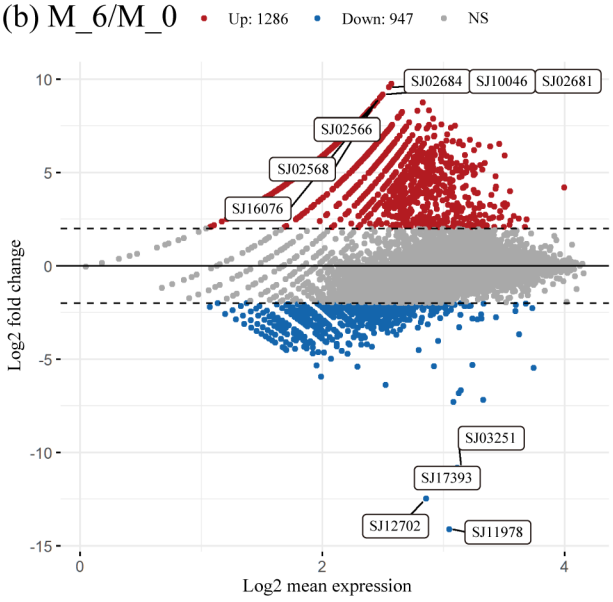

Female

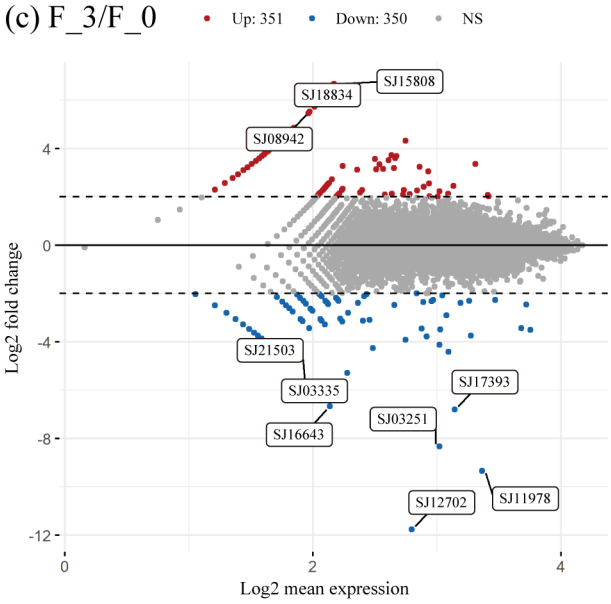

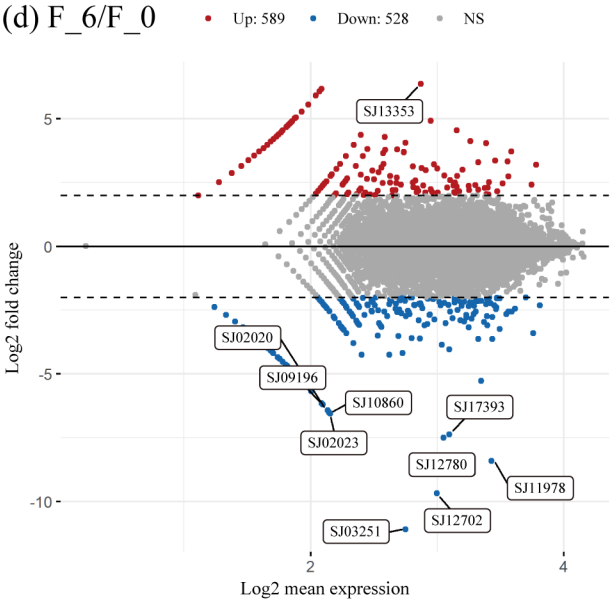

Plate 18

(a) Upregulation

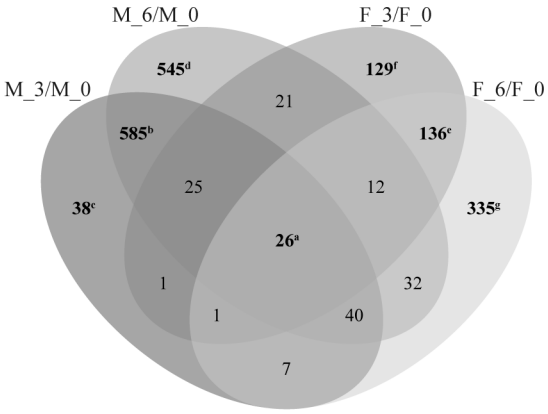

(b) Downregulation

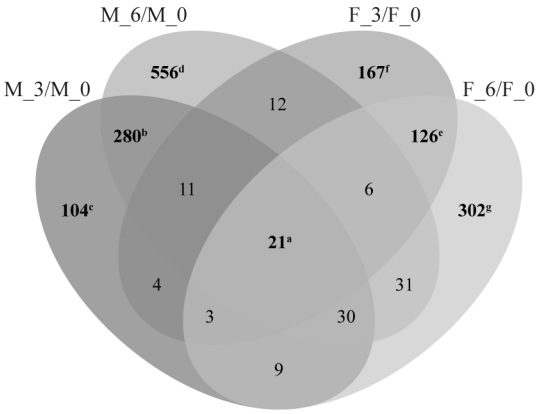

Alginate synthesis pathway

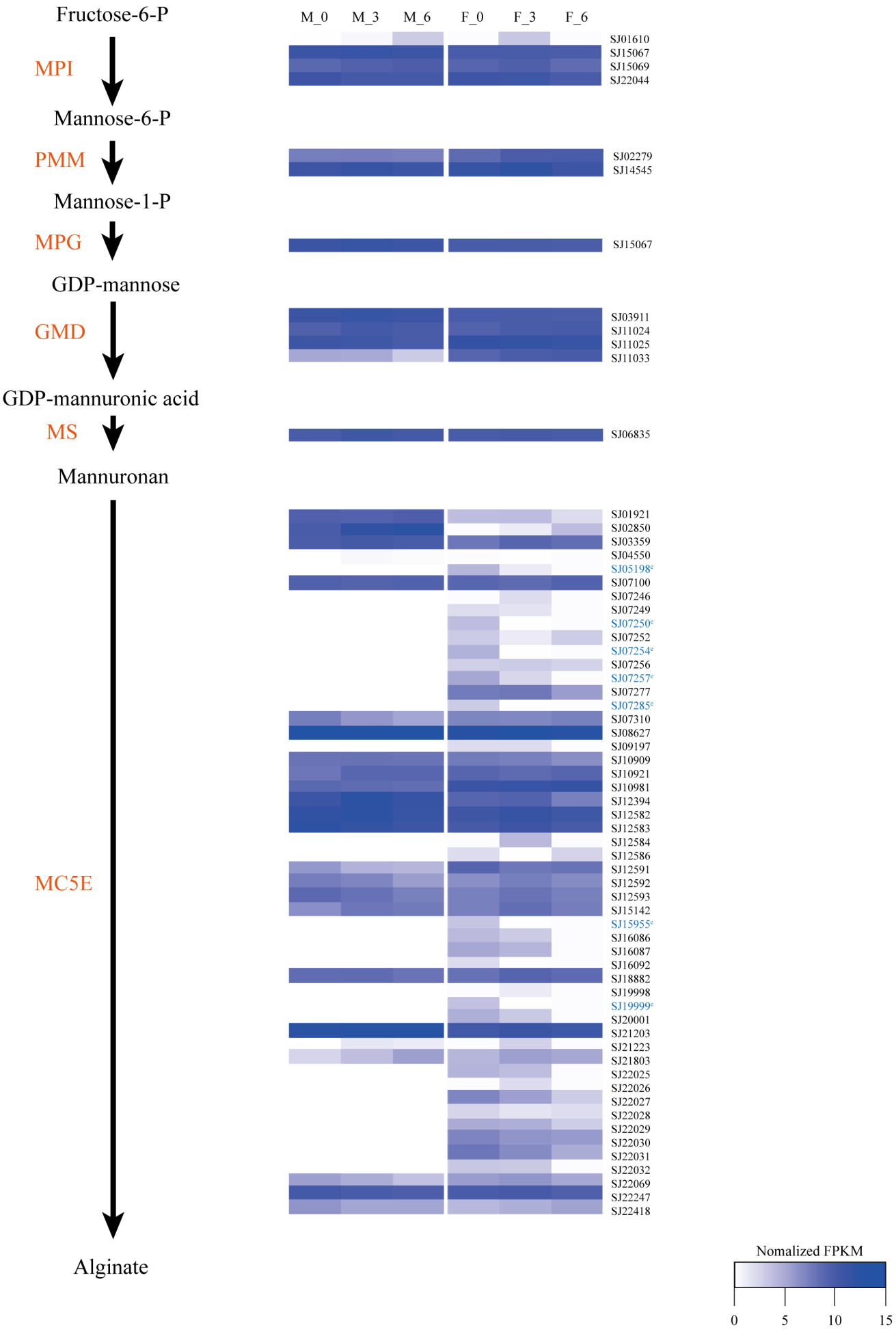

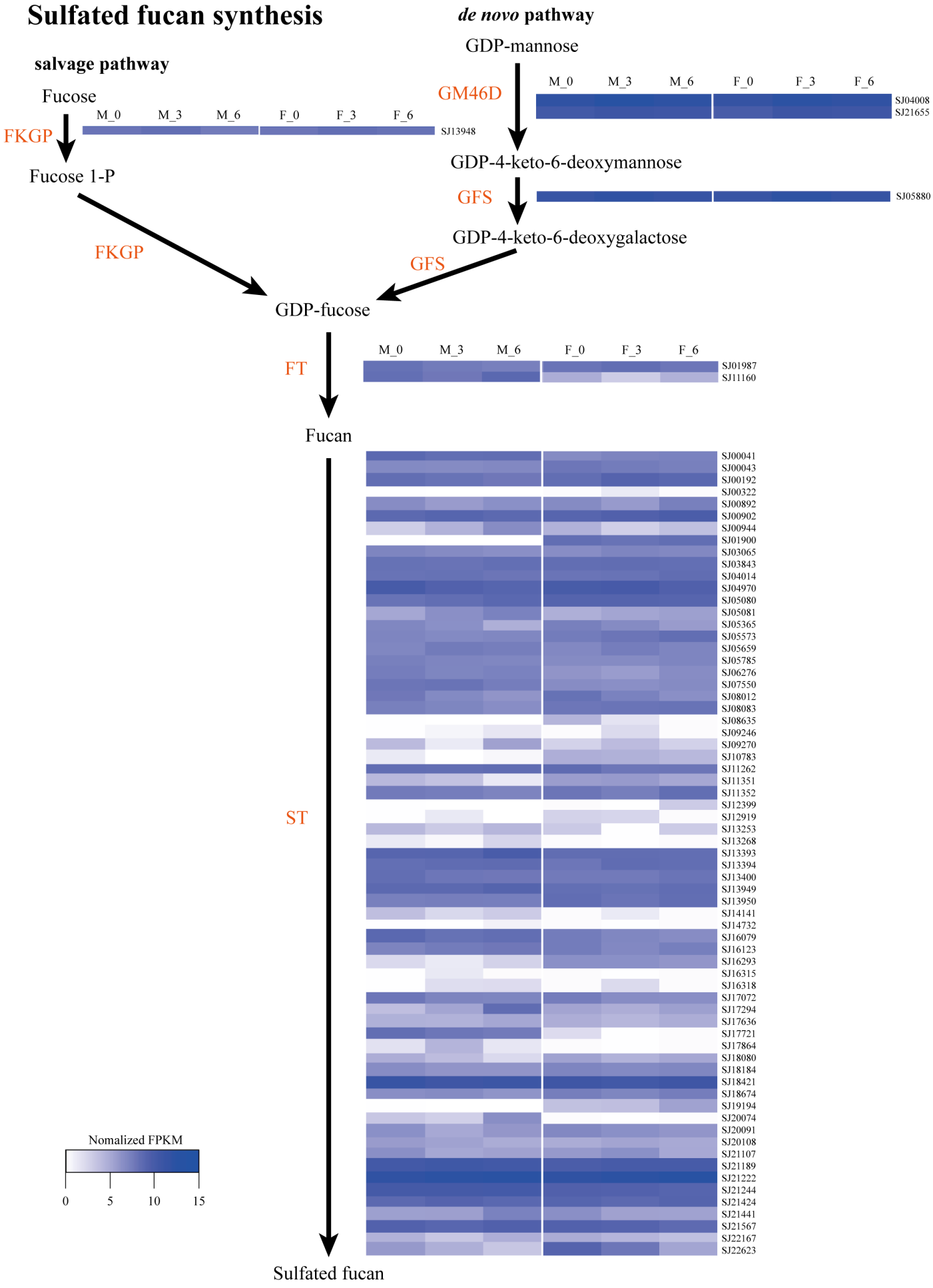
Sulfated fucan synthesis
de novo pathway
salvage pathway
GDP-mannose
Fucose
GM46D
FKGP
M_0 M_3 M_6 F_0 F_3 F_6
SJ13948
SJ04008
SJ21655
Fucose 1-P
GDP-4-keto-6-deoxymannose
GFS
SJ05880
GDP-4-keto-6-deoxygalactose
FKGP
GFS
GDP-fucose
FT
SJ01987
SJ11160
Fucan
ST
SJ00041
SJ00043
SJ00192
SJ00322
SJ00892
SJ00902
SJ00944
SJ01900
SJ03065
SJ03843
SJ04014
SJ04970
SJ05080
SJ05081
SJ05365
SJ05573
SJ05659
SJ05785
SJ06276
SJ07550
SJ08012
SJ08083
SJ08635
SJ09246
SJ09270
SJ10783
SJ11262
SJ11351
SJ11352
SJ12399
SJ12919
SJ13253
SJ13268
SJ13393
SJ13394
SJ13400
SJ13949
SJ13950
SJ14141
SJ14732
SJ16079
SJ16123
SJ16293
SJ16315
SJ16318
SJ17072
SJ17294
SJ17636
SJ17721
SJ17864
SJ18080
SJ18184
SJ18421
SJ18674
SJ19194
SJ20074
SJ20091
SJ20108
SJ21107
SJ21189
SJ21222
SJ21244
SJ21424
SJ21441
SJ21567
SJ22167
SJ22623
Nomalized FPKM
0 5 10 15
Sulfated fucan

Plate 21

Cellulose synthesis pathway

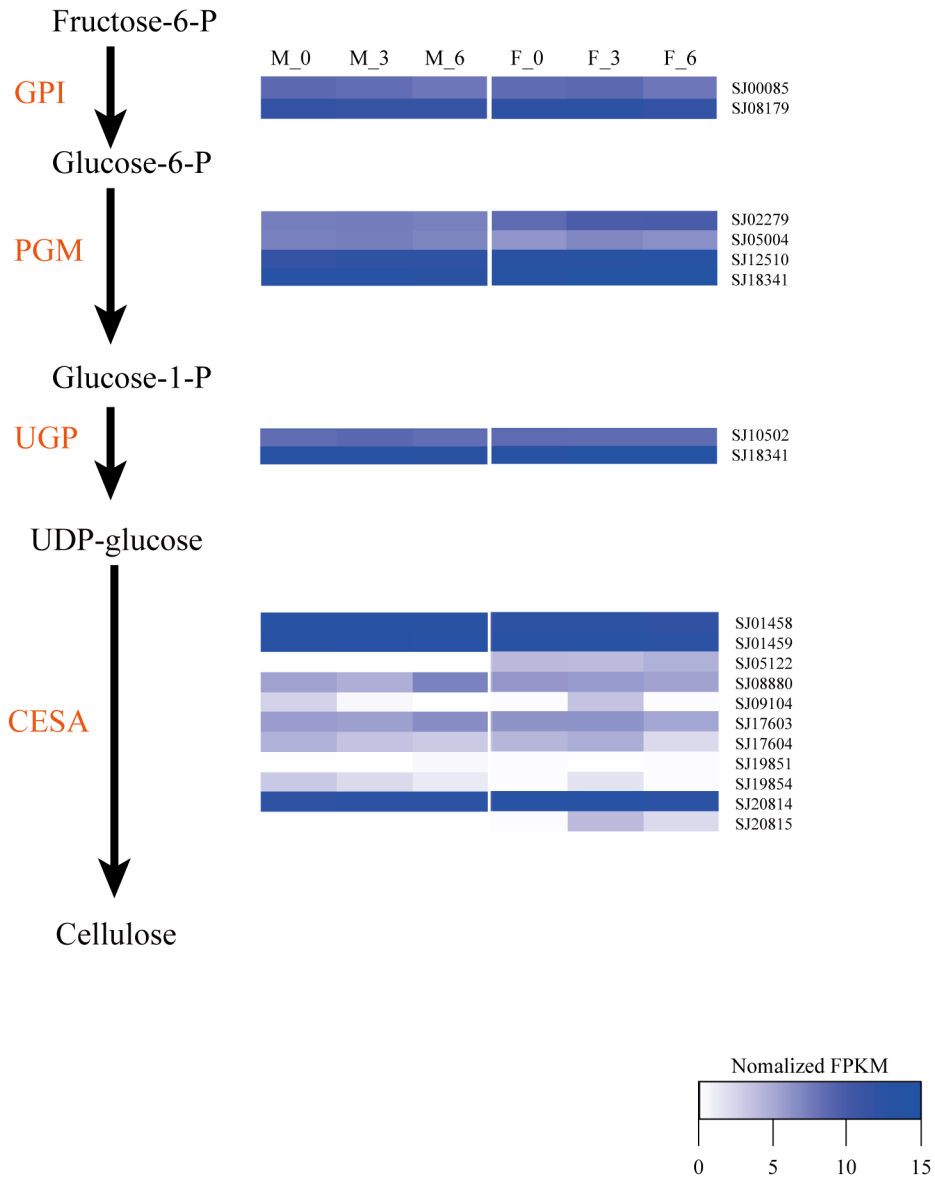

Plate 22

Laminaran synthesis pathway